A STUDY OF PHOSPHOLIPID ASSOCIATING PEPTIDES

A thesis presented in partial fulfilment

of the requirements for the

degree of Ph.D. in

Chemistry at

Massey University

DEREK ROBIN KNIGHTON

1983

ABSTRACT

This thesis describes the solid-phase synthesis of a series of 5 peptides and their subsequent purification by conventional chromatography and semipreparative reversed-phase HPLC. The efficiencies of these 2 methods of purification have been compared. The peptides are: peptide 208, VSSLLSSLKEYWSSLKESFS; peptide 199, RALASSLKEYWSSLKESFS; peptide 202, LESFLKSWLSALEQALKA; peptide 203, LESFKVSWLSALEEYTKA; and peptide 209, LESFLLSWLSAKEQALKA. The peptides were chosen so that each would exhibit a slightly different non-polar face when it adopted an α-helical conformation. Peptides 202 and 209 have exactly the same amino acid composition but differ in that a leucine and a lysine residue have changed positions. This results in the non-polar face of peptide 209 containing one less leucine relative to peptide 202.

The retentions of the series of peptides in several reversed-phase HPLC systems were measured by gradient elution. These systems utilised the following solvent system: Solvent A = 1% triethylammonium phosphate, pH 3.2, Solvent B = 80% 2-propanol, 20% solvent A. Radial-PAK CN, Radial-PAK C18 and μBondapak alkylphenyl columns were used. When a linear gradient from 0 to 100% Solvent B was used the retention of the peptides on the Radial-PAK CN column were: peptide 202, 54.75; peptide 208, 51.5; peptide 209, 49; peptide 203, 48; and peptide 199, 44; (expressed as a percentage of the gradient). The isocratic elution of the peptides were studied in the same solvent system on a μBondapak alkylphenyl column by varying the organic solvent content of the mobile phase. The retention of the peptides could not be correlated with the total hydrophobicity of the peptides but could be correlated with the total hydrophobicity of the non-polar side of each peptide when in the α-helical conformation. This result suggests that the peptides adopt an α-helical conformation when binding to the reversed-phase and suggest an adsorption rather than a partitioning mode of binding.

The isocratic elution of peptide 202 in the same system was studied at 4 different temperatures. Construction of van't Hoff plots allowed the calculation of the standard enthalpies of association of peptide 202 with the reversed phase. The standard enthalpy of association of peptide 202 at 39% Solvent B was -12 kcal/mol.

The affinity of the peptides for dimyristoyl phosphatidylcholine (DMPC) was determined by monitoring turbidity clearance and by determining fluorescence emission wavelength changes of the tryptophan residues upon binding of the peptides to phospholipid vesicles. The peptides affinities for DMPC could be correlated with their retention on the HPLC systems detailed above and with their number of cationic residues.

Application of this relationship to the total number of synthesised apolipoprotein fragments allows a very accurate division (92% correct) between those fragments which will and those which will not bind to phosphatidylcholines. This relationship also appears to be applicable to peptides which are not apolipoprotein in origin and may also be useful in modelling β-endorphin - opiate receptor interactions.

The hydrophobic effect is discussed in relation to simple systems and to RP-HPLC and phospholipid binding. The conclusion is drawn that the hydrophobic effect is not always entropy driven.

PREFACE

This thesis examines the process of peptide interactions with reversed-phase bonded silicas as a model for the interaction of proteins and peptides with lipids. As such, the work is relevant to the study of lipoproteins (and hence to atherosclerosis), membrane proteins, cell receptor binding and perhaps to protein structure in general since proteins are synthesised in the presence of phospholipids in the endoplasmic reticulum.

The work is set out in three main sections. Section A is an introduction outlining the importance of peptide-lipid and protein-lipid interactions to the functioning of biological systems. It also outlines the aims and philosophy of this work. Section B relates the synthesis and purification of a series of 5 peptides used to model the lipid-protein interactions. Section C discusses the hydrophobic effect, relates an investigation of the binding of a peptide series to the nonpolar surfaces of reversed-phase bonded silica and dimyristoyl phosphatidylcholine and discusses the relationship between these two processes. On the basis of these results a modified theory of protein-phospholipid interactions is proposed.

ACKNOWLEDGEMENTS

The author wishes to acknowledge the following. Drs W.S.Hancock and D.R.K.Harding for their constant support and encouragement throughout this work. The Chemistry, Biochemistry and Biophysics Department of Massey University for the provision of Departmental Demonstratorship. The other members of the peptide synthesis group, Jim Napier, Dick Poll, Shona Spicer, Dave Elgar, Anna Wallace, and Grant Taylor for their support and comradeship. Dr G.Midwinter for numerous amino acid analyses. Jenny Trow for the drawing of most of the figures in Chapter 3. Martin Hender for compiling the program found in section A.3 from a flow chart supplied by the author. Erin Temperton for expert and patient typing of this manuscript. Margaret Knighton for her understanding and patience, and for the many hours spent typing the first draft.

Page

TABLE OF CONTENTS

Abstract ii

Preface iv

Acknowledgements v

Table of Contents vi

Table of Figures xiii

Table of Tables xx

PART A

CHAPTER 1 GENERAL INTRODUCTION

1.1 The Importance of Protein-Lipid Interactions 1

1.1.1 Some General Considerations 1

1.1.2 Serum Albumin 2

1.1.3 Phospholipid Transfer Proteins 2

1.1.4 Membrane Structure 3

1.1.5 Membrane Bound Enzymes 4

1.1.6 Membrane Transport Proteins 4

1.1.7 Cell Receptors 4

1.1.8 Cell Toxins 5

1.1.9 The Insertion of Proteins Into and Across Membranes 5

1.2 Serum Lipoproteins 6

1.3 Lipoprotein Metabolism 12

1.4 Disease States of the Lipoprotein System 14

1.5 The Apolipoproteins 16

1.6 Methods of Investigation 17

Page

1.7 Aim of Thesis 17

1.8 The Design of the Model Apolipoprotein Peptide Series 18

PART B

CHAPTER 2 SOLID-PHASE PEPTIDE SYNTHESIS

2.1 Introduction 22

2.1.1 The Basic Problem. 22

2.1.2 The general Scheme of Solid-Phase Peptide Synthesis. 22

2.1.3 Advantages and Disadvantages of Solid-Phase Peptide Synthesis. 24

2.1.4 Synthesis Modifications. 25

2.2 Experimental

2.2.1 Equipment and Chemicals. 25

2.2.2 Method. (a) Preparation of amino acid resins. 27

(b) The synthesis procedure. 27

CHAPTER 3 PURIFICATION OF PEPTIDES

3.1 Introduction 30

3.2 Equipment and Chemicals 30

3.3 The Purification of Peptide 202 32

3.4 The Purification of Peptide 203 44

3.5 The Purification of Peptide 208 52

Page

3.6 The Purification of Peptide 209 55

3.7 The Purification of Peptide 199 58

3.8 Demonstration of purity 62

3.9 Conclusion 66

PART C

CHAPTER 4 BACKGROUND FOR THE HYDROPHOBIC EFFECT

4.1 Introduction. 67

4.2 The Theory of the Hydrophobic Effect. 69

4.3 Hydrophobic Hydration and Simple Model Systems. 70

4.3.1 The Solubility of Nonpolar Gases in Water. 70

4.3.2 Water-Organic Solvent Partitioning. 71

4.4 Hydrophobic Interactions and More Complex Systems. 72

4.4.1 The Hydrophobic Effect and Reversed-Phase HPLC. 72

4.4.2 Hydrophobic Interactions and Amphiphile Association. 75

4.4.2.1 Micelle Formation. 75

4.4.2.2 Phospholipid - Simple Solute Interactions. 76

4.4.2.3 Phospholipid - Protein and Phospholipid -Peptide Interactions. 78

4.4.2.4 Protein - Protein interactions. 80

4.5 Conclusion. 84

Page

CHAPTER 5 ANALYTICAL REVERSED PHASE HPLC

5.1 Introduction 87

5.1.1 Definitions. 87

5.1.2 Equations. 88

5.1.3 The Controversy Over Mechanisms of Retention. 89

5.1.4 Peptides and Reversed Phase HPLC. 90

5.2 Experimental 91

5.2.1 Equipment and Chemicals. 91

5.2.2 Solvent Systems. 92

5.2.3 Methods. 93

5.2.3.1 Gradient elution of peptides in 1% TEAP. 93

5.2.3.2 Isocratic elution of peptides in 1% TEAP. 94

5.3 Results and Discussion 94

5.3.1 Gradient Elution of Peptides in 1% TEAP. 94

5.3.2 Isocratic Elution of Peptides in 1% TEAP. 98

5.3.3 The Effect of Temperature upon the Retention of Peptide 202. 104

5.3.4 The Gradient Elution of Peptides in 0.1M Ammonium Bicarbonate. 110

5.3.5 The Silanophilic Retention of Peptide 202. 112

5.4 Conclusion 113

CHAPTER 6 PHOSPHATIDYLCHOLINE BINDING

6.1 Introduction 115

6.1.1 The Amphipathic Helix Model. 115

Page

6.1.2 Refinement of the Amphipathic Helix Model. 116

6.1.3 The Influence of Charged Residues on the Association of Phosphatidylcholine With Apolipoproteins and Their Fragments. 117

6.1.3.1 Evidence that Ion-pair Interactions May Not Stabilise Alpha-Helices. 119

6.1.3.2 Evidence for Stabilisation of Negatively Charged Phospholipid-Polypeptide Association Via Electrostatic Interactions. 120

6.1.3.3 The Interaction of Electrolytes With Uncharged Phospholipids (Phosphatidylcholines). 122

6.1.4 Fluidity and Protein-Phospholipid Association. 124

6.1.5 Thermodynamic Considerations. 124

6.1.5.1 The Thermodynamics of Alpha-Helix Formation. 124

6.2 Experimental 128

6.2.1 Fluorescence Measurements 128

6.2.2 Turbidity Clearance Measurements 129

6.2.3 Equipment and Procedures 129

6.3 Results and Discussion 130

6.3.1 Egg Phosphatidylcholine Binding 130

6.3.2 Dimyristoyl Phosphatidylcholine Binding 130

CHAPTER 7 THE CORRELATION BETWEEN PHOSPHOLIPID BINDING AND REVERSED-PHASE HPLC RETENTION

7.1 Introduction. 135

7.1.1 The Similarity Between the Two Processes. 135

Page

7.2 Results and Discussion. 136

7.2.1 The Correlation Between Reversed-Phase HPLC Retention and Phospholipid Binding. 136

7.2.2 The Amphipathic Threshold Model - A Modified Amphipathic Helix Model for Apolipoprotein-Phosphatidylcholine Association. 138

7.2.2.1 The Incorrectly Assigned Peptides. 140

7.2.2.2 The Effectiveness of the Current Phosphatidylcholine Binding Model. 141

7.2.2.3 Explanation of the Cationic Residue Effect. 143

7.2.2.4 Other Possible Explanations of the Cationic Residue Effect. 143

7.2.2.5 The Choice of Hydrophobicity Scale. 145

7.2.2.6 The "Fine-Tuning" of the Amphipathic Threshold Model. 147

7.2.2.7 Implications of the Amphipathic Threshold Model. 148

a) An alternative to the discrete binding site. 148

b) Why a threshold? 150

c) How is the cationic contribution expressed. 150

7.2.3 Application of the Amphipathic Threshold Model to Non-apolipoprotein Peptides. 152

7.3 Conclusion. 158

APPENDIX

A.1 The Effect of Various Guard Columns on the HPLC Separation of Peptide 203 From Contaminating Peptides. 160

A.2 Hydrophobicity Scales. 163

Page

A.3 Computer Program for the calculation of Non-Polar Side Hydrophobiciities of peptides. 165

A.4 Plots of Various Hydrophobicity Parameters v's Retention of Peptide in an Acidic Reversed-Phase HPLC System for the Synthetic Peptide Series. 171

A.5 Purification of Acetonitrile for HPLC. 179

A.6 Abbreviations. 180

A.7 A List of Peptides Plotted in Figures 7-2 and 7-3. 181

REFERENCES 183

Page

LIST OF FIGURES

CHAPTER 1

Figure 1-1 Correspondence of Major Lipoprotein Classes Categorised by Ultracentrifugation and Plasma Electrophoresis. 7

Figure 1-2 The Major Metabolic Routes of Lipoproteins. 12

Figure 1-3 The Relative Positions of Nonpolar Amino Acids in the Sequences of the Apolipoprotein Model Peptides Series. 19

Figure 1-4 The Character of the Nonpolar Sides of the Apolipoprotein in Model Peptide Series Depicted in the Alpha-Helical Conformation. 21

CHAPTER 2

Figure 2-1 The Directions of Synthesis Utilised in the Biosynthesis and Chemical Synthesis of Peptides. 23

Figure 2-1 A Schematic Representation of Peptide Synthesis. 24

CHAPTER 3

Figure 3-1 The Sequence of Chromatographic Techniques and Deprotection Reactions Used in the Purification of Peptide 202. 32

Figure 3-2 The Gel Filtration of Crude Trp(CHO)-Peptide 202 on a 33

Page

G-10 Sephadex Column.

Figure 3-3 The Gel Filtration of Trp(CHO)-Peptide 202 on a G-50 Sephadex Column. facing p. 34

Figure 3-4A The Gel Filtration of Trp(CHO)-Peptide 202 on a G-25 Sephadex Column. 35

Figure 3-4B The Reversed-Phase HPLC Analyses of Fractions Collected from a Gel G-25 Filtration Separation of Trp(CHO)-Peptide 202. 35

Figure 3-5A The Semi-Preparative Reversed-Phase HPLC Purification of Trp(CHO)-Peptide 202 after Gel Filtration Chromatography. 36

Figure 3-5B The Reversed-Phase HPLC Analysis of HPLC Purified Trp(CHO)-Peptide 202. 36

Figure 3-6 A Comparison of the UV Spectra of Trp(CHO)-Peptide 202 and Peptide 202. 38

Figure 3-7 The Ion-Exchange Purification of Peptide 202 on SP-C25 Sephadex. 39

Figure 3-8 The Reversed-Phase HPLC Analysis of Fractions from an Ion-Exchange Purification of Peptide 202. 40

Figure 3-9A The Semi-Preparative Reversed-Phase HPLC Purification of Peptide 202 After an Ion-Exchange Purification. 42

Figure 3-9B The Reversed-Phase HPLC Analysis of HPLC purified Peptide 202. 42

Figure 3-10 The Semi-Preparative Reversed-Phase HPLC Purification of Peptide 202 on a Radial-PAK C18 Column. 44

Figure 3-11 The Sequence of Chromatographic Techniques and Deprotection Reactions Used in the Purification of Peptide 203. 45

Page

Figure 3-12 The Ion-Exchange Purification of Peptide 203 on SP-C25 Sephadex. 47

Figure 3-13 The Ion-Exchange Purification of Peptide 203 on a DEAE Ion-Exchanger. 48

Figure 3-14 The Reversed-Phase HPLC Analysis of Fractions from the DEAE Ion-Exchange Purification of Peptide 203. 50

Figure 3-15

A&B The Semi-Preparative Reversed-Phase HPLC Purification of Peptide 203. 51

Figure 3-15C The Reversed-Phase HPLC Analysis of HPLC Purified Peptide 203. 51

Figure 3-16 The Sequence of Chromatographic Techniques and Deprotection Reactions used in the Purification of Peptide 208. 52

Figure 3-17A The Semi-Preparative Reversed-Phasse HPLC of Peptide 208. 54

Figure 3-17B The Reversed-Phase HPLC Analysis of HPLC Purified Peptide 208.

Figure 3-18 The Sequence of Chromatographic Techniques and Deprotection Reactions used in the Purification of Peptide 209. 55

Figure 3-19A The Semi-Preparative Reversed-Phase HPLC Purification of Peptide 209. 57

Figure 3-19B The reversed-Phase HPLC Analysis of HPLC Purified Peptide 209. 57

Figure 3-20 The Sequence of Chromatographic Techniques and Deprotection Reaction Used in the Purification of Peptide 199. 58

Figure 3-21 The Effect of Increasing the Concentration of Ammonium 60

Page

Formate in Solvent A on the Retention of Trp(CHO)-Peptide 199 in Reversed-Phase HPLC.

Figure 3-22A The Semi-Preparative Reversed-Phase HPLC Purification of Peptide 199. 61

Figure 3-22B The Reversed-Phase HPLC Analysis of HPLC Purified Peptide 199. 61

Figure 3-23 The Reversed-Phase HPLC Analysis of Synthetic Peptides at Neutral pH. 63

Figure 3-24 The Reversed-Phase HPLC Analysis of Synthetic Peptides at Acidic pH. 64

Figure 3-25 The UV Absorbance Spectra of the Purified Peptides. 66

CHAPTER 5

Figure 5-1A Plots of the Total Hydrophobicity of Each Peptide Calculated on the Meek 3 Scale v's Point of Elution of Peptide in an Acidic Reversed-Phase HPLC System. 96

Figure 5-1B Plots of the Total Nonpolar Side Hydrophobicity of Each Peptide Calculated on the Meek 3 Scale v's Point of Elution in an Acidic Reversed-Phase HPLC System. 96

Figure 5-2 The Isocratic Elution of Peptide 208 at Diiferent Concentrations of Organic Solvent. 98

Figure 5-3 Plots of k' v's % Solvent B for the Isocratic Elution of the Synthetic Peptide Series. 99

Figure 5-4 Plots of Ink' v's % Solvent B for the Isocratic Elution of the Synthetic Peptide Series. 100

Figure 5-5 Plots of Ink' v's % Solvent B for the Isocratic Elution 105

Page

of Peptide 202 at Different Temperatures.

Figure 5-6 Plots of Ink' v's 1/T K for the Isocratic Elution of Peptide 202 at Different Concentrations of Organic Solvent. 106

Figure 5-7 Plots of Ink' v's Enthalpy of Association for Isocratic Elution of Peptide 202 at Different Temperatures and Concentrations of Organic Solvent. 107

Figure 5-8 Plot of ΔH° v's ΔS° for the Isocratic Elution of Peptide 202 at Different Concentrations of Organic Solvent. 109

Figure 5-9A Plot of the Total Hyrophobicity of Each Peptide Calculated on the Meek 1 Scale v's Point of Elution of Peptide in a Neutral pH Reversed-Phase HPLC System. 112

Figure 5-9B Plot of the Total Nonpolar Side Hydrophobicity of Each Peptide Calculated on the Meek 1 Scale v's Point of Elution of Peptide in a Neutral pH Reversed-Phase HPLC System. 112

Figure 5-10 Plot of k' v's %Isopropanol for the Retention of Peptide 202 at Neutral pH. 113

CHAPTER 6

Figure 6-1 The Non-Polar Side Hydrophobicity of the Peptide Series Calculated Using the Meek 3 Scale v's the Decrease in Absorbance at 325nm of DMPC Suspensions Upon Introduction of Peptide. 134

Page

CHAPTER 7

Figure 7-1 The Reversed-Phase HPLC Retention of the Peptide Series v's Their Affinity for DMPC. 137

Figure 7-2 The Demonstration of the Amphipathic Threshold Model. 139

Figure 7-3 The Demonstration of the Current Amphipathic Helix Model. 142

Figure 7-4 The Application of the Amphipathic Threshold Model to the Phosphatidylcholine Binding of Non-Apolipoprotein Peptides. 154

Figure 7-5 The Calculated Affinity For Phospholipid v's Rat Brain Opiate Receptor Affinity for Deletion Peptides of Porcine Beta-Endorphin. 157

APPENDIX

Figure A-1 A Comparison of the Efficiency of Separation of Peptide 203 With and Without a Guard Column. 161

Figure A-2 The Effect of Various Guard Columns on the HPLC Separation of Peptide 203 from its Contaminating Peptides. 162

Figure A-3 The Efficiencies of the Various Guard Columns Alone. 162

Figures

A-4 to A-17 Plots of Various Hydrophobicity Parameters v's Retention of Peptide in an Acidic Reversed-Phase HPLC System for Each Hydrophobicity Scale (as listed below).

Figure A-4 Meek 1. 172

Page

Figure A-5 Meek 2. 172

Figure A-6 Meek 3. 173

Figure A-7 Meek 4. 173

Figure A-8 Sasagawa 1. 174

Figure A-9 Sasagawa 2. 174

Figure A-10 Bull & Breese. 175

Figure A-11 Jones. 175

Figure A-12 Rekker. 176

Figure A-13 Manavala. 176

Figure A-14 Pliska 1. 177

Figure A-15 Pliska 2. 177

Figure A-16 Wolfenden. 178

Figure A-17 Kyte & Doolittle. 178

Page

LIST OF TABLES

Table 1-1	Concentration of Major Plasma Lipoproteins in Normal Fasting Humans.	8
Table 1-2	Size and Molecular Weights of the Different Lipoprotein Classes.	9
Table 1-3	Lipid Composition of the Different Lipoprotein Classes.	9
Table 1-4	Protein Composition of the Different Lipoprotein Classes.	10
Table 1-5	Phopholipid Composition of the Different Lipoprotein Classes.	11
Table 1-6	A Description of the Disease States of the Lipoprotein System.	15
Table 1-7	Properties of the Apolipoproteins.	16
Table 2-1	The Synthesis Protocol for the Addition of the Nth Amino Acid.	28
Table 3-1	The Amino Acid Analyses of the Purified Peptides.	65
Table 4-1	The Free Energies of Partitioning Per Methylene Group for n-Alcohols in Aqueous-Phospholipid Systems.	76
Table 4-2	An Estimation of the Free Energy Terms Involved in a Disordered to Native Transition of a 100 Residue Protein.	81
Table 4-3	A Summary of the Thermodynamics of Various Processes Driven by the Hydrophobic Effect.	84
Table 5-1	Positions of Elution from Different Reversed-Phase HPLC Columns with Linear Gradients.	85
Table 5-2	The Calculated Free Energy Difference Between Aqueous-Hydrocarbon Transfers for Leucine and Lysine.	103
Table 5-3	The Variation in the Calculated Value of ΔG° with Different Values of the Phase Ratio.	110

Page

Table 5-4	A Comparison of the Retention of the Peptide Series on a Radial-PAK CN Column with Neutral and Acidic Solvent Systems.	111
Table 6-1	The Frequency of Cationic and Anionic Pairs of Residues at Particular Spacings in the Primary Sequence of a Theoretical Amphipathic Helix.	119
Table 6-2	Enthalpies of Alpha-Helix Formation Found in Different Studies.	126
Table 6-3	Turbidity Changes and Fluorescence Emission Maximum Wavelength Changes on Addition of DMPC to Peptide Solutions.	131
Table 6-4	The Fluorescence of Peptide 209 in Various Buffers.	132
Table 6-5	Intrinsic Fluorescence of Peptides at Different Temperatures.	133
Table 7-1	The Accuracy of Different Phosphatidylcholine-Peptide Association Models in Distinguishing Phosphatidylcholine-Binding Peptides.	147
Table 7-2	A List of Non Apolipoprotein Peptides With Known Phosphatidylcholine Affinity.	153
Table A-1	Details of Different Hydrophobicity Scales.	163
Table A-2	The Hydrophobicities of the Amino Acids Measured by Different Scales.	164
Table A-3	A List of Peptides Plotted in Figures 7-2 and 7-3.	181

PART A

CHAPTER 1 GENERAL INTRODUCTION

1.1 The Importance of Protein-Lipid Interactions

Protein-lipid interactions are essential to many biological functions, however, despite vast resources which have been dedicated to this area we have only an elementary knowledge of the mechanisms of such interactions. There can be no doubt that the study of protein-lipid interactions is one of the most important frontiers of biochemistry for without a firm understanding of these interactions we are powerless to describe the full nature of the structures and processes of biological systems. The author hopes to convey in the remainder of this section the importance and diversity of protein-lipid interactions.

1.1.1 Some General Considerations

The study of the structure of lipid-protein complexes has been severely hampered by a lack of X-ray crystallographic data due to the extreme difficulty of obtaining crystalline complexes. However, from the one high resolution structure which has been obtained (bacteriochlorophyll-containing protein), Mathews has drawn some valuable conclusions about the structure of lipid-protein complexes which is neatly summed up as follows: "...the final structure of a lipid-protein complex need not be dominated by lipid-lipid interactions, nor by lipid-protein interactions. Since protein structures are relatively rigid (at least compared to lipids in a bilayer), the protein will be less able to modify its structure to accommodate the lipid than the lipid is free to adjust its structure to conform to that of the protein. Therefore while the protein structure may be dominant in determining the structure of the overall complex, the lipids will contribute to the overall stability of the complex not only through their favourable interactions with the protein, but also by favourable interactions among themselves. The interactions between the lipid tails are of the type hydrocarbon-hydrocarbon and the lipid tail-protein interactions are also hydrocarbon-hydrocarbon. Obviously the energetics are similar whether the lipid is surrounded by protein or by other lipid, just as long as the lipid environment is not polar." (1). Thus Mathews touches upon the importance of the hydrophobic effect in stabilising lipid-protein complexes.

1.1.2 Serum Albumin

Albumin is the most abundant protein in human plasma. It has the interesting property of being able to bind hydrophobic ligands such as fatty acids, lysolecithin, bilirubin, tryptophan, steroids, thyroxine, drugs and dyes (2). Consideration of the amino acid sequence, the disulphide bridges, the high content of alpha-helix, the location of Pro residues and the necessity to enclose hydrophobic faces has led to the proposal of a 3 dimensional structure for serum albumin. This structure is comprised of 3 largely independent hydrophobic ligand binding regions (domains) each of which is composed of 6 antiparallel α-helical sections arranged in a hexagonal pattern which enclose a hydrophobic channel in which hydrophobic ligands could be accommodated (2). Such a model is consistent with the restricted mobility of the bound fatty acid hydrocarbon chain found by spin label studies (2).

1.1.3 Phospholipid Transfer Proteins

According to a recent review (3), intracellular phospholipid transfer proteins are extensively found in the tissues of mammals and have also been found to occur in plants, yeast and a facultatively photosynthetic bacterium. Although the function of these soluble proteins is uncertain it is believed that they contribute to the metabolism of phospholipids by transfer of specific classes of phospholipid from their site of synthesis, the endoplasmic reticulum, to membranous locations which have a deficit of this class of phospholipid because of growth or metabolism. In doing this it is thought that these proteins maintain membranes in a steady state with respect to their phospholipid content. Distinct proteins exist for the transfer of different phospholipid classes. One such protein the phosphatidylcholine transfer protein from bovine liver has been extensively characterised and the hydrophobic residues with which the acyl chains of the phospholipid interact have been determined. This protein can transfer one phosphatidyl-choline molecule at a time and must relinquish it upon subsequent binding to a phospholipid bilayer. The binding of phosphatidylcholine transfer protein to phospholipid bilayers is increased with an increase in the phosphatidic acid or phosphatidyl serine content of the bilayers. As structures of these proteins become available much insight into lipid-protein interactions will be gained.

Phospholipid transfer proteins have also been found in human plasma where they are proposed to have an important role in distributing phospholipids between the various lipoprotein complexes and extracellular surfaces (4).

1.1.4 Membrane Structure

Membranes are fundamental to the existence of biological systems since they form a physical barrier to the dispersion of cell and organelle contents and also allow the passage of substances into and out of cells and organelles to be regulated. Proteins are an integral part of this barrier. The amount of protein in different membranes varies greatly being 76% and 22% of the total dry weight of inner mitochondrial membrane and bovine myelin membrane respectively (5). Membrane proteins may be categorised by their depth of penetration into the bilayer matrix. Intrinsic proteins are embedded in the bilayer and destruction of the membrane is required for their isolation while extrinsic proteins lie outside the bilayer and may be separated without destroying the membrane. The extrinsic proteins spectrin and actin compose a network just inside the plasma membrane of erythrocytes (6). This network forms a cytoskeleton which is considered important in controlling the deformability of the cell and its shape. The association of other membrane proteins with this network is unclear. Some intrinsic membrane proteins appear to have a purely structural role in the membrane e.g. structural protein of inner mitochondrial membrane (7) and basic protein of myelin (8). Another type of intrinsic membrane protein, the glycoproteins, apparently function to anchor their carbohydrate moiety to the membrane and thus identify the cell to the immune-system. An example of this type of protein is glycophorin from erythrocytes (9).

The intrinsic membrane proteins are more hydrophobic (at least in certain domains) than are soluble proteins, however, both hydrophobic interactions and polar interactions are likely to be important in determining the association and orientation of these proteins within the membrane (10). The function of the many intrinsic membrane proteins are diverse and essential. Each specialised cell and organelle possesses specialised membrane bound proteins essential to the function of the organelle and cell. Some of these proteins are discussed separately below to emphasise the importance of lipid-protein interactions to the life process.

1.1.5 Membrane Bound Enzymes

A large number of membrane bound enzymes require the lipid phase to function properly. The protein-lipid complexes of the mitochondrial electron transport chain, mitochondrial ATPases and photosynthetic reaction centres are examples of these (11). A well characterised example of an enzyme not requiring the lipid phase for activity is cytochrome b5, an NAD linked reductase from liver mitochondria. This enzyme is composed of a large enzymatically active region which is soluble in aqueous solution and a hydrophobic membrane binding region (12). The membrane binding region penetrates to the middle of the bilayer then loops back (so that its amino and carboxyl termini are on the same side of the bilayer) and is believed to be highly structured (13).

1.1.6 Membrane Transport Proteins

The maintenance of a high concentration of potassium ions and low concentration of sodium ions inside cells is essential to the function of many cell processes. The concentration gradient is maintained by a so called sodium-potassium pump, an integral protein of the cell membrane which actively transfers potassium into the cell and sodium out of the cell at the expense of ATP. It has been estimated that half of the ATP utilisation in resting muscles and a higher fraction of that in the nerve cells is due to the maintenance of this gradient (14). Negatively charged phospholipids appear to be essential for the activity of this membrane bound enzyme (15). Phospholipid is also essential for the activity of calcium-magnesium ATPase, an enzyme responsible for the transfer of calcium across the plasma membrane (15).

1.1.7 Cell Receptors

Many hormones appear not to enter cells but to bind to specific protein receptors of cell membranes. These receptors require the lipid of the membrane for functionality and correct topological arrangement (16). The mechanism of action of twenty different hormones involves the activation of adenylate cyclase, a membrane bound enzyme found on the cytoplasmic side of the cell membrane, which catalyses the formation of cyclic AMP. It is not known how the binding of the hormone to its specific cell receptor affects the activation of this enzyme however it is likely that the receptor extends through the membrane (17). Phospho-lipid-peptide interactions have been implicated in the binding of the

peptide hormones adrenocorticotropin, glucagon and beta-endorphin to their respective cell receptors (16,18,19).

1.1.8 Cell Toxins

The disease cholera is characterised by a massive loss of body fluid through the intestinal epithelium. It is caused by a protein, cholera toxin, produced by Vibrio cholerae bacteria. The protein is composed of 2 subunits one of which is responsible for the binding of the protein to the lipids on the outside of the epithelial plasma membrane while the other subunit penetrates the membrane and activates adenylate cyclase (20). This activation causes the clinical characteristics of the disease. Lipid-protein interactions are also important in the mechanism of action of various other cell toxins notably melittin (21,22). Phospholipase A-2 from snake and spider venoms have been shown to bind to phospholipid micelles via an interfacial binding site whereupon its catalytic rate increases dramatically (23). In addition the lysis or phagocytosis of foreign cells in a mammalian host is mediated by the protein-membrane interactions of complement factors and the foreign cell membrane (31).

1.1.9 The Insertion of Proteins Into and Across Membranes

Many proteins are synthesised with a hydrophobic leader peptide which is subsequently cleaved enzymatically e.g. preproinsulin contains a 24 amino acid leader peptide (24). These leader peptides are involved in the transport of the protein across the endoplasmic reticulum membrane. A theory has been advanced which accounts for the spontaneous transfer of proteins across membranes and the anchorage of other proteins to the membrane by the formation of a "helical hairpin" which is inserted at right-angles to the bilayer (25). According to the theory the polarity of the helices dictates whether or not the protein is spontaneously exuded through the membrane and how the protein is lodged in the membrane.

1.2 Serum Lipoproteins

The serum lipoproteins are, perhaps, the most extensively characterised protein-lipid system. Because so much is known about plasma lipoproteins and because the findings of this thesis are most directly

applicable to this system, the plasma lipoproteins are discussed separately in the following sections.

Serum Lipoproteins are the major vehicle for lipid transport in vertebrates and have also been found in crustaceans and insects (26). Within the different species of the animal kingdom there is a large diversity in the constitution of serum lipoproteins, the amounts of each lipoprotein class and the metabolism of lipids. It is interesting to note that analogous proteins to human apolipoproteins A-I and B are widely distributed in the HDL and LDL, respectively, of vertebrate lipoproteins (26).

Although much is known about the clinical aspects of apolipoproteins, many of the underlying aspects of metabolism and structure are poorly understood. For example: why are certain proteins lost and others collected by lipoproteins in certain stages of their metabolism? Is the major function of the apolipoproteins structural, receptor recognition or enzyme activation? What is the mechanism for the development of atherosclerosis and how is this mechanism related to the lipoprotein system at the molecular level? If the full answers to these questions are to be found, we must understand protein-lipid interactions to a much higher degree of finesse.

The remainder of this introduction is concerned only with human serum lipoproteins (referred to simply as lipoproteins) since a detailed discussion of the animal lipoproteins is beyond the scope of this work.

Lipoproteins have been categorised into 4 major types based on their different electrophoretic mobilities and their different densities as shown in figure 1-1. The different classes are usually referred to in terms of their density i.e. as high density lipoprotein (HDL), low density lipoprotein (LDL), very low density lipoprotein (VLDL) and chylomicrons.

In addition subclasses of HDL have been found which differ slightly in density (HDL_2 and HDL_3). The intermediate density lipoproteins (IDL) are derived from VLDL but their concentration does not build up in the plasma since they are rapidly taken up by the liver or further metabolised to LDL by the action of lipoprotein lipase.

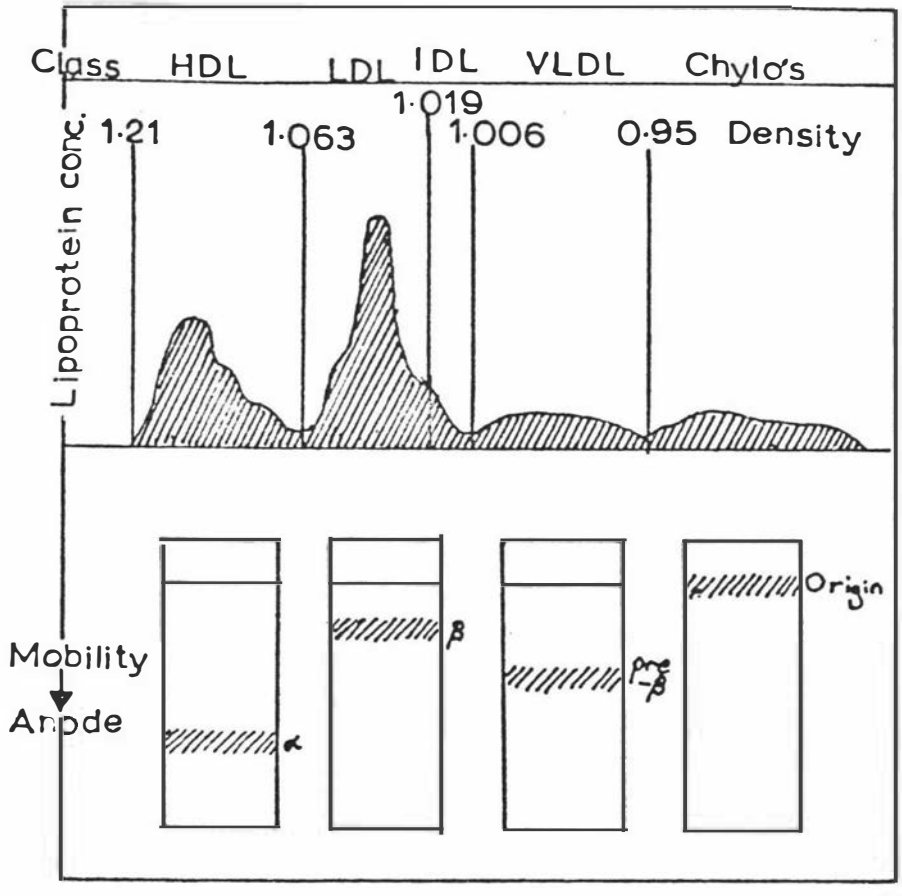

Figure 1-1 Correspondence of Major Lipoprotein Classes Categorised by Ultracentrifugation and Plasma Electrophoresis: The upper diagram shows the ultracentrifugation schlieren pattern for whole plasma while the lower diagram shows the electrophoretic mobility of each of the major density classes, from reference (27).

Even when we limit our consideration of lipoprotein concentrations to one species (i.e. humans) we find a large variation in the individual lipoprotein levels. In particular a significant difference exists between concentrations of lipoproteins in men and women. The concentration of lipoproteins in fasting subjects is shown in Table 1-1.

Table 1-1 Concentrations of Major Plasma Lipoproteins in Normal Fasting Humans

	Males		Females	
Class	μM	mol %	μM	mol %
VLDL	0.1	0.7	0.04	0.2
IDL	0.04	0.3	0.03	0.1
LDL	1.6	10	1.3	6
HDL_2	1.5	9	4.8	23
HDL_3	12.7	80	15.1	71
chylo's[a]	-	-	-	-

a) chylomicrons are introduced into the bloodstream after a fatty meal but are quickly cleared from the blood, chylo's = chylomicrons.
--- from reference (28), Table 2.

As can be seen from the table HDL_3 is the most abundant lipoprotein on a molar basis. The lower incidence of atherosclerosis in pre-menopausal women compared to men has been attributed to their higher levels of HDL (29). The ratio of the concentrations of LDL to HDL is considered to be an important determinant in the development of atherosclerosis (30). The normal concentrations of lipoproteins are greatly changed in many diseases of the lipoprotein system as discussed in section 1.4.

The lipoprotein particles of each lipoprotein class differ in aspects other than density and electrophoretic mobility. There are large differences in the size and molecular weight of the particles as shown in Table 1-2.

Table 1-2 Size and Molecular Weights of the Different Lipoprotein Classes

Class[a]	Density (g/ml)	Molecular Weight (D)	Particle Diameter (nm)
chylo's	<0.93	>400,000,000	75-1200
VLDL	0.93-1.006	10-20,000,000	30-80
IDL	1.006-1.019	5-10,000,000	25-35
LDL	1.019-1.063	2,300,000	18-25
HDL_2	1.063-1.125	360,000	9-12
HDL_3	1.125-1.210	175,000	5-9

(a) chylo's = chylomicrons, from reference (28), Table 1.

Furthermore, the lipid and protein composition of the lipoprotein classes differ markedly, as is shown in Tables 1-3 and 1-4 respectively. It is these differences which most ably demonstrate the complex nature of this lipid transport system.

Table 1-3 Lipid Composition of the Different Lipoprotein Classes[a,b]

Class[c]	Total lipid (%)	Phospho-lipids (%)	Esterified cholesterol (%)	Unesterified cholesterol (%)	Tri-glycerides (%)
chylo's	97-99	7-9	3-5	1-3	<u>84-89</u>
VLDL	90-95	15-20	10-15	5-10	<u>50-65</u>
IDL	80-85	22	22	8	<u>30</u>
LDL	75-80	15-20	<u>35-40</u>	7-10	7-10
HDL_2	55	<u>35</u>	12	4	5
HDL_3	50	<u>20-25</u>	12	3-4	3

a) The predominant lipid class in each lipoprotein class is underlined.

b) By weight of dry lipoprotein, the balance of material is protein. Data from reference (27), Table 3-9.

c) chylo's = chylomicrons.

Table 1-4 Protein Composition of the Different Lipoprotein Classes [ab]

	Chylo's	VLDL	IDL	LDL	HDL_2	HDL_3
ApoA-I	0-3	0-3	0	trace	85	70-75
ApoA-II	0-1.5	0-0.5	0	trace	5	20
ApoD	1	0	-	-	0	1-2
ApoB	10-22	40-50	50-60	95-100	0-2	0
ApoC-I	5-10	5	<1	0-5	1-2	1-2
ApoC-II	15	10	2.5	0.5	1	1
ApoC-III	40	20-25	17	0-5	2-3	2-3
ApoE	5	5-10	15-20	0	3-5	trace

a) The predominant protein in each lipoprotein class is underlined.

b) % by weight of dry delipidated lipoprotein. From reference (27), Table 3-10.

The protein components of the lipoproteins are particularly important since the metabolic fate of the particle depends upon its constituent proteins.

Current models of apolipoprotein-lipid complex formation involve protein, cholesterol and phospholipids at the surface of the lipoprotein particle while triglycerides and cholesterol esters form a nonpolar core (32). It is therefore of interest to investigate the types of phospholipid with which the protein is associated. An analysis of the composition of the phospholipid in the lipoprotein classes is found in Table 1-5. As can be seen phosphatidylcholine is the predominant phospholipid in all lipoprotein classes. For this reason most studies involving model lipoprotein formation have involved complex formation between phosphatidylcholines and apolipoproteins or their fragements (32-34).

Table 1-5 Phospholipid Composition of the Different Lipoprotein Classes

Class	% of Total Phospholipids [a]					
	PC	SP	Lyso PC	PE	PI	PS
chylo's	78.5	11.7	4.2	5.6	-	-
VLDL	59.7	14.8	5.0	4.6	3.6	1.5
LDL	63.7	25.9	2.7	2.2	1.6	0.8
HDL_2	73.8	14.5	2.0	3.3	2.4	0.9
HDL_3	77.1	9.2	4.0	2.5	2.4	0.6

a) PC = phosphatidylcholine, SP = sphingomyelin
Lyso PC = lysolecithin, PE = phosphatidylethanolamine,
PI = phosphatidylinositol, PS = phosphatidylserine.
Data from reference (34), Table 1B.

The complexity of this lipoprotein system is evident in the variability of the composition of the lipoprotein classes, as shown throughout this section. At this point some discussion of the current theories of lipoprotein metabolism may be informative.

1.3 Lipoprotein Metabolism

The major routes of lipoprotein metabolism as perceived at present are depicted in figure 1-2.

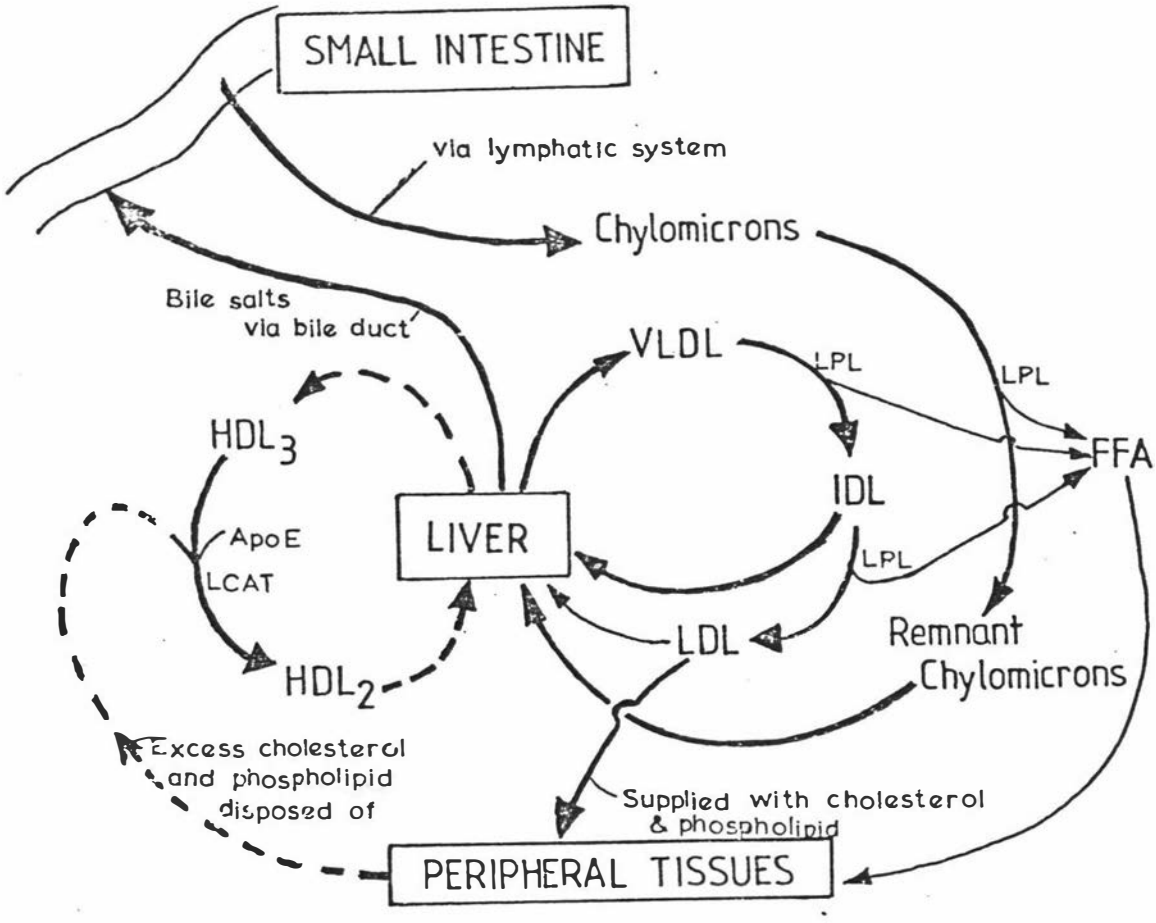

Figure 1-2 The Major Metabolic Routes of Lipoproteins. FFA = Free fatty acids, LPL = lipoprotein lipase, LCAT = lecithin cholesterol acyl transferase. Dashed arrows denote uncertain pathways. The loss of apoliproteins during metabolism of VLDL and the action of various transfer proteins have been omitted from this diagram in the interest of simplicity. Based on information from references (35,36).

Recent in vitro studies have shown that macrophages take up modified LDL (i.e. LDL which has been reacted with reagents to chemically modify its lysine or arginine side chain groups and render them uncharged) and hence become loaded with cholesterol esters (37). Furthermore the cholesterol ester loaded macrophages will release free cholesterol and ApoE independently, provided that a sink for the cholesterol is present (e.g. HDL) (36). This is an extremely interesting discovery since macrophages loaded with cholesterol esters are known to form foam cells which are apparently active in formation of atherosclerotic plaque (38). The damage of LDL by chemical modification of the ApoB moiety (which stops LDL uptake by cell receptors thus stagnating the damaged LDL pool until uptake by the macrophage which recognises the damaged protein) has been related to the epidemiological atherosclerotic risk factors of smoking, diabetes and alcoholism (39). This damage might be respectively caused by Schiff base formation of the aldehyde moieties from cigarette smoke (40), glucose (41) and acetaldehyde (42) with the lysine residues of ApoB.

High affinity receptor mediated uptake of lipoproteins by the liver and other tissues is an extremely important facet of lipoprotein metabolism. It has been demonstrated that native ApoB and ApoE are essential for recognition by the receptors (43). The structure and chemistry of ApoB is not well defined at present due to the difficulty of solubilising this apolipoprotein. A recent breakthrough involving the blocking of active sulphydryl groups (cysteine) has resulted in soluble ApoB and therefore rapid progress in the structure and chemistry of ApoB is foreseen (44). ApoE is more readily studied and hence the complete sequence of ApoE is available (45). Furthermore, the region of ApoE involved in binding to the receptors has been identified as a very dense region of cationic residues (48). The chemical modification of some of the arginine or lysine residues of ApoE results in a protein with no affinity for the receptors (47). ApoE will not bind to high affinity cell receptors when delipidated. The addition of phospholipid restores the binding affinity thus demonstrating that phospholipids are essential to the correct orientation or structure of the ApoE protein (46).

At this point it is interesting to investigate the various clinically observed disease states of the lipoprotein system since this will further

confirm the importance of the protein components in the metabolism of lipoproteins.

1.4 Disease States of the Lipoprotein System

The clinical features of the various disease states can be broadly categorised into two classes: those when the concentration of a lipoprotein class is greatly increased (hyperlipoproteinemias) and those when the concentration of a lipoprotein class is greatly lowered (hypolipoproteinemias). A brief description of the various identified disease states is found in Table 1-6. It is notable that the causes of the disease states so far found have all involved the deficiency of a particular apolipoprotein or receptor or a deficiency of the activity of the enzymes lipoprotein lipase or LCAT. This is indicative of the importance of the protein components of this system. It is also notable that no hyperlipoproteinemia characterised by elevated levels of HDL is known. A current diagnostic method for identifying 'at risk' patients involves the ratio of HDL to LDL. This diagnostic method can be explained if the role of HDL is to transport excess cholesterol back to the liver and the role of LDL is to supply cholesterol to the peripheral tissues (35,49). Thus the delicate balance of cholesterol metabolism is seen as a deciding factor in the progression of atherosclerosis with an imbalance resulting in deposition of cholesterol in "fatty streaks" or atherosclerotic plaque in the arteries of the individual.

Table 1-6 A description of the Disease States of the Lipoprotein System

Name of Disease	Incidence	Clinical Observations	Probable Cause
Hyperlipo-proteinemias[a]:		increased concentration of:	
Type I	Rare	chylomicrons	Deficiency in lipoprotein lipase
Type II[b]	-	LDL or LDL+VLDL incr fat in blood	Deficiency of LDL receptors (peripheral cells)
Type III[b]	Rare	abnormal lipoprotein = floating β - lipoprotein	ApoE-III deficiency (50)
Type IV[b]	-	VLDL	unknown
Type V	Rare	VLDL + chylomicrons Abnormal lipoprotein-X	unknown
Hypolipo-proteinemias:		lowered concentration of:	
A-beta-lipo-proteinemia	-	chylomicrons, LDL and VLDL	No synthesis of ApoB
Tangiers[b] disease	Rare	HDL (1.5%), Plasma cholesterol and phospholipids. Also build up of cholest-erol in lymph system	Lack of peptidase for $ApoA\text{-}I_2 \rightarrow ApoA\text{-}I_4$ (51)
LCAT deficiency	-	HDL + VLDL (increased lipoprotein-X)	LCAT deficiency

a) The hyperlipoproteinemias are numbered according to the increasing electrophoretic mobility of the increased species.

b) Disease associated with an increased risk of atherosclerosis. Data from reference (27).

1.5 The Apolipoproteins

The apolipoproteins are extremely important components of the lipoproteins. Firstly they are apparently important for stabilising the structure of lipoprotein particles. Several theories of lipoprotein structure have been proposed. The common feature of most of these theories is an outer coating of phospholipid and apolipoproteins approximately one molecule thick with an internal core of more hydrophobic lipids (32). Secondly the protein components determine the metabolic fate of the lipoprotein particle by activating the enzymes LCAT (ApoA-I and ApoC-I) and Lipoprotein Lipase (ApoC-II) at the surface of HDL and VLDL particles respectively and by attaching the particles to cell receptors ready for subsequent endocytosis (ApoB and ApoE).

Most of the apolipoproteins have been intensively studied and some of their properties are listed in Table 1-7.

Table 1-7 Properties of the Apolipoproteins

Apolipoprotein	Molecular Wgt	Amino Acids	Calculated α-helix Content	
			lipid-free	+ lipid
ApoA-I[c]	28,300	243	55%	70%
Apo-II	17,380	2x77[a]	35%	40%
ApoB[d]	8,000-300,000	-	-	25%
ApoC-I[c]	6,600	57	56%	73%
ApoC-II[b]	8,800	78	23%	-
ApoC-III	8,700	79	22%	54%
ApoD	20,000	-	-	-
ApoE[d]	33,000	-	66%?	-

a) ApoA-II is a dimer of a 77 amino acid peptide.

b) Activates lipoprotein lipase.

c) Activates LCAT (lecithin cholesterol acyltransferase).

d) Important in cell surface receptor recognition.

From references (27,32).

It is notable that almost all of the apolipoproteins exhibit an increase in α-helical conformation upon binding to phospholipids. This information has led to the amphipathic helix theory for apolipoprotein-phospholipid association, see section 6.1.1. A more in-depth discussion of the phospholipid-protein interactions which occur in lipoproteins can be seen in section 6.1. Suffice it to say at present that these non-covalent interactions are extremely important to the correctly functioning lipoprotein system.

1.6 Methods of Investigation

Because lipoproteins are so complex, approaches to their study have been designed to minimise the large number of variables found in the natural systems. One method frequently used in the study of apolipoprotein-phospholipid association is the examination of the interaction of an isolated apolipoprotein with a single phospholipid. This can be done with spectroscopy (NMR, ESR with spin labels, CD, fluorescence measurements, turbidity clearance), calorimetry (DSC and microcalorimetry), stoichiometry of the isolated products, kinetic studies of the association reaction and X-ray techniques. A wide range of such measurements have been made and the reader is referred to references (32), (34) and (52) for reviews of this topic.

Another approach to finding out more about apolipoprotein-phospholipid interactions has involved the synthesis of series of peptides corresponding to sections of the apolipoproteins. The study of the phospholipid binding characteristics of these peptides has revealed much about the mechanisms of apolipoprotein-phospholipid interactions (33,54). A similar approach has been utilised in this thesis as can be seen in the following sections.

1.7 Aim of Thesis

The aim of this thesis is to test the hypothesis that the interaction of potentially amphipathic helical peptides with a reversed-phase high performance liquid chromatography packing is in some way related to the peptides' ability to bind to phospholipid. Inherent in this aim is a concomitant examination of the accuracy of the amphipathic helix model in describing peptide-phospholipid association. The hypothesis is

tested through the synthesis and purification of a series of 5 model apolipoprotein peptides and the subsequent study of their reversed-phase* and phospholipid binding properties. The series of peptides used is designed to be similar in length, amino acid content and compatibility with the amphipathic helix model. However, each peptide possesses subtle changes to the character of its nonpolar side when in an α-helical conformation. A full explanation of the design of the peptide series actually used is found in the following section.

1.8 The Design of the Model Apolipoprotein Peptide Series

The design of the peptide series is based upon the sequence of a model apolipoprotein peptide named LAP-20 (55,56) which is known to bind strongly to phospholipid, and the sequence of ApoA-I (225-243)** which includes a presumed "lipid binding region" of ApoA-I, ApoA-I (225-232) (57). The series of peptides were chosen to link these two sequences so that the position and number of nonpolar amino acids changed subtly throughout the series. The sequences of the peptide series and the relative positions of their nonpolar residues can be seen in figure 1-3. Peptide 209, of the series not shown in figure 1-3, is identical to peptide 202 except that Lys_6 and Leu_{12} have been interchanged. Each of the peptides has a Trp residue to enable fluorescence wavelength shift measurements upon binding of the peptides to phospholipids.

There are some difficulties involved in designing such a series. The 2 peptides at opposite ends of the series are of different length and contain different amino acids in all polarity classes. Furthermore, the series was designed to enable the testing of LCAT activation caused by a proposed LCAT activating sequence (59) when bonded to each of these peptides. This involved the shortening of the sequences at their amino terminals relative to LAP-20. Such a shortening brings the nonpolar sides of the proposed LCAT activating sequence and the peptide series into line when they are bonded together. The Arg-Ala sequence at the amino terminal of peptide 199 represents the first 2 amino acids of the carboxyl terminal of the proposed LCAT activating sequence. No attempt

* For a definition of reversed-phase see section 5.1.1.

** A peptide enclosing this region, ApoA-I (220-245), has been shown to also bind to phospholipid (58).

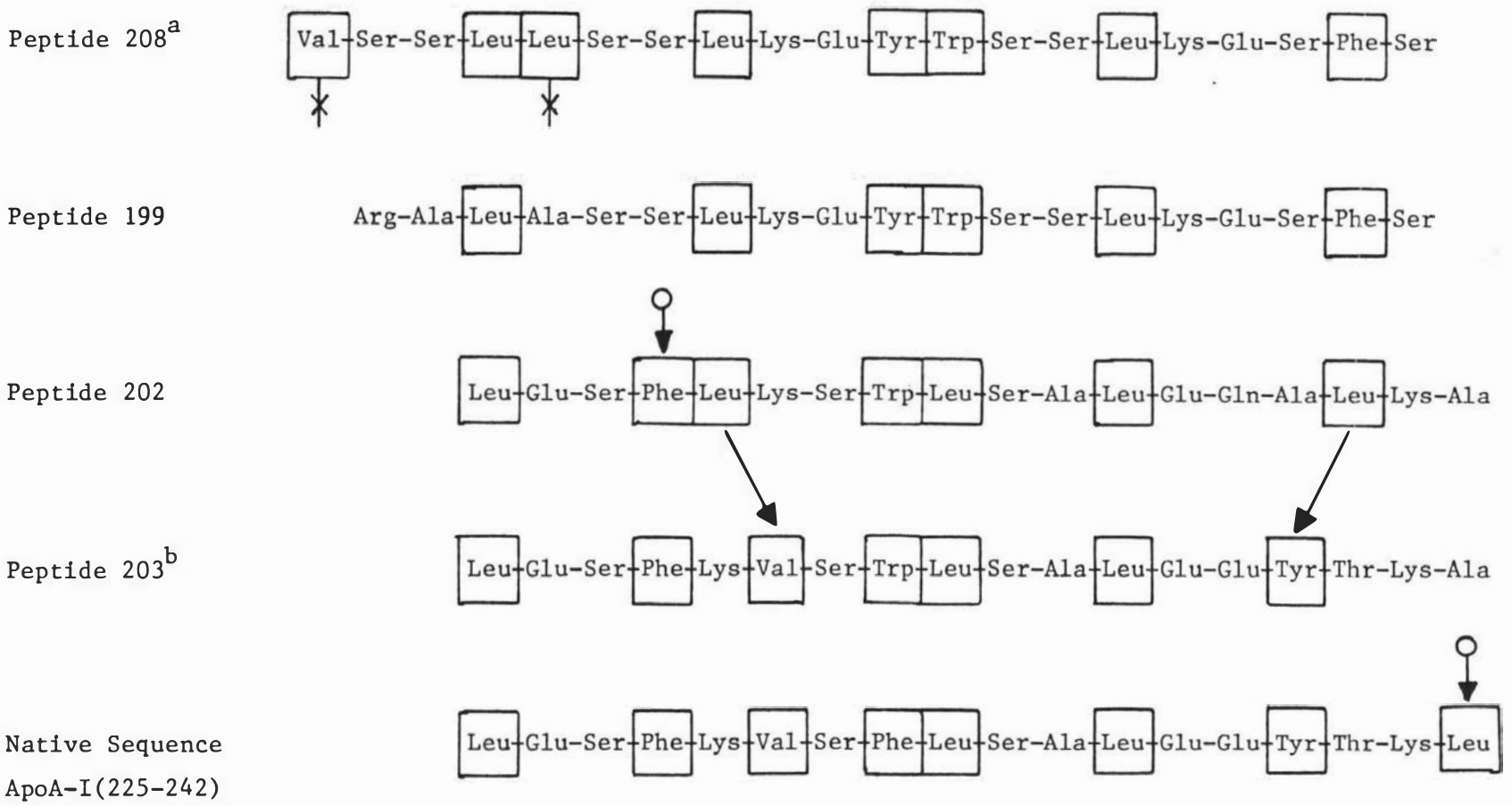

Figure 1-3 The Relative Positions of Nonpolar Amino Acids in the Sequences of the Apolipoprotein Model Peptide Series. Nonpolar amino acids are shown enclosed by boxes. The symbols ⚲, ↘ and ✳ denote the inclusion, transfer and substitution or omission respectively of a nonpolar amino acid at that position compared to the next peptide in the sequence.

a) Peptide 208 has been synthesised by others and was named LAP-20 in these studies (55,56).

b) Peptide 203 is Trp^{232}, Ala^{242} - ApoA-I (225-242).

to test the different LCAT activating properties of these peptides was made in this study. Some other aspects of the series need discussion. The carboxy terminal Leu of the native sequence is not included in the sequence of peptide 203 because of conflicting reports. The amino acid in this position has been identified as Leu 242 by Baker et al. (57) and as Lys 241 by Brewer et al. (60). The differences between the polar and intermediately polar amino acids in the sequences of LAP-20 and the native peptide are largely changed in the peptide 199 to peptide 202 transition.

A pictorial representation of the character of the nonpolar sides of the peptide series drawn in the α-helix formation* is shown in figure 1-4. This clearly shows the compact nature of the hydrophobic sides of peptides 208 and 202 compared to the more disperse hydrophobic sides of peptides 209 and 203.

* The α-helix conformations are depicted in an opened-out form of an α-helix net (61).

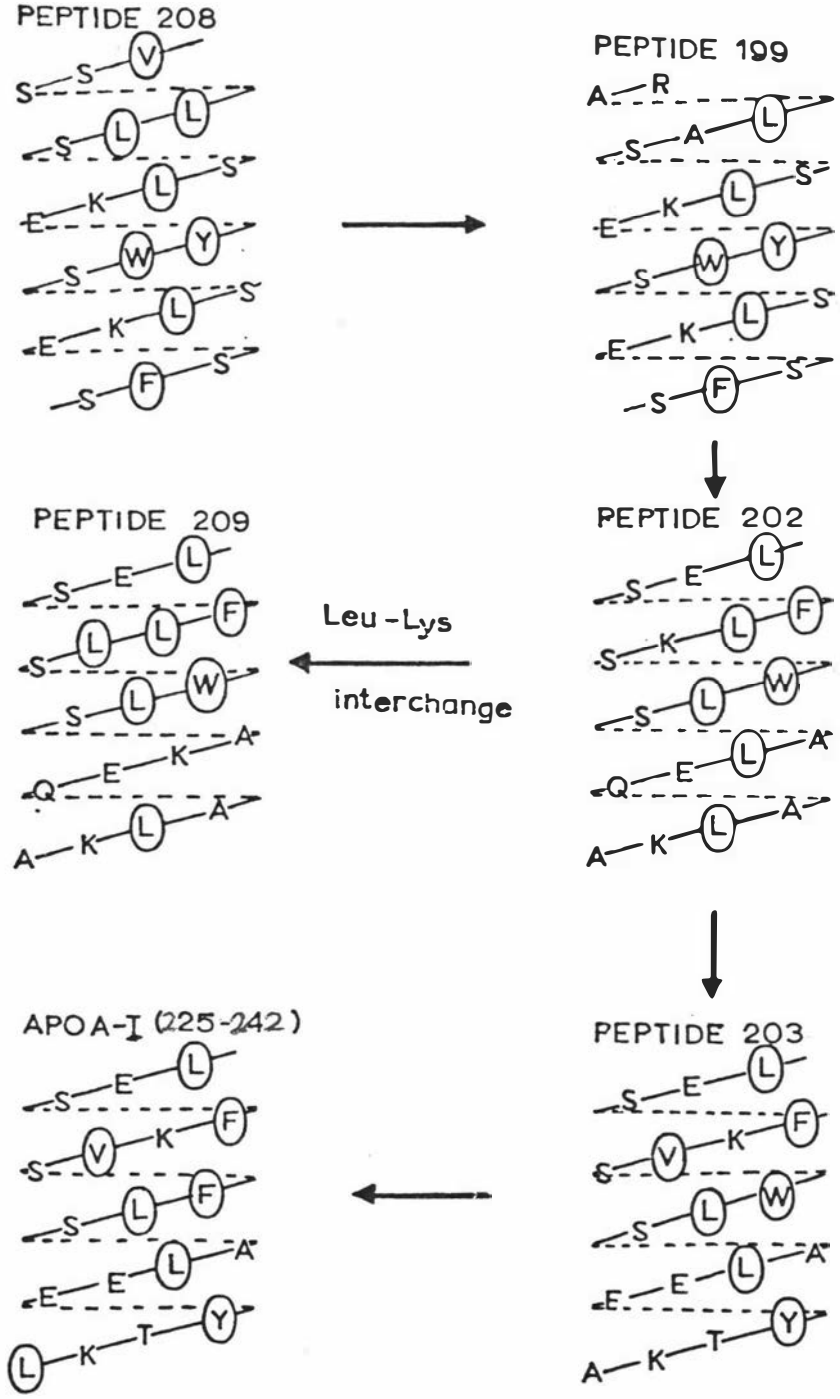

Figure 1-4 The Character of the Non-polar Sides of the Apolipoprotein Model Peptide Series Depicted in the α-Helical Conformation. The amino acids are represented in the one letter code: A = Ala, E = Glu, F = Phe, K = Lys, L = Leu, Q = Gln, R = Arg, S = Ser, T = Thr, V = Val, W = Trp, and Y = Tyr.

PART B

Part B of this thesis consists of the synthesis of the series of peptides by solid-phase peptide synthesis (Chapter 2) followed by their purification by conventional chromatography and semi-preparative reversed-phase HPLC (Chapter 3).

CHAPTER 2 SOLID-PHASE PEPTIDE SYNTHESIS

2.1 Introduction

2.1.1 The Basic Problem

There is one basic problem in peptide synthesis. This is to achieve the correct order of amino acids in the synthesised product while retaining the optical integrity of each amino acid. Of course, this cannot be accomplished by adding unblocked amino acids to each other under conditions where peptide bonds will form since by this approach little control could be exercised over the number and order of amino acids in the product. To overcome this problem the synthesis must be performed sequentially with each coupling being completely unambiguous, i.e. only one free amino group and one activated carboxyl group must be present.

The formation of the peptide bond is in itself a simple dehydration as shown in reaction 2-1.

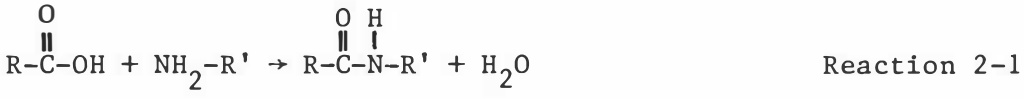

Reaction 2-1

The simplicity of this reaction belies a fundamental problem of peptide synthesis. This is the requirement for very high yields of coupling without side reactions occurring. Thus extremely efficient methods of activating the carbonyl group must be used which are also unreactive to the peptide bond and to any side-chain functional groups.

2.1.2 The General Scheme of Solid Phase Peptide Synthesis

Usually peptides are chemically synthesised from the carboxyl terminal amino acid to the amino terminal amino acid. This is opposite to the direction of synthesis utilised by the ribosome in the biosynthesis of protein, figure 2-1. The main reason that the peptide chemist does

not synthesise peptides in the "natural" direction is that high levels of racemised amino acids accumulate in the peptide. This racemisation, which occurs via oxazolone formation, is almost completely halted when urethane protected amino acids are used to build the peptide from the carboxyl terminal end (63).

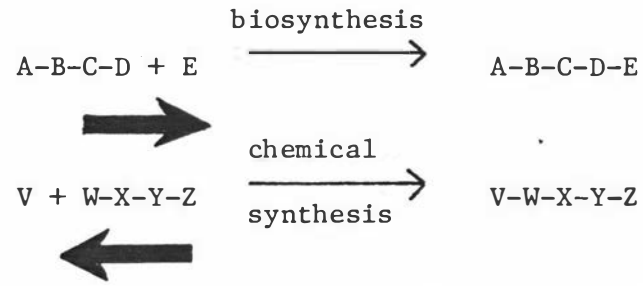

Figure 2.1 The Directions of Synthesis Utilised in the Biosynthesis and Chemical Synthesis of Peptides. The amino terminal is on the left and the carboxy terminal is on the right of the peptide. Each letter represents an amino acid residue. The large arrows indicate direction of synthesis.

To achieve the result of an unambiguous synthesis, the peptide must be assembled peptide bond by peptide bond. This can be accomplished as shown in figure 2-2, provided that any reactive side-chain groups are efficiently blocked throughout the synthesis. A more complete discussion of peptide synthesis can be found in other sources (64,65).

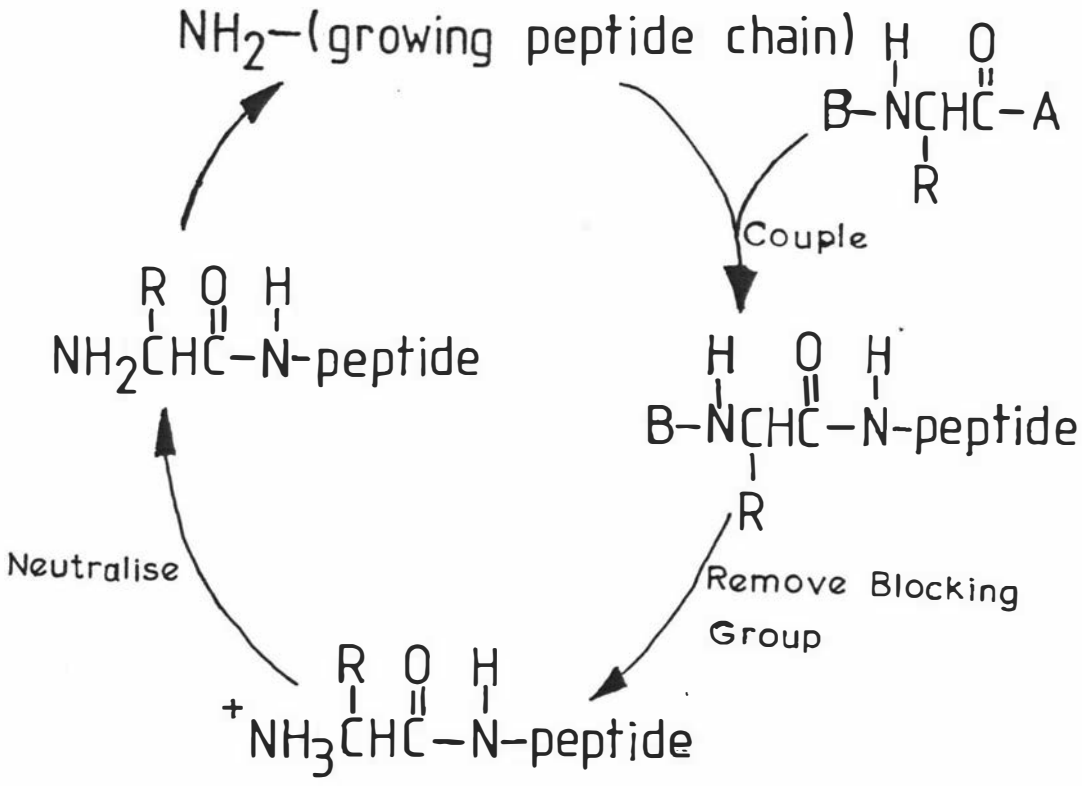

Figure 2-2 A Schematic Representation of Peptide Synthesis.
This figure shows the cyclic nature of the synthesis procedure.
A = a good leaving group.
B = a temporary amino blocking group.

2.1.3 The Advantages and Disadvantages of Solid-Phase Peptide Synthesis

The major advantage of Solid-Phase Peptide Synthesis (SPPS) is the ease with which the synthesis can be automated. Since the growing peptide is always linked to an insoluble polymer resin (the solid-phase) a simple filtration removes the reagents and by-products, thus after washing the peptide-resin is ready for the next treatment. Compare this with solution-phase peptide synthesis where the changing solubility and chromatographic behaviour of the growing peptide may require changes to the conditions of reaction and separation of the product at each cycle. Another advantage of SPPS is that due to the ease of separating the product, double couplings can easily be employed. The use of a second coupling reaction, when the yield from the first is already

high, results in a very large excess of activated Boc-amino acid which assists to drive the coupling reaction to completion.

A disadvantage of SPPS is that since the peptide cannot be purified after each cycle contaminating peptides may accumulate due to termination, deletion and side-reactions. Some of these impurities are extremely difficult to separate from the product.

2.1.4 Synthesis Modifications

Lipophilic peptides have been demonstrated to be difficult to synthesise (66,67,75). The problems encountered in these and other syntheses have led to the modification of synthesis conditions to optimise the yields of peptides. Such modifications include better solvation by shrinking and swelling the resin at each cycle (68) and the use of less cross-linked polymer resins (69), eliminating the formation of quaternary amine groups on the resin by using the more hindered base N,N-diisopropylethylamine (DIEA) instead of triethylamine in the neutralisation step (70), the use of double couplings to increase yield (71), the use of acetylation after each coupling to eliminate deletion peptides (72), the use of more stable side chain protecting groups e.g. -Lys(Cl-z)- (73) and finally the use of resin-peptide linkages which are more stable to acidolytic cleavage than the benzyl ester of the Merrifield type peptide-resins (74,75). All but the last modification have been included in the synthesis of the peptide series described here.

2.2 Experimental

2.2.1 Equipment and Chemicals

The peptides were synthesised using a Schwartz-Mann peptide synthesiser.

The following Boc* amino acids were obtained from indicated sources:

Nα-t-Butyloxycarbonyl-N^{g}-Tosyl-L-Arginine (Boc-Arg(Tos)),
Nα-t-Butyloxycarbonyl-L-Glutamine (Boc-Gln),
Nα-t-Butyloxycarbonyl-N^{ε}-2-Chlorobenzyloxycarbonyl-L-Lysine·
t-Butylamine (Boc-Lys(Cl-z).TBA),

* Boc = t-butyloxycarbonyl

Nα-t-Butyloxycarbonyl-L-Phenylalanine (Boc-Phe),
Nα-t-Butyloxycarbonyl-N^{in}-Formyl-L-Tryptophan (Boc-Trp(CHO)),
Nα-t-Butyloxycarbonyl-O-Benzyl-L-Tyrosine (Boc-Tyr(Bzl)),
Nα-t-Butyloxycarbonyl-L-Valine (Boc-Val)*,
Nα-t-Butyloxycarbonyl-O-Benzyl-L-Serine (Boc-Ser(Bzl)) and
Nα-t-Butyloxycarbonyl-O-Benzyl-L-Threonine (Boc-Thr(Bzl)),

were purchased from Peptide Research Foundation, Osaka, Japan.

Nα-t-Butyloxycarbonyl-L-Alanine (Boc-Ala),
Nα-t-Butyloxycarbonyl-L-Glutamic Acid γ-Benzyl Ester (Boc-Glu(OBzl)),
Nα-t-Butyloxycarbonyl-L-Leucine (Boc-Leu) and
Nα-t-Butyloxycarbonyl-L-Valine (Boc-Val)*,

were purchased from Schwartz-Mann.

N,N'-Dicyclohexylcarbodiimide (DCC) was of redistilled purity, purchased from Protein Research Foundation. Trifluoracetic acid (TFA) was purchased from Halocarbon Products Corporation, Hackensack, NJ, USA and was further purified by distillation in a system protected from moisture with a $CaCl_2$ Drying tube.** N,N-Diisopropylethylamine was purchased from Sigma and purified by reflux over calcium hydride for 1 h followed by distillation. Pyridine was laboratory reagent grade purchased from Ajax Chemicals, Sydney, Australia, and purified by reflux over calcium hydride for 3 h followed by distillation. Acetic anhydride was A.R. grade purchased from Koch-Light Laboratories Ltd., Buckinghamshire, England, and was purified by reflux over calcium hydride for 1 h followed by distillation. N,N-Dimethylformamide (DMF) was A.R. grade purchased from Ajax Chemicals. It was purified by adding calcium hydride (10 g/l DMF) and evacuating for 8 h followed by distillation under vacuum (B.pt. at 10 mm Hg = 39.9°C). Absolute ethanol was laboratory reagent grade purchased from May and Baker, Dagenham, England. Dichloromethane (CH_2Cl_2) was laboratory grade reagent purchased from Smith Biolab. It was purified by redistillation followed by passage through a 40 x 3 cm alumina column.

* Schwartz-Mann Boc-Val was used for the synthesis of peptide 203. Boc-Val from Peptide Research Foundation was used for the synthesis of peptide 208.

** A 2l scale was found to be convenient. Note <u>do not</u> use calcium hydride as a dehydrating reagent for TFA.

The chloromethylpoly(styrene-co-divinylbenzene) resin used to make the amino acid resins was 1% divinylbenzene (200-400 mesh) and had a chlorine substitution value of 0.75 mmol/g resin. It was purchased from Lab Systems Inc., California, USA as "Merrifield resin".

2.2.2 Method

(a) Preparation of amino acid resins:

Peptides 202, 203 and 209 were prepared from Boc-Ala-Merrifield resin which was prepared by the caesium salt method (76). Boc-Ala (10 g) was dissolved in 75 ml ethanol and 25 ml water and the pH adjusted to 7.0 with an aqueous solution of approx. 1 M caesium bicarbonate. The neutral solution was taken to dryness under vacuum then subjected to freeze-drying. The Boc-Ala-O^-, Cs^+ (yield = 100%) was used directly in the next step. 17.6 g of Boc-Ala-O^-, Cs^+ (a 2 fold excess) was dissolved in 175 ml DMF and added to 25 g of the chloromethyl-Merrifield resin. The mixture was stirred overnight at 50°C then washed with DMF, DMF:water (9:1), DMF and ethanol and finally dried in a vacuum dessicator over P_2O_5. The product obtained had a substitution of 0.33 mmol alanine/g of resin.*

Peptides 199 and 208 were prepared from a Boc-Ser(Bzl)-Merrifield resin prepared by the method of Stuart and Young (77). To 25 g of the Merrifield resin and 11.2 g of Boc-Ser (Bzl) (1 fold excess) in 175 ml of absolute ethanol was added 7.2 ml of triethylamine. The mixture was refluxed gently for 24 h then filtered and the resin washed with 100 ml of ethanol (3x), water (3x), methanol (3x) and dichloromethane (3x). The fines were separated by decanting the bulk of the resin from dichloromethane then the resin was filtered and dried over P_2O_5 in a vacuum dessicator overnight. The product obtained had a substitution of 0.25 mmol serine/g resin.*

(b) The synthesis procedure:

The cyclic process used to synthesise the peptides is depicted in Table 2-1. The coupling method used was an *in situ* symmetrical anhydride coupling.

* Obtained by amino acid analysis of an hydrolysate of the resin. Conditions of hydrolysis: - concentrated HCl: propionic acid (1:1) at 140°C for 3 h under vacuum, see reference (78).

Table 2-1 The Synthesis Protocol for the Addition of the Nth Amino Acid

Boc-(amino acid)$_{(n+1)}$-peptide-resin treated as follows:

Treatment Repetition	Time Shaken	Reagent	Reagent Volume	Category of Process
3x	1 min	CH_2Cl_2	30 ml	Washing and
3x	1 min	EtOH	30 ml	solvation of
3x	1 min	CH_2Cl_2	30 ml	resin
2x	1 min	$(AcO)_2O$:Pyr(12:88)	25 ml	Acetylation of
2x	10 min	" " "	25 ml	unprotected
4x	1 min	CH_2Cl_2		amine[a,e] washes
1x	5 min	TFA:CH_2Cl_2(1:1)	20 ml	Deprotection
1x	30 min	" " (1:3)	40 ml	removal of Boc
3x	1 min	CH_2Cl_2	30 ml	Washing and
3x	1 min	EtOH	30 ml	solvation
3x	1 min	CH_2Cl_2	30 ml	of resin
2x	5 min	DIEA:CH_2Cl_2(1:19)	30 ml	Neutralisation
6x	1 min	CH_2Cl_2	30 ml	Washes
1x	5 min	2mmol Boc-amino acid	10 ml	First
1x	60 min	1mmol DCC in CH_2Cl_2	10 ml	coupling
1x	60 min	" " "	10 ml	reaction[b,c,d,f]
5x	1 min	CH_2Cl_2	30 ml	Washes
1x	5 min	2mmol Boc-amino acid	10 ml	Second
1x	60 min	1mmol DCC in DMF	10 ml	coupling
1x	60 min	" " "	10 ml	reaction[b,c,d,f]

Boc-(amino acid)$_n$-(amino acid)$_{(n+1)}$-peptide-resin

re-enter cycle above with n=n-1

Syntheses were performed on a scale of 2 g Boc-amino acid-resin for all peptides except the synthesis of peptide 199 which was performed on a scale of 3 g Boc-amino acid resin.

Boc-Lys(Cl-z) was released from its t-butylamine salt immediately before its use by dissolving the required amount of Boc-Lys(Cl-z). TBA in dichloromethane and shaking with cold 1 N HCl in a separating funnel. The aqueous layer was then discarded and the process repeated twice. The dichloromethane layer was washed with water until the washings were neutral then reduced in volume on a rotary evaporator. The volume of this solution was then made up to the required volume and loaded into the peptide synthesiser.

Footnotes to Table 2-1

a) Also acetylated in this step are free -OH groups produced on the resin by acidolytic cleavage of peptide (62).

b) In most cases the amino acid was dissolved directly in dichloromethane, however, DMF:Dichloromethane (5:16) was used as solvent for Boc-Trp(CHO), Boc-Tyr(Bzl), Boc-Gln and Boc-Leu. Boc-Lys(Cl-z) was released from its t-butylamine salt immediately before use by the procedure indicated below.

c) In each of the coupling steps the reagents are added sequentially to the reaction vessel without removal of the previous reagent.

d) In the case of the coupling of the third amino acid from the carboxyl terminal an inverse addition of these reagents was used i.e.

1x 5 min shake with 1 mmol DCC in CH_2Cl_2
1x 60 min shake with 2 mmol Boc-amino $acid_{(n-1)}$
1x 60 min shake with 1 mmol DCC in CH_2Cl_2

e) $(AcO)_2O$:Pyr = acetic anhydride:pyridine.

f) 1-Hydroxybenzotriazole (0.27 g) was added to the Boc-amino acid solution for each coupling of Boc-Gln.

CHAPTER 3 PURIFICATION OF PEPTIDES

3.1 Introduction

Each of the peptides was purified as described in their individual sections. All the peptides were purified by semi-preparative reversed-phase HPLC as a final step. In addition peptides 202 and 203 were purified by ion-exchange chromatography and peptide 202 by gel filtration chromatography. It is usually considered preferable to purify peptides based on at least two different criteria (e.g. charge and size by ion-exchange and gel-filtration respectively). However in the course of this work it was shown that ion-exchange and gel-filtration do not have any advantage over reversed-phase HPLC and indeed the latter technique appears to be vastly superior. It was therefore decided to purify peptides 208, 209 and 199 only by reversed-phase HPLC after a desalting gel-filtration step. The purification of peptide 199 is considered last as it requires special conditions for elution in the reversed-phase HPLC step.

3.2 Equipment and Chemicals

Hydrogen Fluoride Cleavage

The liquid hydrogen fluoride (HF) cleavage and deprotection reactions were performed in a Type II HF-Reaction Apparatus from Protein Research Foundation (Japan) with liquid HF from Matheson Gas Products (USA). The HF was dried by placing about 0.5 g of CoF_3 in the first distillation chamber. The peptide-resin was placed in the second distillation chamber with anisole from Prolabs, France (laboratory reagent stored over molecular sieves) and a stirring bar. The required amount of HF was distilled from the first chamber by placing the second chamber into liquid air. The mixture was brought to $0^{o}C$ with an ice-water bath. The HF was removed by evacuating the second chamber through a reaction tower (Protein Research Foundation) containing calcium oxide and teflon shavings. The trifluoroacetic acid used in the extraction of peptide has been described in the experimental section of chapter 2, section 2.2.1.

Gel Filtration and Ion-Exchange Column

G-10 Sephadex gel filtration separations were performed in a glass column fitted with a no. 2 glass sinter. The G-50 Sephadex gel filtration

and ion-exchange separations were performed in Pharmacia columns with plunger adaptors.

Urea (puris grade) was purchased from Koch-Light and was dissolved in water to the required concentration and filtered through Whatman No. 5 filter paper. Any isocyanate present in the solution was removed immediately before use by passage through a column of Amberlite MB-3 mixed bed ion-exchange resin (30 cm x 7 cm dia.). The conductivity of 6 M urea was reduced to 1.2 micro MHO by this method. All manipulations with urea solutions were performed in a refrigerated room at approximately 10^{o}C to minimise isocyanate formation.

The eluted peptides were recognised by their absorbance at 280 nm using an 8300 Uvicord II detector and control unit coupled to a type 6520-8 chopper-bar recorder (LKB, Bromma). Conductivity was monitored with a type CDM2e conductivity meter (Radiometer, Copenhagen) connected to a flow-through cell. Fractions were collected using a model 7000 Ultrorac fraction collector (LKB).

Salt concentration gradients for ion-exchange chromatography were prepared using a GM-1 gradient mixer from Pharmacia.

Deformylation

Guanidine hydrochloride was sequenal grade purchased from Pierce Chemicals Co. (Rockford, Illinois, USA). Ethanolamine (2-aminoethanol) was laboratory grade purchased from Ajax Chemicals (Sydney, Australia) and purified by distillation from calcium hydride.

Reversed-Phase HPLC

The HPLC equipment used is described in the experimental section of chapter 5. All HPLC separations in this chapter were performed at ambient temperature. A guard column (Waters Associates) filled with a reversed-phase packing (usually Bondapak C18/porasil B) was essential in order to stop the Radial-PAK cartridges from degrading too quickly in the slightly alkaline mobile phases used in the preparative separations. Ammonium formate was a laboratory reagent purchased from Ajax Chemicals (Sydney, Australia).

UV Spectra

UV spectra were obtained on a Shimadzu MPS-5000 spectrophotometer with a path length of 1 cm, scan speed 3 min/400 nm.

3.3 The Purification of Peptide 202

A scheme of the sequence of chromatographic techniques and deprotection reactions used in the purification of peptide 202 is shown in figure 3-1.

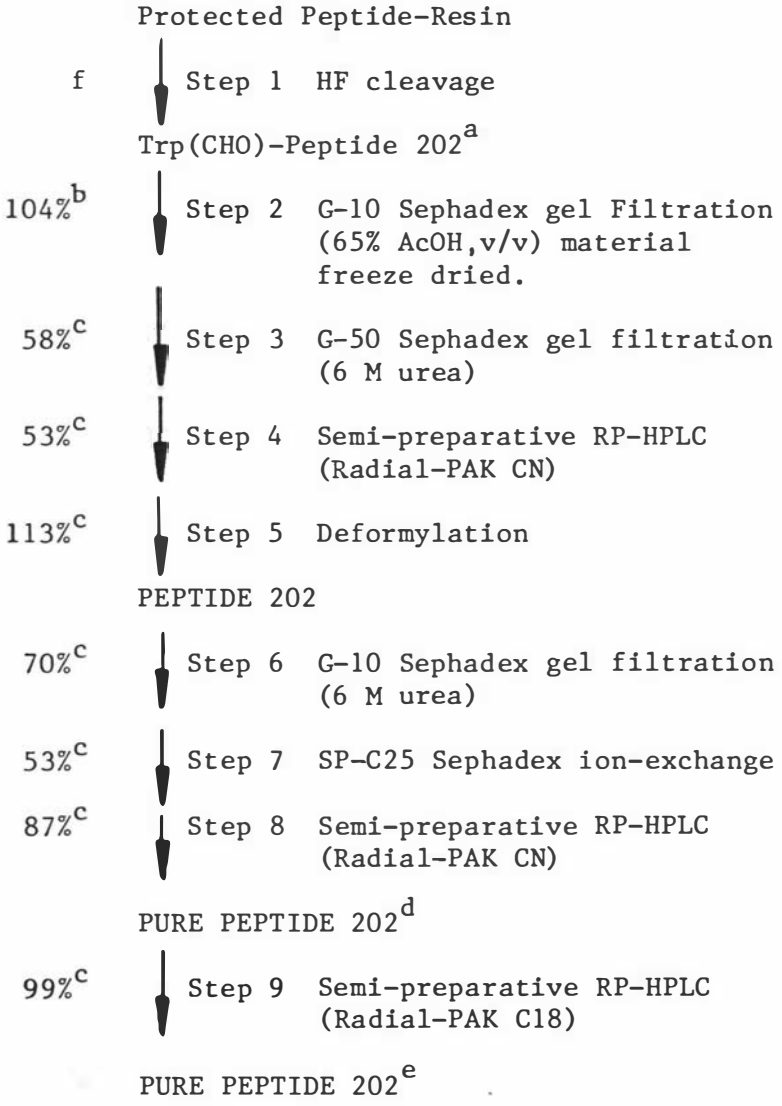

Figure 3-1 The sequence of Chromatographic Techniques and Deprotection Reactions Used in the Purification of Peptide 202

a) Trp(CHO)-Peptide 202 is peptide 202 with its tryptophan residue protected by a formyl group.
b) Based on weight of product.
c) By UV absorbance, (ε_{280} = 5200 $1.mol^{-1}.cm^{-1}$, M.Wt. peptide 202 = 2034, M.Wt. Trp(CHO)-peptide 202 - 2062)
d) Used in reversed-phase HPLC studies (Chapter 5)
e) Used in phospholipid binding studies (Chapter 6)
f) The yield of peptide in Step 1 is included in Step 2

3.3.1 Hydrogen Fluoride Cleavage - Step 1

To 1.4 g resin-peptide was added 4 ml anisole and 20 ml liquid hydrogen fluoride (HF). The mixture was stirred for 1 hr at 0°C then the hydrogen fluoride was removed under vacuum. The resin was washed with 20 ml diethyl ether (5x) to remove the anisole. The peptide was then separated from the resin by treatment with 20 ml trifluoracetic acid followed by filtration (5x). The collected filtrate was evaporated under reduced pressure to an oil.

Amino acid analysis of the trifluoroacetic acid treated resin confirmed that 99% of the peptide had been cleaved from the resin by the liquid hydrogen fluoride treatment.

3.3.2 G-10 Sephadex Gel Filtration of the Crude Peptide - Step 2

The oil from Step-1 above was dissolved in 27 ml of 65% acetic acid and loaded onto a G-10 Sephadex gel filtration column (32 cm x 5.5 cm dia.) at approximately 10°C. The eluted fractions containing the bulk of absorbance at 280 nm were pooled, as indicated in figure 3-2, diluted to approximately 1 ℓ in volume with water and freeze dried. Yield = 540 mg of off-white powder. This represents a 104% yield based on the original substitution of alanine on the resin.

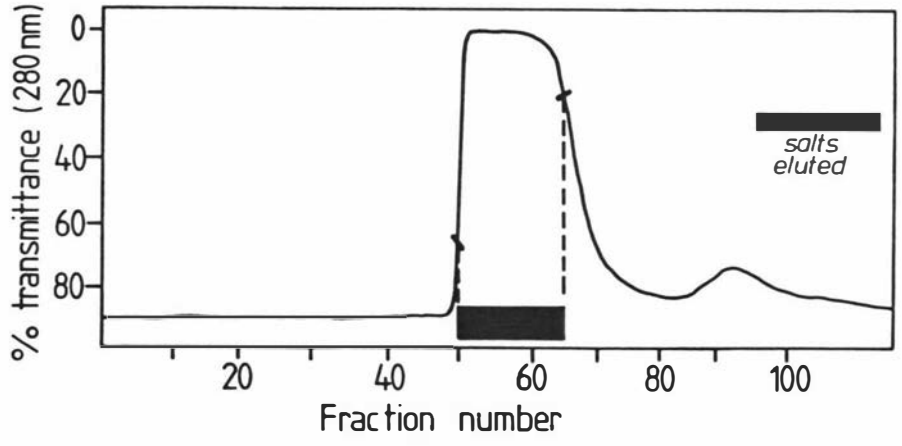

Figure 3-2 The Gel Filtration of Crude Trp(CHO)-Peptide 202 on a G-10 Sephadex Column.

Conditions of Gel Filtration:
Sephadex Type: G-10 Sephadex
Column Dimensions: 32 cm x 5.5 cm dia.
Eluent: 65% acetic acid (v/v). Each fraction contained 5.8 ml.
Sample: The total trifluoroacetic acid soluble fraction of peptide cleaved from 1.4 g of peptide-resin loaded in 27 ml of 65% acetic acid at fractions 1-5.

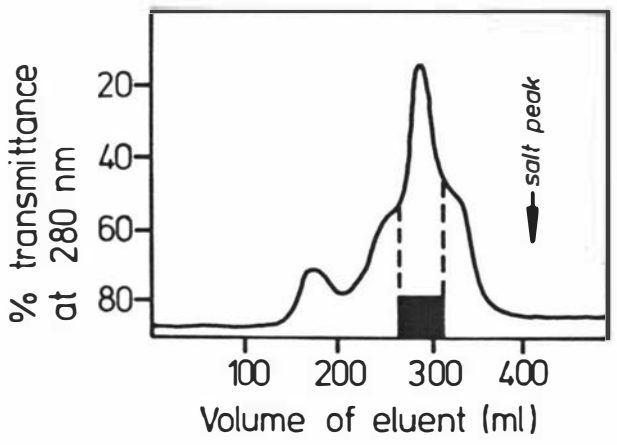

Figure 3-3 The Gel Filtration of Trp(CHO)-Peptide 202 on a G-50 Sephadex Column.

Conditions of gel filtration: -

Sephadex Type: 84 cm x 2.6 cm dia.

Eluent: 6 M urea, 0.02 M ammonium acetate, pH 7.5.

Sample: 101 mg (weighed) Trp(CHO)-Peptide 202 loaded in 8 ml of eluent (97 mg by UV absorbance; ε_{300} = 5200 $1.mol.^{-1}cm^{-1}$, M.Wt. = 2062

Recovery: Collected peak contains 58% of the 300 nm absorbance of the loaded sample. Total recovery of UV absorbing material = 91%.

Those fractions corresponding to the bar under the graph were pooled ready for HPLC purification.

3.3.3 G-50 Sephadex Gel Filtration - Step 3

The product isolated in Step 2 was further treated by gel filtration on a G-50 Sephadex column.

101 mg of Trp(CHO)-peptide 202 was dissolved in 8 ml of 6 M urea, 0.02 M ammonium acetate, pH 7.5 and applied to a G-50 Sephadex fine column (84 cm x 2.6 cm dia.) and eluted with the above solvent. The eluted fractions corresponding to the largest peak were pooled as described in figure 3-3. The collected peak represented 58% of the 300 nm absorbance of the loaded sample.* HPLC analysis of fractions collected from a G-25 Sephadex gel filtration of this peptide, see figures 3-4B and 3-4A respectively, have demonstrated that the fore peak contains little Trp(CHO)-peptide 202** and further has demonstrated that reversed-phase HPLC may be a more effective way of isolating products than is the gel filtration used in Step 3.***

3.3.4 Semi-Preparative RP-HPLC - Step 4

The pooled fractions from the G-50 gel filtration separations contained 138 mg**** of Trp(CHO)-peptide 202 in 92 ml of solution. The peptide was further purified (and in the same process desalted) by semi-preparative reversed-phase HPLC on a Radial-PAK CN column. This was accomplished in several runs by loading variable amounts of the pool (not exceeding 15 ml) directly into the system via pump A***** after dilution

* The total recovery of all 300 nm absorbing material was 91%. Lower recoveries e.g. 70% were observed when polyacrylamide resins were used in earlier attempts to purify this peptide by gel filtration.

** This was confirmed by amino acid analysis which showed that only 2.5% of the weight of the freeze-dried forepeak was due to amino acids.

*** Subsequent purification of peptides 203, 208, 109 and 199 relied on the superior separation properties of reversed-phase HPLC to separate the different sized peptide contaminants.

**** By UV absorbance $\varepsilon_{300} = 5200\ 1.mol^{-1}.cm^{-1}$, M.Wt. = 2062

***** Note that it is necessary to remove the solvent manifold filter from pump A when loading viscous solvents containing urea or guanidine hydrochloride. Failure to carry out this preparation results in the pump drawing liquid faster than it can pass the filter and hence inevitably to the introduction of air into the pump heads. As fast a flow rate was used as was compatible with the 2500 psi pressure limit for the RCM-100 radial compression module.

Figure 3-4A The Gel Filtration of Trp(CHO)-Peptide 202 on a G-25 Sephadex Column.

Conditions of Gel Filtration: -
Sephadex Type: G-25 Sephadex Fine
Column Dimensions: 77 cm x 2.6 cm dia.
Eluent: 6 M urea, 0.02 M ammonium acetate, pH 7.5
Sample: 30 mg Trp(CHO)-Peptide 202 loaded in 4 ml of eluent.

The eluted fractions were pooled into 3 solutions (a,b&c) as indicated in the figure.

Figure 3-4B The Reversed-Phase HPLC Analysis of Fractions Collected from a G-25 Gel Filtration Separation of Trp(CHO)-Peptide 202.

Conditions of Elution: -
Column: Radial-pak CN
Guard Column: None
Solvent A: 0.1 M ammonium bicarbonate, pH 7.8
Solvent B: 2-propanol:acetonitrile:solvent A, (3:3:4, v:v:v)
Detection: 280 nm, 0.2 AUFS
Sample: 500 µl of each of the fractions a,b&c from the gel filtration in part A of this figure. The UV spectra of the pools suggest the following loadings of peptide 202 were used:
a) 0.13 mg
b) 3.25 mg
c) 0.11 mg
(ε_{300} = 5200 $l.mol^{-1}.cm^{-1}$, M.Wt. = 2062)
Flow Rate: 1.0 ml/min.
Gradient: Linear, 0-100% solvent B over 60 min.

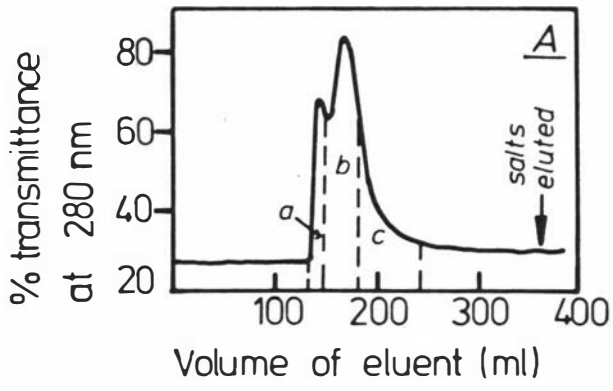
% transmittance at 280 nm
80
60
40
20
A
a
b
c
salts eluted
100
200
300
400
Volume of eluent (ml)

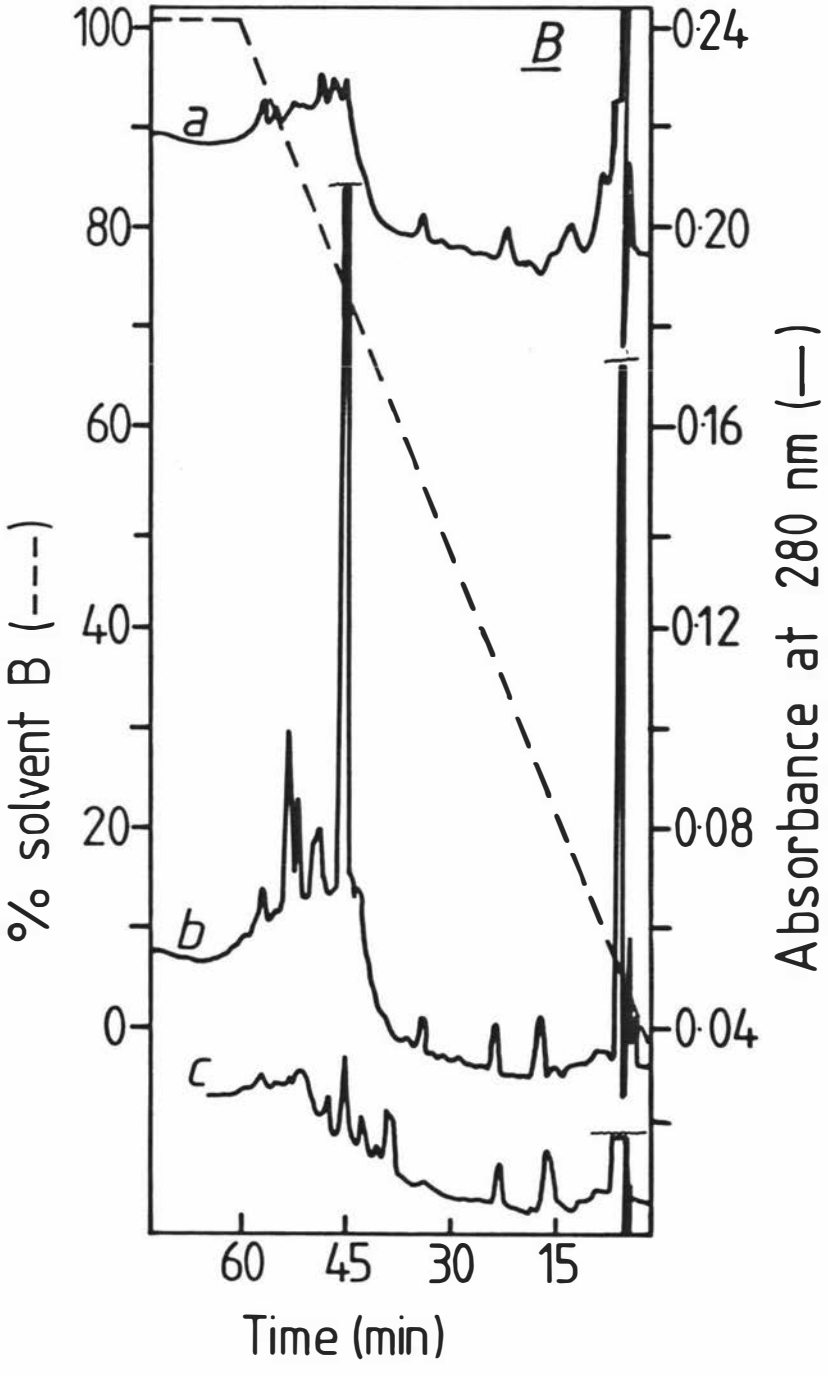
B
a
b
c
100
80
60
40
20
0
% solvent B (---)
0·24
0·20
0·16
0·12
0·08
0·04
Absorbance at 280 nm (—)
60
45
30
15
Time (min)

Figure 3-5A The Semi-Preparative Reversed-Phase HPLC Purification of Trp(CHO)-Peptide 202 after Gel Filtration Chromatography.

Conditions of Elution: -
Column: Radial-pak CN
Guard Column: None
Solvent A: 0.1 M ammonium bicarbonate
Solvent B: 2-propanol:acetonitrile:solvent A, (3:3:4, v:v:v)
Detection: 280 nm, 2.0 AUFS
Sample: 15 ml of the pooled fractions from the G-50 gel filtration of Trp(CHO)-Peptide 202 diluted to approximately 45 ml with solvent A and loaded directly through pump A at 1.5 ml/min. Mass of sample = 22.5 mg. (ε_{300} = 5200 $1.mol^{-1}.cm^{-1}$, M.Wt. = 2062)
Flow Rate: 1.0 ml/min.
Gradient: Linear, 0-100% solvent B over 60 min.

Figure 3-5B The Reversed-Phase HPLC Analysis of HPLC Purified Trp(CHO)-Peptide 202.

Conditions of Elution: - as in A with the following modifications
Detection: 280 nm, 0.1 AUFS
Sample: 50 µl of the pooled HPLC purified fractions. Mass = 49 µg.

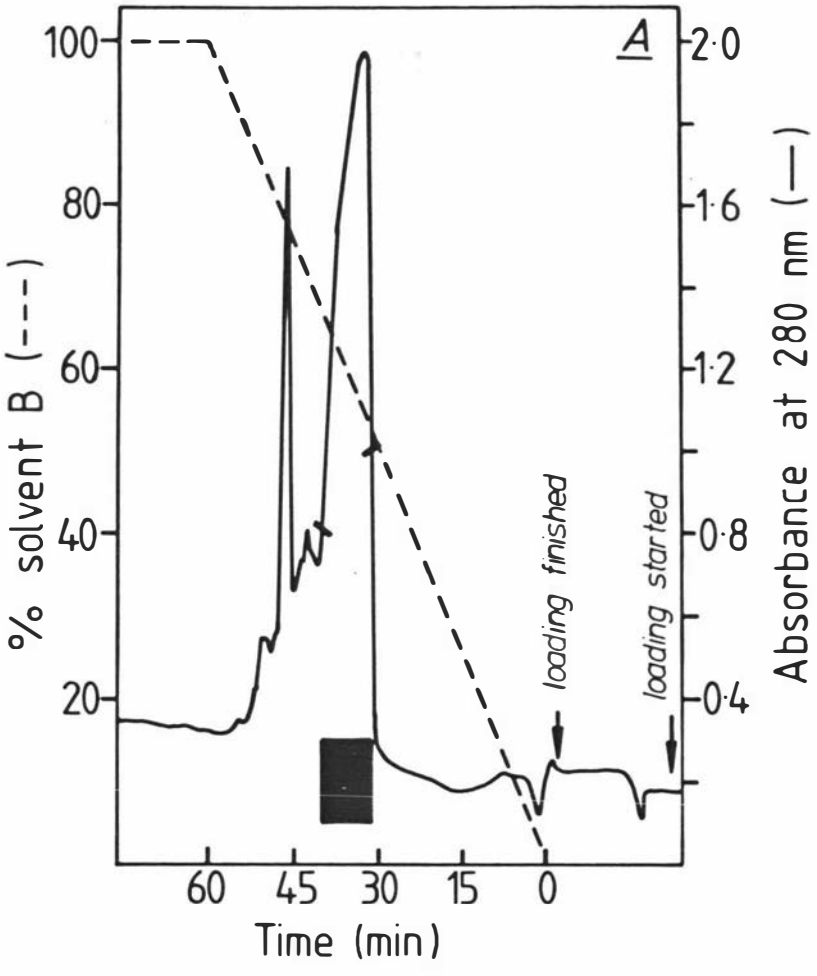
A
100
80
60
40
20
% solvent B (---)
2·0
1·6
1·2
0·8
0·4
Absorbance at 280 nm (—)
loading finished
loading started
60
45
30
15
0
Time (min)

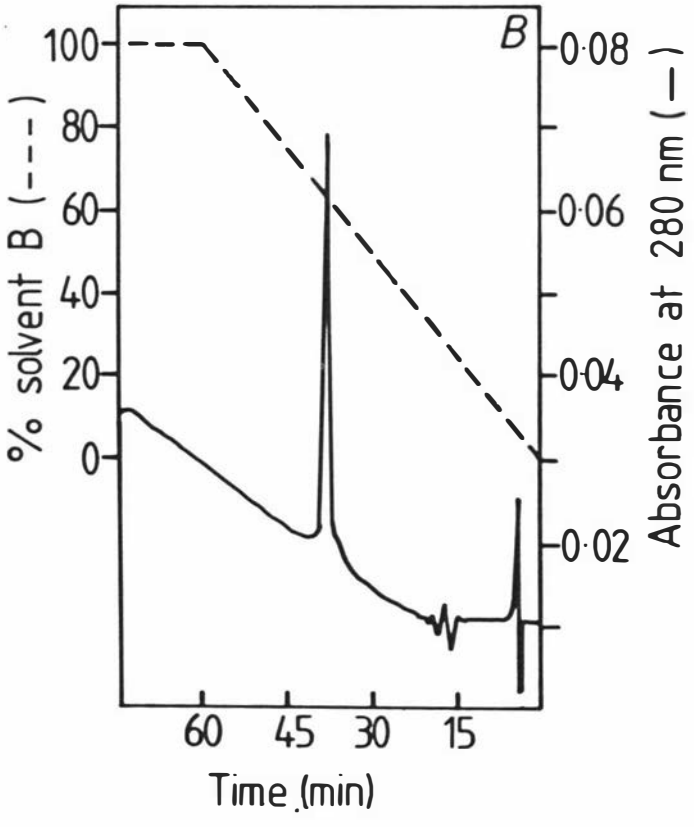
B
100
80
60
40
20
0
% solvent B (---)
0·08
0·06
0·04
0·02
Absorbance at 280 nm (—)
60
45
30
15
Time (min)

with solvent A (1:2, v:v). The conditions of the separation have been given in figure 5A which details the purification of 15 ml of the Trp(CHO)-peptide 202 solution. Evidence of over-loading was identified in this separation by the skewed peak shape. However, the reversed-phase HPLC analysis of the pooled fractions collected from all runs demonstrated that the separation produced peptide of an excellent purity (figure 5B*). The mass of peptide in the pooled fractions was 73 mg of Trp(CHO)-peptide 202 representing a yield of purified peptide of 53%. Note however that re-injection of the HPLC purified peptide results in a 92% recovery.

3.3.5 Deformylation - Step 5

To 35 ml of the pooled HPLC fractions from Step 4 was added 35 ml of water and 40.5 g guanidine hydrochloride** to produce a solution of the peptide in 4.2 M guanidine hydrochloride and approx. 5% 2-propanol and 5% acetonitrile (v/v) with an apparent pH of 7.7.*** The solution was cooled to 4°C and 9.8 ml of ethanolamine was added and the solution stirred for 5 min. The apparent pH was monitored at 10.9-11.0.*** After this time the reaction was quenched by titration with hydrochloric acid (conc.) to pH 6.2. The UV spectra before and after the treatment are shown in figure 3-6. Yield = 113%****.

* Note that the elution point of Trp(CHO)-peptide 202 has decreased from 74% solvent B (figure 3-4B) to 64% solvent B consistent with loss of some reversed phase in the high pH solvent system without protection from a guard column. This observation was made regardless of loading.

** The deformylation of Trp(CHO)-peptide 202 did not proceed in the absence of guanidine hydrochloride.

*** Not adjusted for temperature or solvent effects.

**** Based on UV absorbance (ε_{280} Trp = ε_{300} Trp(CHO) = 5200 $l.mol^{-1}.cm^{-1}$).

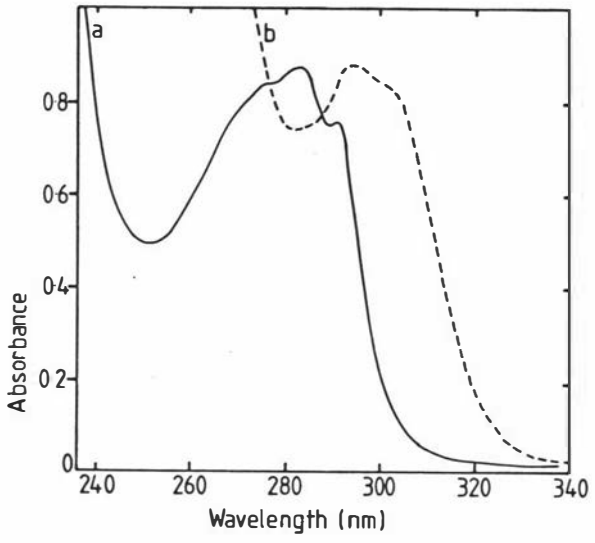

Figure 3-6 A Comparison of the UV Spectra of Trp(CHO)-Peptide 202 and Peptide 202.

Peptide 202 (————),

Trp(CHO)-peptide 202 (– – – –).

Recovery: 113% assuming ε_{280} Peptide 202 = ε_{300} Trp(CHO)-peptide 202.

3.3.6 G-10 Sephadex Gel Filtration - Step 6

Before proceeding to the ion-exchange separation (Step 7) it was necessary to remove the guanidine hydrochloride from the deformylation mixture.

A sample of 60 ml of the neutralised deformylation mixture was loaded onto a G-10 Sephadex column (30 cm x 5.5 cm dia.) equilibrated with 6 M urea, 0.02 M ammonium acetate at a pH of 4.5.* The 280 nm absorbing fractions were pooled (90 ml). The recovery of peptide 202 in this step was 70%.**

* It was necessary to use conditions which were not acidic due to the sensitivity to oxidation of the unprotected tryptophan as evidenced by the broadening of the UV absorbance spectrum of the peptide in 65% acetic acid.

** Based on absorbance at 280 nm.

3.3.7 SP-C25 Sephadex Ion-Exchange - Step 7

The desalted peptide solution (91 ml) containing 15.7 mg of peptide 202 was loaded onto a column of SP-C25-120 Sephadex (15 cm x 1.6 cm dia.) which had been equilibrated with a solution of 6 M urea (cyanate free), 0.02 M ammonium acetate, pH 4.5. After binding, a 0.02 M to 0.3 M ammonium acetate gradient was started with 2 peaks being eluted at conductivities of 2.5 and 5.2 m MHO as shown in figure 3-7. The collected fractions contained 53% of the absorbance at 280 nm of the loaded sample.

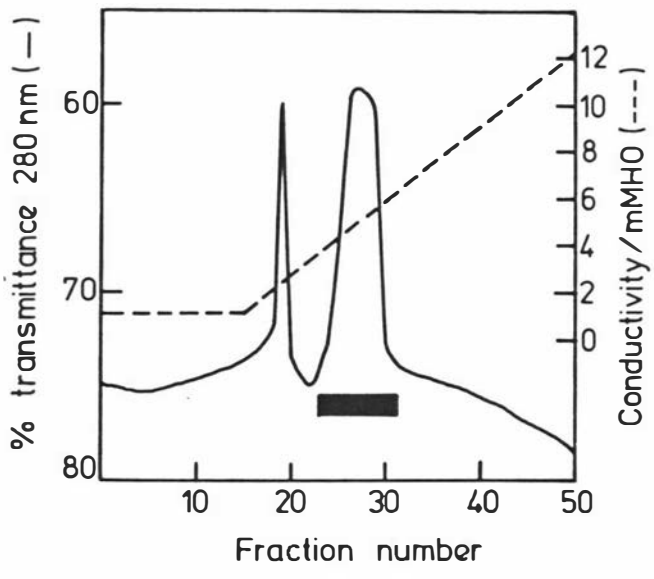

Figure 3-7 The Ion-Exchange Purification of Peptide 202 on SP-C25 Sephadex

Conditions of Elution: -

Ion-Exchanger: SP-C25-120 Sephadex

Column Dimensions: 15 cm x 1.6 cm dia.

Eluent: 6 M urea, gradient from 0.02 M to 0.3 M ammonium acetate, pH 4.5 (each fraction was approx. 8 ml in volume)

Sample: 91 ml of eluent from a desalting gel filtration separation on G-10 Sephadex containing 15.7 mg of peptide 202 (ε_{280} = 5200 $l.mol^{-1}.cm^{-1}$, M.Wt. = 2034)

Recovery: 53% based on absorbance at 280 nm.

A very similar profile as in figure 3-7 was found on elution of peptide 202* from SP-C50 Sephadex with a sodium chloride gradient. The reversed-phase HPLC analysis of these two peaks, which eluted at similar conductivities to the preparation detailed above i.e. at conductivities of 2.6 and 4.2 mMHO, are shown in figure 3.8.

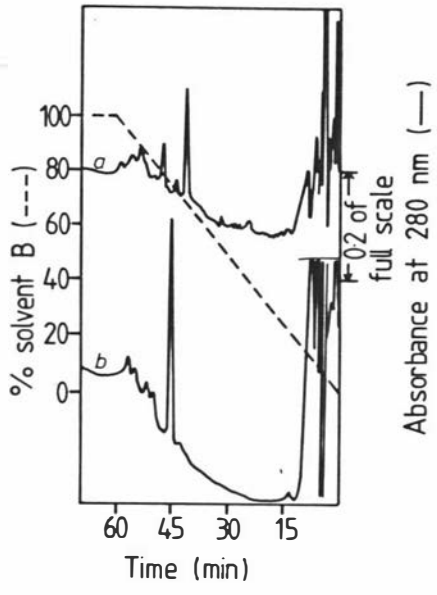

Figure 3-8 The Reversed-Phase HPLC analysis of Fractions from an Ion-Exchange Purification of Peptide-202.

Conditions of Elution: -
As for figure 3-4B with the following modifications.
Samples: a) 78 µg of peptide from the 1st peak of an ion-exchange purification of peptide 202.

b) 28 µg of peptide from the 2nd peak of an ion-exchange purification of peptide 202.

Detection: 280 nm, a) 0.2AUFS, b) 0.1AUFS

* This sample had been subjected only to Steps 1,2,5 and 6 of this purification scheme, see figure 3-1.

This figure clearly shows that reversed-phase HPLC can be utilised in this instance to separate peptides which differ in charge.* Amino acid analysis of the two ion-exchange peaks showed identical amino acid content, however, the first peak eluted (at a conductivity of 2.6 m MHO) contained 0.6 eq. of ethanolamine.** Since this peptide is eluted before peptide 202 on the cation exchange resin, the modification of one of the free amino groups of the peptide is implicated. This modification could involve the formation of a substituted urea with the carbonyl moiety coming from the formyl protection for tryptophan. Such a reaction could possibly proceed via an N-substituted formamide. The hypothetical N-substituted formamide might then be reduced by 2-propanol to an N-substituted isocyanate intermediate which could be subsequently attacked by an amino group as is found for carbamylation of proteins in urea solutions containing high levels of isocyanate (79).

3.3.8 Semi-Preparative Reversed-Phase HPLC - Step 8

The pooled fractions from the ion-exchange separation used in Step 7 was purified and desalted on a Radial-PAK CN column by semi-preparative reversed-phase HPLC. A sample of 53 ml of eluent from the SP Sephadex column (figure 3-7) containing 6.8 mg*** of peptide 202 was neutralised to pH 8.0 with concentrated ammonia,**** filtered through a sample clarification kit fitted with a HAWP 01300 Millipore filter and loaded into the HPLC system directly through pump A at a flow rate of 1.0 ml/min. The conditions of elution have been given in figure 3-9A. The volume of eluent corresponding to the bar in this figure was pooled. It contained 87% of the 280 nm absorbance loaded.

* Hence no ion-exchange step was used in the purification of peptides 208, 209 and 199.

** Calculated from the amino acid analysis chromatograph assuming ethanolamine has a colour factor with ninhydrin equal to that of glycine. Ethanolamine was eluted slightly before lysine on the amino acid analysis chromatograph.

*** By UV absorbance, ε_{280} = 5200 $1.mol^{-1}.cm^{-1}$, M.Wt. = 2034.

**** The pH of the sample must be similar to the pH of the eluent or gaseous carbon dioxide will form inside the HPLC column.

Figure 3-9A The Semi-Preparative Reversed-Phase HPLC Purification of Peptide 202 after an Ion-Exchange Purification.

Conditions of Elution:-
Column: Radial-pak CN
Guard Column: Bondapak phenyl/Porasil B
(37-75 microns, 0.15 g)
Solvent A: 0.1 M ammonium bicarbonate, pH 7.8
Solvent B: 2-propanol:acetonitrile:solvent A, (3:3:4, v:v:v)
Detection: 280 nm, 2.0 AUFS
Sample: 53 ml of a neutralised fraction from the ion-exchange purification of peptide 202 loaded through pump A.
Total mass of sample = 6.8 mg.
(ε_{280} = 5200 $1.mol^{-1}.cm^{-1}$, M.Wt. = 2034).
Flow Rate: 1.0 ml/min
Gradient: Linear, 0-100% solvent B over 60 min.

Figure 3-9B The Reversed-Phase HPLC Analysis of HPLC Purified Peptide 202.

Conditions of Elution: - as in A with the following modifications.
Guard Column: None
Detection: 280 nm, 0.1 AUFS
Sample: 20 µl of the pooled HPLC purified fractions of peptide 202. Mass of sample = 16 µg
(ε_{280} = 5200 $1.mol^{-1}.cm^{-1}$, M.Wt. = 2034).

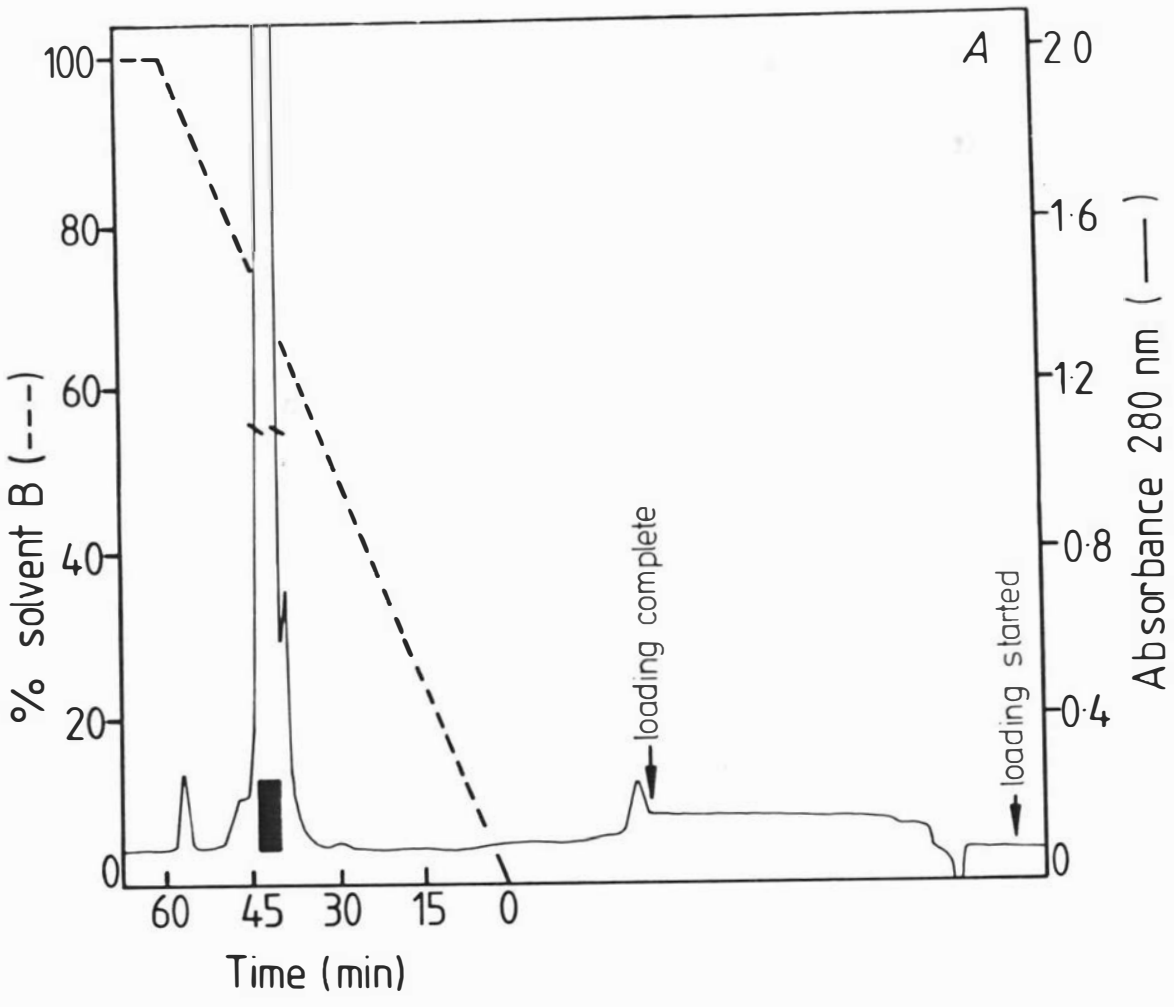
A
100
80
60
40
20
0
% solvent B (---)
2·0
1·6
1·2
0·8
0·4
0
Absorbance 280 nm (——)
loading complete
loading started
60
45
30
15
0
Time (min)

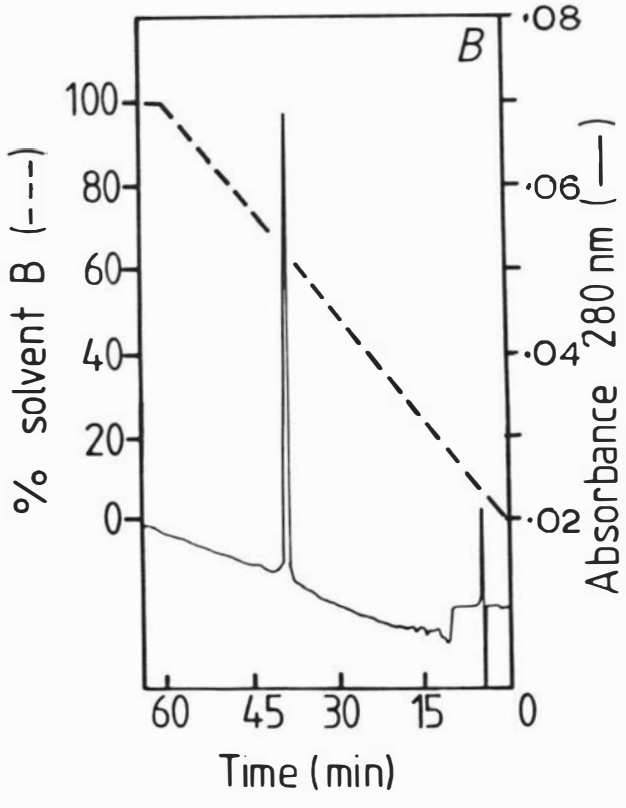
B
100
80
60
40
20
0
% solvent B (---)
·08
·06
·04
·02
Absorbance 280 nm (——)
60
45
30
15
0
Time (min)

The collected fractions for each of the 4 HPLC runs were pooled and diluted 1:4 with 0.1 M ammonium bicarbonate to give a final volume of 37 ml.* The purity of the peptide was checked by analytical HPLC, figure 3-9B.** An extremely high purity was observed. For further criteria of the purity of this peptide see section 3.8. This pool of HPLC purified peptide 202 was used for the HPLC studies of this peptide in Chapter 5, however a further step was necessary for peptide which was to be used in the phospholipid binding studies (Chapter 6).

3.3.9 Semi-Preparative Reversed-Phase HPLC - Step 9

The peptide samples to be used in the phospholipid binding studies should have exactly the same organic solvent content. This content was defined as 5% isopropanol. For this reason the purified peptide 202 was again subjected to reversed-phase HPLC, figure 3-10. The diluted sample of peptide 202 from Step 8 was filtered through a sample clarification kit fitted with a HAWP 01300 Millipore filter and loaded onto the Radial-PAK C18 column through pump A. The collected fraction (5.2 ml) containing 99% of the UV absorbance of the sample was immediately diluted to 46 ml with 0.1 M ammonium bicarbonate.*** This solution, containing 5% 2-propanol, was further diluted with 2-propanol:0.1 M ammonium bicarbonate (5:95) until the absorbance of the solution at 280 nm was 0.2 absorbance units. This solution was used directly in the phospholipid binding study. The overall yield of purified material was 10.3%.****

* No additional peaks were found when the absorbance at 230 nm was monitored.

** This dilution is necessary as some peptide precipitates on standing the concentrated eluent overnight at $4^{o}C$.

*** Peptide 202 was eluted at approx. 64.5% solvent B, but the actual concentration of solvent B in the eluent is approx. 54.5% due to the 6 ml volume between the solvent mixing manifold and the detector outlet. Thus a dilution to 46 ml with solvent A is required to bring the concentration of 2-propanol to 5%.

**** Based on UV absorbance (ε_{280} = 5200 $1.mol^{-1}.cm^{-1}$, M.Wt. = 2034) and the initial substitution of the amino acid - Merrifield resin.

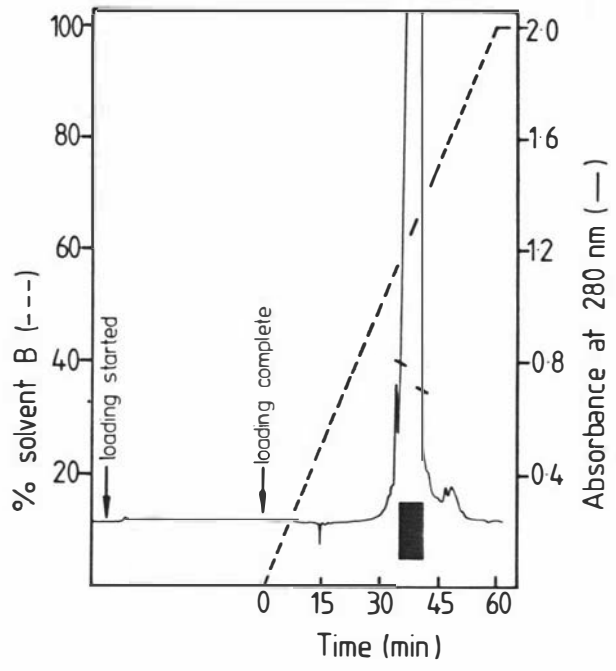

Figure 3-10 The Semi-Preparative Reversed-Phase HPLC Purification of Peptide 202 on a Radial-PAK C18 Column.

Conditions of Elution: -
Column: Radial-PAK C18
Guard Column: Bondapak C18/Porasil B
Solvent A: -0.1 M ammonium bicarbonate, pH 7.8
Solvent B: 2-propanol: Solvent A, 80:20 (v:v)
Detection: 280 nm, 2.0 AUFS
Sample: 17.2 mg peptide 202 in 30 ml of diluted solvent B from figure 3-9A
Flow Rate: 1.0 ml/min
Gradient: Linear 0-100% solvent B over 60 min
Recovery: 99%

3.4 The Purification of Peptide 203

An evaluation of the influence of various guard column packings on the separation of this peptide by reversed-phase HPLC is shown in the Appendix, section A.1.

A scheme of the sequence of chromatographic techniques and deprotection reactions used in the purification of peptide 203 is shown in figure 3-11.

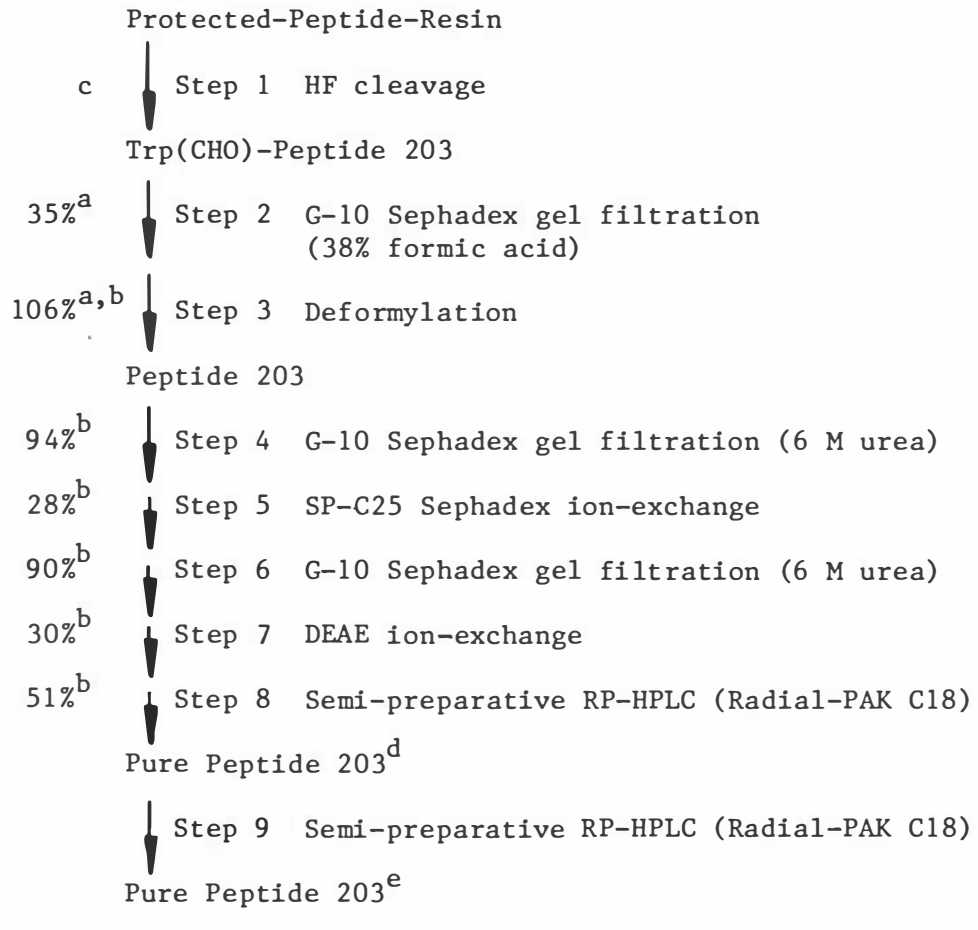

Figure 3-11 The sequence of Chromatographic Techniques and Deprotection Reactions Used in the Purification of Peptide 203.

a) Yield based on weight.

b) Yield based on UV absorbance, ε_{280} = 5200 $l.mol.^{-1}.cm^{-1}$, M.Wt. Trp(CHO)-peptide 203 = 2129, M.Wt. peptide 203 = 2101.

c) Yield included in Step 2 yield.

d) Used in reversed-phase HPLC studies (Chapter 5).

e) Used in phospholipid binding studies (Chapter 6).

3.4.1 Hydrogen Fluoride Cleavage - Step 1

4.9 g of peptide 203 - resin was treated in exactly the same way as peptide 202 - resin in section 3.3.1. The crude Trp(CHO)-peptide 203 was also separated from the resin in exactly the same way.

3.4.2 G-10 Sephadex Gel Filtration - Step 2

The crude Trp(CHO)-peptide 203 was subjected to gel filtration on a G-10 Sephadex column of similar dimensions to the column used in section 3.3.2 for the purification of Trp(CHO)-peptide 202. The peptide was purified in several batches using 38% formic acid as eluent.* The eluent fractions containing the bulk of the 280 nm absorbing material were pooled, diluted approximately 4 fold with water and freeze-dried. After freeze-drying 498 mg of light purple coloured gum was obtained which corresponds to a yield of 35% based on the original substitution of alanine on the resin.

3.4.3 Deformylation - Step 3

260 mg of Trp(CHO)-peptide 203 was dissolved in 108 ml of water to which 61.9 g of guanidine hydrochloride had been added. The solution was cooled to $4^{o}C$ and 15.15 ml of ethanolamine added to give a total volume of 150 ml (4.3 M in guanidine hydrochloride). The solution was stirred for 5 min then titrated to pH 6.2 with glacial acetic acid. Yield = 106%.**

3.4.4 G-10 Sephadex Gel Filtration - Step 4

The peptide 203 prepared in Step 3 (section 3.4.4) was loaded onto a G-10 Sephadex column (32 cm x 5.5 cm dia.) equilibrated with 6 M urea, 0.02 M ammonium acetate, pH 6.5, to remove the peptide from the deformylation mixture. The fractions corresponding to the 280 nm UV absorbing material were pooled. Recovery = 94%.

3.4.5 SP-C25 Sephadex Ion-Exchange - Step 5

The peptide 203 from Step 4 (section 3.4.4) was purified by cation-exchange chromatography as described below.

A solution of 130 mg*** of peptide 203 in 127 ml of 6 M urea, 0.02 M ammonium acetate, pH 6.5 was titrated to pH 4.5 with acetic acid and sorbed onto an SP-C25-120 Sephadex ion-exchange column (18 cm x 1.6 cm

* Due to the low solubility of Trp(CHO)-peptide 203 in acetic acid solutions, an acetic acid solution could not be used as the eluent for these columns.

** Based on UV absorbance of deformylated sample (ε_{280} = 5200 $l.mol^{-1}.cm^{-1}$, M.Wt. = 2101) and weight of the Trp(CHO)-peptide sample.

*** Based on UV absorbance (ε_{280} = 5200 $l.mol^{-1}.cm^{-1}$, M.Wt. = 2101)

dia.) which had been equilibrated with 6 M urea, 0.02 M ammonium acetate at pH 4.5. The sample was eluted with a 0-0.5 M NaCl gradient and the two peaks collected as shown in figure 3-12. The fractions corresponding to the peak labelled "b" in figure 3-12 contained peptide 203 (28% of the loaded absorbance at 280 nm, peak "a" contained 13% of the loaded absorbance at 280 nm).

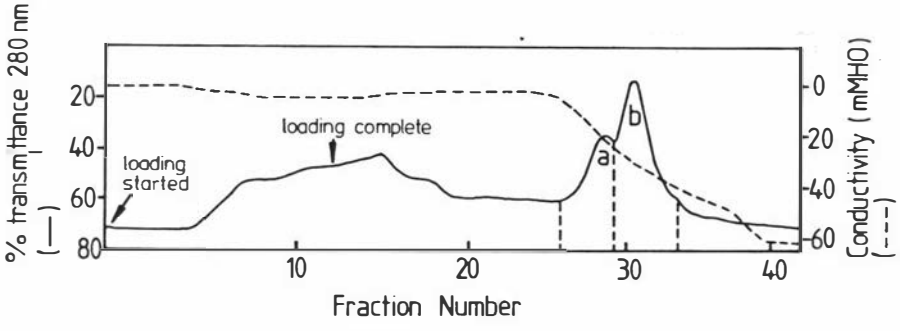

Figure 3.12 The Ion-Exchange Purification of Peptide 203 on SP-C25 Sephadex.

Conditions of Elution: -
Ion-Exchanger: SP-C25-120 Sephadex.
Column Dimensions: 18 cm x 1.6 cm dia.
Eluent: 6 M urea, 0.02 M ammonium acetate, pH 4.5, each fraction was approx. 9.5 ml in volume.
Gradient: 0-0.5 M NaCl.
Sample: 130 mg peptide 203 in 127 ml of eluent buffer (6 M urea, 0.02 M ammonium acetate) titrated to pH 4.5 with acetic acid. After loading, the column was washed with 120 ml of eluent before the gradient was started.
Recovery: Peak b represents 28% of the loaded UV absorbance (280 nm).

3.4.6 G-10 Sephadex Gel Filtration - Step 6

The collected fractions corresponding to the peak labelled "b" in figure 3-12 were rechromatographed through step 4 (section 3.4.4). The desalted solutions were then pooled. Recovery = 90%.*

* Obtained by UV absorbance (ε_{280} = 5200 $1.mol^{-1}.cm^{-1}$, M.Wt. = 2101).

3.4.7 DEAE Ion-Exchange - Step 7

A solution of 28.5 mg of SP Sephadex purified and desalted peptide 203 in 130 ml of 6 M urea, 0.02 M ammonium acetate was titrated to pH 8.0 with potassium hydroxide and loaded onto a column of Whatman DE32 ion-exchanger (30 cm x 1.5 cm dia.). The column was washed with 80 ml of 6 M urea, 50 mM in potassium dihydrogen phosphate, titrated to pH 8.0 with potassium hydroxide and the sample eluted with a 5 mM to 500 mM gradient of potassium dihydrogen phosphate. Only one peak was eluted as shown in figure 3-13 and this represented a 30% recovery of the loaded peptide.*

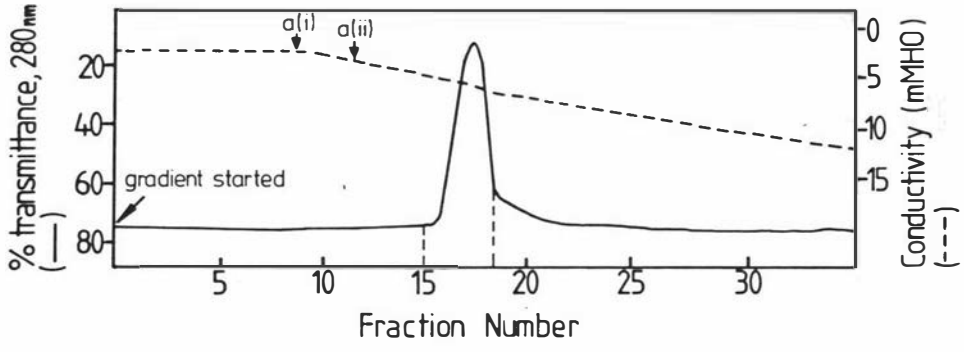

Figure 3-13 The Ion-Exchange Purification of Peptide 203 on a DEAE Ion-Exchanger.

Conditions of Elution: -
Ion Exchanger: Whatman DE32
Column Dimensions: 30 cm x 1.5 cm dia.
Eluent: 6 M urea, gradient from 5 mM to 200 mM potassium dihydrogen phosphate titrated to pH 8.0 with potassium hydroxide. Gradient started at fraction 0. Each fraction contained 5.5 ml of eluent.
Sample: 28.5 mg of peptide 203 in 130 ml of 6 M urea, 0.02 M ammonium acetate titrated to pH 8.0 with potassium hydroxide.

The marked positions a(i) and a(ii) indicate the points of elution of two poorly resolved peaks eluted when a sample from peak "a", figure 3-12 is chromatographed under the same conditions described here.

* Based on absorbance at 280 nm.

The fractions corresponding to this peak were pooled. A reversed-phase HPLC analysis of this pool clearly showed that the two ion-exchange steps had failed to completely remove several impurities, figure 3-14, trace (b). Trace (a) of figure 3-14 shows the reversed-phase HPLC analysis of the pooled peak "a" fractions from the SP-Sephadex ion-exchange step (section 3.4.5, figure 3-12).* A comparison of traces (a) and (b) of figure 3-14 shows that many eluted peaks are common to both HPLC absorbance traces indicating that only a partial separation of the components can be achieved by ion-exchange chromatography. This is another example where reversed-phase HPLC has the potential to achieve a better purification of a peptide based on the peptide's hydrophobicity, than ion-exchange chromatography can achieve based on the peptide's charge.

3.4.8 Semi-preparative RP-HPLC - Step 8

The pooled fractions from the DEAE ion-exchange step containing 11.5 mg of peptide 203** in 18 ml of eluent from Step 7 (section 3.4.7), were loaded directly onto the reversed-phase HPLC system. The separation achieved is described in figure 3-15A. The collected fraction (indicated in the figure) was diluted 4 fold with solvent A, and rechromatographed in the same solvent system, figure 3-15B. The solution was diluted to 22 ml with solvent A.*** This solution was used directly in the HPLC studies of Chapter 5. The purity of the peptide in this solution is shown in figure 3-15C. The total yield of purified material for this step was 51%, however, a recovery of 97% for the second chromatograph, figure 3-15B, was recorded.**

* The pooled peak "a" fractions were subjected to DEAE ion-exchange chromatography before the HPLC analysis. The peptide eluted under the same conditions as in Figure 3-13 as two poorly separated peaks indicated by a(i) and a(ii). The sample analysed in figure 3.14A came from the peak eluted at a(ii) in figure 3-13. Analysis of the a(i) peak is not shown because it was very similar to the a(ii) peak analysis.

** Based on UV absorbance (ε_{280} = 5200 $1.mol^{-1}.cm^{-1}$, M.Wt. = 2101).

*** At a concentration of 0.4 mg/ml in a concentration of approx. 9% solvent B and a temperature of 4°C peptide 203 precipitates in quite large amounts. The precipitate is however readily solubilised by the addition of more than 9% solvent B solution.

Figure 3-14 The Reversed-Phase HPLC Analysis of Fractions from the DEAE Ion-Exchange Purification of Peptide 203.

Conditions of Elution:

Column: Radial-pak C18

Guard Column: None

Solvent A: 0.1 M ammonium bicarbonate

Solvent B: 2-propanol:acetonitrile:solvent A, (3:3:4,v:v:v)

Detection: 230 nm, 0.1 AUFS

Samples: a) 13 µg of peptide[a] from the (aii) peak of The DEAE ion-exchange purification of peak "a" from the SP- ion-exchange purification (figure 3-12).

b) 11 µg of peptide 203[a] from the DEAE ion-exchange purification.

c) A blank run showing peak at 46% solvent B.

Flow Rate: 1.0 ml/min.

Gradient: Linear, 0-100% solvent B over 60 min.

a) Based on UV absorbance (ε_{280} = 5200, M.Wt. = 2101).

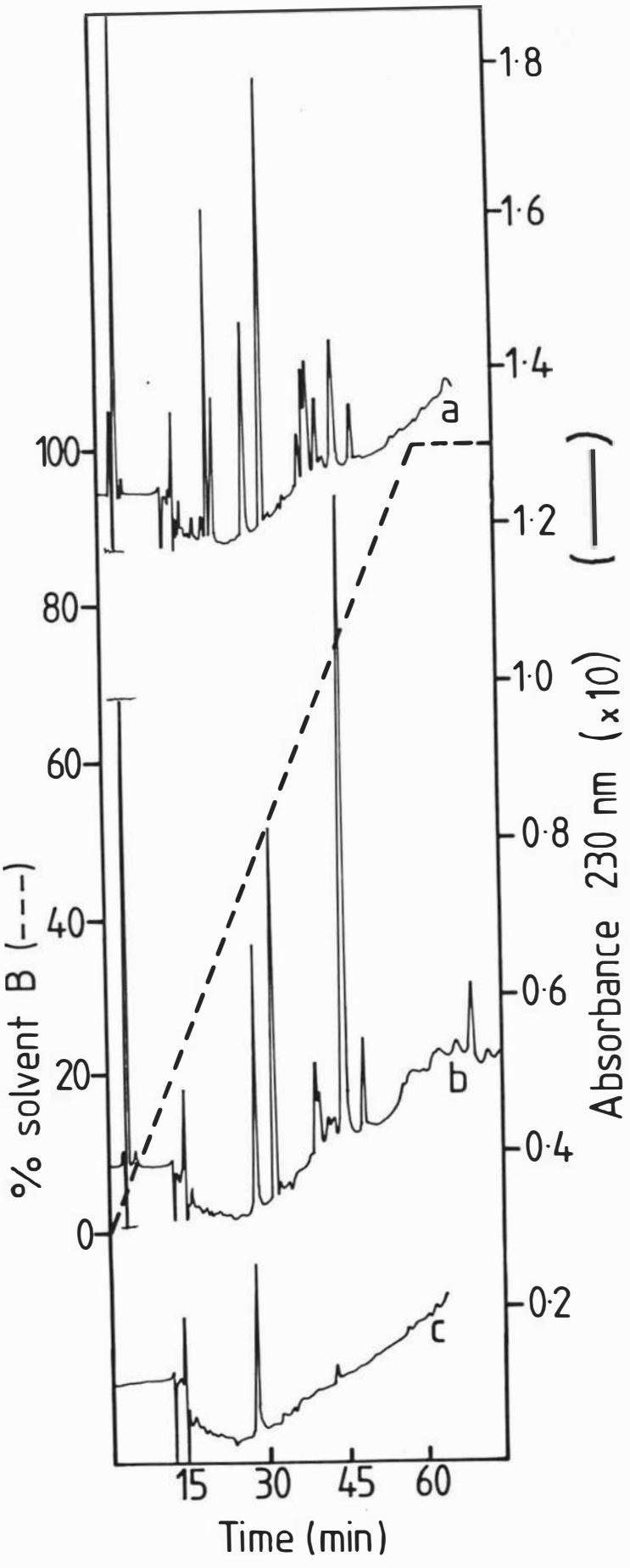
1·8
1·6
1·4
1·2
1·0
0·8
0·6
0·4
0·2
100
80
60
40
20
0
a
b
c
% solvent B (---)
Absorbance 230 nm (x10)
15
30
45
60
Time (min)

Figure 3-15 A&B The Semi-Preparative Reversed-Phase HPLC Purification of Peptide 203.

A. Shows the RP-HPLC purification of DEAE ion-exchange purified peptide 203.

B. Shows the rechromatography of the fraction collected in A.

Conditions of Elution: -
Column: Radial-pak C18
Guard Column: Bondapak C18/Porasil B
Solvent A: 0.1 M ammonium bicarbonate, pH 7.9
Solvent B: 2-propanol:acetonitrile:solvent A 3:3:4, (v:v:v)
Detection: A 240 nm, 2.0 AUFS
B 290 nm, 2.0 AUFS
Sample: A - 11.5 mg of peptide 203 in 18 ml of eluent from the DEAE ion-exchange column.
B - 6.1 mg of peptide 203 in 2 ml of eluent from B diluted to 8 ml with solvent A.
Flow Rate: 1.0 ml/min.
Gradient: Linear, 0-100% solvent B over 60 min.
Recovery A: 53% of 280 nm absorbance
B: 97% of 280 nm abosrbance

Figure 3-15C The Reversed-Phase HPLC Analysis of HPLC Purified Peptide 203.

Conditions of Elution: - as for figure 3-15A&B with the following modifications.
Detection: 230 nm, 0.2 AUFS
Sample: 15 µl of the pooled, diluted, HPLC purified fractions containing 5.6 µg of peptide 203 (by UV absorbance ε_{280} = 5200 $1.mol^{-1}.cm^{-1}$, M.Wt. = 2101).

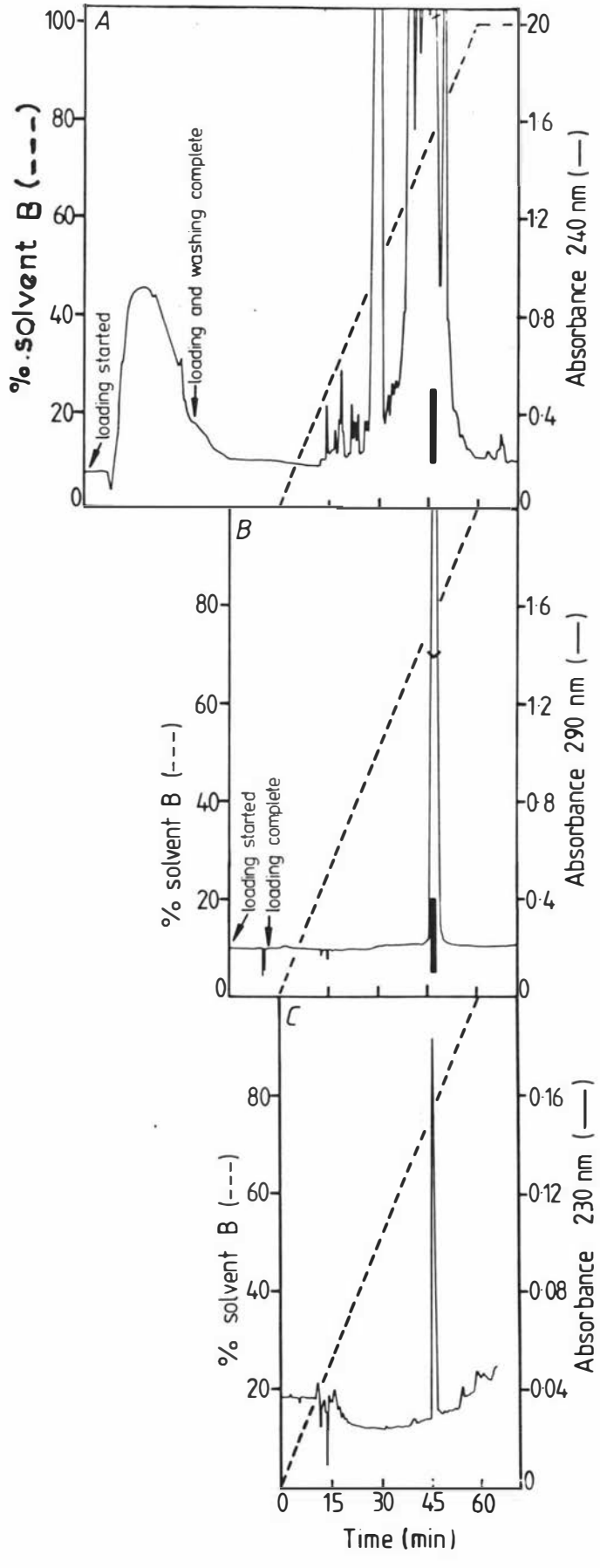
A
% solvent B (---)
Absorbance 240 nm (—)
loading started
loading and washing complete
B
% solvent B (---)
Absorbance 290 nm (—)
loading started
loading complete
C
% solvent B (---)
Absorbance 230 nm (—)
Time (min)

3.4.9 Semi-preparative RP-HPLC - Step 9

To standardise the amount of organic solvents present in the samples of peptide 203 used in the phospholipid binding studies it was necessary to subject the HPLC purified peptide 203 to one more HPLC purification. For this purification the same system was used as in section 3.3.9 for the equivalent step of the purification of peptide 202. This system contains only 2-propanol as the organic solvent and thus acetonitrile is removed from the solution. The peptide was eluted from the radial-PAK C18 column at 58% solvent B (cf. 64% solvent B for peptide 202). The peptide 203 containing fractions were pooled and diluted with 2-propanol: 0.1 M ammonium bicarbonate (5:95) until the optical density of the solution at 280 nm was 0.2. This solution was then used in the lipid-binding studies. The overall yield of purified peptide was 1.3%.

3.5 The Purification of Peptide 208

A scheme of the sequence of chromatographic techniques and de-protection reactions used in the purification of Peptide 208 is shown in figure 3-16.

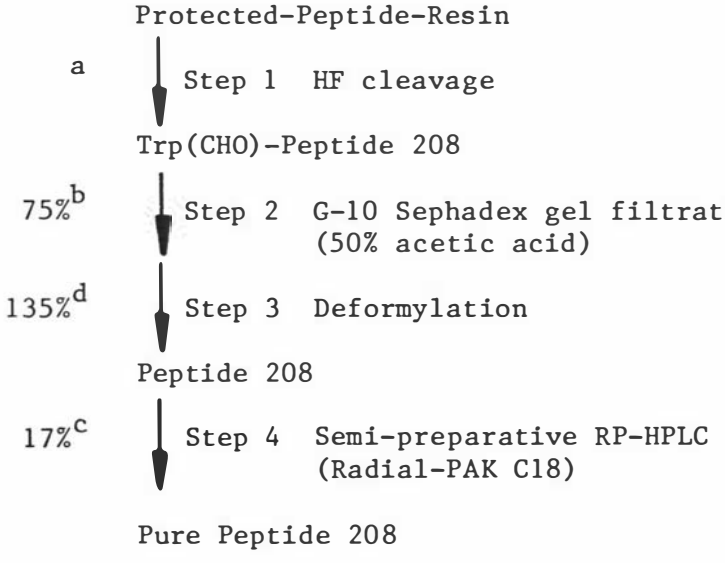

Figure 3-16 The Sequence of Chromatographic Techniques and Deprotection Reactions used in the Purification of Peptide 208.

a) Yield in Step 1 included in Step 2.

b) By weight, M.Wt. Trp(CHO)-peptide 208 = 2306.

c) By UV absorbance, ε_{280} = 5200 $1.mol^{-1}.cm^{-1}$

d) Assuming ε_{280} Trp = ε_{300} Trp(CHO).

3.5.1 Hydrogen Fluoride Cleavage - Step 1

A sample of 3.7 g of Trp(CHO)-peptide 208-resin was treated in exactly the same way as Trp(CHO)-peptide 202-resin in section 3.3.1. The crude Trp(CHO)-peptide 208 was also separated from the resin in exactly the same way except that a solution of trifluoroacetic acid: dichloromethane, 1:1 (v:v) was used to extract the peptide from the resin.

3.5.2 G-10 Sephadex Gel Filtration - Step 2

The total amount of freeze-dried product from Step 1 above was dissolved in 60 ml of 50% acetic acid and separated by gel filtration in 2 batches. The conditions of the separation were identical to those used for the separation of Trp(CHO)-peptide 202 in a G-10 Sephadex gel filtration, section 3.3.2, except that 50% acetic acid was used as eluent. The total yield of peptide at this stage was 856 mg (75%).*

3.5.3 Deformylation - Step 3

A sample of 79.1 mg of Trp(CHO)-peptide 208 was dissolved in 100 ml of water and 57.3 g of guanidine hydrochloride. This solution was cooled to 4°C and 14 ml of ethanolamine was added. The solution was stirred for 5 min while the pH was monitored (apparent pH = 11.8-11.9). After this time the solution was titrated to pH 7.8 with 6 N hydrochloric acid. UV spectra before and after the deformylation showed that the deformylation had been completed.

3.5.4 Semi-preparative RP-HPLC - Step 4

A 60 ml portion of the neutralised deformylation mixture containing approx. 26 mg of peptide 208 was diluted 3 fold with 0.1 M ammonium bicarbonate and loaded directly onto a Radial-PAK C18 column via Pump A of the HPLC system. The sample was eluted and the eluted peptide 208 collected as shown by the bar in figure 3-17A.

The collected fractions from the 3 batches were pooled and diluted to 20 ml with 0.1 M ammonium bicarbonate, pH 7.8. The recovery of peptide from Step 4 was 17%,** however, the recovery of a sample of the

* Based on the initial substitution of serine on the resin.

** Based on weight of Trp(CHO)-peptide 208 and UV spectrum of purified 208 (ε_{280} = 5200 $1.mol^{-1}.cm^{-1}$, M.Wt. = 2278).

Figure 3-17A The Semi-Preparative Reversed-Phase HPLC of Peptide 208.

Conditions of Elution: -

Column: Radial-pak C18

Guard Column: Bondapak C18/Porasil B

Solvent A: 0.1 M ammonium bicarbonate

Solvent B: 2-propanol:solvent A, 80:20 (v:v)

Detection: 305 nm, 2.0 AUFS

Sample: 26 mg of peptide 208 in deformylation mix: solvent A, 1:2 (v:v), loaded through pump A. Volume = 180 ml

Flow Rate: 1.0 ml/min.

Gradient: Linear, 0-80% solvent B over 60 min.

Figure 3-17B The Reversed-Phase HPLC Analysis of HPLC Purified Peptide 208.

Conditions of Elution: - as for figure 3-18B with the following changes.

Detection: 280 nm, 0.1 AUFS

Sample: 48 µg of HPLC purified peptide 208

Gradient: Linear, 0-80% solvent B over 120 min.

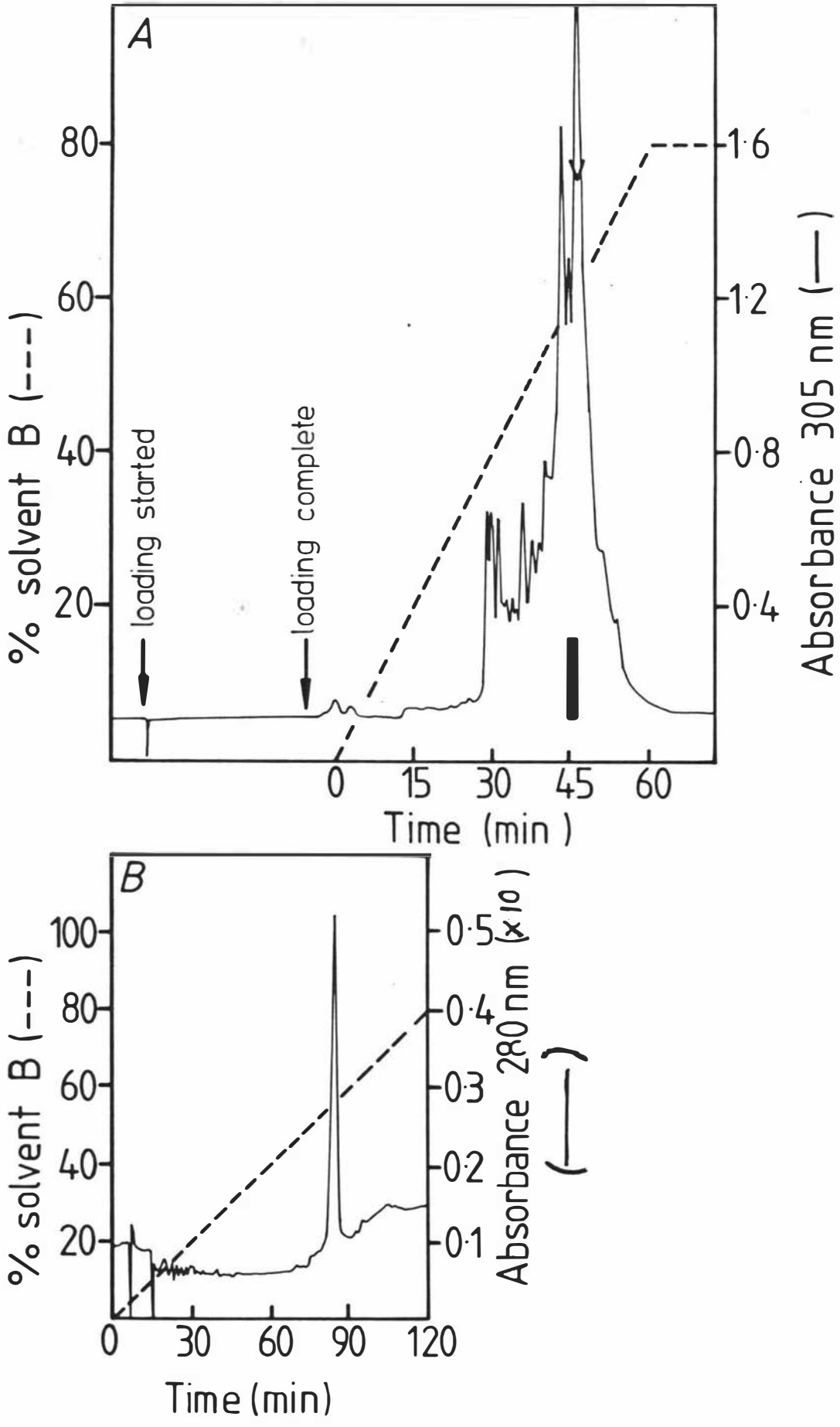
A
80
60
40
20
% solvent B (---)
loading started
loading complete
1·6
1·2
0·8
0·4
Absorbance 305 nm (—)
0
15
30
45
60
Time (min)
B
100
80
60
40
20
% solvent B (---)
0·5
0·4
0·3
0·2
0·1
Absorbance 280nm (x10) (—)
0
30
60
90
120
Time (min)

purified peptide rechromatographed by Step 4 was 96%. The overall yield of peptide by this method was 13%. The purified peptide was analysed by reversed-phase HPLC and shown to be very pure, figure 3-17B.* Further criteria of the purity of this peptide are given in section 3.8.

A sample of the peptide solution was diluted with 0.1 M ammonium bicarbonate until the concentration of 2-propanol was 5% and then further diluted with 2-propanol:0.1 M ammonium bicarbonate (5:95) until the absorbance of the solution at 280 nm was 0.2 absorbance units (as for peptide 202 in section 3.3.9). This solution was used directly in the phospholipid binding studies.

3.6 The Purification of Peptide 209

A scheme of the sequence of chromatographic techniques and deprotection reactions used in the purification of peptide 209 is shown in figure 3-18.

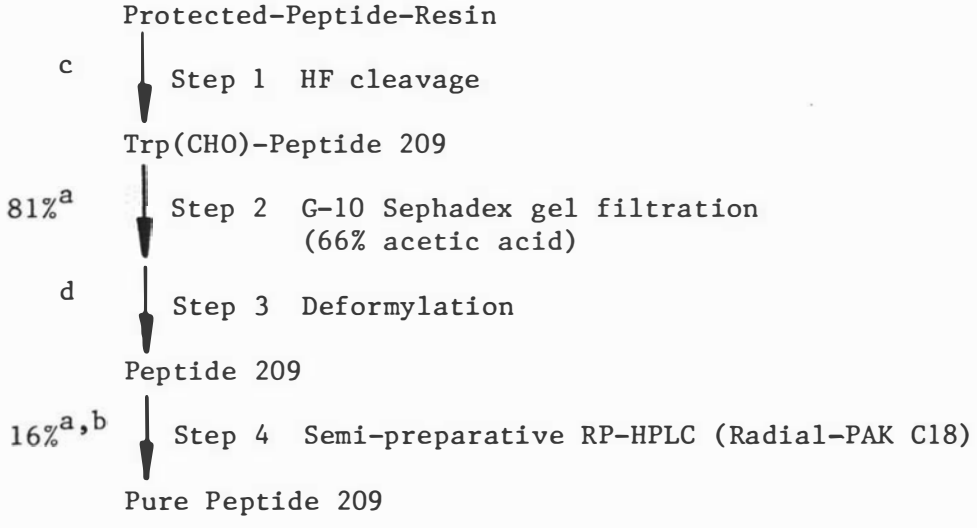

Figure 3-18 The Sequence of Chromatographic Techniques and Deprotection Reactions Used in the Purification of Peptide 209.

a) Yield based on weight (M.Wt. Trp(CHO)-peptide 209 = 2062).

b) Recovery based on UV spectrum (ε_{280} = 5200, M.Wt. peptide 209 = 2034).

c) Yield of peptide in Step 1 included in Step 2.

d) Yield of peptide in Step 3 included in Step 4.

* Note that the shallower gradient used in this analytical separation compared with the preparative separation causes elution at a lower concentration of solvent B as is usually found (80).

3.6.1 Hydrogen Fluoride Cleavage - Step 1

The liquid HF cleavage was performed on 3.8 g of peptide-resin and the crude product extracted in exactly the same way as for peptide 202, section 3.3.1.

3.6.2 G-10 Sephadex Gel Filtration - Step 2

The freeze-dried crude product extracted above was separated on a G-10 Sephadex gel filtration column and freeze-dried exactly as for Trp(CHO)-peptide 202 (section 3.3.2) except that 66% acetic acid was used as eluent. Yield = 1.10 g. This represents an 81% yield based on the original substitution of alanine on the resin.

3.6.3 Deformylation - Step 3

A sample of 23.7 mg of Trp(CHO)-peptide 209 from Step 2 above was added to a solution of 20 ml 6 M guanidine hydrochloride in 2-propanol: 0.1 M ammonium bicarbonate, 1:4 (v:v).* The solution was cooled to 4°C and 2.8 ml of ethanolamine was added. The solution was stirred for 5 min during which time the apparent pH was 10.90-10.98. The solution was then titrated to pH 7.5 with 6 N hydrochloric acid.

3.6.4 Semi-preparative Reversed-Phase HPLC - Step 4

The neutralised solution from Step 3 above was diluted to 100 ml with 0.1 M ammonium bicarbonate, pH 8.0 (Solvent A) and loaded onto a radial-PAK C18 column as described in figure 19A. It was necessary to use an 8 h gradient and include only the back of the main peak in the collected fraction due to a contaminant which was eluted immediately before the main peak. The yield of purified peptide 209 was 16%,** however, the recovery of a reinjected sample was 81%. The purified peptide was analysed by reversed-phase HPLC and shown to be very pure and completely free of the contaminant mentioned above, figure 19B. The peptide is eluted slightly earlier in the gradient when large quantities are loaded, i.e. 76% solvent B for the preparative run compared

* The peptide was not appreciably soluble in 6 M guanidine hydrochloride at neutral pH which necessitated the addition of organic solvent to effect solubility.

** Lowered by the need to collect only the back half of the peptide 209 peak. N.B. It is preferable to collect the front and back of a peak separately when contaminating products are eluted very close to the peak.

Figure 3.19A The Semi-Preparative Reversed-Phase HPLC Purification of Peptide 209.

Conditions of Elution: -

Column: Radial-pak C18

Guard Column: Bondapak C18/Porasil B

Solvent A: 0.1 M ammonium bicarbonate, pH 7.9

Solvent B: 2-propanol:solvent A, 80:20 (v:v)

Detection: 280 nm, 2.0 AUFS

Sample: 23.7 mg of peptide 209 in 20 ml of deformylation reaction mixture diluted to 100 ml with solvent A and loaded through pump A at 3.0 ml/min.

Flow Rate: 1.0 ml/min.

Gradient: Linear, 0-100% solvent B over 8 h.

Yield of pure peptide = 16% (based on weight of Trp(CHO)-peptide 209 and UV absorbance of purified peptide, ε_{280} = 5200 $l.mol^{-1}.cm^{-1}$, M.Wt. = Trp(CHO)-peptide 209 = 2062, M.Wt. peptide 209 = 2034).

Figure 3-19B The Reversed-Phase HPLC Analysis of HPLC Purified Peptide 209.

Conditions of Elution: - as for figure 3-19A with the following modifications.

Guard Column: None

Detection: 280 nm, 0.1 AUFS

Sample: 74 µg of purified peptide 209[a]

a) Based on UV spectrum (ε_{280} = 2500 $l.mol^{-1}.cm^{-1}$, M.Wt. = 2034)

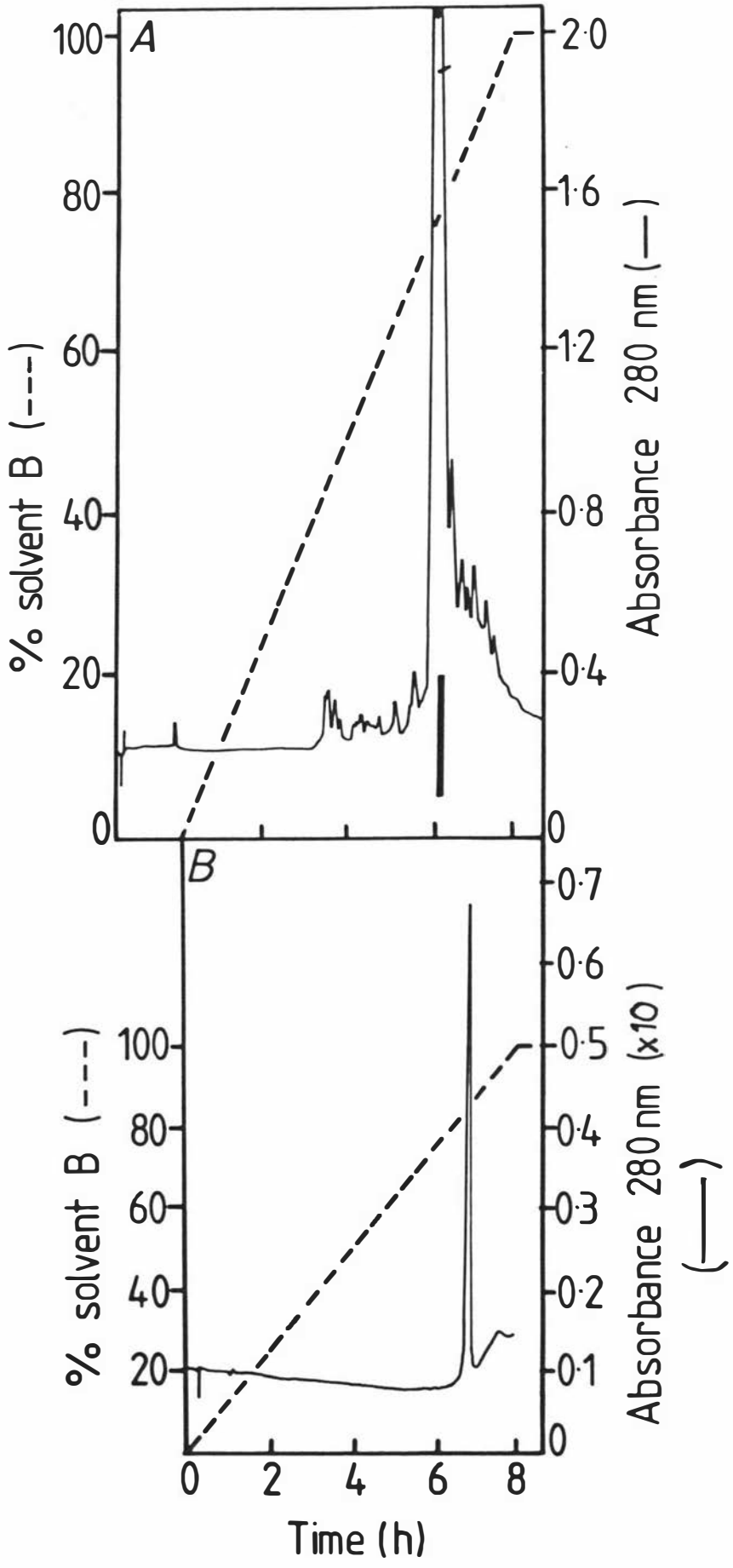
A
B
100
80
60
40
20
0
% solvent B (---)
2·0
1·6
1·2
0·8
0·4
0
Absorbance 280 nm (—)
0·7
0·6
0·5
0·4
0·3
0·2
0·1
Absorbance 280nm (x10) (——)
0
2
4
6
8
Time (h)

with 85% solvent B for the analytical run, which is a general loading phenomenon of reversed-phase HPLC (81). Further criteria of purity have been given in section 3.8.

3.7 The Purification of Peptide 199

A scheme of the sequence of chromatographic techniques and deprotection reactions used in the purification of Peptide 199 is shown in figure 3-20.

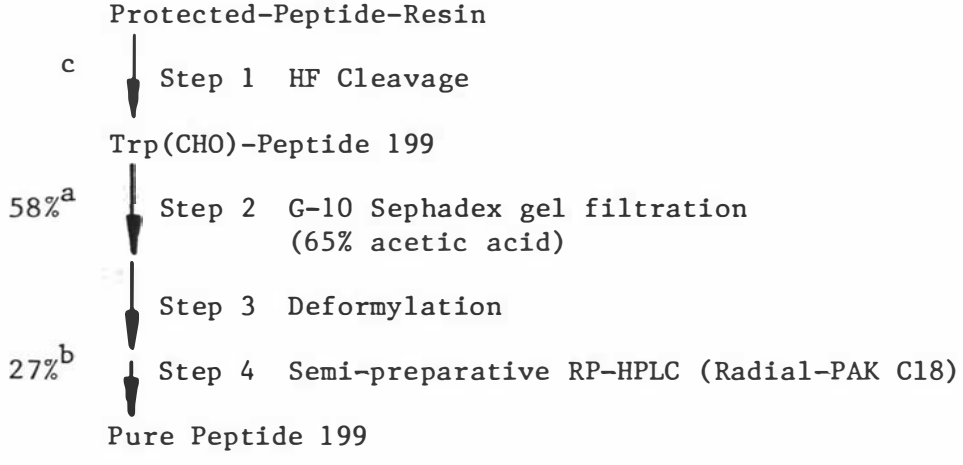

Figure 3-20 The Sequence of Chromatographic Techniques and Deprotection Reactions Used in the Purification of Peptide 199.

Where applicable the yields or recovery of the various steps are given as percentages.

a) By weight (M.Wt. of Trp(CHO)-peptide 199 = 2163).

b) By UV spectrum (ε_{280} = 5200 $1.mol^{-1}.cm^{-1}$, M.Wt. peptide 199 = 2135).

c) Yield of Step 1 included in Step 2.

3.7.1 Hydrogen Fluoride Cleavage - Step 1

The total sample of 5.3 g of peptide-resin was treated in the identical manner to the peptide-resin in section 3.3.1 except that trifluoracetic acid:dichloromethane, 1:1 (v:v) was used to extract the peptide from the resin.

3.7.2 G-10 Sephadex Gel Filtration - Step 2

The total of the extracted, freeze-dried material from Step 1 above was treated exactly as crude Trp(CHO)-peptide 202 in section 3.3.2, yield = 940 mg. This represents a 58% yield based on the original substitution of serine on the resin.

3.7.3 Deformylation of Trp(CHO)-Peptide 199

A sample of 37.7 mg of Trp(CHO)-peptide 199 (freeze-dried powder from the gel filtration on G-10 Sephadex in 65% acetic acid) was added to a solution of 14.3 g guanidine hydrochloride in 25 ml of water. A small amount of material was insoluble and this was removed by filtration through a Millipore HAWP 0.45 membrane filter fitted to a millipore sample clarification kit. The temperature of the solution was brought to 4°C and 3.5 ml of ethanolamine was added causing the pH to rise from 4.0 to 11.3.* The solution was stirred for 5 mins at 4°C (during which time the pH decreased slowly to 11.1) then the solution was neutralised to pH 6.3 by the addition of 6 N HCL.

3.7.4 Semi-preparative Reversed-Phase HPLC - Step 4

Peptide 199 behaved very differently compared to the other peptides with respect to retention on a reversed-phase HPLC system at neutral pH. This will be discussed further in section 5.3.5. In the 0.1 M ammonium bicarbonate system used for purifying the other peptides a very broad peak was observed upon elution of peptide 199 from a Radial-PAK CN column. With the same solvent system and a Radial-PAK C18 column no peak was eluted. It was reasoned that the anomalous behaviour of this peptide was caused by the interaction of ionised silanol groups with the basic groups of the peptide. It was also reasoned that an increased concentration of ammonium ions would reduce this interaction and therefore 0.5 M ammonium bicarbonate was tried as the aqueous component of the mobile phase. This solvent proved very difficult to work with, however, due to formation of carbon dioxide bubbles in the detector and therefore the less volatile salt, ammonium formate was tried. Peptide 199 was retained less and eluted with greater efficiency with increasing concentrations of ammonium formate in the mobile phase. Figure 3-21 shows the effect of increasing concentration of ammonium formate in solvent A upon the elution profile of Trp(CHO)-peptide 199. The neutralised solution from the deformylation reaction (section 3.8.1) was divided into 4 approximately equal portions and purified by 4 separate runs in the HPLC system detailed in figure 3-22A. The collected peaks (see bar in

* pH meter was standardised at approximately 23°C and no attempt to adjust these pH values for the decrease in temperature has been made.

Figure 3-21 The Effect of Increasing the Concentration of Ammonium Formate in Solvent A on the Retention of Trp(CHO)-Peptide 199 in Reversed-Phase HPLC.

Conditions of Elution: -

Column: Radial-PAK C18

Guard Column: Bondapak C18/Porasil B

Solvent A: Concentration ammonium formate as shown for each trace, pH 6.3

Solvent B: 2-propanol:solvent A, 80:20 (v:v)

Detection: 280 nm, 0.1 AUFS

Sample: 120 µg Trp(CHO)-peptide 199 in 250 µl 6 M guanidine hydrochloride

Flow Rate: 1.0 ml/min.

Gradient: Linear, 0-80% solvent B over 60 min.

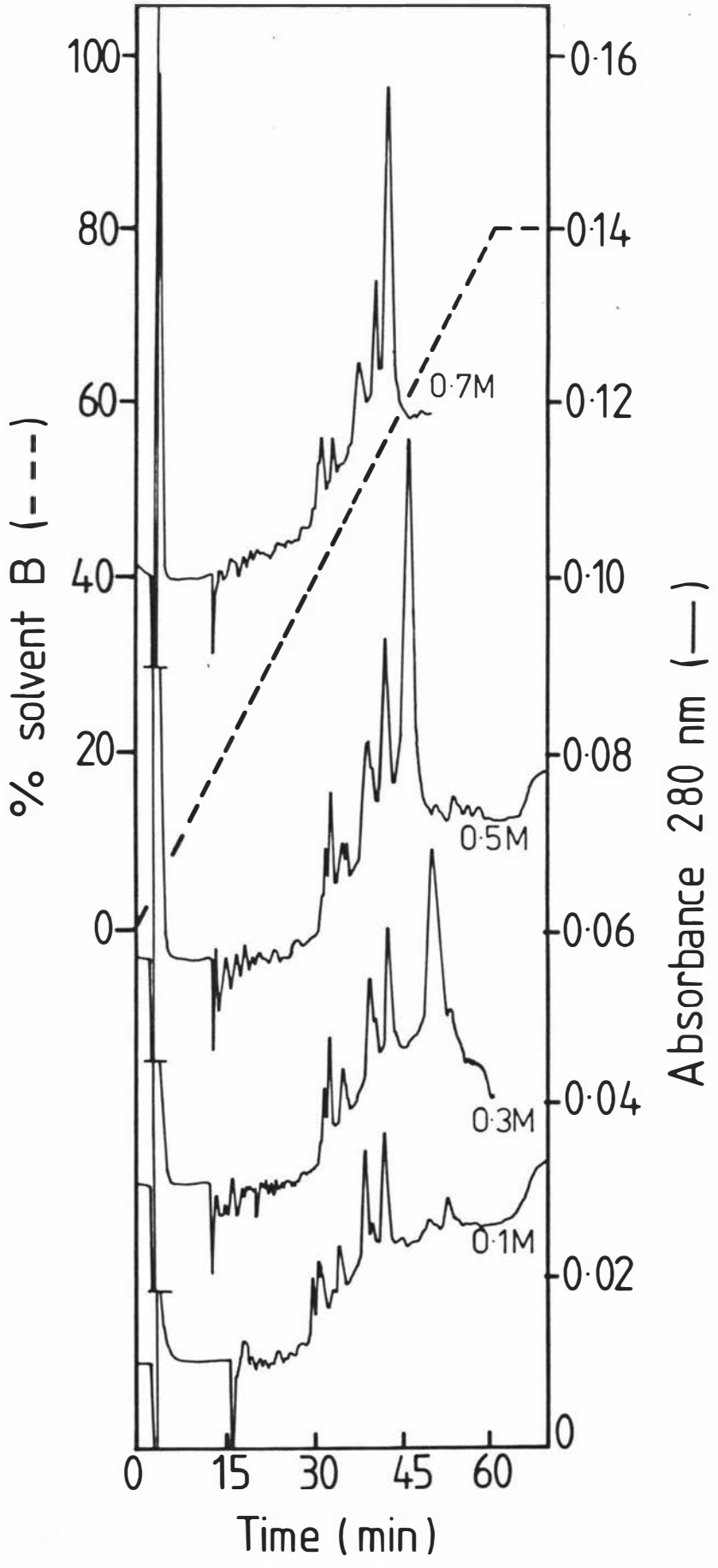
100
80
60
40
20
0
% solvent B (- - -)
0·16
0·14
0·12
0·10
0·08
0·06
0·04
0·02
0
Absorbance 280 nm (—)
0·7M
0·5M
0·3M
0·1M
0
15
30
45
60
Time (min)

Figure 3-22A The Semi-Preparative Reversed-Phase HPLC Purification of Peptide 199

Conditions of Elution: -
Column: Radial-PAK C18
Guard Column: Bondapak C18/Porasil B
Solvent A: 0.5 M ammonium formate, pH 6.3
Solvent B: 2-propanol:solvent A, 4:1 (v:v)
Detection: 305 nm, 2.0 AUFS
Sample: 9.4 mg peptide 199[a] in 12.5 ml of the neutralised deformylation mixture, diluted to 40 ml with solvent A, filtered,[b] and loaded through pump A at 2.0 ml/min.
Flow Rate: 1.0 ml/min.
Gradient: Linear, 0-80% solvent B over 60 min.
Recovery: the collected peak represents a 27% recovery[c] of purified peptide. Rechromatography of this sample results in a 95% recovery.[c]

Figure 3-22B The Reversed-Phase HPLC Analysis of HPLC Purified Peptide 199.

Conditions of Elution: -
Column: Radial-PAK C18
Guard Column: Bondapak C18/Porasil B
Solvent A: 1.0 M ammonium formate, pH 6.3
Solvent B: 2-propanol:solvent A, 4:1 (v:v)
Detection: 280 nm, 0.2 AUFS
Sample: 60 µg[c] of HPLC purified peptide 199 in 800 µl 6 M guanidine hydrochloride
Flow Rate: 1.0 ml/min.
Gradient: Linear, 0-100% solvent B over 2 h

a) Based on weight of Trp(CHO)-peptide 199 used in deformylation.

b) Millipore HAWP 0.45 membrane filter.

c) By UV spectra (ε_{220} = 5200 $l.mol^{-1}.cm^{-1}$, M.Wt. = 2135)

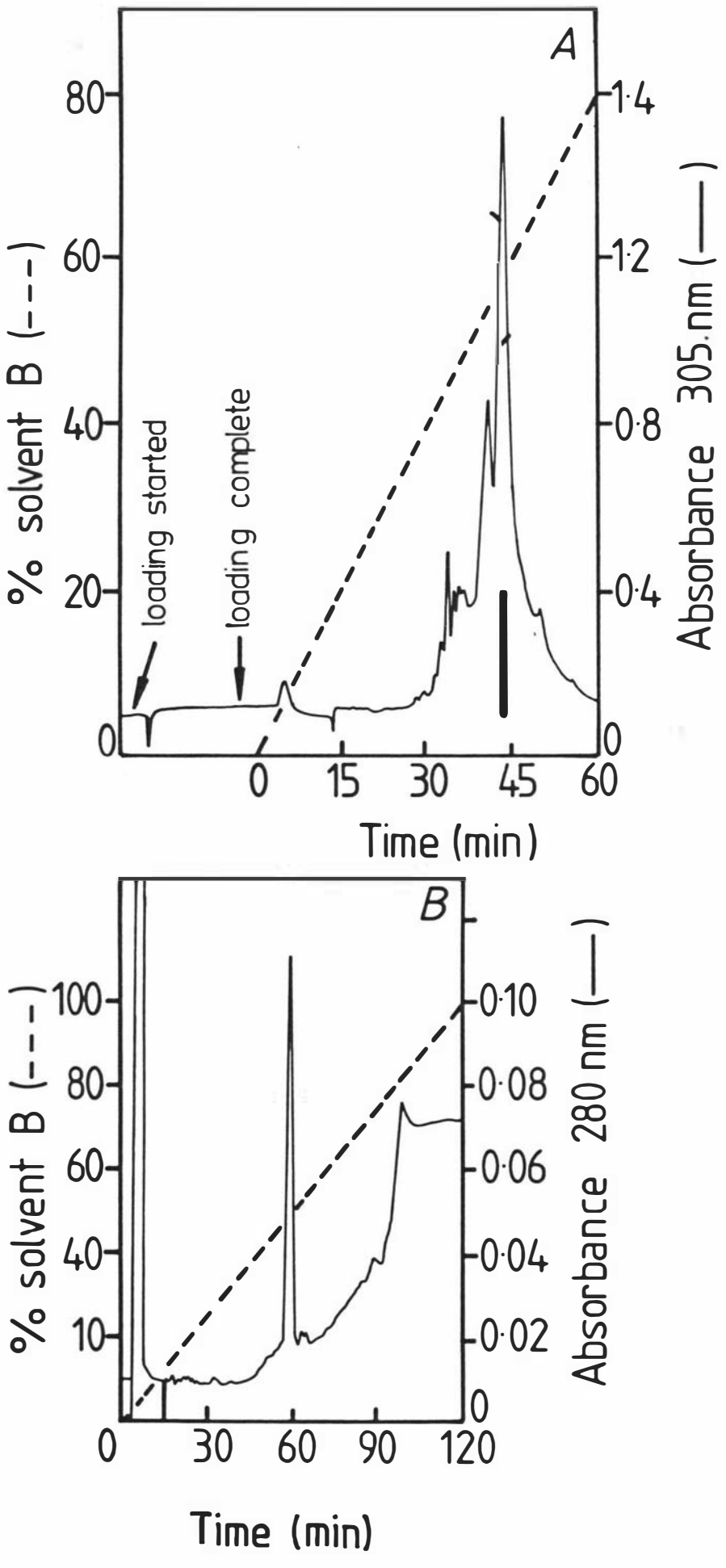
A
80
60
40
20
0
% solvent B (---)
1·4
1·2
0·8
0·4
0
Absorbance 305 nm (——)
loading started
loading complete
0
15
30
45
60
Time (min)
B
100
80
60
40
10
% solvent B (---)
0·10
0·08
0·06
0·04
0·02
0
Absorbance 280 nm (——)
0
30
60
90
120
Time (min)

figure 3-22A) were pooled and diluted to 22 ml* with 78 mM ammonium bicarbonate to bring the concentration of ammonium ions to 0.1 M and the concentration of 2-propanol to 5%. A sample of this solution was diluted with 5% 2-propanol in 0.1 M ammonium bicarbonate until the absorbance of the solution at 280 nm was 0.2 absorbance units. This solution was used in the phospholipid binding study. The purity of the peptide can be judged by the reversed-phase HPLC analysis of a sample of the HPLC purified peptide 199, figure 3-22B. Further criteria of purity are given in section 3.8. The yield of recovered peptide was 27% however a rechromatographed sample of the purified peptide was eluted with a 95% recovery.**

3.8 Demonstration of Purity

Each of the HPLC purified peptides has been analysed by a reversed-phase HPLC system at neutral pH and shown to be homogeneous, figure 3-23. The use of 2 reversed-phase HPLC systems at different pHs has been shown to be an extremely powerful analytical method of separating closely related peptides (165,185).*** Therefore the purified peptides were also analysed in a 1% triethylammonium phosphate system at pH 3.2. The results of this analysis are shown in figure 3-24. All of the peptides show good purity, however, peptide 199 contains a low level of impurities (trace f). Trace (a) shows the characteristic baseline found in a blank gradient with the TEAP system.

The amino acid analysis of the hydrolysates of each of the purified peptides is given in table 3-1. These analyses are in excellent agreement with the theoretical number of amino acids in each peptide.

* It is important to dilute the collected fraction because the concentration of peptide on elution is high enough to cause precipitation of the peptide.

** By UV spectrum (ε_{280} = 5200 $l.mol.^{-1}$ cm^{-1}, M.Wt = 2135)

*** References (82) and (83) also give examples of the separation of very closely related peptides by reversed-phase HPLC.

Figure 3-23 The Reversed-Phase HPLC Analysis of Synthetic Peptides at Neutral pH.

This figure describes the analysis of each of the synthetic peptides on different reversed-phase HPLC systems as described in the noted figure legends.

A: - peptide 202 (see figure 3-9B)

B: - peptide 208 (see figure 3-17B)

C: - peptide 209 (see figure 3-19B)

D: - peptide 203 (see figure 3-15C)

E: - peptide 199 (see figure 3-22B)

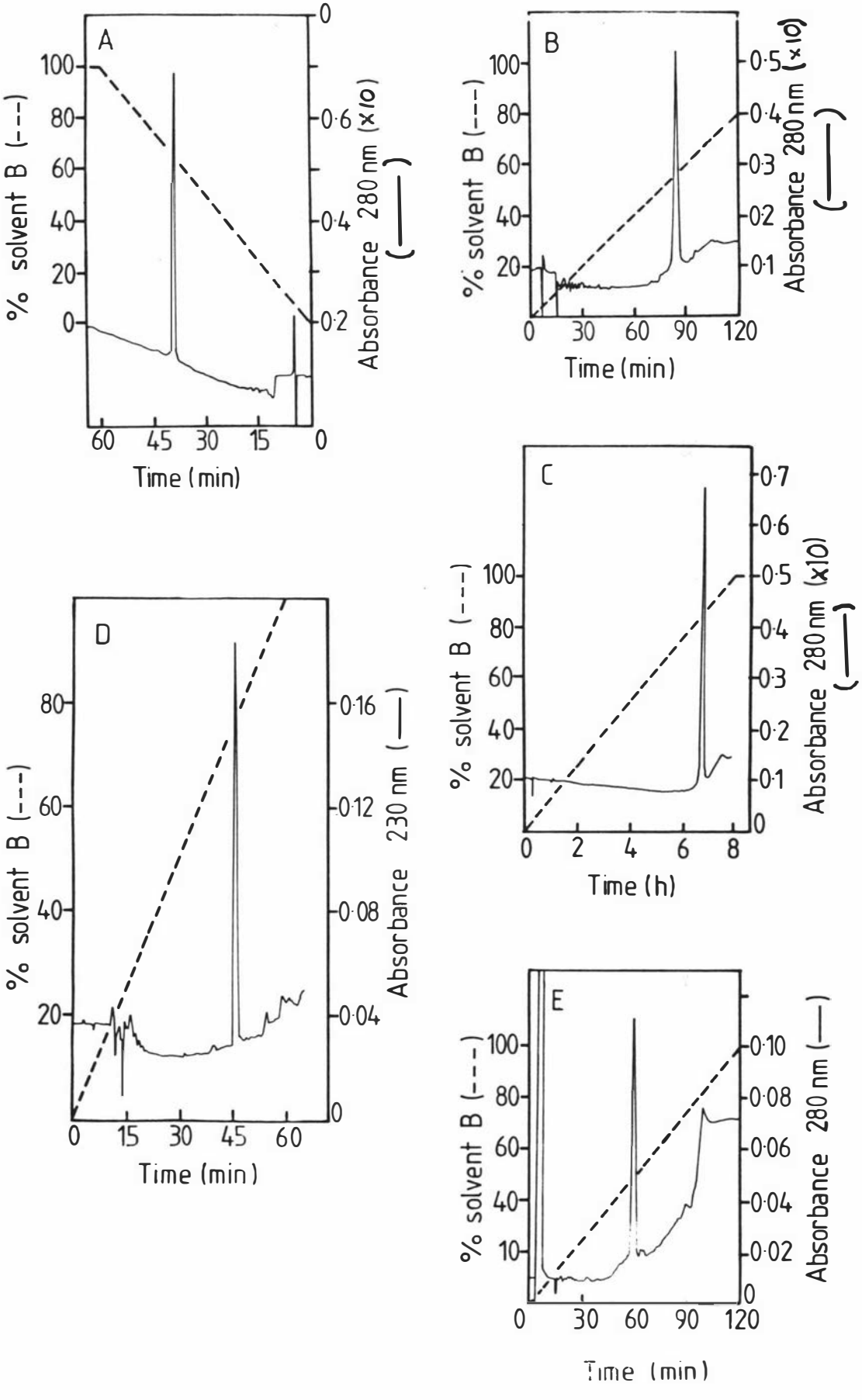
A
% solvent B (---)
Absorbance 280 nm (×10) (——)
Time (min)
B
% solvent B (---)
Absorbance 280 nm (×10) (——)
Time (min)
C
% solvent B (---)
Absorbance 280 nm (x10) (——)
Time (h)
D
% solvent B (---)
Absorbance 230 nm (——)
Time (min)
E
% solvent B (---)
Absorbance 280 nm (——)
Time (min)

Figure 3-24 The Reversed-Phase HPLC Analysis of Synthetic Peptides at Acid pH.

Conditions of Elution: -

Column: μBondapak alkylphenyl

Guard Column: None

Solvent A: 1% triethylammonium phosphate, pH 3.2

Solvent B: 2-propanol; solvent A, 4:1 (v:v)

Detection: 280 nm; a,b,c,&d 0.2 AUFS; e 1.0 AUFS, f 0.1 AUFS

Samples: a) Blank run (no sample)

b) 13 μg of peptide 202

c) 16 μg of peptide 208

d) 32 μg of peptide 203

e) 72 μg of peptide 209

f) 18 μg of peptide 199

Peptides 208 and 203 were injected in 3 M guanidine hydrochloride

Flow Rate: 1.0 ml/min.

Gradient: Linear 0-100%B over 60 min.

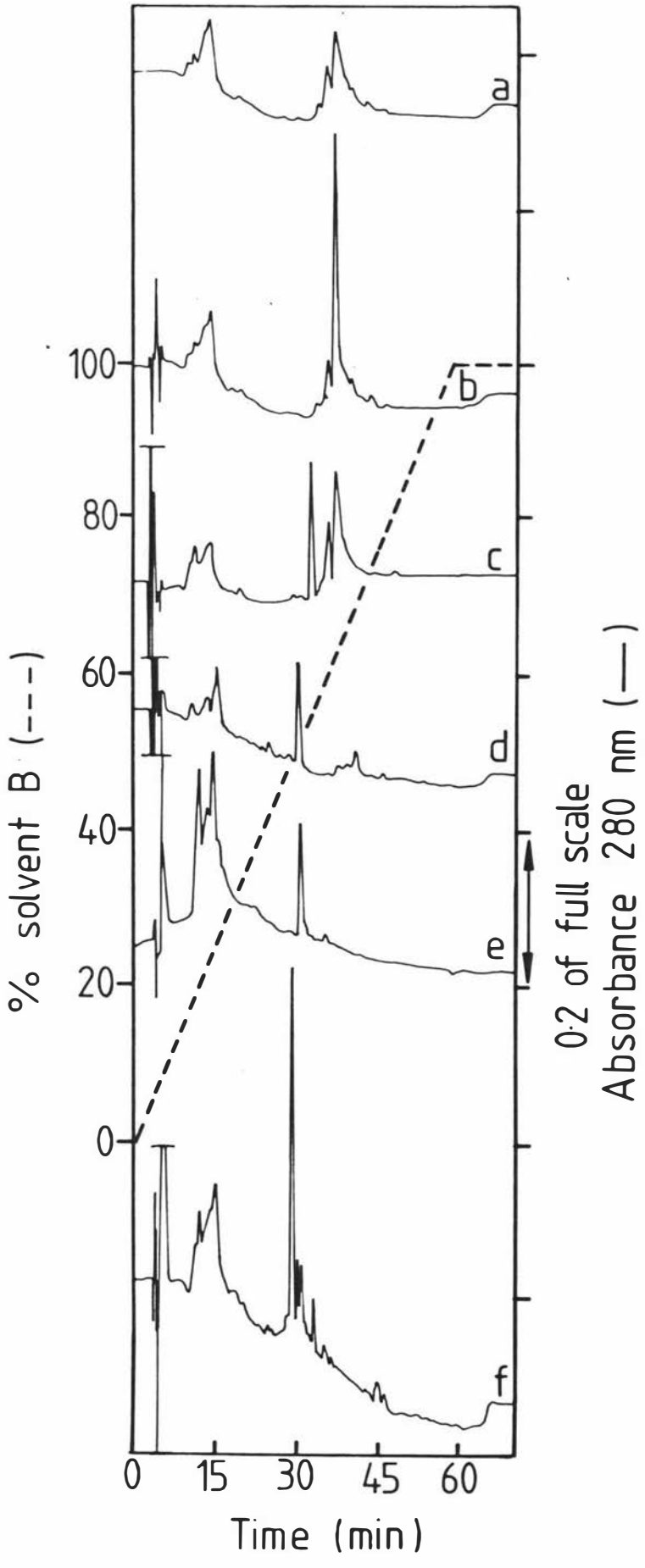
a
b
c
d
e
f
100
80
60
40
20
0
% solvent B (---)
0 15 30 45 60
Time (min)
0·2 of full scale
Absorbance 280 nm (—)

Table 3-1 The Amino Acid Analyses of the Purified Peptides.

Amino Acid	Ratio of Amino Acids in Peptide Hydrolysate [a,e]				
	Peptide 202	Peptide 203	Peptide 208	Peptide 209	Peptide 199
Thr[b]	-	0.8(1)	-	-	-
Ser[b]	2.5(3)	2.3(3)	5.6(8)	2.2(3)	5.9[c](6)
Glu+Gln	3.0(2+1)	2.8(3)	2.0(2)	3.0(2+1)	2.0(2)
Ala	3.1(3)	1.9(2)	-	3.1(3)	1.9(2)
Val	-	0.9(1)	0.9(1)	-	-
Leu	5.0(5)	3.0(3)	4.0(4)	5.0(5)	3.0(3)
Tyr[b]	1.1(1)	1.0(1)	1.2(1)	1.1(1)	1.0(1)
Phe	1.1(1)	1.0(1)	1.2(1)	1.1(1)	1.0(1)
Lys	2.0(2)	1.8(2)	1.9(2)	2.0(2)	2.0(2)
Arg	-	-	-	-	1.0(1)
Trp[d]	N.D.(1)	N.D.(1)	N.D.(1)	N.D.(1)	N.D.(1)

a) Conditions of hydrolysis: 6N HCl, 22 h, 110°C in evacuated tubes.

b) Values not corrected for oxidation except where stipulated by footnote (c).

c) Values corrected for oxidation by quantitation of a series of timed hydrolyses and extrapolation back to zero time.

d) N.D. = not determined. Analysis of the UV spectrum of each peptide shows that each peptide contains approximately 1 residue of tryptophan (ε_{280} = 5200 $1.mol^{-1}.cm^{-1}$).

e) Values in parenthesis are the theoretical ratios of amino acids in the peptides.

The UV spectra of the purified peptides are well defined as shown in figure 3-25. The shoulder at 275 nm is not apparent in peptides 203, 208 and 199 due to the presence of tyrosine in these peptides which has a small absorbance at this wavelength.

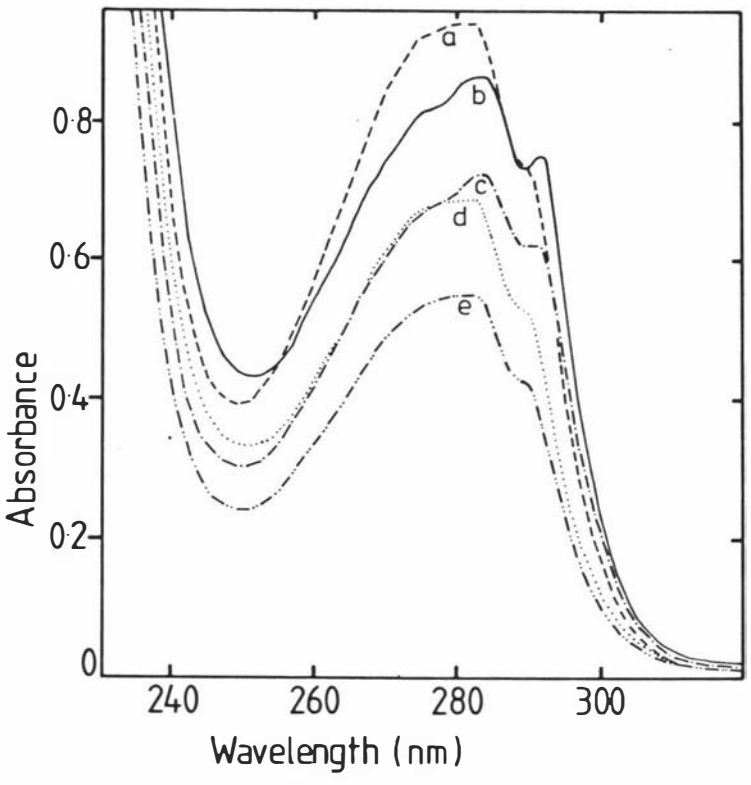

Figure 3-25 The UV Absorbance Spectra of the Purified Peptides.

UV spectra of the HPLC purified peptides at variable concentration before dilution to an equal concentration.

a) Peptide 203 (-----)

b) Peptide 202 (——————)

c) Peptide 209 (-·-·-)

d) Peptide 199 (.....)

e) Peptide 208 (-··-··-)

3.9 Conclusion

The purification of lipophilic peptides has been shown to be difficult by some low yields of purified peptides which have been observed (84, 85). This is partially due to the low solubility of these peptides in aqueous solvents and their tendency to aggregate. Semi-preparative reversed-phase HPLC, e.g. figures 3-5A, 3-9A, 3-15A, 3-17A, 3-19A and 3-22A, would appear to be an excellent alternative to the time consuming and sometimes low yielding conventional chromatography of these peptides. Not only is it fast and convenient but the homogeneity of the isolated product is excellent.

PART C

CHAPTER 4 BACKGROUND FOR THE HYDROPHOBIC EFFECT

4.1 Introduction

The following chapter is a discussion of the present understanding of the hydrophobic effect and its relationship to the various processes which are apparently driven by this effect. This discussion will provide a basis for the understanding of the role of the hydrophobic effect in the association of peptides with reversed phase bonded silicas (HPLC) and with phospholipids and hence enhance the continuity of the remainder of the text.

The hydrophobic effect is evident as the observed unwillingness of nonpolar substances to interact with aqueous environments (86-90,95). The term hydrophobic implies a hatred for water, however, this is not the case. To quote Hartley: "The antipathy of the paraffin-chain for water, is however, frequently misunderstood. There is no question of actual repulsion between individual water molecules and paraffin chains, nor is there any very strong attraction of paraffin chains for one another. There is, however, a very strong attraction of water molecules for one another in comparison with which the paraffin-paraffin or paraffin-water attractions are very slight, as is well known from the work of Harkins on cohesion of liquids. It is this water-water attraction which satisfies itself by the extrusion of paraffin chains ....." (89). Considering the relatively simple concept of the hydrophobic effect outlined above, it is surprising to find the large degree of controversy and confusion which exists in this field (88,93,99). A common misconception is that the observed affinity of hydrophobic groups for each other in the presence of water is the result of van der Waals' bonding between the hydrophobic groups (7,91,92). This improper consideration has no doubt arisen from the use of the expression "hydrophobic bonding" which implies a direct form of bonding between hydrophobic groups (93). It has been reasoned that van der Waals' forces would not be influenced by temperature (as the hydrophobic effect is). Furthermore these non-covalent interactions are also found between water and hydrocarbons (88,93,94,96). A comparison of the strengths of bonding has revealed that van der Waals' forces are an order of magnitude smaller than hydrophobic interactions (152).

From the outset we must consider two types of process driven by the hydrophobic effect which are often not separated and thus jointly referred to as "the hydrophobic effect". These are defined by Ben-Naim (94).

(a) Hydrophobic Hydration refers to the relative preference of a solute for two solvents when one of these solvents is water. This process is described by standard thermodynamics of transfer. It should be noted that only solute-solvent and solvent-solvent interactions are considered.

(b) Hydrophobic Interaction refers to the interaction between two or more nonpolar or amphipathic solute molecules in water. This term replaces the hydrophobic bond used previously.*

In the limit of very large aggregates formed by hydrophobic interactions, the process of hydrophobic interaction becomes hydrophobic hydration. This is because each added solute molecule is accommodated in the interior of the aggregate, completely separate from the aqueous environment, and therefore is effectively partitioning into another solvent (94).

Hydrophobic interactions have been postulated to be an integral part of the processes of conformational changes of biopolymers, binding of substrate to enzyme, the association of subunits to form a multi-subunit enzyme and processes involving high levels of aggregation such as formation of biological membranes and the organisation of biological molecules to form a functional unit in a living system (88,94,95). Considering the importance of these processes it is surprising to find that our present knowledge and understanding of hydrophobic interactions is only in its very elementary stages (94).

It should be noted that in the following discussion the processes of hydrophobic hydration and hydrophobic interaction will always be expressed in the direction of decreasing interaction with water, e.g. water to hexanol partitioning, nonpolar solute association and the transfer of nonpolar gases from water into the gas phase (degassing).

* The term apolar bond is a more general definition not requiring aqueous solution and thus this term is better replaced by solvophobic interactions or apolar interactions.

The most studied systems investigating the hydrophobic effect involve relatively simple water to gas or water to organic solvent transfers. Such studies will be summarised in the opening part of this chapter, sections 4.3.1 and 4.3.2. Later sections will be dedicated to more complex systems involving many sorts of interactions, sections 4.4.1 and 4.4.2. The results of studies on simple systems are often quoted to support various experimental observations, however, it should be recognised that in some ways the simple processes are quite different from the complex processes. Therefore the direct utilization of results from the simple systems to explain more complex processes should be conducted with caution. A summary of the contrasts between the thermodynamics of the processes is given in section 4.5.

4.2 The Theory of the Hydrophobic Effect

According to Ben-Naim there is no completely satisfactory theoretical treatment of hydrophobic hydration which allows the calculation of the standard free energy of hydration (97). Semi-theoretical methods have therefore been employed all of which involve serious approximations especially when applied to such a complex fluid as water. Nevertheless the theory of hydrophobic interactions has been dealt with in detail by Ben-Naim (90). This author has severe reservations about the predictions of pairwise hydrophobic interactions since knowledge of the full pair correlation functions which are used to calculate the free energy change on dimerisation is far from satisfactory (98). In addition to the extreme technical difficulties involved in calculating the full pair correlation functions, the lack of appropriate experimental data means that the success or failure of a particular treatment cannot even be qualitatively assessed. For this reason Ben-Naim suggests that the major effort in the field of hydrophobic interactions should be focused on the experimental rather than the theoretical side of the problem. In view of these uncertainties current theoretical models for hydrophobic interactions will not be discussed here and the reader is referred to Ben-Naim (90) for details of these models. Hall has said that superficially the arguments may look impressive but on closer examination it turns out that often they are essentially sterile (143).

4.3 Hydrophobic Hydration and Simple Model Systems

4.3.1 The Solubility* of Nonpolar Gases in Water

There has been intense study in the area of solubility of nonpolar gases in water as discussed in a recent review (103). It is important to realise that studies of the thermodynamics of these simple systems require some assumptions as to the ideal behaviour of the gas and the resulting solution. As a consequence, the activity coefficients of the gas and solution may be incorrect resulting in the calculation of incorrect entropy values. The degree of influence these assumptions have on thermodynamic quantities is uncertain at present (99).

A constant feature of the solubility of nonpolar gases in water appears to be the large positive entropy of degassing (negative entropy of solution) which is the major term in the free energy calculation over a wide range of temperature. It has been proposed that the cause of this large positive entropy change is the increased mobility of water molecules released from proposed regions of high order ("ice-like" structure) at the nonpolar solute-water interface (100,101). An alternative theory has been proposed by Wertz (102) who claims that the large positive entropy change observed on the degassing of a large number of gaseous solutes can be explained simply by the gain in entropy of the solute molecule itself.**

Another observation is apparently common to all the gas solubility systems studied. This is the large value of the change in heat capacity (ΔC_p) for the water to gas transition which is exhibited by the non-linear Van't Hoff plots (ΔG v's $1/T$). Such a nonlinear dependence of the enthalpy change on temperature has been viewed by Tanford as being caused by the varying structure of water as temperature is changed (100, see also section 4.3.2).

* In terms of the defined direction of reaction being the hydrated to the nonhydrated state the process might be better described as the degassing of nonpolar gases from water.

** Ben-Naim and Tanford have claimed that such an entropy change would not be large enough to explain the overall change in entropy.

4.3.2 Water - Organic Solvent Partitioning

The process of water-organic solvent partitioning is another easily studied area of hydrophobic hydration. This process has much in common with the previously discussed solubility of nonpolar gases in water. Many studies have shown the decreasing tendency of nonpolar and amphiphilic solutes to partition into water with the increasing non-polar character of the solute (105-107). The dominant term in the free energy equation is again the large positive entropy change for the hydrated to nonhydrated transfer (87,100,106). In addition non-linear van't Hoff plots are found implying that the heat capacity change (ΔC_p) is large for the partition transfer (87,100). It is worthwhile noting that the entropies and enthalpies of transfer are most often calculated near the minima for the solubility of the solutes in water at different temperatures (e.g. 25^{o}C). At higher temperatures the ΔH contribution may well be much more important. Tanford has noted anomalous entropy and heat capacity effects in the solubility of alkanes in aqueous solution (100). The heat capacity of the solubilization of the alkane is not constant but is itself a function of temperature, as evidenced by non-linear van't Hoff plots. Tanford attributes the observed change in heat capacity to the change in state of water molecules brought about by the presence of the dissolved hydrocarbon (100). Furthermore Tanford notes that, whereas the free energy of the transfer increases linearly with increasing hydrocarbon chain length and seems to depend upon hydrocarbon-water interfacial area, the corresponding enthalpy and entropy functions show no corresponding regularity (100). This indicated to Tanford that the water molecules of the hydrocarbon-water interface do not have a unique way of arranging themselves, but that different arrangements are possible depending on the precise spacial requirements. He concluded that these different arrangements must differ in enthalpy and entropy, but must do so in a mutually compensating fashion so that no irregularity in free energy can be detected. Tanford postulates the existence of two states of water molecules at the hydrocarbon water interface, one with a high enthalpy and entropy state (strong hydrogen bonding at interface) and one with a lower enthalpy and entropy state, which differ very little in free energy (100). An increase in temperature would shift the equilibrium to the higher enthalpy state resulting in the anomolous heat capacities observed.

4.4 Hydrophobic Interactions and More Complex Systems

4.4.1 The Hydrophobic Effect and Reversed Phase HPLC

It is generally accepted that the hydrophobic effect* is responsible for the retention of nonpolar or amphipathic solutes on nonpolar supports when the mobile phase is aqueous (108-110). The mobile phases used in reversed phase chromatography often contain mixtures of water and polar organic solvents e.g. methanol and acetonitrile. There is a difficulty here since the hydrophobic effect is applied only to completely aqueous solutions. To circumvent this difficulty the Solvophobic Theory (111) has been applied to reversed-phase chromatography by Melander and Horvath (109,146). Sinanoglu originally used the theory in order to explain the coil to helix transition of DNA in different solvents (111). He correlated the observed high stability of coiled DNA in aqueous solution with the high cohesiveness of water and the decrease in solvent cavity surface area caused by stacking of the bases in the coiled conformation. Furthermore an analysis of the thermodynamic contributions expected revealed that the most important contribution to the coil to helix transition was a negative enthalpy caused by the decrease in solvent cavity area (111). This is compatible with the observed decrease in stability of helical DNA with increased temperature.

There is a conceptual point to be made here. The solvophobic theory encompasses solvents which do not contain water at all, whereas, hydrophobic effects are presumed to be caused by the special properties of water. Therefore inherent in the solvophobic theory is the notion that the special cohesiveness of water is merely an extreme in a continuum of solvent cohesiveness (111). This concept is supported by the approximate obedience of many liquids including water to a linear

* The more general term "hydrophobic effect" is used here since it is unclear whether the solute is completely partitioned into the nonpolar support and its adsorbed layers of nonpolar mobile phase components or whether the bound solute maintains some interaction with the mobile phase. These two mechanisms of interaction, partition and adsorption respectively, are currently under evaluation thus it is uncertain which of the respective terms hydrophobic hydration and hydrophobic interaction applies to reversed phase chromatography.

relationship between surface tension of solvent and the standard free energy of solution of argon in the solvent (112).

The solvophobic theory is expressed in terms of the free energy change calculated for the dissolution of a solute from a hypothetical gas phase at atmospheric pressure into a particular solvent. This calculation may be split up into two components being the formation of a cavity in the solvent for the solute molecule and the interactions of the solute with solvent caused by van der Waals' interactions, electrostatic interactions and entropy change associated with the restricted volume of the solute relative to the gas phase. A general prediction of this theory is that the retention factor k' should decrease with decreasing surface tension of the solvent. This is not a simple relationship however because microscopic surface tension is not directly related to bulk surface tension and in fact microscopic surface tension cannot be determined for solvent mixtures without various assumptions. By this theory the free energy of the interaction of a solute with the reversed phase is a function of the interfacial surface tension, the static dipole moment of the solute, the contact surface area of the associated species, the polarizability of the solute, the molecular surface area and volume of the solute, the static dielectric constant of the solvent, the phase volume, the mole volume of solute and the temperature (110).

As with the other phenomena of the hydrophobic effect many reversed phase HPLC studies are available to demonstrate that increasingly nonpolar solutes have decreasing affinity for the aqueous mobile phase. Linear plots of ln k' v's alkyl carbon number have been obtained for many solutes and systems (113-116).

Several studies have also been made at different temperatures thus allowing the calculation of enthalpies of retention. Van't Hoff plots (ln k' v's $1/T^{o}K$) are characteristically linear for the studies completed so far (116-118,141,145,146). This implies there is no change in the heat capacity for the transfer of solute from mobile phase to the stationary phase at least in the temperature range at which these studies were carried out. If Tanford's hypothesis of the dual nature of the thermodynamic states of water (i.e. high temperature and low temperature states)(103) is correct we might expect to find curved van't Hoff plots for all processes involving the hydrophobic effect.

The occurrence of linear van't Hoff plots in reversed phase HPLC therefore implies that either Tanford's hypothesis is incorrect or some other contribution to the enthalpy of association exactly balances the effect of the changing enthalpy state of water with temperature in the HPLC systems. It could be said that the presence of organic solvents disturbs the thermodynamics of the pure water system and that therefore the thermodynamic quantities calculated in HPLC systems are not relevant to the hydrophobic effect. Such a statement may be refuted by consideration of linear lnk'v's organic solvent composition plots which show that no sudden change in the mechanism of retention occurs on the addition of organic solvent to pure water (148,149). Secondly it is a fact that even in reversed-phase systems containing no organic solvents, an increase in temperature decreases retention showing that ΔH is negative (141,145,146).

Most importantly the negative enthalpies of association exhibited in the reversed-phase HPLC systems are a very important contribution to the retention and appear to dominate the free energy term (116-118, 147).

The calculation of entropy values for the association of solutes with reversed-phase bonded silicas (HPLC) requires the estimation of the phase ratio, ϕ, which reflects the amounts of mobile and stationary phases. No rigorous calculation of the value for ϕ has been demonstrated.* However, to within a large margin for error in the ϕ value, the values obtained for entropy changes in the HPLC systems indicate that the enthalpy of association is the predominant term in the calculation of free energy of association of the solute. Contrary to the role of entropy change in the simple systems, the entropy of association appears to be a negative quantity in reversed-phase HPLC, i.e. the entropy change does not favour association of the solute with the reversed phase bonded silica.

* The mechanism of binding to reversed phases is uncertain at present. Due to this uncertainty, calculation of the phase ratio is subject to error (see section 5.1.3).

4.4.2 Hydrophobic Interactions and Amphiphile Association

4.4.2.1 Micelle Formation

Hydrophobic interactions play an important role in the aggregation of amphiphiles such as phospholipids to form the stable structures of membranes and lipoproteins. According to Tanford the aggregation of amphiphiles to form micelles in aqueous solution involves the influence of two opposing forces (120). The attractive force arises from hydrophobic interactions concerned with the nonpolar moiety.* The repulsive force arises from the polar moiety and prevents growth of the micelles to large size. (Even in systems where very large micelles are formed a repulsive force must be present in order to prevent the amphiphile separating into an entirely distinct phase). The growth of the micelle is arrested when the free energy changes caused by the two forces acting on an amphiphile molecule aggregating with a formed micelle are exactly equal and opposite. In the case of ionic amphiphiles electrostatic repulsion between like charges is a major factor in the repulsive force. The amphiphile's polar groups on the outside of the micelle are forced closer together by an increase in micelle size. In the case of non-ionic amphiphiles the repulsive force is due to the preference of polar groups for hydration rather than self association with the polar groups becoming closer together (and hence less hydrated) with increasing micelle size. In the cases where the amphiphile is a lipid with 2 acyl chains as with phosphatidylcholines, bilayers are formed to decrease the surface area covered by the polar head groups (120). Tanford predicts a 60% greater negative free energy of association of these amphiphiles (compared to monoacyl lipids) caused by hydrophobic interactions. This greater attractive force must be balanced by a greater repulsive force between polar head groups in size stable vesicles. Thus the potential associated with charge repulsions are higher in diacyl lipid aggregates compared to monoacyl lipid aggregates. Considering the importance of the repulsive forces between head groups

* An important factor in micelle formation is that a minimum number of amphiphiles must become associated with each other before the hydrocarbon-water interface can be effectively eliminated. This gives rise to the phenomenon of critical micelle concentration (i.e. a minimum concentration of amphiphile must be present before any micelles are formed).

of diacyl phospholipids, any attempt to explain the binding (or partitioning) of other amphiphiles, e.g. peptides, to phospholipids must entail an analysis of the effect of the added amphiphile on the repulsive forces. This is particularly relevant when the amphiphile is charged as in the case of peptide-phospholipid interactions.

It is worthwhile to note that the area per phospholipid head group increases moving from the gel to liquid crystalline state. This process has a direct analogy with melting of solids in 3 dimensions. The high co-operativity of the pure phospholipid transition can be explained by the freedom of thermal energy transfer between hydrocarbon chains and the similarity of all amphiphile environments. Little is known about the thermodynamics of micelle formation (143).

4.4.2.2 Phospholipid - Simple Solute Interactions

Very little data is available for partitioning of organic molecules between aqueous solution and phospholipids or membranes. One system which has been investigated is the partitioning of n-alcohols into various membranes and phosphatidylcholine dispersions. Free energies per methylene group of the n-alcohols calculated from the partition equilibrium concentration were in good agreement as shown in Table 4-1.

Table 4-1 The Free Energies of Partitioning Per Methylene Group for n-Alcohols in Aqueous-Phospholipid Systems

Partitioning System	ΔG_{CH_2} [a]	Ref
Aqueous/erythrocyte ghosts	-0.695	(123)
Aqueous/toad bladder membranes	-0.780	(124)
Aqueous/DMPC liposomes[b]	-0.540	(91)
Aqueous/DPPC liposomes[b]	-0.745	(125)
Aqueous/egg yolk P.C. liposomes	-0.630	(125)
Aqueous/octanol	-0.705	(125)

a) The incremental free energy per methylene group for partitioning from the aqueous component to the phospholipid component in kcal per mole of methylene groups.

b) DMPC = dimyristoyl phosphatidylcholine,
DPPC = dipalmitoyl phosphatidylcholine.

Thus for the n-alcohols at least the free energy per methylene group of the transition from water to various phospholipids varied little and was approximately equal to the value of -0.690 kcal/mol calculated for the octanol/water partition system. This is good evidence that the same driving force is responsible for both effects, i.e. that the hydrophobic effect influences the partitioning through a high free energy of the hydrated hydrocarbon moiety. The contribution of the alcohol group itself varied considerably depending upon the phospholipid, with values of between +0.790 and +3.0 kcal/mol for the free energy of transfer, probably dependent upon the environment of the alcohol moiety.

A novel partitioning system has recently been studied (126). It consisted of various amphiphiles (including phospholipids) adsorbed to a reversed-phase HPLC packing (Corasil-C18). The free energy of partitioning per methylene group for n-alcohols in this system had an average value of -701 cal/mol. This compares very favourably with the aqueous-phospholipid partitioning systems above. The use of microparticulate packings in this system promises to provide an exciting model for aqueous-phospholipid partitioning systems.

The enthalpies and entropies of partitioning of n-alcohols in an aqueous-DMPC system have been determined by Katz and Dimond (91). They found that above the phase transition temperature of DMPC the transfer of n-alcohols from aqueous solution to DMPC was exothermic i.e. ΔH was negative. Furthermore the entropy change ΔS was also negative. Thus it appears that the thermodynamics of alcohol partitioning between aqueous solution and phospholipids has more in common with reversed-phase HPLC systems than with water-organic solvent partitioning systems. This point has been used by Wise as an argument for using HPLC systems as models for aqueous solvent-membrane partitioning (126). Below the phase transition temperature of DMPC the partitioning of n-alcohols in the water-DMPC system has positive values for both ΔH and ΔS (91). This has been interpreted as being due to the disruption of the crystallinity of the "frozen" acyl chain groups of the DMPC which dominates any other contributions.

4.4.2.3 Phospholipid-Protein and Phospholipid-Peptide Interactions

The amphipathic helix model proposed by Segrest and others to explain phospholipid-apolipoprotein association presents strong *a priori* evidence for the importance of hydrophobic interactions in this process. Indeed there is considerable evidence that hydrophobic interactions contribute to phospholipid-apolipoprotein association (32,119,121,144). Assman *et al.* have interpreted their NMR results as indicating that hydrophobic interactions between phospholipid acyl chains and nonpolar amino acid residues are more important than hydrophilic interactions (119). Similar conclusions were drawn by Stoffel *et al.* based on their results (121). In these studies it appeared that only the regions of the acyl chains furthest from the phospholipid head group exhibited significant decreases in relaxation times (T1) consistent with the tighter packing of these regions on binding to protein. However, it was recognised that the regions of the acyl chains closer to the phospholipid head group were already tightly packed in the absence of apolipoprotein. Andrews *et al.* have observed a reduction in the cooperativity of the acyl chain motion upon addition of apoHDL to DMPC (121). This results in an increase in the temperature range of the gel to liquid-crystalline (fluid) phase transition temperature. Many other studies have shown similar increases in the range of the phase transition temperature upon addition of protein (52). Furthermore these authors interpreted the lack of specificity of the association as being due to the lack of specificity and direction which hydrophobic interactions exhibit. Perhaps one of the most significant indications that the hydrophobic effect is important in phospholipid-apolipoprotein interactions comes from work by Chen *et al.* (144). In these studies ApoC-I was labelled with nitroxide or ^{13}C enriched at methionine-38. EPR spectra of the nitroxide labelled ApoC-1 had correlation times of 0.22 ns and 0.35 ns in the absence and presence of DMPC respectively. This indicated that the methionine residue was restricted in motion in the DMPC complex. NMR spectra of the ^{13}C enriched ApoC-1 in a disaggregated form (1.6 M Gdn.HCl) had a line width and spin-lattice relaxation time of 2.6 Hz and 970 ms respectively. These values substantially changed if the protein was allowed to interact with DMPC (4.7 Hz and 380 ms) or allowed to attain its native conformation (6.0 Hz and 320 ms). These results are consistent with the hypothesis that

hydrophobic residues are significantly more tightly packed in the DMPC complex or in the native state compared to the denatured state. The large changes observed in the EPR and NMR spectra of the methionine analogue must be compared with the much smaller changes observed in the spectra of phospholipids upon association with apolipoproteins (119,121). Therefore this study is evidence that the transfer of hydrophobic residues from an aqueous to a more nonpolar environment is a very important contribution to both phospholipid-protein association and to native protein conformation. Further evidence for the change in environment of the nonpolar residues of apolipoproteins upon association with phospholipid comes from fluorescence studies (32). The transfer of tryptophan and tyrosine residues from an aqueous environment to a more nonpolar environment results in a change in the fluorescence emission maximum of these residues. Such changes have been observed in many studies of apolipoprotein-phospholipid association (32). In summary it appears that hydrophobic interactions may well be one of the major contributions to phospholipid-protein association. It should be noted, however, that the high average hydrophobicity of a protein is not sufficient to ensure complex formation with phospholipid (150). In this regard it appears that the secondary and tertiary structure of the protein in relation to its hydrophobicity are extremely important facets of the interaction (section 6.1.1).

The thermodynamics of phospholipid-protein and phospholipid-peptide associations are extremely complicated and are only beginning to be studied. The problem is that the overall thermodynamics reflect the combined result of a number of processes which include: phospholipid phase changes, bilayer to micellar phospholipid structural changes, conformational changes and self association of the protein (complex enough by themselves), interaction of the polar amino acid residues with the phospholipid head groups, transfer of hydrophobic amino acid residues to the interior of the hydrocarbon region of the phospholipid aggregate, and the perturbation of the phospholipid environment caused by the last two processes. At present it is not possible to separate the different contributions to the overall thermodynamics.

We know that in many protein-phospholipid association reactions, hydrophobic amino acids are transferred from a more or less aqueous environment to the more nonpolar environment of the phospholipid acyl chain region. The free energy change of this process would appear to

be one of the major contributions to the driving force of protein-phospholipid association from a priori considerations (127,128). However, in view of the complete lack of data available quantitating the hydrophobic interactions in lipid-protein systems we must be very cautious in selecting a model system to describe these hydrophobic interactions. For example the assignment of hydrophobicities to amino acid side chains from experiments on amino acids need not be a good model for the same side chains in a protein. In addition we should not assign an enthalpy or entropy to the process until it can be proved that the model used mimics the thermodynamics of the hydrophobic interactions in the protein-phospholipid system. The authors of some recent studies have simply assumed that the hydrophobic interactions influence the free energy of association of protein and lipids only through a positive change in entropy (127,128). Furthermore these authors noted that when the enthalpies of association of apolipoproteins with phospholipid and the enthalpies of conformational change for apolipoproteins under varying conditions are plotted against the % α-helix change a fairly good correlation is observed (127,128). This was used as evidence that the enthalpy of association observed in protein-phospholipid association was a direct result of the change in α-helix structure. However, the degree of α-helix change is not independent of the degree of association with phospholipid or with the overall conformation of the protein. In addition, hydrophobic interactions are extremely important in protein-phospholipid association and in determining protein structure (section 4.4.2.4). Therefore we could with some justification suggest that the similarity of the enthalpies of the two processes might arise from the hydrophobic interactions which are common to both processes.

A more detailed account of some aspects of lipid-protein association will be given in chapter 6.

4.4.2.4 Protein-Protein Interactions

Hydrophobic interactions have been cited as a major contribution to the stability of proteins as shown in Table 4-2.

Table 4-2 An Estimation of the Free Energy Terms Involved in a Disordered to Native-Transition of a 100 Residue Protein at 37°C, from reference (130).

Source of free energy change	ΔG (kcal/mol)
Conformational entropy	+340
Conformational enthalpy	-100
Hydrophobic interactions[a]	-130
Hydrogen bonds	-10
Ionic bonds	-10
TOTAL	+90

a) The authors admit that the calculated free energy from hydrophobic interactions may be too high due to the assumption that 65 of the 100 residues are apolar and all are transferred from an aqueous environment to one resembling 100% ethanol in the random coil to native structure transition. Nevertheless the hydrophobic interactions still dominate the other bonding considerations.

The total of the contributions to protein stability in Table 4-2 is positive indicating that the native conformation would not be favoured. Of course proteins do have native conformations and therefore we would expect the total of the contributions to be a negative free energy. This suggests that the stability of the native structure of proteins might be small and indeed the free energy of denaturation of proteins is commonly between 10 and 50 kcal/mol (131). Thus the forces stabilising the native structure of a massive protein molecule are much smaller than the strength of one covalent bond e.g. 458 kJ/mol (109 kcal/mol) for the H-H bond in H_2 (132). The predicted influence of temperature on stability of the proteins is to decrease stability by decreasing the hydrophobic interactions and the hydrogen bonding (133). This is disputed by Ben-Naim using a semi-theoretical approach based on the methane-water system (134). Other authors also belong to this school of thought (86,95). Ben-Naim asserts that an increase in temperature will result in increased stability of the protein due to both hydrophobic hydration and hydrophobic interactions. The fact that proteins decrease in stability with increase in temperature is clearly at

variance to this assertion. Ben-Naim was therefore "forced" to conclude that the hydrophobic effect was relatively unimportant to the structure of proteins (134). It should be noted that in this treatment the protein was assumed to be a number of methane molecules linked together by a massless backbone. No attempt was made to correct for the loss of entropy experienced by a methane molecule on "becoming" for example the very restricted methyl group of an alanine residue of a protein. Such considerations have been emphasised by Wertz (102). Furthermore the assertion is at variance to the effect of temperature on hydrophobic interactions in other complex systems (section 4.5). We must therefore suspect that the thermodynamics of the methane-water system may not be directly applicable to the more complex systems.

A recent study of the effect of different denaturant concentrations on the thermal stability of several proteins has indicated that approximately 80% of the negative enthalpy of protein folding is due to hydrophobic interactions (135). Thus there is evidence to suggest that, far from being insignificant, hydrophobic interactions are a major factor in stabilising native protein structure. It should be noted that this study indicated that the enthalpy of the hydrophobic effect was the driving force of protein stability and not the entropy as is usually considered based on the simple methane-water model.

Furthermore, it has been noted for some time that hydrophobic residues tend to be found only on one side of α-helical regions of proteins (136-138). A recent method of predicting secondary structure of proteins which utilised only the hydrophobicities of the residues and their sequence* achieves a very high success rate (80% of residues are correctly assigned to α-helix and β-sheet regions) (139). This success rate is at least comparable with those of other secondary structure prediction methods which have quite low success rates (between 50 and 60% for the three states; helix, sheet and loop) (140). Let us consider this startling evidence. Why should a simplistic consideration of the positions of hydrophobic residues in the primary sequence of proteins yield such an accurate prediction of secondary

* In this prediction method sequences with alternating polar and nonpolar residues are identified as β-sheet regions. Sequences in which the distribution of polar and nonpolar residues is such that an an amphipathic helix may form, are identified as being α-helical.

structure? It is difficult to arrive at any other conclusion than that the hydrophobic effect is a primary stabilising force for protein secondary structure.

4.5 Conclusion

A summary of the thermodynamics of the various processes driven by the hydrophobic effect is shown in Table 4-3.

Table 4-3 A Summary of the Thermodynamics of Various Processes Driven by the Hydrophobic Effect

Process[e]	Dominant term in ΔG	Sign of ΔH[a]	Sign of ΔS	Reference
Solubility of nonpolar gases[d]	ΔS	variable	+ve	(86,103)
Water-organic solvent partitioning	ΔS	variable	+ve	(86,106)
Reversed-phase HPLC	ΔH	-ve	-ve	(116-118,147)
Water-Phospholipid partitioning[b]	ΔH	-ve	-ve	(91)
Phospholipid-protein association	?	?	?	-
Protein refolding	?	-ve	?	(135)
DNA helix to coil transition[c]	ΔH	-ve	?	(111)

a) "Variable" denotes a temperature dependent change of sign.

b) Above the phase transition temperature.

c) Obtained by a theoretical treatment of the solvophobic theory.

d) In water.

e) Defined in the direction of most aqueous to least aqueous environment of the nonpolar groups.

Although all of these processes require much more study there seems to be a general dichotomy in the thermodynamics of the various systems. The simple systems (water solubility of nonpolar gases and water-organic solvent partitioning) appear to be driven largely by a positive entropy change at least at 25°C where the enthalpy changes are small.* In these systems the enthalpy change is temperature dependent. Contrast these systems with the more complex systems of reversed-phase HPLC, phospholipid-protein association and protein refolding where the negative change in enthalpy is dominant and appears to be independent of temperature. Therefore, there may be a real danger in using simple systems as models for hydrophobic effects in more complex systems.

One possible explanation for the difference between these systems is that in the simple systems the non-hydrated solute is in a state of high entropy e.g. as a gas or dissolved in organic solvent while in the more complex system the non-hydrated solute is in a state of low entropy caused by binding to a hydrophobic surface. It is worthwhile noting that even though ΔH is positive for the simple systems with small solutes at 25°C, larger solutes can have negative enthalpies of partitioning (104). Furthermore even with small solutes the incremental enthalpy change per methylene group for a series of alkanes is negative at 25°C (151). This is confirmed by Tanford's data (100). The incremental enthalpy change per methylene group for nonionic surfactant association is also negative (143).

If the various processes driven by the hydrophobic effect are not identical in their thermodynamics, what is the unifying factor between them? Primarily this is, of course, the decreasing tendency to associate with an aqueous environment (expressed by a negative ΔG for the processes described in Table 4-3) found with the increasing nonpolar character of the solute. Another unifying factor in these processes may be the variable nature of their enthalpy and entropy contributions to the free energy change. As noted earlier the free energy of transfer increases linearly with increasing hydrocarbon chain length (and seems to depend upon hydrocarbon-water interfacial area), whereas the corresponding enthalpy and entropy functions show no corresponding regularity (100). Tanford proposed that the two thermodynamic states of water molecules

* At higher temperatures the enthalpy change may well become very important, a fact which is neglected in most treatments of the hydrophobic effect in these systems.

at a hydrocarbon-water interface (see section 4.3.1) must differ in enthalpy and entropy in a mutually compensating way. This unusual interdependence of entropy and enthalpy has been noted in several other hydrophobically driven processes and has been termed enthalpy-entropy compensation.* Each of the processes of alkane solubility (100,104), reversed phase HPLC retention (114,141,142), protein denaturation (135) and phospholipid/water partitioning (91) demonstrate enthalpy-entropy compensation. If this phenomenon can be related to the structure of water at the hydrocarbon-water interface then enthalpy-entropy compensation may be a unifying factor for all processes driven by the hydrophobic effect. Such a concept might easily be generalised to all solvents and solvent mixtures by considering their degree of cohesiveness and its influence upon solvent structure at the solute-solvent interface.

* Enthalpy-entropy compensation is the linear dependence of the free energy of reaction with the enthalpy of the reaction and hence is also the linear dependence of the enthalpy of reaction with the entropy of reaction at constant temperature (141).

CHAPTER 5 ANALYTICAL REVERSED-PHASE HPLC

5.1 Introduction

This introduction is not intended as a comprehensive description of reversed-phase HPLC. Neither is it intended as a complete review of the literature of various aspects of this chromatographic technique. For detailed works on these topics the reader is referred to the following authors: Snyder and Kirkland (108), Melander and Horvath (109), Hearn (110) and Hancock and Sparrow (153). The latter two works are concerned mainly with reversed phase HPLC of peptides and proteins. The function of this introduction is to familiarise the reader with the terminology and theory which will be used to discuss the results. A discussion of hydrophobic and solvophobic effects and their significance to reversed-phase HPLC has been given in section 4.4.1.

5.1.1 Definitions

REVERSED-PHASE: A hydrophobic layer bonded to a particulate matrix (usually silica). This is termed a "reversed-phase" because the mobile phase is more polar than the stationary phase which is opposite to the situation in (so called) normal phase or adsorption chromatography.

HIGH PERFORMANCE LIQUID CHROMATOGRAPHY *(HPLC): The use of a very small and uniform particle size (typically 5 or 10 microns) and a highly uniform packing for stationary phases in liquid chromatographic applications. These factors limit eddy diffusion, and minimise pore volume allowing a more rapid exchange of solute between the mobile phase inside the pores and mobile phase outside the pores. Both of these effects result in decreased band spreading and therefore an increase in performance. The major advances in this technique have involved the use of a silica matrix to which has been chemically bonded various nonpolar moieties. Pyrocarbon reversed-phases on silica matrices and organic resins are also being investigated for the purposes of HPLC (109).

* HPLC formerly stood for "high pressure liquid chromatography" due to the high pressures involved in forcing solvent between the very small particles which constitute the stationary phase. It is now generally accepted that the high performance of the technique is its distinguishing feature.

5.1.2 Equations

The basic equation linking the observed phenomena of retention volume or retention time of a sample solute with a useful chromatographic parameter is equation 5-1.

$$k' = \frac{t_r - t_o}{t_o} = \frac{v_r - v_o}{v_o} \qquad \text{Equation 5-1}$$

In this equation k' is the capacity factor reflecting the proportions of sample associated with the stationary and mobile phases, t_o and v_o are the retention time and volume of an unretained sample respectively, and t_r and v_r are the retention time and volume of the solute under chromatographic consideration (154).

The capacity ratio (k') is related to the thermodynamic equilibrium constant (K) by Equation 5-2 (149).

$$k' = K\phi \qquad \text{Equation 5-2}$$

where ϕ is the phase-ratio reflecting the ratio of the amounts of stationary phase and mobile phase.

The phase-ratio, ϕ can be calculated by Equation 5-3

$$\phi = \frac{\text{volume of stationary phase}}{\text{volume of mobile phase}} \qquad \text{Equation 5-3}$$

$$\simeq \frac{\text{weight of stationary phase}}{\text{volume of mobile phase}}$$

$$\text{Since } \Delta G^o = -RT\ln K \qquad \text{Equation 5-4}$$

then by Equations 5-2 and 5-4

$$\ln k' = \frac{-\Delta G^o}{RT} + \ln \phi \qquad \text{Equation 5-5}$$

$$\text{also } \Delta G^o = \Delta H^o - T\Delta S^o \qquad \text{Equation 5-6}$$

thus by Equations 5-5 and 5-6

$$\ln k' = \frac{-\Delta H^o}{RT} + \frac{\Delta S^o}{R} + \ln \phi \qquad \text{Equation 5-7}$$

Equation 5-7 shows that the temperature dependence of k' is completely determined by the standard enthalpy of binding (ΔH^o). This holds true if ΔS^o is constant with changing temperature as evidenced by linear van't Hoff plots. We should contrast the temperature dependence of k' with the temperature dependence of ΔG^o, which is completely determined by ΔS^o (Equation 5-6). Thus the effect of temperature change on chromatographic equilibria is mediated through the enthalpy and not the entropy of the interaction (141).

5.1.3 The Controversy Over Mechanisms of Retention

There is considerable controversy over the mechanism of solute retention in reversed-phase HPLC. Although initially a partition mechanism was assumed, with the solute dissolving in the pseudo-liquid of the reversed-phase, there is now mounting evidence that the partition mechanism does not apply (147, 154). Recent studies are compatible with an adsorption or mixed adsorption-partition mechanism (147,154).

When we consider the retention mechanism in relation to calculation of the phase ratio, ϕ, it becomes apparent that the equation used for the calculation of ϕ (section 5.1.2) may not be entirely accurate. If the sample is bound to the reverse phase only at the interface between mobile and stationary phases, i.e. by the adsorption mode, then the volume of the stationary phase could be said to be irrelevant. The sample would not interact with the entire volume of the reversed-phase. Equation 5-3 is based on a partition mechanism (147).

A similar problem in relating the capacity factor to the thermodynamic equilibrium constant is found in normal phase chromatography (adsorption chromatography). In this instance the mechanism of retention can only be adsorption. Thus in these systems the value of ϕ (called v_a) reflects the surface area of the stationary phase per weight unit of adsorbent (183). However, in the case of adsorption chromatography a measurement of surface area can be made by the BET method (183). This method estimates the surface area of adsorbent (e.g. silica) by the weight of nitrogen gas which will adhere to it. No comparable technique has been developed for estimating reversed-phase surface area.

Furthermore the available surface of reversed-phase decreases with increasing size of solute due to the exclusion of solute from small pores.

This is especially relevant to the reversed-phase HPLC of proteins. We can say, therefore, that the value of ϕ for solutes which are retained by an adsorption mechanism will be affected by the particular silica used, the length of alkyl chain bonded (since the surface area inside a pore will decrease with increasing alkyl chain length and the size of the solute). Some recent studies have also shown that the void volume varies substantially with the percentage of organic solvent in the mobile phase (174). If this is possible then ϕ may also vary with the percentage of organic solvent. The unavailability of accurate values for ϕ necessarily prohibits the calculation of accurate values for ΔG^{o} and ΔS^{o} from equations 5-5 and 5-7. However accurate values of ΔG^{o} and ΔS^{o} can be found relative to another solute in the same system.

5.1.4 Peptides and Reversed-Phase HPLC

The use of reversed-phase HPLC to characterise and purify peptides and proteins is now an intensive area of study (80, 153-168). These studies demonstrate the power of this technique in the analytical and preparative chromatography of sensitive biological molecules. A number of studies have attempted to correlate the hydrophobicities of the constituent amino acids of peptides with the retention of the peptides on a reversed-phase HPLC system (80,155,157,158,163). On the whole these studies show some correlation between total hydrophobicity of the constituent amino acids and the retention of peptides on RP-HPLC. However retention of larger peptides were often incorrectly predicted and this was attributed to the secondary structure of the peptides (80,158). Thus the most important parameter for RP-HPLC retention has been proposed as the molecular hydrophobicity reflecting the hydrophobic residues actually exposed to the reversed-phase (80). The concept of secondary structure of peptides has been used as an explanation for peptides which depart from predicted v's actual elution time plots, however, little constructive evidence for this exists. This thesis directly supports the hypothesis that peptides retain or adopt a considerable degree of structure when bound to the stationary phase of a RP-HPLC system. Furthermore it points to the amphipathic helical conformation as an important determinant of binding in peptides predisposed to this conformation.* The study indicates that it is the nonpolar part of this structure that is responsible for the highly specific separations of peptides achieved.

* See section 6.1.1.

5.2 Experimental

5.2.1 Equipment and Chemicals

The HPLC system consisted of two M6000A solvent pumps, controlled by a M660 solvent programmer and attached to a U6K universal liquid chromatograph injector (Waters Assoc., Milford, MA, USA). Detection was accomplished with an M450 variable-wavelength UV spectrophotometer (Waters Assoc.) coupled to an Omniscribe two-channel recorder (Houston Instruments, Austin, TX, USA). Samples were introduced into the injector with a microlitre 825 syringe (Hamilton, Reno, NV, USA). Where a Radial-PAK column was used, as detailed in the results section, a Waters RCM-100 radial compression module was attached to the above system. Studies which utilised the Radial-PAK columns were conducted at ambient temperature.

Where temperature was controlled, as indicated in the text, a Pye series 104 chromatograph oven was used. In these studies a length of 35 cm of 0.51 mm internal diameter stainless steel tubing was incorporated into the system between the column and injector. This length of tubing was completely enclosed inside the oven to pre-equilibrate the temperature of the solvent before it entered the column.* The heat exchanger was not removed from the Waters 450 variable wavelength detector as a stable baseline could not be obtained without it. The absorbance was therefore monitored at room temperature.

The reversed-phase bonded silica columns used were a Radial-PAK C18 (10 micron, 8 mm x 100 mm), a Radial-PAK CN (10 micron, 8 mm x 100 mm) and a μBondapak alkylphenyl column (10 micron, 3.9 mm x 300 mm). The isopropanol used was BDH laboratory reagent grade. It was purified for 4 h followed by distillation under the same conditions using a 110 cm fractionation column equipped with a vacuum mantle and filled with 6 mm glass rings. The purification was performed on 10l batches and the first 2l was not used for chromatographic separations. The purified alcohol was stored under oxygen free nitrogen in sealed bottles and kept in the dark. The acetonitrile used was laboratory reagent grade

* It is essential when running a liquid chromatographic system at other than room temperature to ensure that the solvent enters the column at the same temperature as the column. This can be achieved by including a length of tubing before the column within the temperature controlled environment. Failure to observe this rule results in a radial temperature gradient at the top of the column with consequent loss of resolution and change of k' values.

purchased from Ajax and was purified in a 4 step process as recorded in the appendix (section A.5). Ammonium bicarbonate was "R" grade purchased from May & Baker Ltd. Orthophosphoric acid 88-90% w/w, 1.750 specific gravity was purchased from May & Baker Ltd. Triethylamine was laboratory reagent grade purchased from Ajax Chemicals. It was purified by reflux over calcium hydride for 4 h followed by distillation from calcium hydride.

5.2.2 Solvent Systems

The aqueous solvents (called solvent A since they were introduced to the system through pump A) were made up from glass distilled water which had been degassed by stirring under vacuum for 30 min. Solvents were filtered and degassed using a Millipore membrane filtration system. The aqueous solvents (solvent A) were filtered through a HAWP04700 membrane filter. 2-Propanol was filtered through a FHLP04700 membrane filter and acetonitrile through a Sartorius SM 0.45 µm membrane filter.

(a) The 1% TEAP System:

- Solvent A was a 1% (v/v) solution of orthophosphoric acid titrated to pH3.2 with purified triethylamine (approx. 20 mls).
- Solvent B was 2-propanol (isopropanol): solvent A, 80:20 formed by adding 200 ml of solvent A to 800 ml of filtered 2-propanol.

The solvents were finally degassed by stirring under vacuum for 30 sec. Solvent A was prepared fresh each day while solvent B was made up as required (never longer than 3 days) and was degassed daily by the final degassing procedure.

(b) The 0.1 M Ammonium Bicarbonate System:

- Solvent A was a 0.1 M solution of ammonium bicarbonate made up freshly each day. The pH of this buffer varied between 7.8 and 8.0.
- Solvent B was acetonitrile: solvent A (80:20) formed by adding 200 ml of solvent A to 800 ml of filtered acetonitrile. Solvent A had to be prepared daily as its pH became more alkaline with the passage of time. Solvent B was made up as required (never longer than 48 hr) and was degassed daily as for the 1% TEAP system.

5.2.3 Methods

5.2.3.1 Gradient Elution of Peptides in 1% TEAP

Peptides were eluted by linear gradients from 100% solvent A to 100% solvent B. The duration of the gradient was always 1 h and was started immediately after the sample had been injected onto the column. The flow rate of solvent was always 1.0 ml/min. Differing quantities of each peptide were injected. For peptides 202 and 208, 28 µg and 16 µg of peptide were injected respectively, with the exception of the study with the alkylphenyl column at 40°C where half these quantities were used. For peptide 209, 125 µg and 56 µg of peptide were injected in the Radial-PAK CN* and 40°C µBondapak alkylphenyl studies respectively. For peptides 203 and 199 18 µg and 19 µg of peptide was used respectively.** All samples were loaded in 3 M guanidine hydrochloride. This was accomplished by adding equal volumes of a stock solution of the peptide and a buffer consisting of 6 M guanidine hydrochloride, 1% TEAP and 0.1% orthophosphoric acid at pH 1.7. The detection of peptides was accomplished at 280 nm at a sensitivity of 0.2 absorbance units full scale (AUFS).

All columns were placed in series with a precolumn filter (Waters Assoc.) and the Radial-PAK C18 column was also in series with a guard column filled with Porasil-B C18 packing. The use of a guard column did not affect the retention time of peptide 202 and the agreement between retention of peptides on this system and the other columns suggest that all 4 peptides were unaffected. The time of elution was interpreted as a % of solvent B measured directly from the chart paper by assuming that there was no time lag between solvent leaving the pump mixing manifold and entering the detector. Where this time lag has been allowed for, by subtracting 10% solvent B from the observed value, the elution conditions found are referred to as adjusted % solvent B.***

* Peptide 209 used in the gradient elution from the Radial-PAK CN column was not deformylated, however only very small changes in retention have been noticed between formylated and deformylated peptide 202.

** These weights are based upon the concentration of peptide determined from its UV absorbance at 280 nm assuming the tryptophan absorbance results in a value of $\varepsilon = 5200\ 1.mol^{-1}.cm^{-1}$. The weight is obtained from the concentration by multiplying by the volume and the calculated molecular weight of peptide.

$$\text{Weight} = \frac{A_{280}}{5200} \times \text{vol} \times \text{M.Wt.}$$

*** For a discussion of this problem of delayed solvent appearance see reference (170).

5.2.3.2 Isocratic Elution of Peptides in 1% TEAP

The isocratic elution of peptides was studied on a μBondapak alkylphenyl column. The various solvent compositions were obtained by using the two pumps used in gradient formation with their different solvents (see section 5.2.2). The gradient mixer was set at initial conditions* and the % solvent B flowing into the system regulated by adjusting the initial conditions thumb-wheel (thus only 1% increments are possible in this system). After changing the isocratic conditions, the sample was not injected until a stable base-line was obtained (usually 20-30 min.). The sample loadings differed for the different peptides. These were: 202, 1.4 μg; 208, 1.7 μg; 209, 28 μg; 199, 1.9 μg; 203, 0.9 μg.** The detection of peptides was accomplished at 220 nm at a sensitivity of 0.04 AUFS.*** Values of k' were calculated using a constant void volume of 2.5 ml.

5.3 Results and Discussion

5.3.1 Gradient Elution of Peptides in 1% TEAP

The retention of each of the 5 synthetic peptides in this work in the TEAP system on 3 different HPLC columns is shown in table 5-1.

* The final conditions mode works just as well however a mixture of the two modes should not be used since small differences in the response of the pumps in these two modes results in quite substantial differences in retention time.

** See footnote in the preceding section, for method of obtaining weight of sample.

*** For detection of peptide 209 absorbance was monitored at 230 nm which necessitated the use of a larger sample compared to the other peptides. The k' of peptide 209 was quite insensitive to the larger loading.

Table 5-1 Positions of Elution from Different Reversed-Phase HPLC Columns with Linear Gradients.

Column	Temperature	Elution of Peptide in Gradient (% Solvent B)[c] 202	208	209	203	199
CN-Radial PAK	ambient	54.75	51.5	49	48	44
μ-Bondapak alkylphenyl	40°C	63	55.5	51.5	51.5	48.5
μ-Bondapak alkylphenyl	ambient	67.5	60	ND[b]	54	53
C18-Radial-PAK[a]	ambient	69	61	ND[b]	58	56

a) A problem encountered with the C18-Radial-PAK column was the appearance of "memory peaks" which presumably arose from tightly bound peptide 202. The peptide could only be removed with repeated blank gradients or isocratic elution at the percentage of solvent B at which the peak was eluted.

b) N.D. = not determined.

c) The solvent system used is the 1% TEAP system, pH 3.2 described in section 5.2.2.
Solvent A: - 1% TEAP, pH 3.2
Solvent B: - 2-propanol:Solvent A (80:20, v:v)
Gradient: - 0-100% Solvent B over 60 min.

It should be noted that for each of the peptides the retention increases with increasing nonpolar character of the bonded phase, i.e. Radial-PAK CN < μBondapak alkylphenyl < Radial-PAK C18. This relationship has been observed elsewhere (162). It should also be noted that the order of elution of the peptide series is identical for all three columns, i.e. 202 < 208 < 209 ≃ 203 < 199.

This observed retention order is difficult to explain in terms of the total hydrophobicities of the constituent amino acids of each peptide. To illustrate this figure 5-1A shows the total hydrophobicities (calculated from Meek 3 hydrophobicity scale - see appendix, section A.2) v's the retention of the peptides. The order of retention is clearly not

Figure 5-1A Plots of the Total Hydrophobicity[a] of Each Peptide Calculated on the Meek 3 Scale[b] v's Point of Elution of Peptide in an Acidic Reversed-Phase HPLC System.[c] This figure shows that the retention order of the peptides cannot be directly related to their total hydrophobicity. In particular the total hydrophobicity of peptides 202 and 209 which contain exactly the same amino acids cannot be related to the different retentions of these peptides.

Figure 5-1B Plots of the Total Nonpolar Side Hydrophobicity[d] of Each Peptide Calculated on the Meek 3 Scale[b] v's Point of Elution in an Acidic Reversed-Phase HPLC System.[c] This figure shows a good correlation between hydrophobicity of the nonpolar side of the peptide and its retention in the HPLC system.

a) Total hydrophobicity of a peptide is defined as the sum of the hydrophobicities of its constituent amino acids.

b) The Meek 3 scale is defined in the appendix, section A.2.

c) The solvent system used has been described in Table 5-1. Each curve represents the retention of the peptides on a different column:

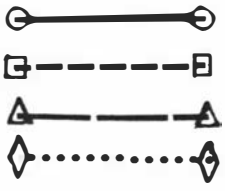

Radial-PAK CN (ambient temp.)
μBondapak alkylphenyl (40°C)
μBondapak alkylphenyl (ambient temp.)
Radial-PAK C18 (ambient temp.)

d) Total nonpolar side hydrophobicity is the maximum hydrophobicity of a peptide when in the α-helical configuration considering only 180° of the face of the helix. These values were calculated using the computer program shown in the appendix, section A.3.

predicted by this method. In particular this appraisal of hydrophobicity cannot explain the difference in retention between peptides 202 and 209 which contain the same amino acids, with only a Lys for Leu interchange making them non-identical. When plots of actual retention v's total hydrophobicity of each peptide are made for each of the available hydrophobicity scales (see appendix, section A.2) none of these scales predict the actual order of retention of the peptides (see appendix, section A.4).

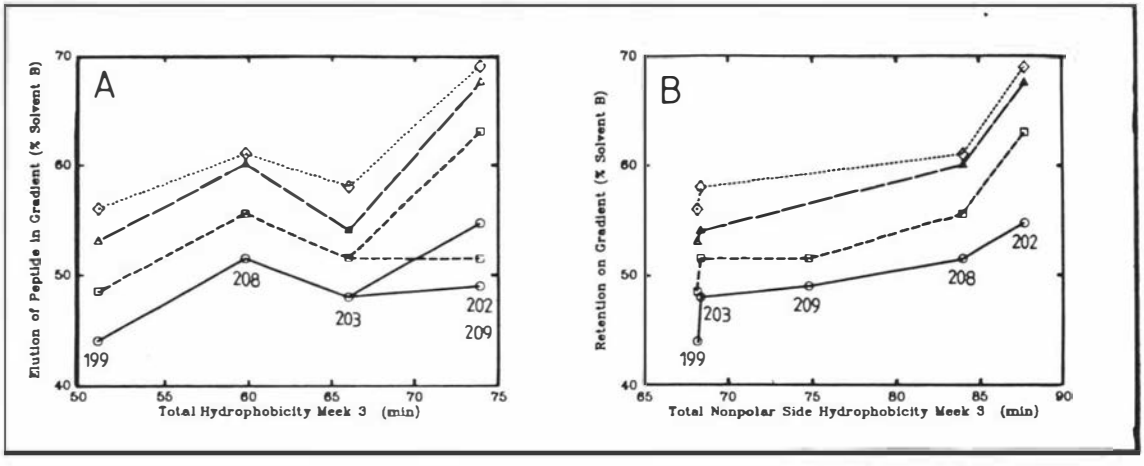

Contrast this inability to predict the correct order of elution of the peptide series with the relationship found if we assume that the peptides are bound to the reversed-phase columns by only the most hydrophobic half of their α-helical structure as detailed in the amphipathic helix model (section 6.1.1). To illustrate this figure 5-1B correlates the total nonpolar side hydrophobicity of the peptide series calculated using the Meek 3 scale (see appendix, section A.2) with the actual retention of the peptides on the 4 different reversed-phase systems. These so called "total nonpolar side hydrophobicities" were calculated by the computer program found in the appendix, section A.3, and represent the hydrophobicity of 180^{o} of the most nonpolar side of the peptide in an α-helical conformation. As can be seen from figure 5-1B consideration of the amphipathic helical properties of the peptides results in a dramatic improvement in the prediction of retention order of the peptide series. This improvement is also seen in other hydrophobicity scales as shown in section A.4 of the appendix. In particular the reversed-phase HPLC scales determined at acid pH (Meek 2, Meek 3, Meek 4 and Sasagawa 2), the tlc scales (Pliska 1 and Pliska 2) and a hydropathy scale (Kyte & Doolittle 1) demonstrate ability to predict the correct elution order. Since peptide 199 contains an extra cationic

residue we may expect it to show some anomalous retention caused by charge repulsion or attraction contributions which are peculiar to the TEAP, reversed-phase HPLC system used in this study. The observed decrease in retention of peptide 199 with respect to its nonpolar side hydrophobicity calculated with a number of the hydrophobicity scales is compatible with a small charge repulsion between cationic residues (Arg & Lys) and triethylammonium ions adsorbed to the reversed phase column. A decrease in retention of positively charged peptides upon addition of alkylammonium ions to the mobile phase has been noted in other studies (184,185). This effect has been explained recently by the "ion-interaction model" which relates the adsorbtion of ion-interaction reagents onto the reversed-phase column with changes in retention of charged solutes (188). Because of this effect the effectiveness of the different hydrophobicity scales in predicting the elution order of the peptide series was based mainly on the peptides which possessed equal charge at the pH of the study (i.e. peptide 199 was largely excluded from the consideration).

The above study presents very interesting evidence for the hypothesis that the amphipathic helix is an important determinant of the reversed-phase HPLC retention of peptides predisposed to this conformation. Many more peptides must be chromatographed in this system before it is known how widely applicable is the observed correlation. It may well be that some of the discrepancies between observed retention times of peptides and their predicted retention times is due to various secondary structures which the particular peptide adopts on the reversed-phase surface (163, 158,80). Indeed some degree of structure has been implied by other studies (163,158,80).

There are some implications here which should be considered. Firstly the mechanism for solute binding in reversed-phase HPLC is currently controversial with partition, adsorption and mixed-mode mechanisms being proposed (section 5.1.3). This study supports an adsorption mechanism since some amino acids apparently do not contribute to the retention. Secondly since peptides apparently bind to phospholipids and to the reversed-phase in this HPLC system via an amphipathic helix, RP-HPLC utilising the 1% TEAP, 2-propanol solvent system may be an excellent way of quantitating the hydrophobic interactions between peptides and phospholipids. The similarity of the thermodynamics of the two processes (section 4.5) is a further argument for this. This concept will be further treated in Chapter 7.

5.3.2 Isocratic Elution of Peptides in 1% TEAP

An extensive study of the isocratic elution of the peptide series in the TEAP system with a μBondapak alkylphenyl column was made. An example of the variation in retention time observed with changing concentration of organic solvent is shown in figure 5-2 for peptide 208. The full results of this study are shown in figure 5-3. This figure clearly shows that the order of retention observed in the gradient elution of the peptides is duplicated in the isocratic study. Indeed an excellent correlation between the extrapolated lnk' at 37% solvent B and the point of elution in the gradient was found. This is expected since increases in retention on gradient elution systems has been related to increases in retention on isocratic systems by a formula (169).

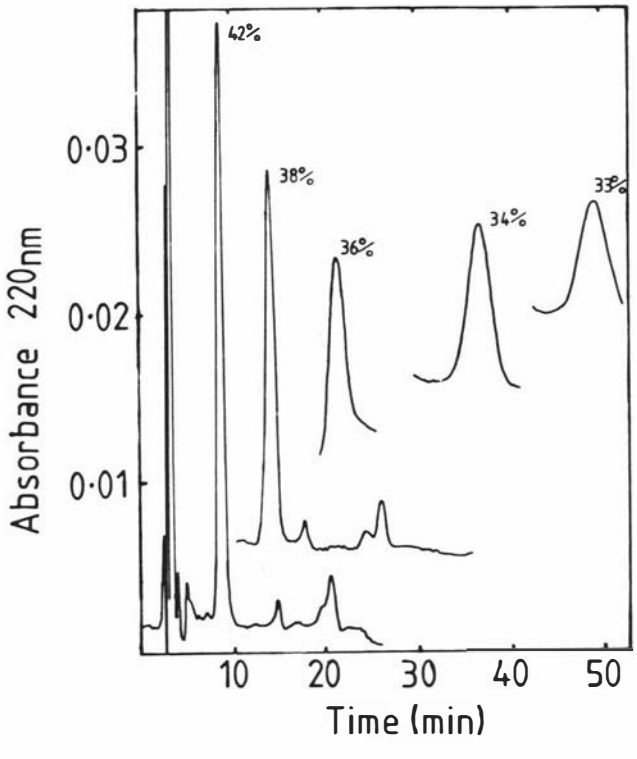

Figure 5-2 The Isocratic Elution of Peptide 208 at Different Concentrations of Organic Solvent.
The percentages shown describe the percentage of solvent B used in the chromatograph as shown.
As is expected a decrease in the concentration of organic solvent causes an increase in retention of the peptides. The conditions used were:

Column: μBondapak alkylphenyl
Solvent A: 1% TEAP, pH 3.2
Solvent B: 2-propanol: Solvent A (80:20, v:v)
Temperature: 40.0°C
Sample: 1.7 μg peptide 208 in 3 M guanidine hydrochloride

Figure 5-3 Plots of k' v's % Solvent B for the Isocratic Elution of the Synthetic Peptide Series. ◆——◆ , peptide 199; o.....o, peptide 209; ■--------■ , peptide 203; □-·-·-·-□ , peptide 208; ●-----●, peptide 202. The chromatographic conditions have been given in figure 5-2. Mass of sample in each study was: peptide 199, 1.9 μg; peptide 209, 28 μg; peptide 203, 0.9 μg; peptide 208, 1.7 μg; peptide 202, 1.4 μg. All samples were injected in 3 M guanidine hydrochloride.

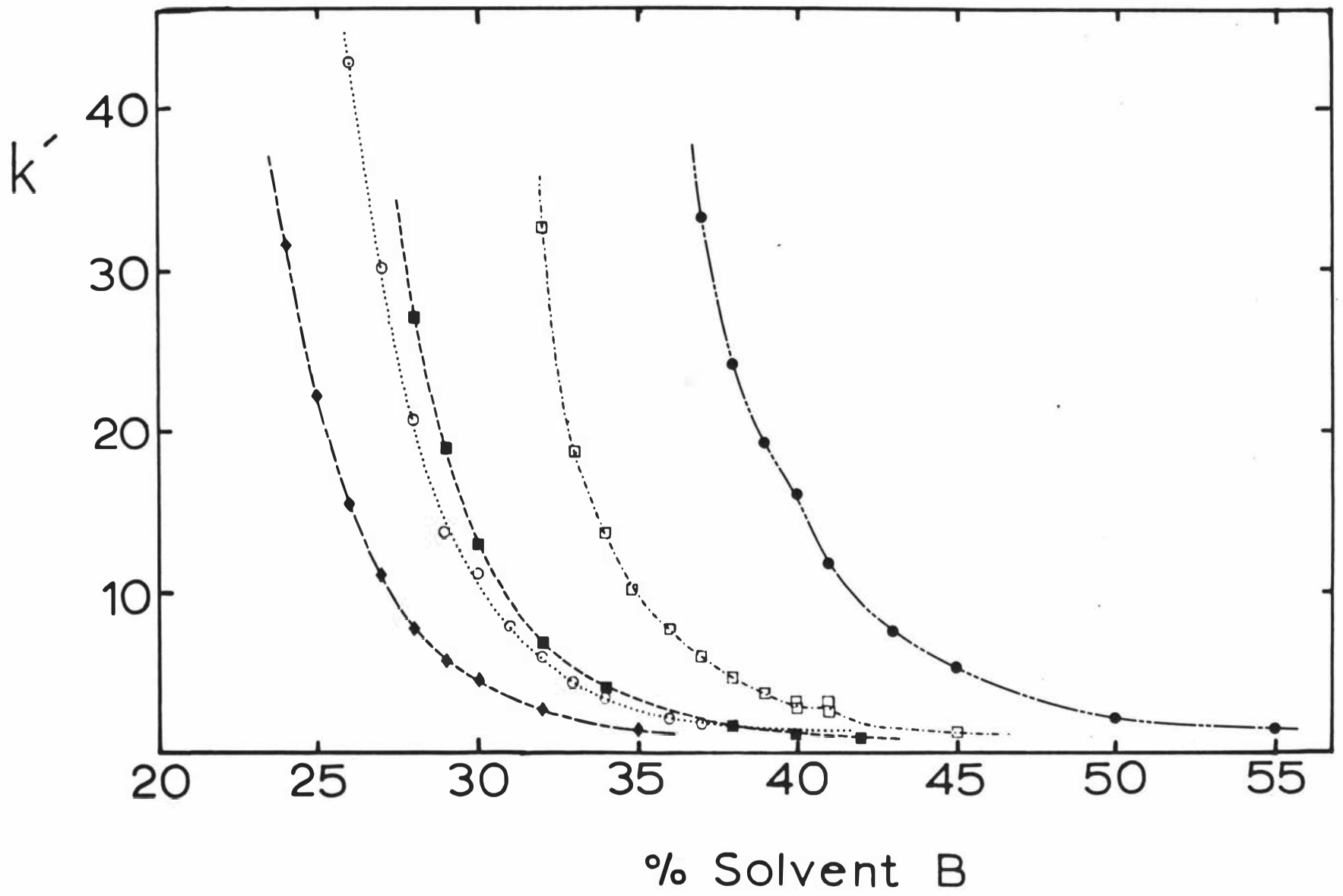
k'
40
30
20
10
20
25
30
35
40
45
50
55
% Solvent B

Figure 5-4 Plots of lnk' v's % Solvent B for the Isocratic Elution of the Synthetic Peptide Series. ◆——◆ , peptide 199; o.....o, peptide 209; ■-------■ , peptide 203; □-·-·-·-□ , peptide 208; ●-----●, peptide 202. The chromatographic conditions have been given in Figures 5-2 and 5-3. The large symbols at the base of the figure represent the composition of mobile phase at the point of elution of the respective peptides under conditions of gradient elution (adjusted % Solvent B). These symbols are enlargements of the smaller symbols portraying the isocratic elution of the same peptide.

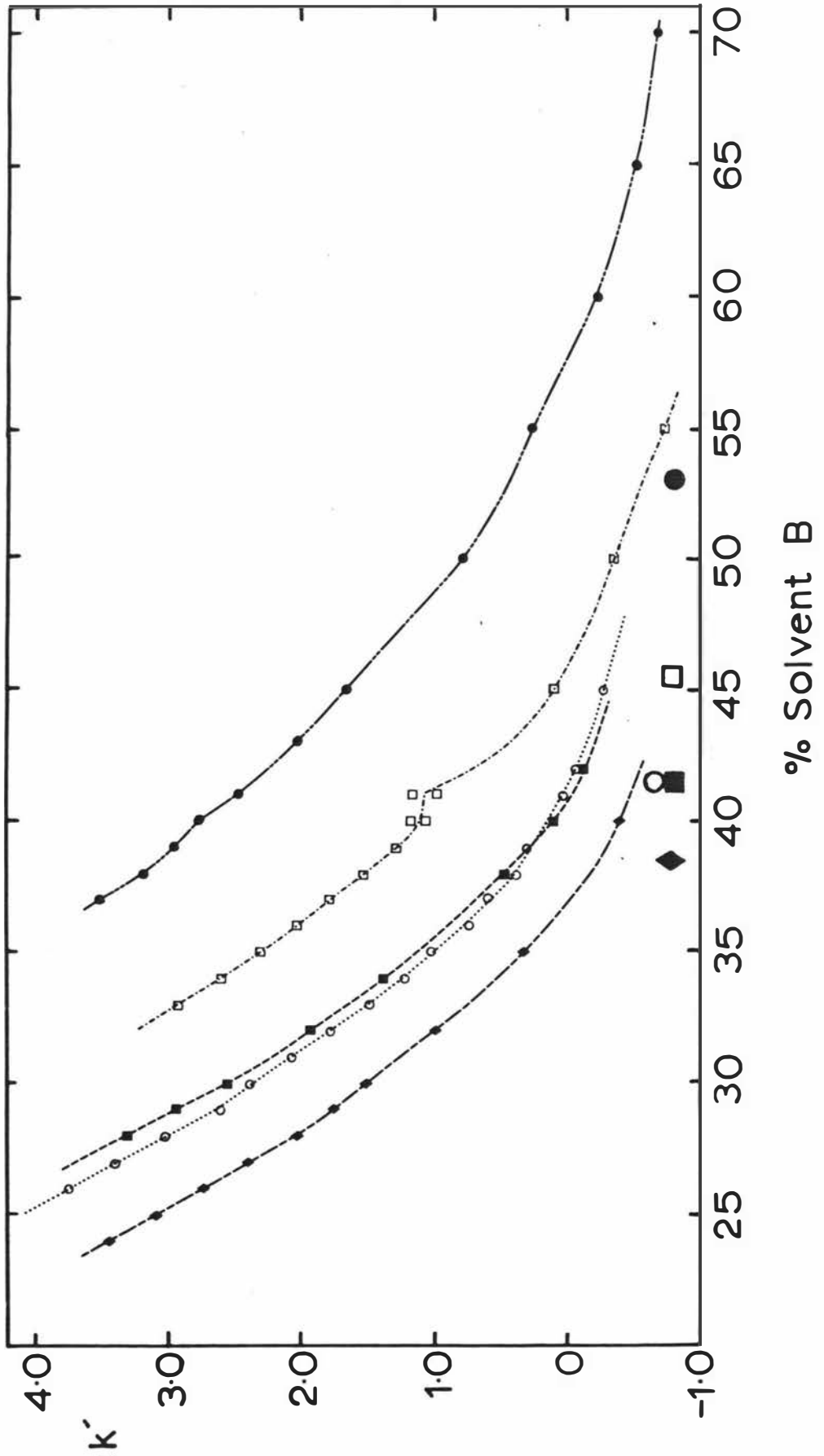
ln k'
4·0
3·0
2·0
1·0
0
-1·0
25
30
35
40
45
50
55
60
65
70
% Solvent B

The peptide series therefore appears to behave normally in their elution properties. The results of the isocratic study have been further analysed to produce plots of lnk' v's composition of mobile phase (figure 5-4). The slopes of the 5 lines shown in figure 5-4 are very similar with the difference between each line approximating a displacement along the "% Solvent B" axis.

A small irregularity in the peptide 208 curve is noticable at 40-41% Solvent B. The retention of this peptide at these concentrations of organic solvent varied somewhat as shown in the figure. A smaller irregularity in the peptide 202 curve can be noticed at 40% Solvent B. Such an irregularity appears consistent with a small change in the reversed-phase surface at this concentration of organic solvent.

The shape of lnk' v's composition of mobile phase plots has been the subject of some controversy (172). Two schools of thought exist being: -

(a) That the plot should be linear and that any deviation from linearity is caused by an inappropriate choice of the void volumn of the column, insufficient control on equilibration time, solute concentration or temperature, or a mixed mode separation perhaps incorporating normal phase interaction with residual silanol groups (171,172).

(b) That such plots obey a quadratic equation and hence will always be slightly curved (169,173).

Whatever the reason, the plots in figure 5-4 are certainly curved at lower elution times but become more linear as retention is increased (i.e. as % solvent B is decreased). Parallel plots of lnk' v's % organic solvent have been observed for simple solutes when the organic modifier is acetonitrile (173) and methanol (189). Parallel plots of lnk' v's % organic solvent have also been observed for peptides and proteins of similar size (160,164). The fact that the lnk' v's % Solvent B plots for each peptide are approximately linear, parallel lines has an important consequence. This shows that the relative retention of the peptides is not greatly affected by the change in concentration of organic solvent. Thus the relative retentions of peptides at a particular concentration of organic solvent may be an accurate measure of the relative hydrophobicities of each peptide in a pure aqueous mobile phase. If this is true we should expect to find that differences in retention

of peptides in reversed-phase HPLC at some concentration of organic solvent accurately reflects the difference in the hydrophobicities of the peptides measured in a fully aqueous system. This hypothesis will be tested below for peptide 202 and its Leu-Lys reversal analogue peptide 209 assuming that both peptides adsorb to the reversed-phase column with an amphipathic helical structure.

Strictly speaking it is possible to obtain values of the free energy of the interaction of peptide with the reversed-phase from equation 5-8.

$$\Delta G^{o} = -RT\ln K = -RT\ln(k'/\phi) \qquad \text{Equation 5-8}$$

The quantity of the phase ratio, ϕ, is elusive however.* When the retention of two solutes is being compared under the same conditions the difference in the free energy of association for the two solutes can be obtained without evaluating ϕ by Equation 5-9.

$$\Delta\Delta G^{o}_{1-2} = \Delta G^{o}_{1} - \Delta G^{o}_{2} = -RT(\ln k'_{1} - \ln k'_{2}) \qquad \text{Equation 5-9}$$

Using this equation the difference between the free energy of association of peptides 202 and 209 at 40°C and 37% Solvent B was calculated to be -2.11 kcal/mol (-8.82 kJ/mol). A comparison between this difference in free energies and the differences between the free energies of transfer of leucine and lysine in various processes is shown in Table 5-2.

* The phase ratio, ϕ, reflects the ratio of the quantities of stationary and mobile phase available to the solute. In a partitioning mechanism this represents the ratio of the volumes of each phase, while in an adsorption mechanism the ϕ is a measure of the surface area of stationary phase to volume of mobile phase. Since the mechanism of retention in RP-HPLC systems is currently under debate it is perhaps premature to calculate free energies of interaction using assumed values of ϕ, see section 5.1.3.

Table 5-2 The Calculated Free Energy Difference Between Aqueous-Hydrocarbon Transfers for Leucine and Lysine.

Scale	Method	$\Delta\Delta G^{o}_{L-K}$	Temp.	Ref.
Knighton	RP-HPLC	-2.11	40°C	this study
Rekker	octanol/H_2O partitioning	-2.11	-	(158,175)
Bull & Breese	surface tension	-2.11	30°C	(129)
Pliska[b]	tlc	-3.75[d]	-	(176)
Pliska[c]	tlc	-2.52[d]	-	(176)
Manavalan	statistical "surrounding hydrophobicity"	-3.54	25°C	(177)

a) $\Delta\Delta G^{o}_{L-K}$ is the difference in free energy of transfer (from an aqueous to a nonpolar environment) between leucine and lysine residues. $\Delta\Delta G^{o}_{L-K} = \Delta G^{o}_{L} - \Delta G^{o}_{K}$ (kcal/mol).

b) Charged lysine.

c) Uncharged lysine.

d) Calculated from $\Delta G^{o} = -RT\ 2.303 \log P$.

The calculated values of $\Delta\Delta G^{o}$ for the scales of Rekker (158,175), Bull & Breese (129) and Pliska (176) agree very favourably with the measured value in the HPLC system. Such agreement is good evidence that only those residues on the most non-polar 180° of face of the amphipathic helix are exposed to the non-polar stationary phase. Furthermore the good agreement between the hydrophobicity scales supports the role of the hydrophobic effect in the processes from which these hydrophobicity scales were deduced including the HPLC system used here. This is an important observation which supports the concept that the relative hydrophobicities of the amino acids are not changed by the presence of organic solvent in the aqueous solution. Such a situation was implied by the linear and parallel lnk' v's % solvent B plots for the series of peptides. These facts are important justification for the use of reversed-phase HPLC derived hydrophobicity data (measured

in the presence of organic solvent) in explanations of the hydrophobic effect in fully aqueous biological systems.

It is interesting to compare the values of $\Delta\Delta G^{o}_{L-K}$ found in table 5-2 with those found with two other hydrophobicity scales. When the scale of Jones is used $\Delta\Delta G^{o}_{L-K}$ is -0.53 kcal/mol which is much lower than the values calculated in table 5-2 (177,178). This scale is based on the solubility of amino acids in aqueous dioxane and ethanol solutions (180-182). It is notable that the hydrophobicity of lysine in this scale was calculated from a consideration of the side chain of norleucine with no contribution from the amino group. Another scale measures the so called "hydropathy" of the amino acid side chains (179). When $\Delta\Delta G^{o}_{L-K}$ is calculated using this scale a value of -11.80 kcal/mol is obtained. This value is much larger than the values calculated in table 5-2. The reason for this is that the hydropathy scale includes the free energy of hydration of the ε-amino group estimated from the gas to aqueous transfer of n-butylamine. The fact that poor agreement is found between $\Delta\Delta G^{o}_{L-K}$ values found with these scales and those of table 5-2 shows that the hydrophobicity of lysine has been wrongly estimated in Jones' scale (180) and that the hydropathy scale of Wolfenden (179) bears little relevance to the hydrophobic effect.

5.3.3 The Effect of Temperature upon the Retention of Peptide 202

Some appreciation of the effect of temperature on retention is shown in the comparison of the gradient elution of the peptide series at 40°C and at room temperature (22-23°C) (table 5-1). The changes in retention caused by temperature are similar in all cases,* which reflects similar values for the enthalpy of association of each of the peptides as illustrated in equation 5-7.

$$\ln k' = \frac{-\Delta H^{o}}{RT} + \frac{\Delta S^{o}}{R} + \ln \phi \qquad \text{Equation 5-7}$$

We have in this treatment assumed that the similar changes in retention in the gradient system would also be reflected in similar changes in ln k' in the isocratic system.**

* The retention of peptide 209 was not evaluated at room temperature and therefore no inference on the temperature dependence of its retention can be made.

** An excellent correlation between the gradient elution of the peptides and their retention in an isocratic system has been found. Data not shown.

The temperature dependence of retention in the isocratic system was investigated for peptide 202. The results of this study are summarised in figure 5-5. The plot of lnk' v's solvent composition appears merely to be translated to lower % Solvent B by an increase in temperature.

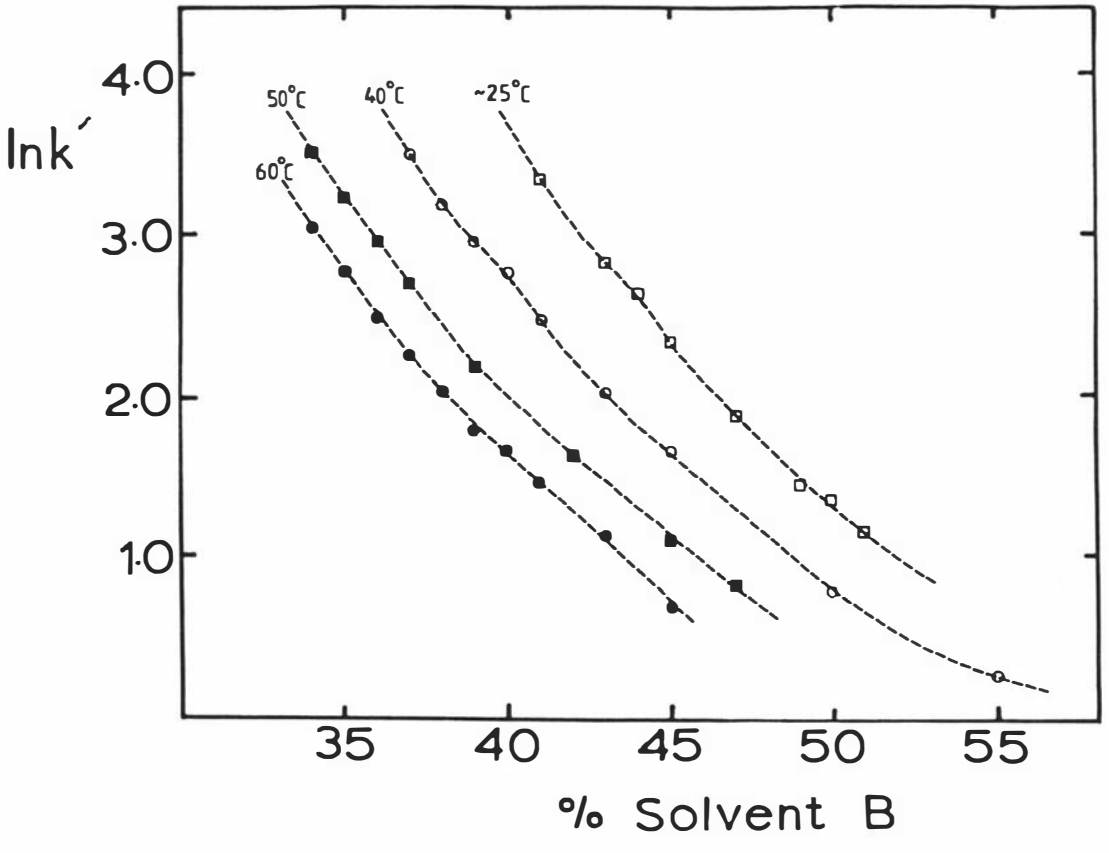

Figure 5-5 Plots of lnk' v's % Solvent B for the Isocratic Elution of Peptide 202 at Different Temperatures.

The chromatographic conditions have been given in figures 5-2 and 5-3. Temperatures of system: ●-----●, 60°C; ■-----■, 50°C; o-----o, 40°C; □-----□, ambient temperature 25±0.5°C.

It is notable that the small irregularity in the curve at ambient temperature and 44% Solvent B persists in the 40°C curve at 40% Solvent B but not at the two higher temperatures. The origin of this irregularity is probably some temperature dependent transition or structural change of the peptide, mobile phase or stationary phase.

The data from figure 5-5 may be graphed in the form of a van't Hoff plot for evaluation of the enthalpies of association of the solute at different solvent compositions, figure 5-6. As shown in this figure a decrease in % solvent B causes an increase in retention (at a particular temperature) and a concurrent increase in $-\Delta H^{o}/R$. The linearity of each plot indicates that when conditions of elution are held constant, apart from temperature, the enthalpy of the association is constant at least over the temperature range used here.

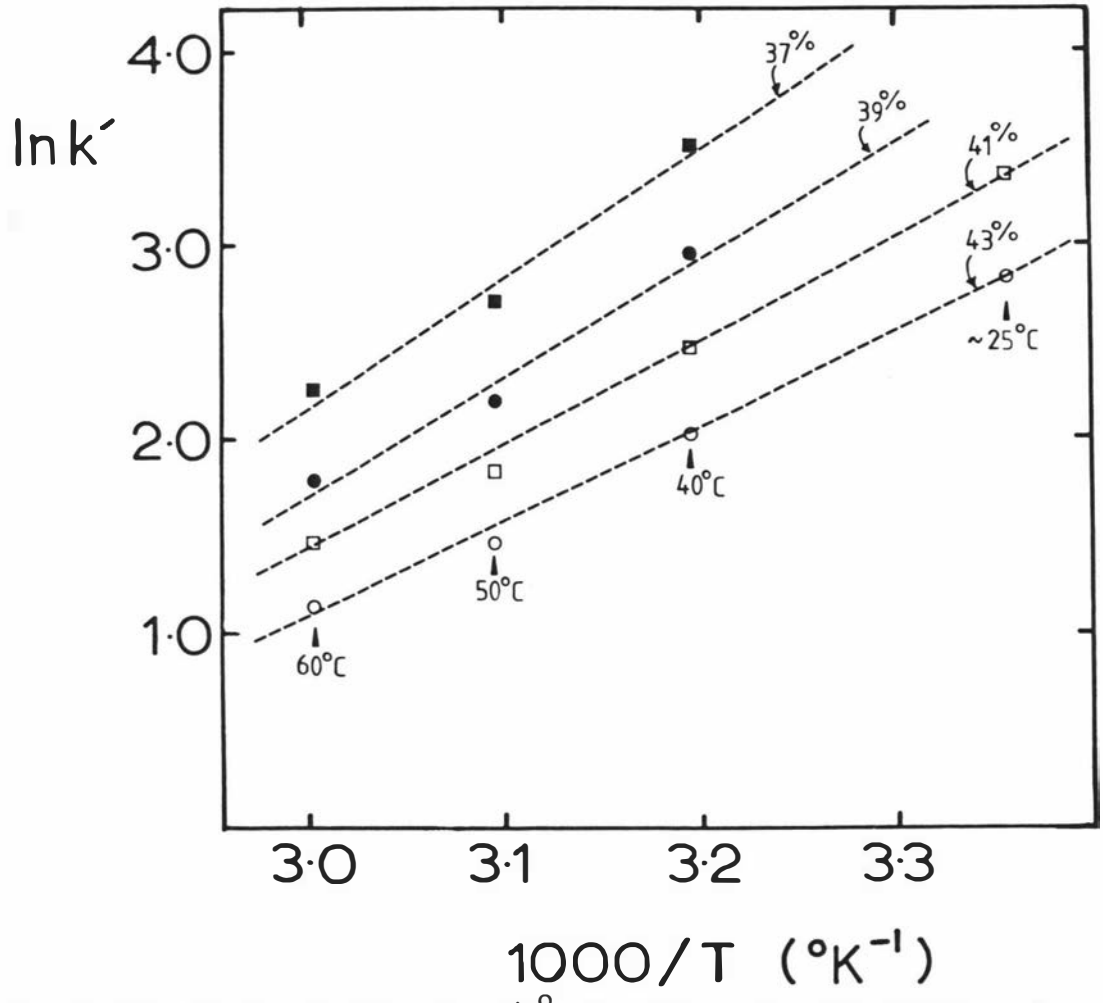

Figure 5-6 Plots of lnk' v's $1/T^{o}K$ for the Isocratic Elution of Peptide 202 at Different Concentrations of Organic Solvent. The chromatographic conditions have been given in figures 5-2 and 5-3. Isocratic conditions: ■-----■, 37% Solvent B; ●-----●, 39% Solvent B; □-----□, 41% Solvent B; o-----o, 43% Solvent B.

An estimation of the errors involved in the composition of solvent shows that the lines drawn in figure 5-6 are within experimental error of the points.

The enthalpies of association calculated from figure 5-6 are summarised in figure 5-7.

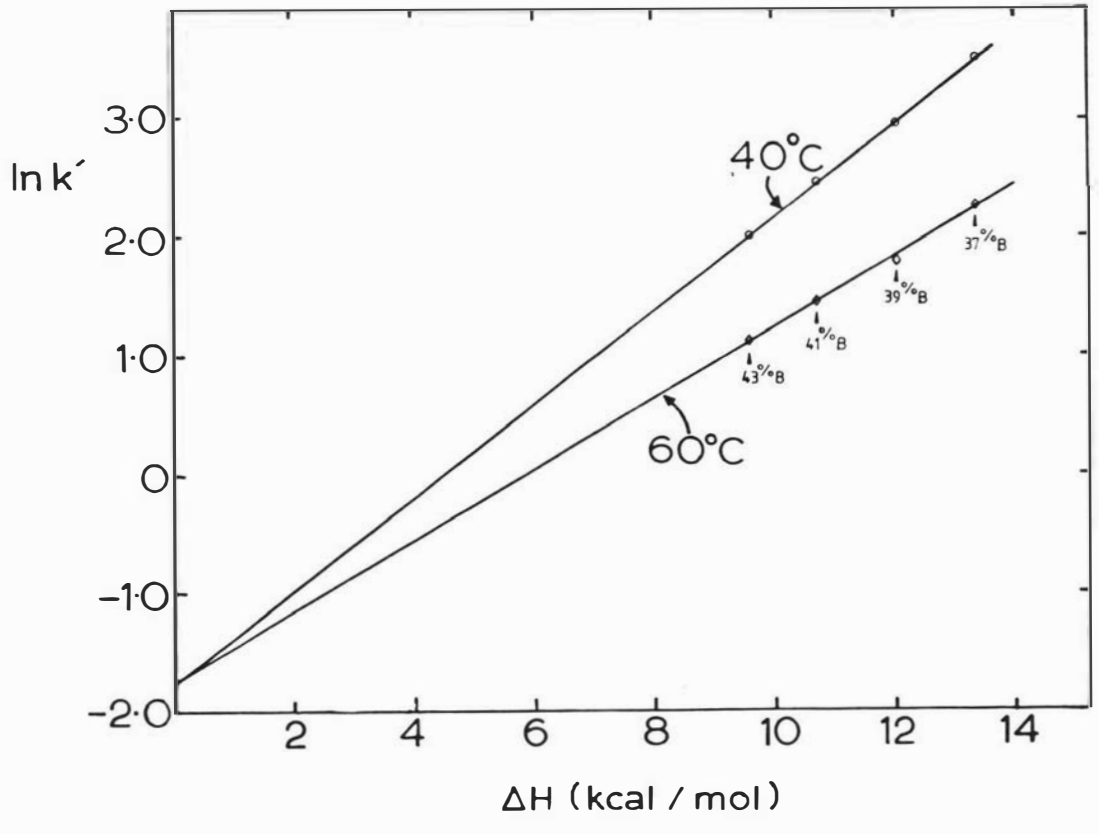

Figure 5-7 Plots of lnk' v's Enthalpy of Association for Isocratic Elution of Peptide 202 at Different Temperatures and Concentrations of Organic Solvent.
The compositions of the mobile phases corresponding to particular enthalpies are shown as % B (% Solvent B).
The lnk' values are plotted for the two temperatures 40°C (⊖——⊖) and 60°C (◊——◊).

This figure clearly shows the linear relationship between the enthalpy of association and lnk' and hence between ΔH^{o} and ΔG^{o} (see equation 5-5). Such relationships have been found in other studies although not as conclusively as in this work (141). In these studies the linear relationship was cited as evidence the enthalpy-entropy compensation was occurring, in other words, that both enthalpy and entropy change in a mutually compensating way so that the nett effect on the free energy change is linear with the enthalpy change. Linear ΔH^{o} v's ΔS^{o} plots at constant temperature (Barclay-Butler plots) are alternative displays of the same phenomenon but since ΔS^{o} is often not directly measurable the former method of displaying enthalpy-entropy compensation is favoured (141). Such a plot of the data can be found in figure 5-8. This figure clearly shows how ΔS^{o} and ΔH^{o} for the association of the peptide with the reversed-phase packing are linearly related. Values of ΔS^{o} were calculated using equation 5-7. The phase ratio was calculated by equation 5-3 assuming that the volume of mobile phase was 2.5 ml, the weight of reversed-phase packing was 2.1 g and the fraction by weight of organic ligands on the packing was 10% ($\phi = 0.084$, $\ln\phi = 2.48$). The use of any other value for the phase ratio would not effect the linearity of this line but would change the intercepts. It is worthwhile stressing that the points shown represent the ΔS^{o} and ΔH^{o} values for either $40^{o}C$ or $60^{o}C$. Thus the effect of temperature on the free energy change for the association is not mediated through changes in ΔH^{o} or ΔS^{o}. It has been shown that reasonably linear plots of lnk' v's ΔH^{o} have been obtained by varying the hydrophobic surface area of the solute (i.e. varying the solute) and varying the concentration of organic solvent (141). This has been used as evidence that the mechanism of interaction of the solutes with the reversed-phase is not changed by changing the solute (141). Similarly the results presented here show linear lnk' v's ΔH^{o} plots obtained by keeping the solute constant (peptide 202) and varying the concentration of organic solvent. This is evidence that the mechanism of interaction of peptide 202 with the reversed-phase column does not change with changing concentration of organic solvent, at least over the limited concentration of organic solvent applicable to this study. The above temperature study therefore confirms the current model of solute reversed-phase interaction and is compatible with the general criteria of the solvophobic theory (see section 4.4.1). The accurate calculation of values for HPLC systems will enable the calculation of the ΔG^{o} and ΔS^{o} of association and thus enable a fuller understanding of the thermodynamics

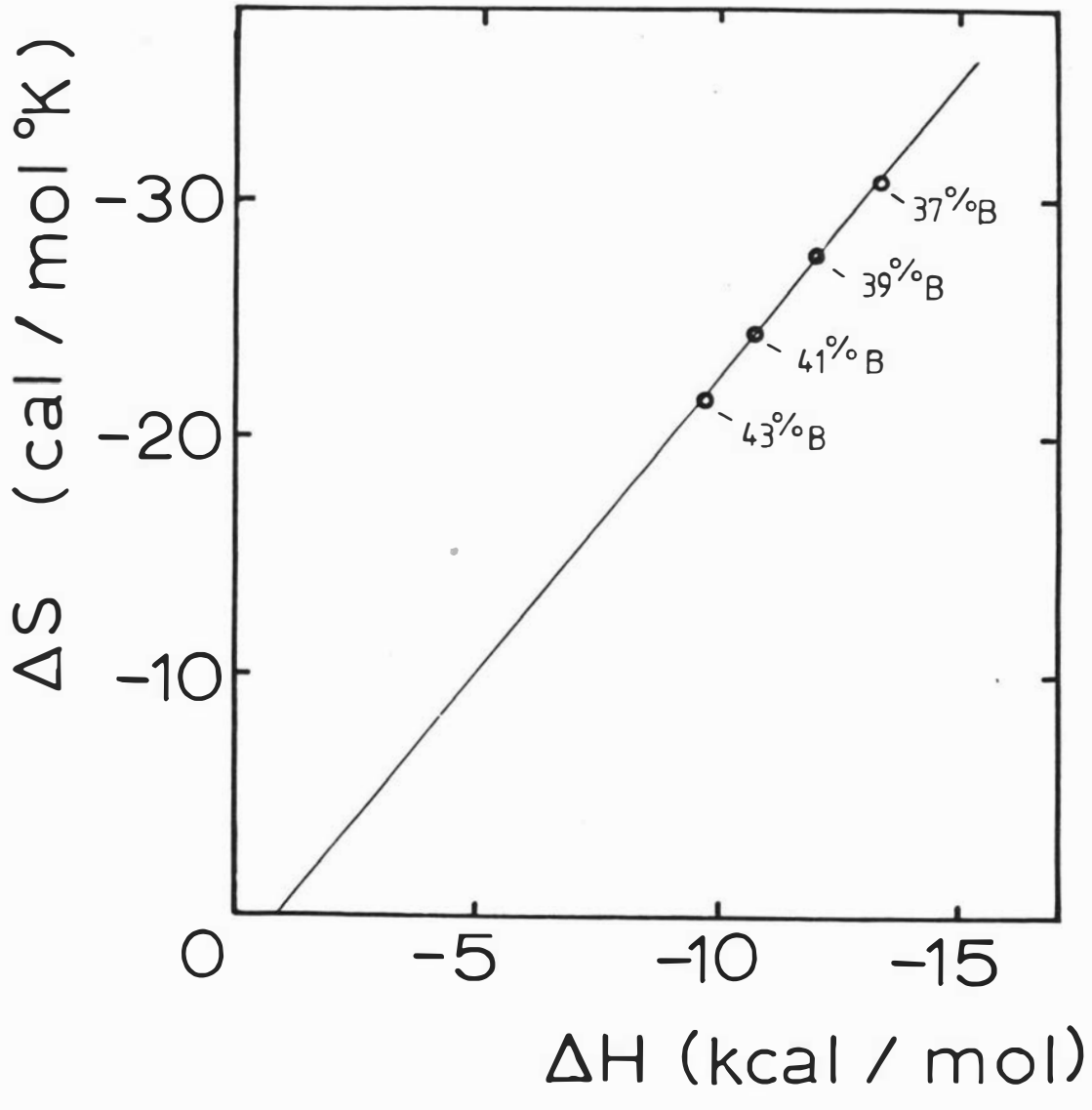

Figure 5-8 Plot of ΔH^{o} v's ΔS^{o} for the Isocratic Elution of Peptide 202 at Different Concentrations of Organic Solvent. The values of ΔS^{o} were calculated using Equation 5-7 using a calculated value for ϕ of 0.084. Chromatographic conditions have been given in figures 5-2 and 5-3. The values of ΔS^{o} are not dependent on temperature.

of the hydrophobic effect as it applies to RP-HPLC and possibly to other phenomena of the hydrophobic effect.

Let us concentrate for a moment upon the value of the enthalpy of association for peptide 202. The value is negative and quite large (13.6 kcal/mol at 37% Solvent B). In fact the enthalpy term dominates the free energy of the interaction even when ϕ is much smaller or larger than its proposed value, Table 5-3. Furthermore the entropy change has the same sign as the enthalpy change and thus works against the enthalpy to reduce the overall negative free energy of interaction.

Table 5.3 Variation in the Calculated Value of ΔG^o with Different Values of the Phase Ratio (ϕ).

ϕ[a]	ΔG^o[b]	$T\Delta S^o$[c]
0.84	-1.94 (-8.1)	-10.11 (-42.30)
0.084	-3.38 (-14.1)	-8.67 (-36.28)
0.0084	-4.81 (20.1)	-7.24 (-30.29)

a) Represented are values of ϕ, 10 times larger and 10 times smaller than the value calculated for ϕ based on equation 5.3.

b) The standard free energy of association of peptide 202 to the reversed-phase at 39% Solvent B and 40°C calculated from $\Delta G^o = -RT(\ln k' - \ln \phi)$ where k' = 19.1.

c) The $T\Delta S^o$ contribution to the free energy of association of peptide 202 to the reversed-phase at 39% Solvent B and 40°C calculated from $T\Delta S^o = \Delta H^o - \Delta G^o$ where ΔH^o is -12.05 kcal/mol (50.42 kJ/mol). Units are in kcal/mol (kJ/mol in parentheses).

The negative sign of the enthalpy is in agreement with other HPLC studies of simple molecules as was discussed in section 4.4.1.

5.3.4 The Gradient Elution of Peptides in 0.1 M Ammonium Bicarbonate.

The retention of the peptide series on a Radial-PAK CN column in a gradient from 0.1 M ammonium bicarbonate to 80% acetonitrile:20% 0.1 M ammonium bicarbonate is shown in Table 5-4.

Table 5-4 A Comparison of the Retention of the Peptide Series on a Radial-PAK CN Column with Neutral and Acidic Solvent Systems.

Peptide	% Solvent B[a,c]	
	0.1 M ammonium bicarbonate (neutral)	1% TEAP[b] (acidic)
202	45.5	54.75
208	46.5	51.5
209	41	49
203	33	48
199	54.5[d]	44

a) Without guard column.

b) From Table 5-1.

c) Temperature ambient, note the difference in the organic solvents in these solvent systems; acetonitrile in the neutral solvent, 2-propanol in the acidic system.

d) Eluted as a very broad peak.

As can be seen the order of elution in the system at neutral pH is quite different compared to the system at acid pH. Note in particular that the order of elution of peptides 202 and 208 has been reversed and that peptide 199 is retained much later in the gradient than all of the other peptides. Fortunately Meek has determined a set of hydrophobicity parameters for amino acids at neutral pH (155). A plot of retention on the above system v's non-polar side hydrophobicity determined on the Meek scale is depicted in Figure 5-9B. Figure 5-9A shows the same retentions correlated with the total hydrophobicity of the peptides. The greatest change in retention on going to the bicarbonate system is that of peptide 199. This peptide is the only one to contain an arginine residue and at this pH, where ionisation of the non-capped Radial-PAK CN silanol groups occurs, it is probable that the peptide is being retained by strong chemisorption as described by Snyder (183) and others (184,185). The elution order of the remainder of the peptides is predicted by figure 5-9B however peptide 203 appears to be eluted some time before it would be predicted from this graph.

Figure 5-9A Plot of the Total Hydrophobicity[a] of Each Peptide Calculated on the Meek 1[b] Scale v's Point of Elution of Peptide in a Neutral pH Reversed-Phase HPLC System.[c] This figure shows little correlation between retention and total hydrophobicity. See text for a more detailed explanation.

Figure 5-9B Plot of the Total Nonpolar Side Hydrophobicity[d] of Each Peptide Calculated on the Meek 1 Scale[b] v's Point of Elution of Peptide in a Neutral pH Reversed-Phase HPLC System.[c] This figure shows good correlation between retention and the total hydrophobicity of the nonpolar face of peptides 209, 202 and 208 which do not differ in charged amino acid content. See text for a more detailed explanation.

a) Total hydrophobicity of a peptide is defined as the sum of the hydrophobicities of its constituent amino acids.

b) The Meek 1 Scale is defined in the appendix section A.2.

c) The chromatographic system used in this experiment was as follows: - column, Radial-PAK CN; Solvent A:- 0.1 M ammonium bicarbonate; Solvent B: - acetonitrile: Solvent A (80:20, v:v), Gradient:linear, 0-100% Solvent B over 60 min.

d) Total nonpolar side hydrophobicity is the maximum hydrophobicity of the peptide when in the α-helical conformation considering only 180^{o} of the face of the α-helix. These values were calculated using the computer program shown in the appendix, section A.3.

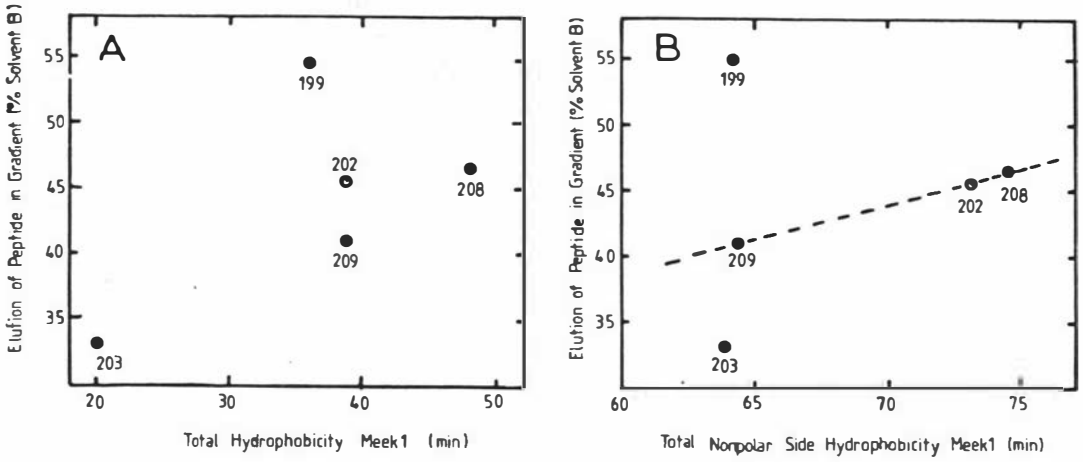

It is pertinent to recap at this stage. In the TEAP system at pH 3.2 the side chain of glutamic acid is uncharged while the side chain of arginine is positively charged. In this system peptide 199 (which is the only one which contains arginine) has a lower than predicted retention (figure 5.18). This could be explained by an ion-exchange effect with adsorbed triethylammonium ions repelling positive charges which approach the reversed-phase. Since the extra glutamic acid residue in peptide 203 is uncharged at this pH, its retention relative to the other peptides will be unaffected by such an ion-exchange effect. In the pH 7.9 system both arginine and glutamic acids are charged. However, in this case the stationary phase is slightly negatively charged due to ionisation of some silanol groups (186).* This would cause a relative decrease in retention of a peptide containing more glutamic acid residues than others (peptide 203) and an increase in retention of peptides containing more cationic residues than others (peptide 199). Such changes in retention can be seen in figure 5-9B.

5.3.5 The Silanophilic Retention of Peptide 202

The retention of peptide 202 on a Radial-PAK CN column in a 1% TEAP system is shown in figure 5-10. This figure describes the decrease in retention caused by increasing organic solvent in the mobile phase followed by increasing retention with further increases of organic solvent.

* This charge has resulted in ionic exclusion of negatively charged peptides in gel permeation chromatography (187).

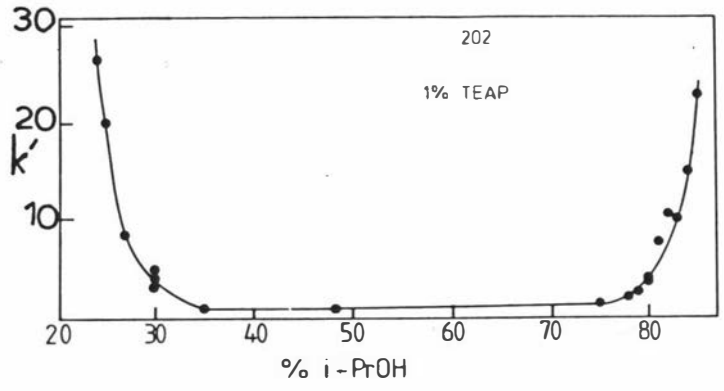

Figure 5-10 Plot of k' v's % Isopropanol for the Retention of Peptide 202 at Neutral pH. The chromatographic conditions were:
Column: Radial-PAK CN
Solvent A: 1% TEAP
Solvent B: isopropanol
Isocratic elution
Sample: 5-6 µg peptide 202 in 3 M guanidine hydrochloride

It has been established that the polar solutes, particularly amines, may bind to siliconaceous stationary phases via a normal phase mode when the mobile phase is sufficiently nonpolar (184,185). One striking property of this two sided relationship is the similarity of the slopes for the normal phase and reversed-phase modes.

5.4 Conclusions

(1) The peptides in the series retain or adopt structure on binding to reversed-phase bonded silicas.

(2) These results are compatible with an adsorption mode of binding of the peptide series onto reversed-phase bonded silica.

(3) The order of elution of the peptides in both acidic and neutral reversed-phase HPLC systems can be explained in terms of an amphipathic helix theory utilising reversed-phase HPLC derived hydrophobicity values. Only the

residues on the most nonpolar half of the helix contribute to the hydrophobic retention.

(4) The ΔH^{o} of association is an important determinant of and probably dominates the binding process.

(5) This study supports a theory of multisite cooperative binding of peptides.

CHAPTER 6 PHOSPHATIDYLCHOLINE BINDING

INTRODUCTION

The complex field of phospholipid-protein (and phospholipid-peptide) association is not well understood. A vast amount of data about these associations has been produced, but progress towards a cohesive theory explaining the data has been very slow. A significant step forward in this progress was the recognition of the amphipathic helix as the predominant structure in the phospholipid-protein interactions.

6.1.1 The Amphipathic Helix Model

The Amphipathic Helix Model was proposed by Segrest *et al*. (190) in order to explain the unusual distribution of amino acids found in the primary sequences of the apolipoproteins and to explain increases in the α-helical contents of the apolipoproteins upon their association with phosphatidylcholines. An amphipathic helix was defined to be a specific region of an apolipoprotein (called a lipid binding region) which was able to attain an α-helical conformation and expose a nonpolar face and a polar face when in this conformation. The charged residues of the amphipathic helix were defined to be disposed so that negatively charged residues occupied a thin strip in the centre of the polar face while positively charged residues occupied the lateral edges of the polar face. This distribution was envisaged to permit close contact between charged amino acid side chains and the oppositely charged groups of the phosphatidylcholine. It was also envisaged that upon association with phosphatidylcholine the nonpolar face of the amphipathic helix would be buried in the hydrocarbon millieu of the micelle while the polar face would be exposed to the polar environment of the hydrated phosphatidylcholine head groups. Thus the association was envisaged to be the result of both hydrophobic and electrostatic interactions. A detailed account of the evidence supporting the role of hydrophobic interactions in phospholipid-apolipoprotein association has been presented in section 4.4.2.3.

This model was subsequently challenged because strong electrostatic interactions between charged amino acids and the charged groups of the phosphatidylcholine could not be substantiated by a decrease in the mobility of the phosphatidylcholine charged head groups (119,122). Segrest responded to this challenge by conceding that the likelihood

of a tight electrostatic interaction was small due to the high degree of solvation which the charged groups would possess and suggested that electrostatic interactions might assist in the initiation of apolipoprotein-phosphatidylcholine association (191). The Amphipathic Helix Model is largely unchanged to this day, however certain refinements have been made to the model (see section 6.1.2).

A search of all available protein sequences revealed 65 sequences compatible with the amphipathic helix model which contained at least two oppositely charged 1-2 or 1-4 ion-pairs (192). Twenty-two of these sequences were from lipid-binding proteins and since this class represented only 2% of the sequences searched, these proteins appeared to be enriched with amphipathic sequences by approximately twenty times more than non-lipid-binding proteins. In another study the incidence of 1-2 and 1-4 ion-pairs is shown to be much higher in apolipoproteins than in globular proteins (32). Clearly some role for the charged amino acids in these sequences is implicated however no satisfactory mechanism for this role has been found. The suggestion that the ion-pairs are involved in stabilising the lipid-protein complexes has been refuted on the grounds that hydration of the charged groups would weaken any electrostatic interaction (128).

6.1.2 Refinement of the Amphipathic Helix Model

The study of a large number of synthetic peptides (33,193) has allowed the determination of certain criteria to distinguish between lipid associating and non-lipid-associating peptides. These criteria attempt to quantify the rather qualitative Amphipathic Helix Model. The determination of the criteria has been handicapped by a lack of knowledge discriminating between the polar and nonpolar interactions of the various peptide-phosphatidylcholine associations. Consequently these criteria have changed several times to accommodate the lipid-associating properties of newly synthesised fragments (33,193-195). These changes have centred on the hydrophobicity required for binding and have changed chronologically from a general statement of the involvement of the hydrophobicity (194), to a minimum average value of -900 cal/residue* for the total number of amino acids in the sequence (194,195), to a general statement of the involvement of the hydro-

* Using hydrophobicity scale of Bull & Breese (129).

phobicity only of the non-polar face (193) and finally to a minimum hydrophobicity of the non-polar face of -850 cal/residue* (33).

Therefore at present the most informed approach to protein-lipid interactions is a modification of the amphipathic helix theory proposed by Sparrow and Gotto (33). These authors state that three criteria must be met before a peptide will bind to phospholipid. The peptide must possess:

(a) The ability to form an amphipathic helix,

(b) A mean residue hydrophobicity of the non-polar face of greater than -850 cal/residue, and

(c) A critical length of 20 amino acids or more for stable phospholipid-peptide interaction. The accuracy of these criteria in determining whether or not a peptide is able to bind phosphatidylcholine is discussed in the following chapter (figure 7-3).

6.1.3 The Influence of Charged Residues on the Association of Phosphatidylcholine with Apolipoproteins and their Fragments

As has already been mentioned in section 6.1.1 the distribution of charged residues found in apolipoproteins indicates that some role exists for this distribution. Indeed there is much evidence to indicate that charged residues are important determinants of phospholipid association. The state of ionisation of some peptides and proteins has a large effect on their association with phosphatidylcholine (PC) (196,197). Upon binding to PC, approximately half of the Glu, Asp and Lys residues of ApoA-I undergo a change in pKa favouring the charged form (197). Using synthetic peptides Sparrow et al. have shown that the replacement of two lysine residues with glutamic acid results in a severe decrease in PC affinity (193). Acylation of the lysine side chains of ApoA-II with maleic anhydride removes the ability of the apolipoprotein to bind egg yolk PC (198). Another study revealed the large enthalpies of association of ApoA-I with DMPC of -90 kcal/mol ApoA-I and -170 kcal/mol ApoA-I at pH 7.4 and 3.1 respectively (233). This demonstrates the importance of charge interactions in the association.

* Using hydrophobicity scale of Bull & Breese (129).

In a study by Hauser et al. (199) the chemical shifts of selected protons of sonically irradiated dispersions of egg yolk phosphatidylcholine were compared with those of porcine HDL_3. Significant differences in the chemical shifts were found at the 2 and 3 carbon positions of the fatty acyl chains, at the methylene groups of the glycerol moiety and at the $POCH_2$ moiety of the choline group. No chemical shift differences were observed for CH_2N or $N(CH_3)_3$. These results were interpreted to mean that the polar head groups and the carboxyl end of the acyl chains of the phosphatidylcholine are situated in different magnetic environments in these two systems. Furthermore, the interaction of the apolipoproteins of porcine HDL_3 with the polar head groups of the phospholipid is implicated although not through specific ionic interactions with the choline methyl groups.

It has been shown that the phospholipid polar head groups and the apolipoproteins are present on the surface of the HDL particle (200,201). In agreement with this it has been shown that all choline methyl groups of HDL are accessible to ferricyanide (202). However, ^{31}P-NMR studies with HDL revealed that 20% of the ^{31}P resonance is unaffected by addition of Mn^{2+} (203). This was interpreted to mean that 20% of the phospholipid head groups interact strongly with the apolipoprotein components of HDL and are therefore unavailable to the Mn^{2+}. It should be noted that only the phosphate moiety is implicated in this interaction.

Similarly NMR measurements of the phospholipid choline methyl groups in porcine LDL showed that about 1/3 of these groups did not contribute a sharp resonance signal below 65°C (202). This may be evidence that these groups are immobilised by the apolipoproteins of LDL. Perhaps the best evidence of the importance of charged residues to the PC association of peptides comes from the inability to accurately predict PC association unless charged residues are taken into account (see section 7.2.2.2).

Other possible functions for the charged residue pattern found in the amphipathic helix should be considered. One of these is the stabilisation of α-helical regions by the formation of ion-pairs.

6.1.3.1 Evidence that Ion-pair Interactions may not Stabilise α-Helices

In considering the function of the distributions of charged residues found in apolipoproteins, it is informative to investigate the frequency of ion-pairs formed in a theoretical amphipathic helix. This helix is similar to that used by Segrest (192) in a computer search of proteins for amphipathic helices. However, in this theoretical amphipathic helix the polar face consists entirely of charged residues. Furthermore the polar face consists of an anionic region flanked by two cationic regions (each region consists entirely of the one type of charged residue).* In Segrest's model the charged residues are arranged in the same manner but are mixed with neutral residues. The frequency of cationic and anionic pairs of residues at particular spacings in the primary sequence are shown in table 6-1.

Table 6-1 The Frequency of Cationic and Anionic Pairs of Residues at Particular Spacings in the Primary Sequence of a Theoretical Amphipathic Helix[b].

Spacing between the cationic and anionic residues	1-2	1-3	1-4	1-5
Frequency of occurrence[a]	6	0	6	4

a) For 18 residues of a repeating 18 residue helix. The pairs of residues are not necessarily non-overlapping, i.e. a residue may be included in more than one pair.

b) As stipulated in the text.

As can be seen from the table, if the charged residues are confined to regions as proposed by the Amphipathic Helix Model then 1-3 ion-pairs are not possible. Instead, a high frequency of 1-2, 1-4 and 1-5 ion-pairs are found. Thus we should realise that the high frequency of ion-pairs of particular spacings in apolipoproteins may simply reflect

* This resulted in the region for the acidic residues being 100° of the helix and the region for the basic residues being 60° to either side of the acid region. The hydrophobic residues were thus confined to the remaining 140° of the helix.

the limited regions which the charged residues may occupy. Therefore, the fact that the distances between the side chain groups of peptides in an α-helical conformation are closest for 1-2, 1-4 and 1-5 pairs of residues (204) may not be significant. It is also worth noting that the frequency of the pairs of residues is unaffected by a complete exchange of the cationic and anionic residues. The fact that such reversed amphipathic helices are not found to a large extent in apolipoproteins (192) and that one peptide's ability to bind to phosphatidylcholine was shown to decrease after such an exchange (205) is evidence that ion-pairing is not the predominant function of these paired residues. It has been argued that the hydration of the charged residues would not allow strong electrostatic interactions between them and indeed no experimental evidence for such strong interactions has been found (32). Thus the function of the paired residues is an enigma. Some innovative theories about their function have been; that they produce an initial orientation of the apoprotein with respect to the phospholipid which favours the interaction of these species during the initial phase of binding, or that the ion-pairs resulting from a 1-4 sequence relationship could function to lock a section of the peptide backbone into an α-helix through preferential hydration of the polar side of the helix (32).

To understand how charged residues can affect the association of peptides and proteins with PC we must develop a fuller understanding of the complex nature of the phospholipid interface.

Considerable information about the influence of charged residues on apolipoprotein-phosphatidylcholine binding may be found in model studies involving lysine and polylysine.

6.1.3.2 Evidence for Stabilisation of Negatively Charged Phospholipid-Polypeptide Association via Electrostatic Interactions

Phospholipids bearing a net negative charge form a small but significant fraction of the lipid pool of most biological membranes. These lipids are phosphatidylserine, phosphatidylglycerol and phosphatidylinositol which bear a net single negative charge, and phosphatidic acid and cardiolipin which bear two net negative charges (206).

There is a tendency for such negatively charged amphiphiles to increase the area they occupy at the surface in order to decrease

lateral repulsion between the adjacent amphiphiles. Increasing the pH and hence the degree of ionisation results in an increase in the area occupied by individual amphiphiles at the surface, thus favouring the liquid-crystalline state of the bilayer where there is a lateral expansion (206). Thus, increases in the pH will depress the lipid phase transition temperature, whereas increases in either ionic strength or cation concentration (both of which will reduce the bilayer surface charge) elevate the lipid phase transition temperature by stabilising the gel (crystalline) state (206).

Recent X-ray diffraction analysis of charged lipid bilayers has demonstrated that as surface charge increases and the lateral packing of the head groups decreases leading to bilayer expansion, the acyl chains only partly follow their example (206). The authors interpreted this as being due to the attractive van der Waals interactions between the acyl chains however the major consideration in this association is most probably hydrophobic interactions which induce a close packing of acyl chains in order to minimise the aqueous-hydrocarbon interface. Thus to maintain the acyl chain packing distances (hence stopping the intrusion of water into the hydrophobic domain) the acyl chains tilt relative to the surface normal. Such tilting results in a decrease in the bilayer thickness and a decrease in the effective interacting length of the acyl chains. This results in a decreased stability of the gel (crystalline) state and hence a decrease in the phase transition temperature (T_c) is caused (206). A similar tilting of acyl chains has been identified in the gel state of phosphatidylcholines suggesting that a similar balance between charged group repulsions and hydrophobic "attractions" is attained in these phospholipids (207).

Poly-L-lysine interacts strongly with negatively charged phospholipids (208-213) causing an increase in the gel to liquid-crystalline transition temperature and an increase in the negative enthalpy of this transition. Furthermore in mixed phospholipid systems the addition of poly-L-lysine can result in the formation of rigid poly-L-lysine lipid domains (211). The major contributing factor in this association has been interpreted as the electrostatic attraction between the positively charged lysine side chains and the negatively charged phosphate moiety (211). Poly-L-lysine binds to the phospholipid in a partially α-helical conformation so that half of the charged side chains interact with the phosphate groups (211).

These experimental observations of the association of poly-L-lysine with negatively charged phospholipids are compatible with the X-ray diffraction studies discussed at the beginning of this section. Thus in a manner analogous to association of calcium ions, the cationic lysine side chains interact with the negatively charged head groups of the phospholipid decreasing the electrostatic repulsion between the head groups thus allowing a lateral condensation of the monolayer. This condensation allows a decrease in the tilt of the acyl chains in the gel state which in turn causes an increase in the effective interacting length of the acyl chains, elevation of the phase transition temperature and an increase in the enthalpy of this transition. Thus the process of binding of polypeptides to phospholipid is influenced both by the polar head groups and the acyl chains of the phospholipid.

6.1.3.3 The Interaction of Electrolytes with Uncharged Phospholipids (Phosphatidylcholines)

There is considerable evidence that charged amino acid residues influence the association of peptides and proteins with phosphatidylcholine (section 6.1.3). As has already been mentioned the reason for this is unknown. It may be informative to discuss the interactions in the light of recent experimental results.

Electrostatic repulsions between like charges on the phosphatidylcholine (PC) head group are important determinants of the expanded state of phosphatidylcholine bilayers (120). There is evidence for acyl chain tilting in the gel phase of PC which supports the expanded nature of the bilayer (207). In contrast the head groups of phosphatidylethanolamine are much closer packed presumably due to the ability of the primary amine group to undergo intermolecular hydrogen bond formation (214,215).

In comparison to negatively charged phospholipids the interaction of poly-L-lysine with neutral, zwitterionic phospholipids is much weaker (209,212). This is surprising in view of the importance of the charge repulsions to the expanded state of phosphatidylcholine. A recent study by Nakagaki and Okamura sheds some light on the matter (216,217). These authors found that uncharged zwitterionic lysine had a much higher affinity for dimyristoyl phosphatidylcholine (DMPC) monolayers than either the mono or dihydrochloride. The uncharged lysine caused a small increase in the area of the monolayer due to the size of the amino acid molecules. Despite the high affinity of uncharged lysine for DMPC

monolayers, evidence was produced to show that no strong interactions existed between the two. Such results are consistent with a decrease in the electrostatic repulsions in the monolayer caused by the insertion of the uncharged lysine resulting in an energetically favourable association. In contrast the charged hydrochlorides of lysine caused large expansions of the monolayer consistent with increased charge repulsion. Such large expansions of the monolayer would be energetically unfavourable due to decreased hydrophobic interactions as outlined above and hence few of the lysine hydrochloride molecules would associate with the monolayer. Thus it is now obvious why polylysine will not interact strongly with PC. The incorporation of a highly positively charged molecule will increase the charge repulsion within the monolayer leading to an energetically unfavourable lateral expansion.

The above study may also explain the importance of the anionic amino acid residues to the association of peptides and proteins with DMPC. Thus Glu and Asp residues may be necessary in order to neutralise the overall charge of the peptide so that expansion of the bilayer due to electrostatic repulsion is prevented.

Therefore the high incidence of 1-2, 1-4 and 1-5 ion pairs found in apolipoproteins may be due simply to the need for overall neutrality and the restricted areas of the amphipathic helix which the charged residues can occupy (section 6.1.3.1). It is interesting to consider which charged residues might be most important to the binding of peptides and proteins to PC. There is more evidence for the effect of cationic residues on the phosphate moiety of PC than for an effect of anionic residues on the choline moiety of PC (section 6.1.3). Furthermore charged amphiphiles are thought to enrich surrounding areas adjacent to their charged groups with oppositely charged ions from solution (206). The anionic migration of DMPC vesicles in electrophoresis (196) suggests that this occurs more readily for the outer choline groups than for the inner phosphate groups. This effect could explain why little change is found in the environment of the choline moiety upon binding to peptides and proteins.

It is also interesting to consider the relative importance of the cationic residues arginine, lysine and histidine. There is increasing evidence that arginine residues are essential for the binding of phosphate containing substrates and cofactors in many enzyme catalysed reactions (218). A specialist role for arginine has been suggested

whereby the major biological function of this residue is the binding of phosphorylated metabolites. The guanidino group is ideally suited to such an interaction due to its planar structure and its ability to form two hydrogen bonds with the phosphate moiety (219). For this reason we might expect arginine to be at least twice as important as lysine or histidine in the association of peptides and proteins with PC.

6.1.4 Fluidity and Protein-Phospholipid Association

Many conflicting results have been found concerning the fluidity of phospholipid bilayers upon the binding of proteins and peptides (32, 220-222,130). These differences have been attributed to the difference in time scale between NMR and ESR techniques (220) and the different types of order which exist i.e. orientational order, conformational order and rigid-body order (222). A detailed discussion of fluidity and gel/liquid-crystalline phase transitions is beyond the scope of this thesis.

6.1.5 Thermodynamic Considerations

The thermodynamics of protein-phosphatidylcholine interaction is complex. Not only does the physical state of the phospholipid (gel or liquid-crystalline) drastically influence the thermodynamics, but the size of the resulting complexes, the nature of the protein-phospholipid interaction, the conformation of the protein in the bound and unbound state and the number of protein molecules per complex also influence this process. The thermodynamic treatment of protein structure is not well developed (135). Therefore it is informative at this point to investigate the current understanding of the thermodynamics of α-helix formation since an increase in α-helix content is usually seen when proteins and peptides bind to phospholipids.

6.1.5.1 The Thermodynamics of α-Helix Formation

There is substantial evidence for the fact that α-helix formation is enthalpically driven (223). However whether or not this enthalpy is the direct result of peptide hydrogen bond formation remains controversial (223,224). Most studies which conclude that the enthalpy of α-helix formation is predominantly the result of peptide hydrogen bonding assume that any hydrophobic effects are predominantly entropic with a small endothermic contribution to the enthalpy as has been proposed by

Scheraga et al. (225) and Tanford (100). This interpretation of the hydrophobic effect has been treated in Chapter 4 together with its possible inapplicability to more complex systems.

At this point it is relevant to examine the results of several studies concerning the hydrophobic effect and protein structure. The amphipathic character of α-helices has long been noted (136). Recently a method for predicting secondary structure of proteins was devised which considered only the hydrophobic character of the amino acids in the sequence (139). This method appears to be at least as successful as other available prediction methods (140). α-Helices are predicted by the new method by searching for alternately non-polar and polar sections of the sequence compatible with an amphipathic helix. Furthermore a recent study reviewing the α-helices of highly resolved protein structures has found that most of the α-helices in these proteins are curved (226). Also the outer hydrogen bonds of the helix exposed to an aqueous environment are longer than the inner hydrogen bonds of the helix exposed to an aqueous environment. Thus it appears that the hydrophobic effect may regulate the secondary structure in proteins and also modify the secondary structure.

Several studies have attempted to determine the enthalpy associated with α-helix formations as shown in table 6-2.

Table 6-2 Enthalpies of α-helix formation found in different studies

Peptide/Protein	Method	ΔH% helical[a]	Reference
Poly-L-Lys	titrn @ varied temp	-0.885	(227)
Poly-L-Glu	titrn @ varied temp	-1.12	(227)
Poly-L-Lys	KCl shock	-1.2	(127)
Poly-L-Glu	pH jump	-2.0	(127)
ApoA-I	thermal denaturation	-1.2	(128)
ApoA-I	pH jump	-2.0	(128)
ApoA-II	b	-2.0	(128)
ApoA-II & C-III	c	-1.3	(127)
ApoA-I	phospholipid binding	-4.0	(128)

a) Units of kcal/mol of α-helical residues.

b) Correlation of change in α-helix conformation with ΔH of phospholipid binding with different concentrations of GdnCl.

c) Correlation of change in α-helix conformation with ΔH of phospholipid binding with different phospholipids.

All experimental values have been exothermic but a wide range of values between -0.085 and -4.0 kcal/mol α-helical residues have been determined. The failure to find a single value of the enthalpy for α-helix formation is evidence that there is some other influence on the observed enthalpy although the variations in experimental conditions, e.g. ionic strength and temperature, may partially explain this failure (128). This other influence may be the hydrophobic effect which will vary according to the amino acid sequence under consideration.* This effect is of particular importance in protein denaturation and phospholipid binding where the formation of a regular hydrophobic face may allow more effective

* Contributions to enthalpy of protein-phospholipid interactions arise from the difference in the sum of the heats of lipid-lipid and protein-protein interactions in the reactants and the heat of lipid-protein interactions in the products (127).

exclusion of water from this area. Such a consideration has not been approached until this study, which has shown that the association of a peptide with reversed-phase silica is enthalpy driven, because it has been accepted that the hydrophobic effect was predominantly an entropic process. It would be expected that the change in secondary structure would reflect the proportion of peptide and protein which changes its hydrophobic environment and hence that the enthalpy contribution from the hydrophobic effect would be closely correlated with the increase in α-helical content of the protein. The particular hydrophobicity of the region of protein and the hydrophobicity of its surrounding environment would result in some scatter of an enthalpy v's change in α-helix content data as is observed (127,128).

The assumption that hydrophobic interactions in complex biological processes are driven only by entropy changes is widespread. The role of hydrophobic interactions in many studies should perhaps be reassessed since the thermodynamics of some complex processes involving hydrophobic interactions do not fit this assumption (see section 4.5). A typical example of the use of this assumption is seen in a study by Massey et al. (127) in which the enthalpy of α-helix formation is assumed to be the only contribution to the enthalpy of association of DMPC with ApoA-II (above the phase transition temperature of the complex). Massey et al. used the theoretically estimated value for the enthalpy of random coil to α-helix transition of -1.32 kcal/mol calculated by Hermans (227) to support this assumption. This value must be regarded as suspect as outlined below. Hermans attributes the enthalpy of α-helix formation to three contributions: - the peptide hydrogen bond, the loss of bond rotations and the hydrophobic bonding caused by the nonpolar character of the amide backbone when it is hydrogen bonded to itself. Hermans' value for the enthalpy of peptide hydrogen bond formation of -1500 cal/mol obtained from a statistical mechanics study by Poland and Scherage (228) is both incomplete and a simplification. Hermans ignores the contribution of hydrogen bonding between water molecules and amide groups in the random coil conformation. When this effect is taken into account the enthalpy for the hydrogen bond formation is estimated to be much smaller at -675 cal/mol of hydrogen bonds (228). Hermans' value for the enthalpy of loss of bond rotations is also questionable since it is assumed that completely free rotation exists about the single bonds of the peptide chain in the random coil conformation while absolutely no torsional oscillations occur about these bonds in the α-helical conformation (229).

The hydrophobic bonding contribution of the total enthalpy of α-helix formation is also questionable since Hermans himself points out the use of Nenethy and Scheraga's (225) hydrophobicity bond strength is questionable in this instance. Thus because of the complicated nature of the random coil to α-helix transition no theoretical treatment is available to test experimental values of enthalpy with certainty. For this reason the contribution to the observed enthalpy of hydrophobic bonding between side chain groups cannot be overlooked, and there may well be a major contribution of enthalpy from this source.

Another reason for questioning the contribution of α-helix formation to the enthalpy of protein-lipid association is that the conformational change and the release of heat do not always occur on the same time scale (240).

6.2 Experimental

6.2.1 Fluorescence Measurements

The intrinsic fluorescence emission spectrum of the tryptophan residue in each peptide was measured on an Aminco SPF-500 Ratio Spectrofluorimeter instrument with the excitation wavelength set at 280 nm and with the band passes for both excitation and emission set at 5 nm. The instrument was used in the normal ratio mode (gain=3). For emission scans the damping was set at 1 second. Except where specified, emission spectra were obtained on samples at room temperature with no attempt to thermostat the cell. The instrument was standardised daily against a standard solution of 18.2 μM tryptophan in deionised water so that this solution had a relative fluorescence of 8% at the emission maximum of 365 nm.

Peptides were prepared for fluorescence measurements by pooling the appropriate HPLC fractions (see Chapter 3) and diluting these with 0.1 M ammonium bicarbonate until the proportion of isopropanol in the solution was 5% (v/v). This solution was then further diluted with 5% isopropanol: 95% 0.1 M ammonium bicarbonate (v:v) until the optical density of the peptide solution at 280 nm was 0.2 AUFS. A sample of 200 μl of the diluted solution was mixed with 3.0 ml of liposome buffer (see section 6.2.3) and the fluorescence emission spectrum measured. Phospholipid was then introduced into the cuvette and after mixing the fluorescence emission spectrum was measured at regular intervals.

6.2.2 Turbidity Clearance Measurements

Chemicals: L-α-Dimyristoyl phosphatidylcholine (DMPC) was 99% pure and was purchased from Sigma Chemical Company. Egg phosphatidylcholine was isolated from fresh egg yolks according to the method of Bergelson et al. (235) and stored under nitrogen in a chloroform-methanol solution containing butylated toluene at -10°C. Potassium bromide was puris A.R. grade from Koch-Light Laboratories Ltd. Sodium azide was laboratory grade from BDH. Ethylenediaminetetra-acetic acid (EDTA) was Univar analytical reagent grade from Ajax Chemicals. Tris (hydroxymethyl)-aminomethane (Tris) was laboratory reagent grade from Hopkin and Williams Ltd.

6.2.3 Equipment and Procedures

The lipid turbidity clearance studies were performed at room temperature in a buffer consisting of 8.5% potassium bromide (w/v). 0.01% sodium azide (w/v). 0.01% EDTA (w/v) and 0.01 M tris as used by Pownall et al. (236) and hereafter referred to as liposome buffer. The buffer was titrated to pH 7.4 with 6 N HCl. A stock suspension of egg phosphatidylcholine was prepared by evaporating a 2:1 chloroform: methanol solution of the phospholipid under an oxygen free nitrogen stream then subjecting the solid to vacuum for 30 min. The resulting 43 mg of solid phospholipid was suspended in 3 ml of liposome buffer and sonicated for 1 minute at approximately 90% output on an MSE L666 probe sonicator. Peptide solutions were prepared as described in section 6.2.1, the fluorescence measurements experimental section. After an initial fluorescence measurement had been made on the peptide solution 80 µl of the stock liposome suspension was injected into the peptide solutions and into a control containing 3.0 ml of liposome buffer and 200 µl of 5% isopropanol:95% 0.1 M ammonium bicarbonate (v:v). The cuvettes were inverted 3 times to effect complete dispersion of the liposomes. Turbidity was measured at regular intervals at 326 nm on a Hitachi model 101 spectrophotometer using liposome buffer as a blank.

A stock suspension of dimyristoylphosphatidylcholine (DMPC) was prepared 2 h before the lipid binding study by sonication of 19.8 mg DMPC in 1 ml liposome buffer for 60 sec at approximately 40°C. Peptide-lipid mixtures were prepared and turbidity measured as for egg phosphatidylcholine except that 100 µl of the stock suspension was added.

6.3 Results and Discussion

6.3.1 Egg Phosphatidylcholine Binding

Within experimental error no decrease in turbidity of the peptide-liposome mixtures was observed relative to the control after an incubation of 3 hours at room temperature (19°C). Furthermore, sonication of the mixtures for 1 minute at room temperature did not decrease turbidity in any of the mixtures by more than 5%. Fluorescence studies were not performed on these samples.

6.3.2 Dimyristoyl Phosphatidylcholine Binding

The decrease in turbidity and change in wavelength of fluorescence emission upon incubation of the peptides with DMPC at 20°C is shown in Table 6-3. Clearly peptides 202, 208 and 199 interact strongly with the phospholipid while peptides 203 and 209 interact less strongly. The decrease in turbidity of phosphatidylcholine liposomes and changes in wavelength of the fluorescence emission spectrum maximum have been shown to be excellent indicators of the formation of peptide-phospholipid complexes (236-238).

Table 6-3 Turbidity Changes and Fluorescence Emission Maximum Wavelength Changes on Addition of DMPC to Peptide Solutions.[d]

Peptide	$\Delta A_{325\ nm}$[a]	Wavelength of Fluorescence[b]		$\Delta\lambda$[c]
		initial	final	
202	.205	363 (0.63)	344 (2.2)	19
208	.103	364 (0.68)	339 (1.6)	25
209	.050	348 (0.54)	348 (1.0)	0
203	.059	363 (0.53)	362 (0.88)	1
199	.095	364 (0.70)	344 (1.3)	20

a) $\Delta A_{325\ nm}$ is the difference in absorbance at 325 nm between the incubated peptide-DMPC mixtures and a control containing no peptide. The absorbance of the control was 0.507 optical density units. The recorded changes in absorbance are the values found 3.5 h after addition of the DMPC suspension. The associations were essentially complete after this time. The values were obtained in one study but are representative of a reproducible effect.

b) The wavelength (nm) of the fluorescence emission maximum was measured initially before the addition of DMPC and finally 3.75 h after the addition of DMPC. The figures in parentheses are the % fluorescence of each emission maximum.

c) $\Delta\lambda$ is the difference between the wavelengths (nm) of the fluorescence emission maxima of the peptide solutions in the presence and absence of DMPC.

d) The approximate molar ratio of DMPC:peptide is 400:1. Temperature = $20^{o}C$.

It is interesting to note that peptide 209 has a low fluorescence emission maximum of 348 nm which is unchanged by the addition of lipid even though the turbidity of the DMPC suspension decreases and the percentage fluorescence increases. The most simple explanation is that peptide 209 self-associates in 8.5% KBr allowing the tryptophan a more non-polar environment which causes the emission maximum to be lowered. This phenomenon has also been noted by Sparrow et al. with LAP-24 (56). Evidence that peptide 209 self-associates under these conditions is shown in Table 6-4.

Table 6-4 The Fluorescence of Peptide 209 in Various Buffers.

Buffer	Wavelength of Emission Maximum (nm)
8.5% KBr*	348
0.1 M NH_4HCO_3	356
5%iPrOH:95% 0.1 M NH_4HCO_3 (v/v)	362
3 M GdnCl,0.1 M NH_4HCO_3	364**

The 8.5% KBr buffer promotes self association by increasing hydrophobic interactions (239). The lower salt concentration in 0.1 M NH_4HCO_3 results in a smaller amount of self-association while the 5% isopropanol solution actively decreases hydrophobic interactions further decreasing the amount of self-association. The use of a 3 M guanidine hydrochloride buffer causes the complete unfolding of the peptide resulting in a more random hydrophobic character which effectively stops self-association. Furthermore, as shown in Table 6-5, peptide 209 is the only peptide which has a fluorescence emission maximum which is temperature dependent. This would be expected if the peptide underwent a temperature dependent self-association and would indicate a negative enthalpy for the self-association. The transfer of the tryptophan residue to a more non-polar environment and the negative enthalpy of the self-association (see section 4.5) are evidence that the hydrophobic effect is important in this interaction.

* From Table 6-1. See experimental section for full buffer components.

** The wavelength of emission for a standard tryptophan solution (2.81 mg/l) in pure water is 365 nm.

Table 6-5 Intrinsic Fluorescence of Peptides at Different Temperatures.

Peptide	20°C	39.8°C
202	363	364
208	364	362
209	348	353,364(sh)*.
203	363	363
199	364	362

Thus although peptide 209 has no shift in fluorescence emission wavelength, an increase in % fluorescence and a decrease in turbidity confirm that it does interact weakly with DMPC. Similarly peptide 203 also interacts weakly while peptides 202, 208 and 199 demonstrate much stronger association with the phospholipid by causing more turbidity clearing and exhibiting large changes in fluorescence emission maxima.

Figure 6-1 shows the results for DMPC turbidity clearance from Table 6-1 plotted against the values for non-polar side hydrophobicity using the Meek 3 scale.**

* The emission spectrum of this peptide at 39.8°C was extremely unstable. The intensity of the fluorescence emission at 365 nm varied between 0.90 and 0.45 percentage fluorescence in a series of peaks which appeared to occur randomly (5 peaks in 6 minutes). Between the peaks the "baseline" of 0.45% fluorescence was also very noisy.

** See appendix, section A.2.

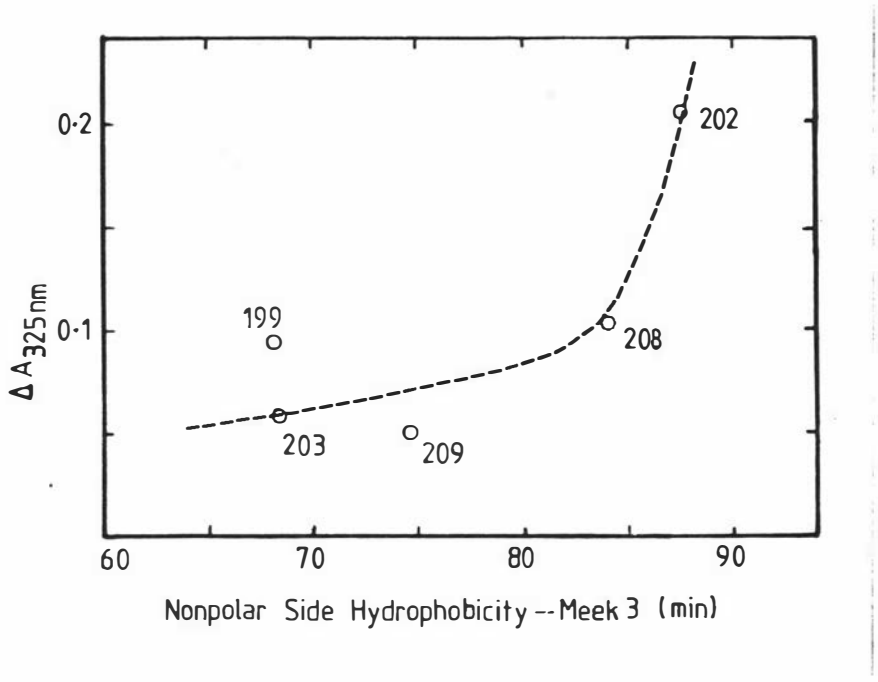

Figure 6-1 The Non-polar Side Hydrophobicity of the Peptide Series Calculated Using the Meek 3 Scale[a] v's the Decrease in Absorbance at 325 nm of DMPC Suspensions Upon Introduction of Peptide.[b]

a) Calculated as for figure 5-1B.

b) From table 6-3.

If peptide 199 is neglected for the time being, the non-polar side hydrophobicity of each peptide seems to explain the order of phospholipid binding ability of the other peptides. The slightly smaller value for 209 may be caused by its self-association since self-association will decrease the concentration of peptide available for binding to the phospholipid. The similarity of this plot with figure 5-1B indicates a striking similarity in the two processes of reversed-phase HPLC binding of peptides and phosphatidylcholine binding of peptides. The two processes will be compared in the following chapter.

CHAPTER 7 THE CORRELATION BETWEEN PHOSPHOLIPID BINDING AND REVERSED-PHASE HPLC RETENTION

7.1 Introduction

The previous two chapters have respectively dealt with the interaction of a series of peptides with reversed-phase bonded silica and with phosphatidylcholine. This chapter investigates the relationship between these two processes. Furthermore, based on this relationship and other information, a modification of the amphipathic helix theory is proposed which describes the binding of peptides to the phosphatidylcholines.

The importance of a quantitative model which describes hydrophobic interactions in biological systems has long been realised. To quote Horvath and colleagues (146) "Owing to the cardinal role of hydrophobic interactions in life processes, there is a need for a physio-chemical method to quantitatively measure the hydrophobicity of biologically active substances. In the light of our present understanding, solvophobic chromatography could be a very useful tool to obtain such information. Moreover stationary phases with hydrophobic surfaces of different configuration could be used as probes to map the detailed hydrophobic profile of biologically interesting compounds."

The isocratic reversed-phase HPLC retention of various compounds has been related to their organic solvent/water partitioning with some success (241-244). Thus it is not a novel idea to correlate reversed-phase HPLC retention of compounds with their affinity for other hydrophobic systems.

7.1.1 The Similarity Between the Two Processes

The binding of a peptide to a reversed-phase bonded silica and to a phospholipid vesicle interface are two closely related processes. In both cases the peptide binds to an interface between a non-polar and polar environment. The nature of the interface is certainly different for the two processes, however, the same driving force exits in both, i.e. the exclusion of the non-polar amino acid side chain groups from the aqueous environment.* The free energy of associations of

* In the case of reversed phase HPLC the aqueous environment contains organic solvent. The applicability of measurements made in this environment to those made in fully aqueous solution has been discussed in section 5.3.2.

a particular peptide with each of the two interfaces are not likely to be equal because the micro-environment of the bound peptide is different in each case. Nevertheless, we should expect to see some degree of correlation between the affinities of a series of peptides for the two interfaces. This is particularly relevant since the retention of the series of peptides on a reversed-phase HPLC system has been shown to occur via the α-helical structure, Chapter 5. Thus the mechanism of binding in both processes involves the same amphipathic helix structure.

It was this analogy which inspired the model described here. This analogy gives a fresh approach to the study of protein-phospholipid interactions and also offers a quantitative formula for the prediction of phospholipid binding by peptides. The degree of success of this formula is further evidence for the amphipathic helical model of apolipoprotein binding. The new approach developed by the author encompasses all three criteria of the current lipid-peptide binding model (section 6.1.2) in one formula and in addition proposes a way of establishing the contribution made by polar interactions. These interactions have been largely ignored by most studies after the initial theory of the amphipathic helix was postulated for reasons given in section 6.1.1.

7.2 Results and Discussion

7.2.1 The Correlation Between Reversed-Phase HPLC Retention and Phospholipid Binding

The correlation observed between reversed-phase HPLC retention and the phospholipid binding ability of the series of peptides synthesised in this study is shown in Figure 7-1 (data from Figures 5-1B and 6-1).

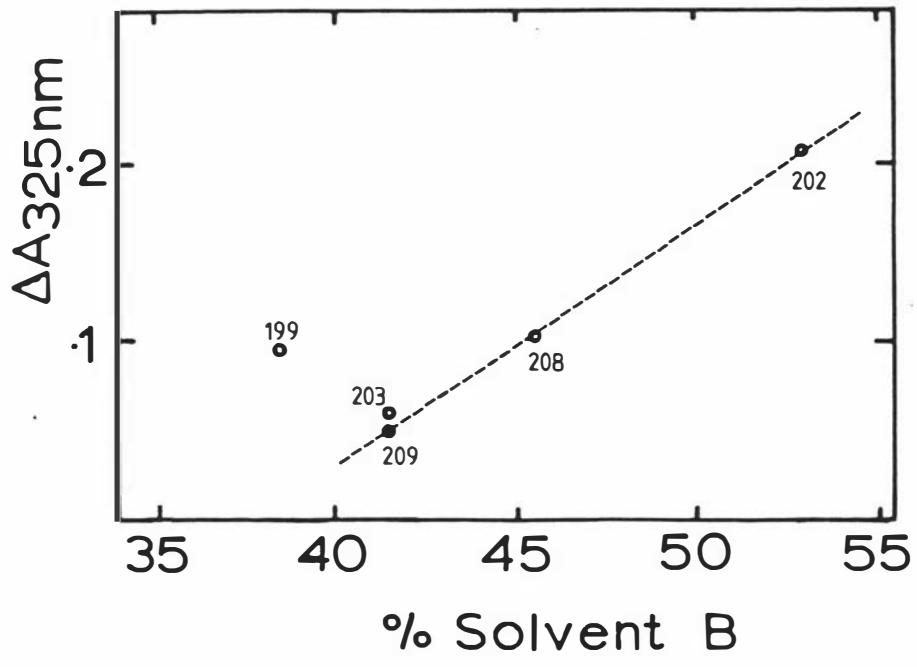

Figure 7-1 The Reversed-Phase HPLC Retention of the Peptide Series v's their Affinity for DMPC.
The reversed-phase system was the μBondapak alkylphenyl, 40°C system described in table 5-1 (Solvent A: - 1% TEAP, pH 3.2, Solvent B: - 2-propanol:Solvent A, 80:20 (v:v). The retentions have been corrected for the 6 ml solvent delay volume by subtracting 10% Solvent B. The affinities for DMPC are taken from table 6-3 and represent the decrease in turbidity of phospholipid suspensions 3.5 h after addition of the respective peptide. Each peptide is identified by its number.

There is an excellent correlation between the reversed-phase HPLC retention and the phospholipid binding capacity of all of the peptides (if we neglect peptide 199 for the meantime). This demonstrates that this HPLC system may be a good model for estimating the hydrophobic component of phospholipid-peptide associations. The fifth peptide, peptide 199, shows a greater ability to decrease the turbidity of DMPC vesicles than would be predicted from either its retention in reversed-phase HPLC (figure 7-1) or its non-polar side hydrophobicity (figure 6-1). It was reasoned that, since peptide 199 contained no hydrophobic residues which the others do not also contain in varying amounts (see section 3.8), the anomolous behaviour of peptide 199 could not be attributed to hydrophobic effects. The most likely

cause of this anomolous behaviour was therefore reasoned to be the extra cationic residue in this peptide. It should be remembered that all of the peptides contain 2 lysines and 2 glutamic acids,* while only peptide 199 contains an arginine residue. Indeed there is much evidence for the existence of interactions between the phosphatidylcholine polar head groups and the cationic residues of phospholipid binding peptides and proteins (section 6.1.3). The question now arises: Is this hypothesis compatible with the numerous studies of the phospholipid binding properties of other synthetic peptides? If the hypothesis is correct then the phosphatidylcholine binding ability of a peptide should depend not only on its non-polar side hydrophobicity** but also upon its number of cationic residues.

7.2.2 The Amphipathic Threshold Model - A Modified Amphipathic Helix Model for Apolipoprotein-Phosphatidylcholine Association

As discussed in section 6.1.3, there can be no doubt that polar residues do have an advantageous effect on phospholipid binding of peptides and proteins. The precise nature of this contribution has proved evasive however. In the modified model portrayed here the major contribution by polar residues is assumed to be the interaction of cationic residues with the anionic phosphates of the phosphatidylcholine head groups on the surface of the liposome or lipoprotein. Thus the two major contributions to binding are the hydrophobic effect, for which an HPLC derived hydrophobicity scale is a good model, and the cationic residue effect for which it is assumed that arginine stabilises the interaction twice as well as lysine or histidine. The Amphipathic Threshold Model is described by figure 7-2. The purpose of this graph is to separate all those peptides which bind to phosphatidylcholine from all those which do not.

* Except for peptide 203 which contains 3 glutamic acid residues.

** See section A.3.

Figure 7-2 The Demonstration of the Amphipathic Threshold Model. Non-polar side hydrophobicity[a] v's cationic contribution[b] of all apolipoprotein fragments and model peptides which have been prepared and studied to determine lipid-binding ability; ●, form stable phosphatidylcholine-peptide complexes; ⊙, interact strongly with phosphatidylcholine but do not form stable complexes; o, do not interact with phosphatidylcholine. A list of the peptides included in this graph can be found in the appendix, section A.7. The threshold has been drawn between the two groups so as to minimise the number of incorrectly assigned peptides. Note that all the peptides are linear and possess no disulphide bridges.

a) Calculated using the scale of Meek *et al*. (157) using the computer program in the appendix, section A.3 with 180^{o} of non-polar face.

b) Cation contribution = 2 x Arg + Lys + His where Arg, lys and His are the total number of arginine, lysine and histidine residues present in a sequence.

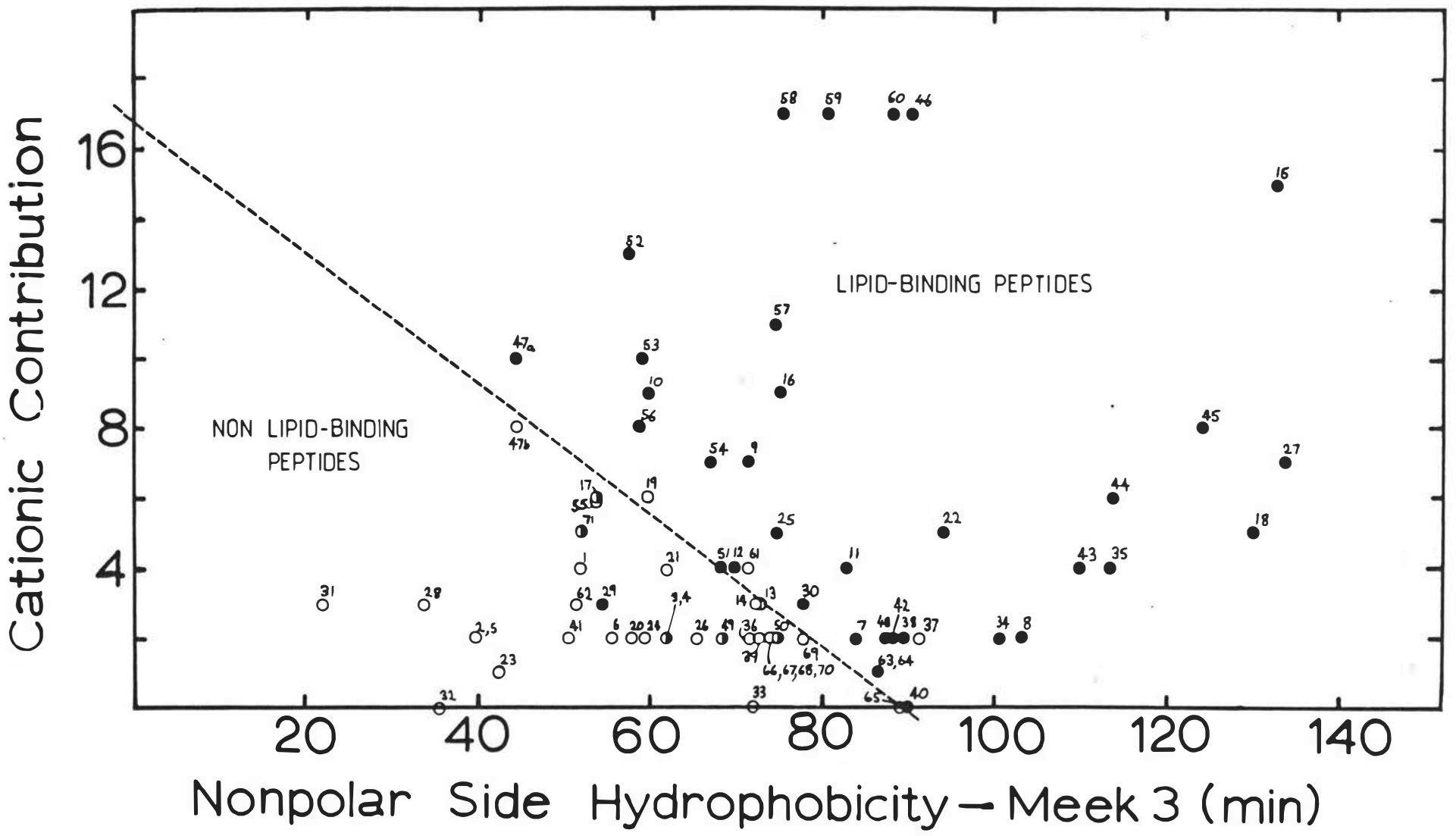
Cationic Contribution
16
12
8
4
20
40
60
80
100
120
140
Nonpolar Side Hydrophobicity – Meek 3 (min)
LIPID-BINDING PEPTIDES
NON LIPID-BINDING PEPTIDES

The Amphipathic Threshold model depicted in figure 7-2 achieves remarkable success in distinguishing between phospholipid binding and non-binding peptides. All but 4 of the 71 peptides studied are correctly assigned to their respective groups, a success rate of 94%. This is even more remarkable when we realise that: a) the hydrophobicity scale used may not exactly mimic the hydrophobicity of the amino acids in the phospholipid environment; b) the calculation of hydrophobicity of the non-polar face is based on only 180^{o} of the circumference regardless of the extent of hydrophobic face and the position of acidic and basic residues; c) no allowance has been made for any distortion to the α-helical structure which could maximise the non-polar face, d) basic residues are counted as having equal contribution to the interaction with phosphatidylcholine irrespective of where they are positioned relative to the non-polar face; e) the relative contributions of arginine, lysine and histidine residues may require refining, and f) there is no standard method for determining whether a peptide is a phosphatidylcholine binding peptide or not and thus the points on the graph represent a mosaic of different phosphatidylcholine binding assays.

7.2.2.1 The Incorrectly Assigned Peptides

Two of the points, corresponding to incorrectly assigned peptides, numbers 19 and 61*, are extremely close to the threshold depicted in figure 7-2 and thus a small adjustment in hydrophobicity scale or cationic residue contribution might easily bring these on the correct side of the threshold. The other two peptides are more difficult to

* It should be noted that the DMPC binding ability of peptide no. 61 has not been reported. Instead its egg phosphatidylcholine binding ability has been reported (205). Peptides appear to bind more readily to DMPC than to egg PC (32) and hence the position of peptide no. 61 on figure 7-2 may be compatible with a slight increase in the threshold for the longer acyl chain phosphatidylcholines found in egg PC. If in fact peptide no. 61 does not bind to DMPC then the most probable reason is the reversal of charged residues relative to the classical amphipathic helix. This means that in this peptide the cationic residues occupy a strip in the centre of the polar face while anionic residues occupy two regions either side of the cationic strip. Any "finetuning" of the Amphipathic Threshold Model should evaluate this effect.

explain. Peptide no. 37 was over-predicted in graphs of all combinations of hydrophobicity scales and polar amino acid contributions attempted. The source of this error may lie in the added charge repulsion this peptide could experience when forming an α-helix. Such charge repulsion results in lowered α-helicity in protonated poly-lysine (227) and melittin (245). The N-terminal sequence of this peptide Leu-Ile-Lys-Lys-Ala- contains 3 positive charges, 1 α-amino group and 2 ε-amino groups. When an α-helical conformation is adopted the α-amino group is positioned extremely closely to the two ε-amino groups. This may lead to α-helix destabilisation and hence to a lowered affinity for phospholipids. The addition of two further residues Thr-Pro- to this peptide results in peptide no. 38, a phospholipid binding peptide. This addition does not substantially change the non-polar side hydrophobicity or the α-helix potential of peptide no. 38 relative to peptide no. 37. However when the peptide is in the α-helical conformation the Thr-Pro-addition separates the α-amino group from the two ε-amino groups.

The other peptide whose phosphatidylcholine affinity was poorly predicted by the Amphipathic Threshold Theory described in figure 7-2 is peptide no. 29. This peptide does not demonstrate a high α-helical content upon binding to phosphatidylcholine (246). This fact suggests that this peptide binds to phosphatidylcholine by some mechanism other than the amphipathic helix with self-association possibly being involved.

7.2.2.2 The Effectiveness of the Current Phosphatidylcholine Binding Model

The current model describing the phosphatidylcholine binding ability of peptides (Sparrow *et al.* reference (33)) has been discussed in section 6.1.2. In contrast to the Amphipathic Threshold Model discussed above, the current model is much less accurate at the prediction of the phosphatidylcholine binding. This model has been applied to all of the synthetic fragments of apolipoproteins and model peptides as for the Amphipathic Threshold Model. The result is shown in figure 7-3. Using this model, 24 of the 71 peptides are incorrectly assigned to the binding and non-binding groups. This represents a success rate of only 66%. Clearly the new model is a vast improvement (cf. 94% success rate).

Figure 7-3 The Demonstration of the Current Amphipathic Helix Model. Average non-polar side hydrophobicity[a] v's number of residues for all apolipoprotein fragments and model peptides which have been prepared and studied to determine lipid-binding ability; ● , form stable phosphatidylcholine-peptide complexes; ◐, interact strongly with phosphatidylcholine but do not form stable complexes; ○, do not interact with phosphatidylcholine. A list of the peptides included in this graph can be found in the appendix, section A.7.

a) Calculated using the Bull and Breese scale of hydrophobicity (see section A.2) using the computer program found in the appendix (section A.3).

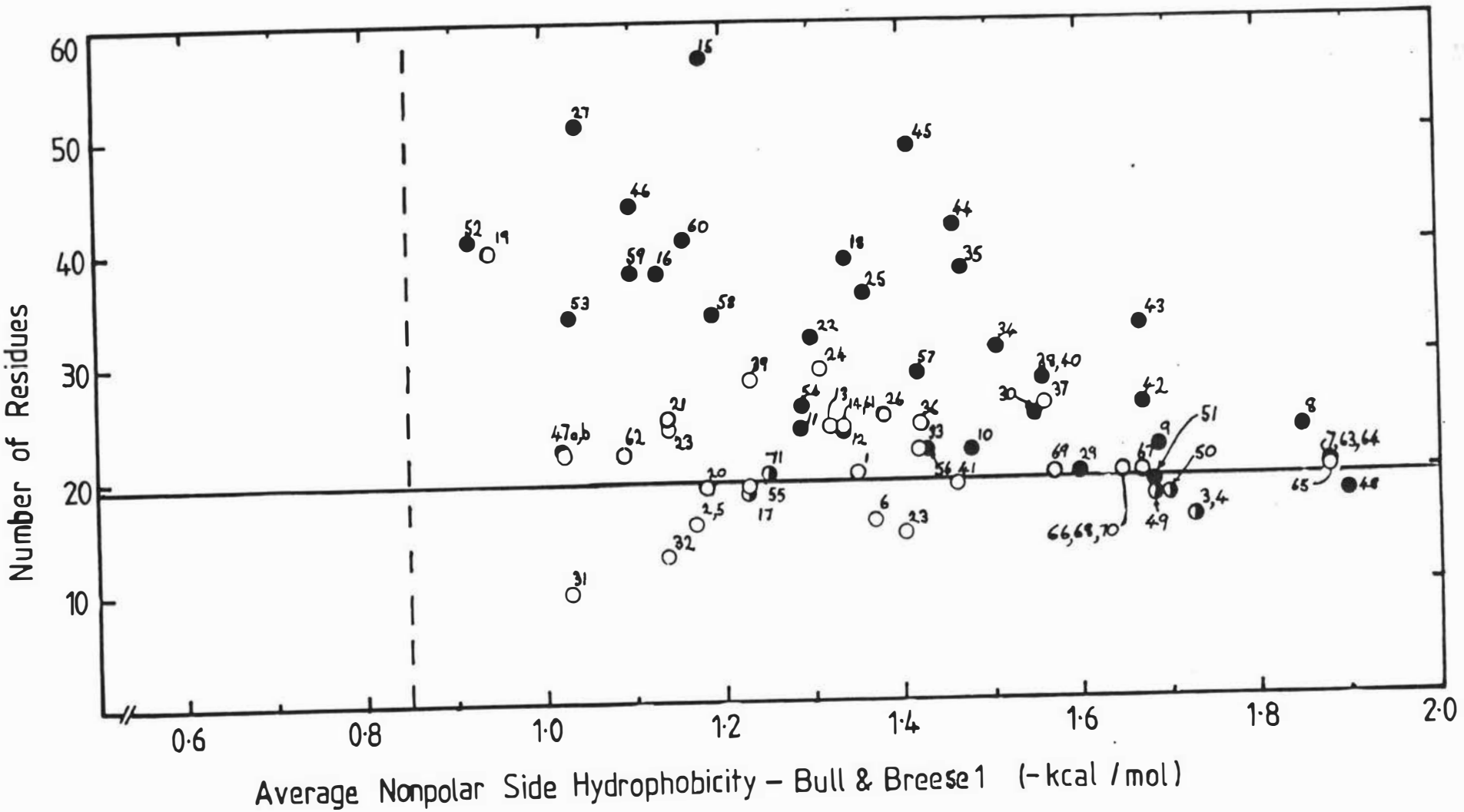
Number of Residues
60
50
40
30
20
10
0·6
0·8
1·0
1·2
1·4
1·6
1·8
2·0
Average Nonpolar Side Hydrophobicity – Bull & Breese 1 (– kcal / mol)

7.2.2.3 Explanation of the Cation Residue Effect

The cationic effect can best be explained by using the example of a recent study (193). In this study a lipid associating peptide LAP-20 and 3 of its homologues were synthesised. Two of the homologues were made by replacing one of two lysine residues in LAP-20 with a glutamic acid residue and the other was made by replacing both lysine residues (peptide nos. 7, 63, 64 and 65 of figure 7-2 respectively). The substitution of only one lysine does not drop the peptide's affinity for phosphatidylcholine below the threshold and therefore the peptide still binds. The substitution of both lysine residues does drop the affinity below the threshold and a non-phosphatidylcholine binding peptide results. Another example is in a study by Mao et al. (195). They have observed that the substitution of a Lys-Lys sequence with Ser-Ser (peptide nos. 38 and 40 of figure 7-2 respectively) does not affect the DMPC binding capacity of their peptide. This change does not decrease the peptide's affinity for phosphatidylcholine below the threshold of figure 7-2 and hence both peptides bind to DMPC.

Evidence for the increased contribution of arginine to the stability of peptide-phosphatidylcholine complexes relative to the other cationic residues comes from the consideration of equal contributions by the cationic residues (more evidence has been given in section 6.1.3). This model is not shown.
In progressing from this model to the Amphipathic Threshold Model (figure 7-2) the phosphatidylcholine binding ability of peptide nos. 47a, 51 and 56 switch from being underestimated to being correctly predicted.* It should be emphasised that small increases in the number of correctly assigned peptides are probably significant since the number of incorrectly assigned peptides decreases from 6 to 4, a vast improvement. The fact that the number is small merely reflects the small number of peptides which lie close to the threshold.

7.2.2.4 Other Possible Explanations of the Cationic Residue Effect

It could be argued that the importance of cationic residues to the phosphatidylcholine binding ability of peptides is merely the expression of another parameter which increases concurrently with

* The phosphatidylcholine binding ability of peptide no. 19 switches from being correctly predicted to being slightly over-estimated by the Amphipathic Threshold Model.

the number of cationic residues. This parameter might be the number of 1-2, 1-4 and 1-5 ion-pairs, the number of acidic residues or total peptide length. When each of these parameters is plotted against the same non-polar hydrophobicity as for the Amphipathic Threshold Model the numbers of incorrectly assigned peptides were 7, 8 and 19 respectively (cf. 4 incorrectly assigned peptides for the Amphipathic Threshold Model, figure 7-2). Peptide length is obviously a poor substitute for the cationic residue contribution in the model, since nearly 5 times the number of incorrectly assigned peptides are found using this parameter compared with the cationic contribution of figure 7-2. However, the situation is less clear for the number of 1-2, 1-4 and 1-5 ion-pairs and the number of acid residues. The successfulness of these parameters in correctly assigning most of the peptides to their binding and non-binding groups most probably reflects the high incidence of 1-2, 1-4 and 1-5 ion-pairs in the peptides studied (32). That is, whenever a cationic residue is present in a sequence it is almost always linked to an anionic residue via a 1-2, 1-4 or 1-5 ion pair. The Amphipathic Threshold Model still gives the least number of incorrectly assigned peptides, however the possibility of contributions from ion-pairs and/or acid residues cannot be overlooked. The synthesis and study of a new series of peptides whose properties lie close to the threshold of figure 7-2 but vary in their ion-pair and acidic residue content may clarify this point. One study, which compared the phosphatidylcholine binding properties of a synthetic peptide with an analogue which was identical except that its cationic and anionic residues were interchanged, suggests that the number of ion-pairs is not as important as the position of the charged residues around the amphipathic helix (205). Also peptide 203 from the current study contains an extra Glu residue compared to the others in the series but no increase in DMPC affinity was observed for this peptide above that explained by its non-polar side hydrophobicity, figure 7-1. These examples suggest respectively that the ion-pairs and acidic residues are not important to the association of peptides with phospholipid. A possible role for acidic residues which has been outlined in section 6.1.3.3 may explain the high incidence of the ion-pairs in apolipoproteins. This role is the neutralisation of the cationic residues since neutrally charged molecules appear to have strongest affinity for the neutrally charged phospholipids.

7.2.2.5 The Choice of Hydrophobicity Scale

The Amphipathic Threshold Model utilises the reversed-phase HPLC derived scale of amino acid hydrophobicities of Meek and Rossetti (157), (see also "Meek 3" in appendix, section A.2). It is interesting to consider the influence of a change in the hydrophobicity scale on the model.* For this reason the number of cationic residues was plotted against Bull & Breese (129) non-polar side hydrophobicity for the total number of synthesised peptides to determine the sensitivity of the model to a change of this nature. Switching to the Bull & Breese scale of hydrophobicity results in an increase in the number of incorrectly assigned phosphatidylcholine binding peptides from 6 to 9. Thus, not only can the reversed-phase HPLC derived scale of hydrophobicities be applied to the phosphatidylcholine binding properties of peptides, but it is also more effective than the scale of Bull & Breese for this purpose. It is notable that although the use of the Bull & Breese hydrophobicity scale causes a significant increase in the number of incorrectly assigned peptides, this number is small compared to the large increase in number of incorrectly assigned peptides which takes place when cationic residues are not taken into account (figure 7-3). Therefore the effect of the change of hydrophobicity scale is relatively minor compared to the effect of neglecting the cationic residues.

The currently accepted model for peptide-phosphatidylcholine association uses the average non-polar side hydrophobicity of peptides (see section 6.1.2). It is therefore of interest to compare the effectiveness of this parameter with that of total non-polar side hydrophobicity. When average non-polar side hydrophobicity (Meek 3) is plotted against the number of cationic residues in each peptide, the graph contains 10 peptides whose phosphatidylcholine binding abilities have been incorrectly assigned. This should be compared to a graph which utilises the total non-polar side hydrophobicity (Meek 3 hydrophobicity scale) and which contains only 6 incorrectly assigned peptides. Although the total hydrophobicity of the non-polar side appears to be significant improvement over the average hydrophobicity of the non-polar side in this regard, more studies

* A list of the graphs constructed and their effectiveness can be found in table 7-1 at the end of this section.

would have to be made before the influence of average non-polar side hydrophobicity could be completely discounted. Such studies would involve the preparation of a series of peptides of different lengths but with a constant number of cationic residues and a constant average non-polar side hydrophobicity. Most studies performed to date do not satisfy these conditions however one study is quite useful in this regard. The relative phosphatidylcholine affinities of the peptides LAP-20 and LAP-24 have been estimated and the longer peptide binds much more strongly. This cannot be predicted from a consideration of average non-polar side hydrophobicity but can be predicted by a consideration of total non-polar side hydrophobicity. Therefore it would appear that the total non-polar side hydrophobicity is the more relevant parameter.

Furthermore it should be noted that there are two stipulations made on the hydrophobicity of peptides in the current Sparrow and Gotto model (33); a minimum length and a minimum average non-polar side hydrophobicity. These two stipulations have the effect of placing a total non-polar side threshold on the peptides. Such stipulations are thus entirely consistent with the Amphipathic Threshold Model.

It is also interesting to note that Sparrow and Gotto (33) suggest that a minimum average non-polar side hydrophobicity of -850 cal/mol is required before a peptide binds strongly to phospholipid. Plotting the number of cationic residues against average non-polar side hydrophobicity for the all the apolipoprotein fragments and model peptides and the fitting of a threshold to optimise the binding-non-binding compartmentalisation results in a minimum average non-polar side hydrophobicity of -1900 cal/mol for a peptide without cationic residues.

Table 7-1 shows the successfulness of the various plots in predicting the phosphatidylcholine binding properties of the peptides. A list of the peptides is given in the appendix, section A.7.

Table 7-1 The Accuracy of Different Phosphatidylcholine-Peptide Association Models in Distinguishing Phosphatidylcholine-binding Peptides.

Hydrophobicity Scale[a]	Other Parameter	No. Incorrect Peptides[b]	Figure
Meek 3 Total N.P.S.H.[c]	2xArg+Lys+His	4	7-2
Bull & Breese Av. N.P.S.H.	No. of residues	24	7-3
Meek 3 Total N.P.S.H.	Arg+Lys+His	6	d
Meek 3 Total N.P.S.H.	No. of 1-2,1-4 & 1-5 ion-pairs	7	d
Meek 3 Total N.P.S.H.	Glu+Asp	8	d
Meek 3 Total N.P.S.H.	No. of residues	19	d
Bull & Breese Total N.P.S.H.	Arg+Lys+His	9	d
Meek 3 Av. N.P.S.H.	Arg+Lys+His	10	d

a) N.P.S.H. = Non-polar Side Hydrophobicity. The Meek 3 and Bull & Breese hydrophobicity scales are detailed in the appendix, section A.2. N.P.S.H. and average N.P.S.H. were calculated using the computer program found in the appendix, section A.3.

b) Number of incorrectly assigned peptides.

c) The Amphipathic Threshold Model.

d) Figure not shown.

7.2.2.6 The "Fine-Tuning" of the Amphipathic Threshold Model

In section 7.2.2 some ways of improving the Amphipathic Threshold Model were proposed. These included the determination of the exact relative contributions of the cationic residues and the maximising of the total peptide-phosphatidylcholine interactions by allowing some flexibility in the α-helical structure and in the depth of penetration of the helix into the phospholipid. Other factors, such as charge repulsion by closely situated charged residues and extensive α-helix

breaker regions (248) or other secondary and tertiary structural features may also need to be taken into account. In order to facilitate the "fine-tuning" of the Amphipathic Threshold Model a uniform approach by the different groups working in this area should be adopted. Ideally an assay of phospholipid binding should be used with standardised conditions for pH, ionic strength, phospholipid type, preparation of vesicles, concentration of both peptide and vesicles, temperature and method of quantitating the amount of phospholipid-peptide interaction. Using the Amphipathic Threshold Model as a guide many peptides can now be synthesised which lie close to the threshold. Subtle changes to the sequences of such peptides should allow a "fine-tuning" of the model. Note that adjustments to the model may be necessary for each type of phospholipid to allow for changes in the interactions between phospholipid charged head groups and the charged amino acids.

7.2.2.7 Implications of the Amphipathic Threshold Model

If the Amphipathic Threshold Model is correct then several implications can be drawn about the mechanism of binding of peptides to phosphatidylcholine.

a) An alternative to the discrete binding site

The new approach offers an alternative to the concept of discrete phospholipid binding sites. In the modified model presented here the length of amphipathic helix is considered continuous and phospholipid-peptide binding occurs only after a certain threshold for the free energy of association has been exceeded.

Historically, discrete amphipathic helical lipid-binding regions were invoked on the basis of predictions of secondary structure within the apolipoproteins (190-192,224) calculated by Chou and Fasman parameters (248). A number of studies were completed on the lipid binding properties of series of synthetic peptides representing gradually increasing portions of these proposed phospholipid-binding regions (33,193). The requirement of a certain minimum length of the sequence for lipid binding to occur was interpreted to mean that discrete lipid binding sites were involved. Such results are readily assimilated into the Amphipathic Threshold Model. The elongation of the sequence eventually causes the peptide to bind phospholipid when the threshold for free energy of association is exceeded. It should be noted that such an interpretation does not limit the phospholipid-binding region

to that region for which α-helicity is predicted. The Chou and Fasman (248) predictions of secondary structure should be regarded as suspect for this application since the α-helix and β-sheet parameters are inherently biased in that they have been calculated from the statistical occurrence of residues in the various secondary structures of water soluble globular proteins (246). Apolipoproteins bear some differences to this group of proteins in that they have no or few cystine disulphide linkages, prosthetic groups or bound ligands which allows a flexibility of conformation not found in other protein classes (32). One of the reasons for the low α-helix potentials calculated for sequences between the proposed amphipathic helical sections of the apolipoproteins is the existence of proline within these regions. The statistical analysis of proline residues within water soluble globular proteins which have had their structures analysed by X-ray crystallography leads one to believe that proline is an α-helix breaker. However, analysis of the sequences in which Chou and Fasman calculations fail to predict α-helical structure found by X-ray crystallography reveal that several of these sequences contain proline in a slightly distorted α-helix (248). Such sequences are found in β-haemoglobin, cytochrome C, cytochrome b5, subtilisin BPN' (248), and in phospholipase A2 (249). It is quite feasible that proline residues found in apolipoproteins merely alter the direction of the helix to accommodate the curvature of the phospholipid or lipoprotein particle as has been proposed by others (32). This reasoning is supported by the periodic occurrence of proline within the structure of apolipoprotein A-I (250). Another function of the proline residues contained in apolipoproteins may be to decrease the α-helicity of these proteins in solution and hence maximise the free energy of association with phospholipid. Alternatively the function may be to decrease the degree of self association and oligimerisation of the apolipoprotein by decreasing the regularity of the non-polar face, as has been noted for β-endorphin (251).

Furthermore several studies have shown that the α-helicity of apolipoproteins increases on binding to phospholipids (32). Apolipoprotein model peptides (33,193), other proteins (212,252,254,255) and unrelated peptides (18,19,21,22,253) also become more α-helical on binding to phospholipids. This stabilisation of the α-helix conformation is also seen in non-polar solvents (19,256,257). Chou and Fasman calculations clearly under-predict α-helical structure of apolipo-

proteins and peptides in the phospholipid environment. Thus the prediction of discrete α-helical sections in apolipoproteins by Chou and Fasman parameters may not be relevant to the lipid bound proteins. There will of course be some sequences which cannot adopt the α-helical configuration even when stabilised by phospholipid but such sequences will be less common than that predicted by the Chou and Fasman calculations. The calculation of an adjusted set of Chou and Fasman parameters for each amino acid is of course hampered by the difficult task of crystallising protein-lipid or peptide-lipid mixtures (1).

b) Why A Threshold?

It is interesting to consider why a threshold for peptide-phosphatidylcholine association should exist at all. The existence of a threshold is not unprecedented in solute-phospholipid interactions. We may draw a parallel here with the partitioning of a series of alkyltrimethyl ammonium halides into membranes (258). When the alkyl chain is up to 6 carbons in length, interaction with membranes is superficial. Longer chain lengths, however, give rise to penetration and much stronger interaction. Clearly in this situation we also have a threshold. The hydrophobicity of the solute increases until a certain value is exceeded and then a strong interaction results.

Since the threshold appears to be obeyed for a large number of different peptides the threshold would appear to be a property of the phospholipid rather than a property of the peptide or peptide-phospholipid complex. Perhaps this property is the large internal pressure of phospholipid bilayers (130). We could expect phospholipid bilayers to squeeze out potential solutes by way of this internal pressure or cohesiveness. Such a proposition is consistent with a study by Phillips et al. (259) in which it was found that the hydrophobic protein β-casein could not penetrate a condensed phosphatidylcholine monolayer but could penetrate an expanded monolayer.

Another way of looking at this problem is to consider the work required to oppose the internal pressure prior to the insertion of a solute. For a given size of solute, there must be a minimum interaction energy of the solute and phospholipid (equal and opposite to the work done opposing the internal pressure) before any interaction will take place. It has been estimated that the internal pressure in distearoyl lecithin monolayer is approx. 26 dyne/cm (130). A very

simplistic calculation of the work required to insert a 20 residue peptide in the form of an α-helix into such a monolayer results in a value of 3.4 kcal/mol.* This should be compared with the threshold non-polar side hydrophobicity of a peptide with no cationic residues. This value is 19.4 kcal/mol.** The two values are of the same order of magnitude, which is encouraging considering the assumptions which have been made. The penetration of water to the 5th methylene groups of the phospholipid acyl chains may account for some of the discrepancy (231). Although this theory seems to be attractive there may be many other possible causes for the threshold in this complex interaction.

c) How is the Cationic Contribution Expressed?

Clearly a contribution of the cationic residues to phospholipid-binding is implicated. The contribution of the alkyl moieties of the side chains of these residues to hydrophobic interactions in complexes is expected to be quantitated by the reversed phase HPLC determined scale used in the revised model. Therefore rather than any added contribution from the alkyl moieties of the cationic residues it must be the cation itself which is involved in extra stabilisation of the peptide-phospholipid complexes.

It may be that the ionic interaction itself does not contribute to the free energy of association, but that the perturbation of the negative potential of the phosphate layer in the phosphatidylcholine decreases repulsive forces between the polar head groups. This would allow closer packing of the head groups which in turn would allow closer packing of the alkyl portions of the phospholipid closest to the interface hence excluding water molecules from this hydrophobic region. The favourable association of cationic residues with phospholipids may therefore be due indirectly to the hydrophobic effect. The closer packing of alkyl chains below cationic residues is compatible with the suggestion by Sparrow and Gotto (33) that hydrophobic residues nearest in sequence to

* Assuming the dimensions of the peptide are 3 nm x 0.3 nm (260) and that the pressure stays constant despite the disturbance of the insertion.

** The Bull and Breese scale of hydrophobicity (129) must be used because the units of this hydrophobicity scale are in energy units while the reversed-phase HPLC derived scale of the Amphipathic Threshold Model has units of minutes.

the ion-pairs on an amphipathic helix are more important than other hydrophobic residues in influencing phospholipid binding. It could be argued that closer packing of the polar head groups would induce large changes in the phosphorous NMR spectra of the phospholipid. However, in the binding of poly-L-lysine to negatively charged phospholipids (where electrostatic interactions are very important) the local order of the phosphate region is not affected (213). Hence a small change in the relaxation time of the phosphorous nuclei upon binding of protein may be compatible with this interpretation. Moreover the increase in the temperature of the gel to liquid crystalline transition of phosphatidylcholine upon binding to apolipoproteins is compatible with a closer packed region of phospholipid surrounding the apolipoprotein. The concept of a more stable phospholipid domain being closest to the apolipoprotein is at variance to the proposal by other authors (128) who reason that the addition of protein perturbs the phospholipid closest to it while inducing remotely the stabilisation of the domain of phospholipid farthest from the protein. It is difficult to envisage how this circumstance might arise.

7.2.3 Application of the Amphipathic Threshold Model to Non-apolipoprotein Peptides

The Amphipathic Threshold Model quantitates the major interactions between apolipoprotein fragments and phosphatidylcholine (PC) but can the model be applied to other peptide-PC associations? A good test of the general applicability of the model is to use it to predict the PC affinity of a completely different pool of peptides. A list of non-apolipoprotein peptides for which PC affinities are known is given in table 7-2. These peptides are plotted in figure 7-4 according to the Amphipathic Threshold Model. Considering the diversity of function of the peptides and the differing conditions of the PC binding assay, the agreement of the PC affinity of these peptides with their predicted PC affinity is remarkable.

As can be seen in figure 7-4 the lack of affinity for PC of human gastrin, somatostatin (reduced), substance P, sleep peptide, angiotensin I, glucagon (19-29), β-endorphin, ACTH (1-10) and salmon calcitonin are correctly predicted by the model. Similarly the model accurately predicts the strong PC affinity of: the surface active peptides delta-

Number	Peptide	Reference
1	human gastrin	(253)
2	somatostatin (reduced)	(253)
3	substance P	(253)
4	sleep peptide	(253)
5	angiotensin I	(253)
6	glucagon	(267)
7	glucagon (19-29)	(253)
8	corticotropin releasing factor	(262)
9	growth hormone releasing factor	(262)
10	β-endorphin	(261)
11	ACTH (1-10)	(16)
12	ACTH (1-24)	(16)
13	delta-haemolysin[a]	(263,264)
14	melittin	(22)
15	cytotoxic peptide	(251)
16	calcitonin (human)[b]	(265)
17	" (porcine)[b]	(265)
18	" (salmon)[b]	(265)
19	porcine phospholipase A2[c]	(266)

Table 7-2 A List of Non Apolipoprotein Peptides With Known Phosphatidylcholine Affinity. These peptides are plotted in figure 7-4.

a) Staphylococcus aureus

b) Residues 1-7 were omitted from the calculation of the non-polar side hydrophobicity due to the 1-7 disulfide linkage and hence the uncertain secondary structure in this region.

c) The interface recognition region of porcine phospholipase A2. The non-polar side hydrophobicity of the N-terminal sequence (1-22) was calculated using the computer program in the appendix (section A.3) and then the hydrophobicity of Tyr_{69} was added to this result since this tyrosine residue has also been implicated in the phospholipid binding process (266).

Figure 7-4 The Application of the Amphipathic Threshold Model to the Phosphatidylcholine Binding of Non Apolipoprotein Peptides. The sequences of the peptides listed in table 7-2 were analysed according to the rules of the Amphipathic Threshold Model (see figure 7-2) and plotted as for figure 7-2. The threshold drawn in this figure has been directly transferred from figure 7-2. Phosphatidylcholine affinities: ●, form stable complexes; ⊙, interact weakly with phosphatidylcholine but do not form stable complexes; o, do not interact with phosphatidylcholine.

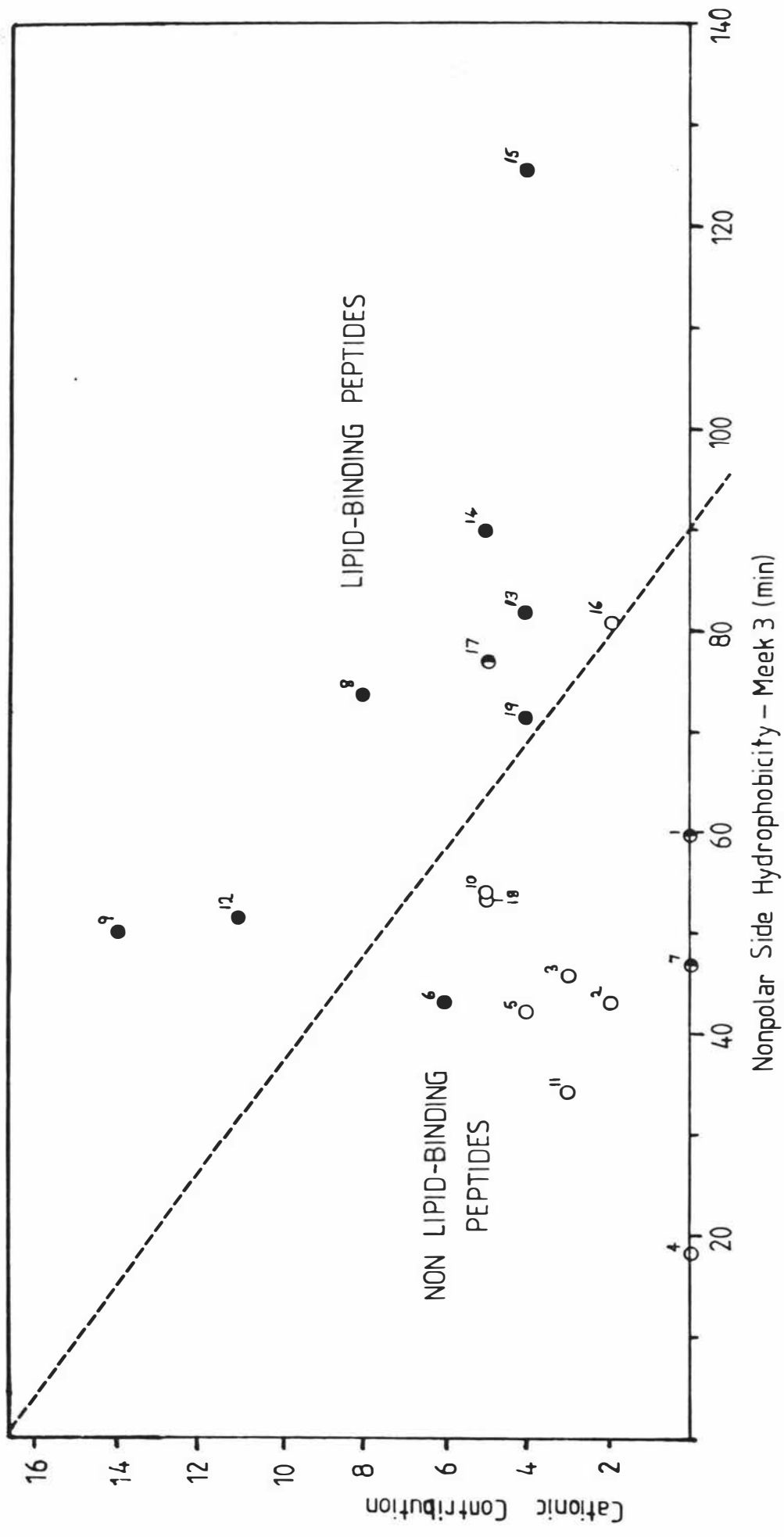
LIPID-BINDING PEPTIDES
NON LIPID-BINDING PEPTIDES
Cationic Contribution
Nonpolar Side Hydrophobicity – Meek 3 (min)
2
4
6
8
10
12
14
16
20
40
60
80
100
120
140

haemolysin, melittin and a cytotoxic peptide with melittin like activity,* the peptide hormones corticotropin releasing factor, growth hormone releasing factor, and ACTH (1-24); and the phospholipid interface recognition site of porcine phospholipase A_2.

The model appears less useful in predicting the PC affinities of human and porcine calcitonins which have only a low affinity for DMPC as evidenced by differential scanning calorimetry (265). The presence of 1-7 disulphide bridges in these peptides may have distorted the amphipathic character of the remainder of the sequences. The model under-predicts the PC affinity of glucagon (No. 6). However, it must be pointed out that glucagon binds to DMPC only over a narrow temperature range near the phase transition temperature and will not apparently bind to DPPC.* Thus the affinity of glucagon for PC is not particularly strong and therefore a position close to the threshold would be expected when glucagon is plotted on figure 7-4. Other authors have suggested that the glucagon molecule can be envisaged as two separate amphipathic helices (1-14 and 19-29) separated by 4 polar residues (269). Calculation of the non-polar side hydrophobicity for these two fragments followed by addition of these values results in the correct prediction of glucogon's DMPC affinity.

It is necessary to explain the inclusion of the phospholipase A_2 sequence in figure 7-4. The affinity of this protein for phospholipids is strong and has been suggested as a model for protein-lipid interactions (23). The interface recognition site of this protein has been studied and the residues responsible for phospholipid binding identified (266). Furthermore the majority of these residues are located in α-helical segments at the N-terminus of this enzyme (249). Thus there is some support for the hypothesis that an amphipathic helix is involved in the interface recognition site of this enzyme. It is notable that the synthesis of a semi-synthetic analogue of porcine phospholipase A_2 in which Arg_6 was replaced with Asn_6, has a decreased affinity for PC monolayers (270). This is in complete agreement with the function of cationic residues defined by the Amphipathic Threshold Model.

An interesting approach to the specificity of interaction of the peptide hormones with their surface receptor is best described using β-endorphin as an example. This peptide will not interact strongly

* The model also predicts a stronger interaction for the cytotoxic peptide compared to melittin as is observed (251).

with PC and therefore lies just below the threshold in figure 7-4 (No. 10). Thus with the added contribution of a specific receptor-β-endorphin interaction the β-endorphin can interact strongly at the cell receptor site while demonstrating no non-specific affinity for other membraneous surfaces. The construction of β-endorphin analogues with more uniform amphipathic helix structures resulted in unpredictable biological potency of these analogues probably due to non-specific interaction with phospholipids (271).

The similarity of the potential amphipathic helix in β-endorphin to those in apolipoproteins together with the increase in α-helix content of this peptide in helicogenic solvents has led to the hypothesis that the potential amphipathic helix is important in the interaction of β-endorphin with membrane phospholipids (19). A two stage interaction was envisaged where β-endorphin would first partition into (or onto) the membrane and then interact with the opiate receptor. Very accurate receptor binding constants for porcine β-endorphin and its deletion peptides are available from this study.* Figure 7-5 shows the correlation between rat brain opiate receptor affinity and the phospholipid binding potential (considering both hydrophobicity and cationic residues according to the Amphipathic Threshold Model) for each of the peptides.

* Porcine β-endorphin lies extremely close to human β-endorphin when plotted on figure 7-4 and hence is expected not to bind to phosphatidylcholine.

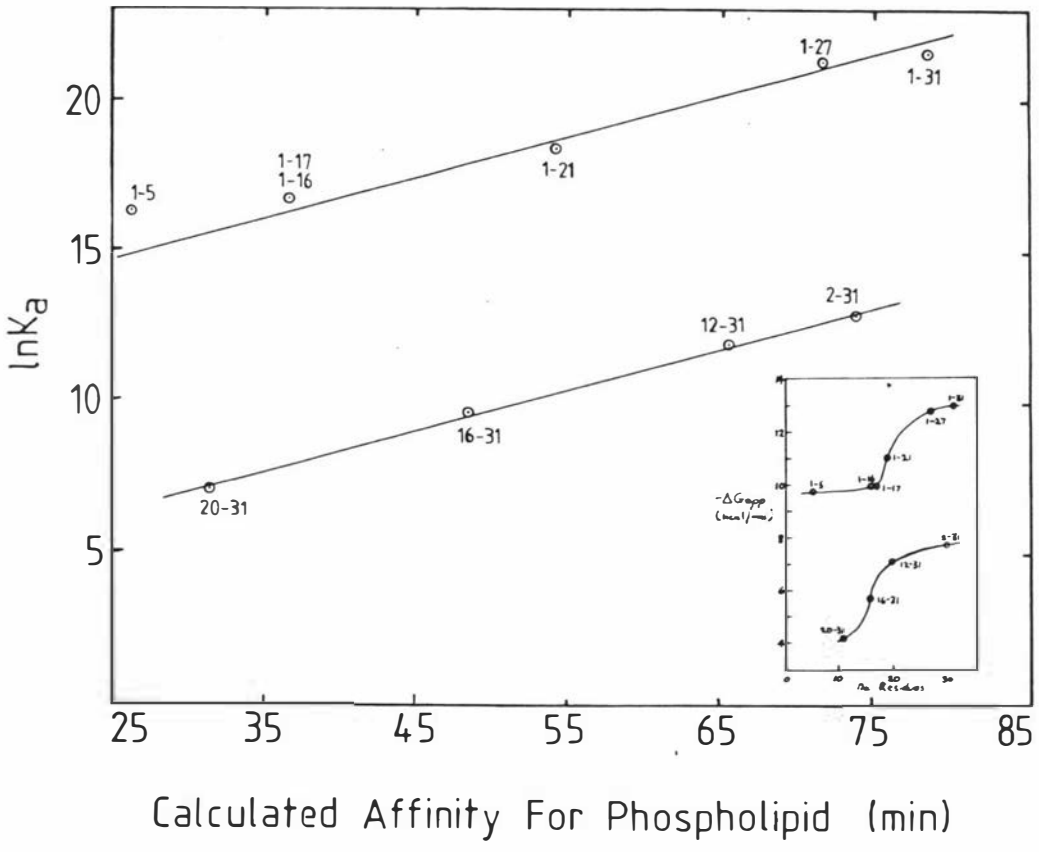

Figure 7-5 The Calculated Affinity For Phospholipid v's Rat Brain Opiate Receptor Affinity for Deletion Peptides of Porcine β-Endorphin.

The phospholipid affinity of each peptide was calculated by finding the total non-polar side hydrophobocity of each peptide (by using the hydrophobicity scale of Meek 3 in the computer program of section A.3) and adding to this a value of 4.52 min for every lysine and histidine residue in the peptide. Thus the two major contributions to phospholipid affinity quantitated by the Amphipathic Threshold Model are combined into one parameter in this graph. The inset shows the best available correlation of receptor affinity with any parameter prior to this study. The receptor affinities were obtained from reference (19) using the equation $K_a = 1/K_d$.

The correlation is exceptionally good. Those peptides which do not contain the amino terminal tyrosine lie on the lower line while those which contain this residue lie on the top line. This confirms that the amino terminal tyrosine residue is extremely important for receptor binding contributing approximately -5.2 kcal/mol to the free energy of binding.* The most striking feature of this graph is that the two lines are parallel. This means that apart from the specific tyrosine interaction with the receptor (and a slightly larger than predicted value for the receptor affinity of the 1-5 fragment, enkephalin, which may be due to the greater flexibility of this short peptide) the affinities of these peptides for the receptor can be quantitatively explained by their predicted affinities for phosphatidylcholine. This is an extremely powerful argument for the participation of membrane lipids in the interaction of β-endorphin with its receptor. The sequence homology of porcine β-endorphin with human, ovine, bovine, camel, equine, rat, ostrich, turkey and salmon β-endorphins (19) may reflect the importance of the amphipathic helix to the mode of binding of this peptide to the receptor in other species.

7.3 Conclusion

The Amphipathic Threshold Model postulated in this work presents a considerable advantage over previous methods of predicting phosphatidylcholine-peptide interactions. The model is applicable to apolipoprotein fragments and also to certain peptide hormones and surface active peptides. The model may also be useful in quantitating peptide hormone-receptor interactions.

The hydrophobicity scale used in the model is based upon the reversed-phase HPLC retention of peptides. Reversed-phase HPLC has been shown to accurately reflect the hydrophobic environment of the phospholipids. In particular a system consisting of a μ-Bondapak alkylphenyl column with a gradient from 1% triethylammonium phosphate (TEAP) pH 3.2 to 80% 2-propanol:20% 1% TEAP was particularly useful in quantitating the

* This specific tyrosine-receptor interaction energy of -5.2 kcal/mol may be compared with the hydrophobicity of tyrosine measured by Bull and Breese (129) of -2.24 kcal/mol. Note, however, that the hydrophobicity of tyrosine is already included in the calculation of phospholipid affinity plotted in figure 7-5.

hydrophobic interactions between peptides and phospholipids. Furthermore the thermodynamics of the reversed-phase HPLC retention may more accurately reflect the thermodynamics of peptide-PC interactions. Using the model as a guide, the synthesis of many peptides can now be attempted to "fine-tune" the hydrophobicity scale and the interactions of the polar residues. No such guide has been available before this study.

APPENDIX

A.1 The Effect of Various Guard Columns on the HPLC Separation of Peptide 203 From Contaminating Peptides

The effect of placing an "in line" guard column before the high performance column in an HPLC system is considered here. As shown in figure A-1 the separation of peptide 203 from its synthetic contaminating peptides is almost unaffected by the placement of a guard column (containing C18/Porasil B packing) between the injector and the Radial-PAK C18 column.

The peptide is eluted slightly later with no decrease in efficiency when the guard column is added to the system.

The effects of 4 different guard columns upon the system used in figure A-1A are shown in Figure A-2. This figure shows that the choice of guard column does not greatly influence the separation. The recoveries would appear to be better when C18/Porasil B or Prep-PAK C18 packings were used in the guard columns however. Comparison with figure A-3 shows that 3 of the guard columns (when used without any other column) have very poor efficiencies (figure A3-A, B & D). These broad peaks are completely eluted before the composition of the mobile phase reaches that required for elution from the Radial-PAK C18 column. Thus the peptide eluted from the guard columns is merely readsorbed in a tight band onto the high performance column in all cases. For this reason the efficiency of the guard column is not relevant provided the elution of the peptide from the guard column is complete well before the peptide begins to be eluted from the high performance column.

Figure A-1 A Comparison of the Efficiency of Separation of Peptide 203 With (B) and Without (A) a Guard Column.

Conditions of Elution: -

Column: Radial-PAK C18

Guard Column: A, none; B, C18/porasil B

Solvent A: - 0.1 M ammonium bicarbonate, pH 7.9

Solvent B: - 2-propanol: acetonitrile: solvent A, (3:3:4, v:v:v)

Detection: A, 230 nm, 0.1 AUFS
B, 230 nm, 0.2 AUFS

Sample: 12.5 µg peptide 203 purified by gel filtration and ion-exchange chromatography (i.e. up to step 7 of figure 3-11, section 3.4) in 6 M urea.

Gradient: linear, 0-100% solvent B over 60 min.

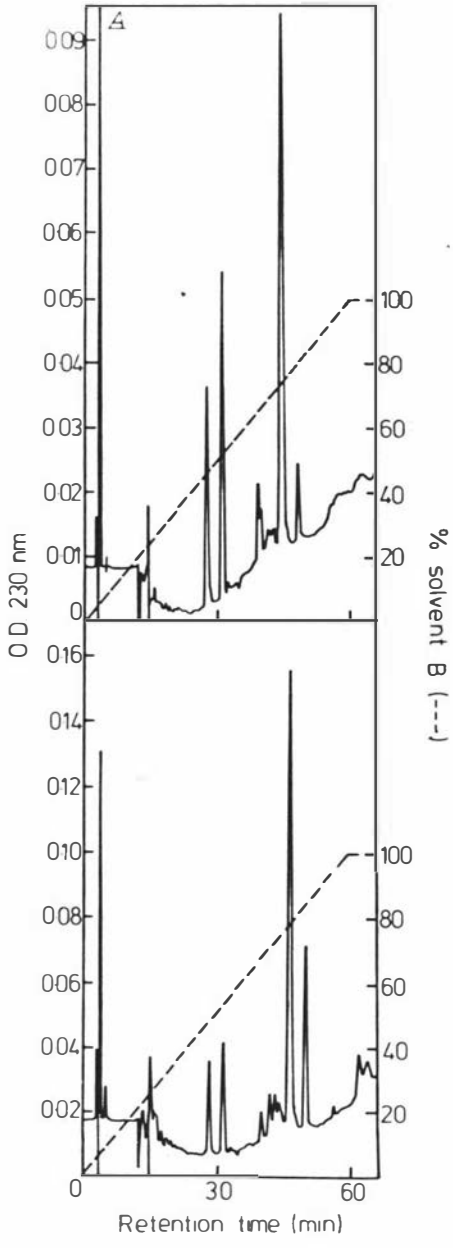
A
0.09
0.08
0.07
0.06
0.05
0.04
0.03
0.02
0.01
0
100
80
60
40
20
0.16
0.14
0.12
0.10
0.08
0.06
0.04
0.02
0
30
60
Retention time (min)
OD 230 nm
% solvent B (---)

Figure A-2 The Effect of Various Guard Columns on the HPLC Separation of Peptide 203 from its Contaminating Peptides. The conditions of elution are identical to those of figure A-1B. The guard column (Waters Associates) had dimensions of 30 x 3.9 mm.

Guard columns: A, C18/Porasil B, 0.13 g.
B, Prep-PAK C18, 0.17 g.
C, Spherisorb ODS.
D, C18/Corasil, 0.35 g.

The guard columns in A, B and D were prepared by the tap-fill method adding the dry packing in four roughly equal amounts. The guard column in C was packed from a slurry under high pressure.

Figure A-3 The Efficiencies of the Various Guard Columns Alone. The conditions of elution are identical to those of figure A-1B except that the Radial-PAK C18 column has been removed. The guard columns have been described in figure A-2.

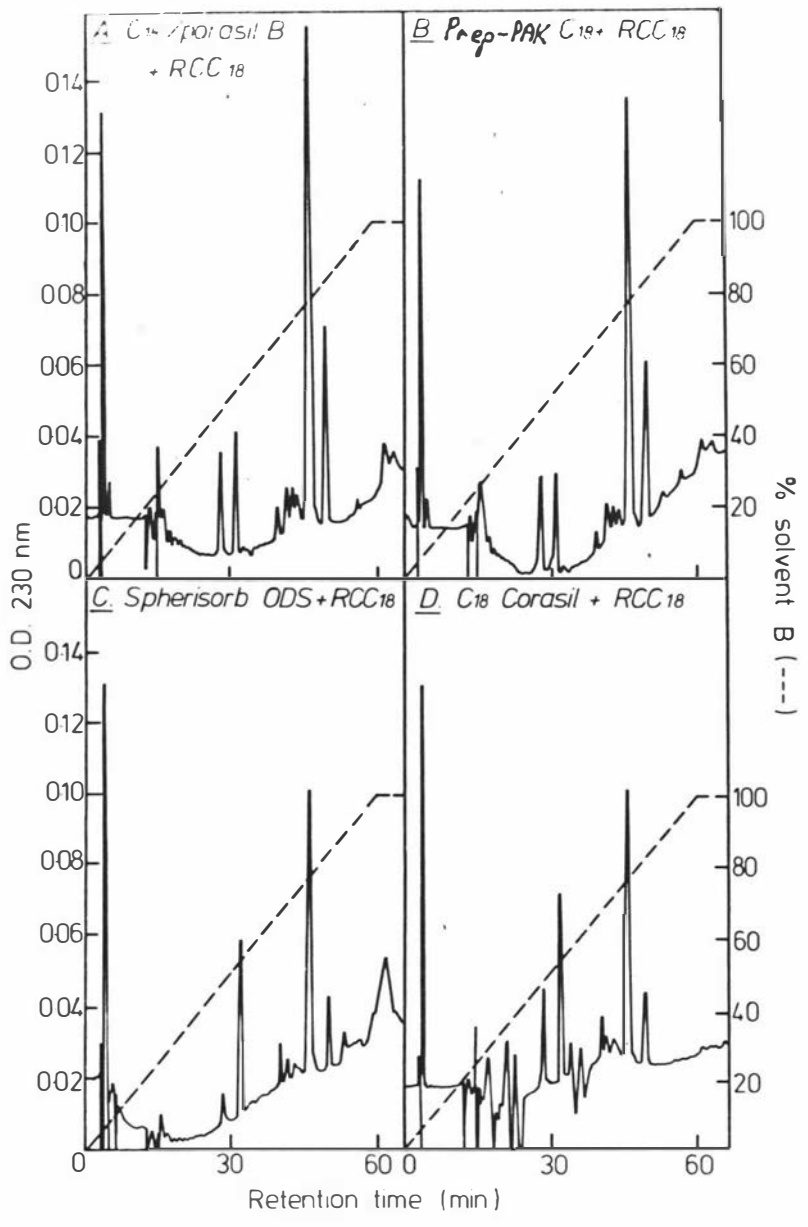
A. C18/porasil B + RCC18
B. Prep-PAK C18 + RCC18
C. Spherisorb ODS + RCC18
D. C18 Corasil + RCC18
O.D. 230 nm
% solvent B (---)
Retention time (min)

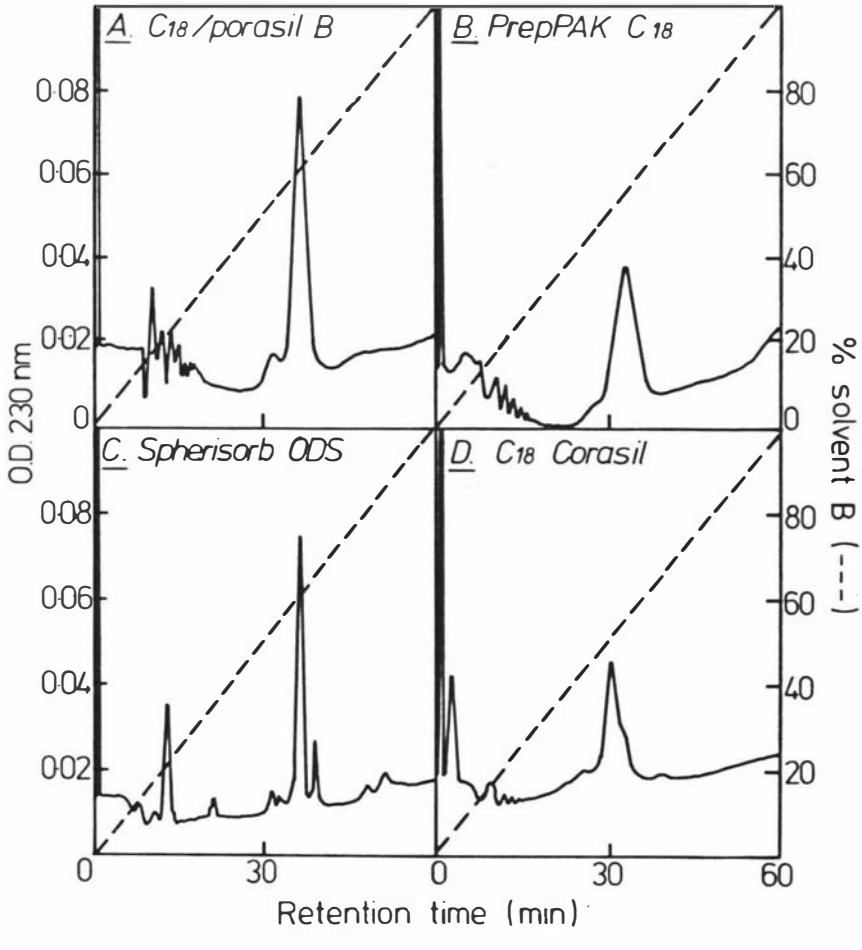
A. C18/porasil B
B. PrepPAK C18
C. Spherisorb ODS
D. C18 Corasil
OD 230 nm
% solvent B (---)
Retention time (min)

A.2 Hydrophobicity Scales

Many methods have been used to quantify the hydrophobic character of amino acids. Table A-1 presents a number of these scales together with their source and the type of experiment used for the quantitation.

Table A-1 Details of Different Hydrophobicity Scales.

Name	Details of hydrophobicity measurement	Reference
Sasagawa 1	HPLC, μBondapak C18, 0.1% TFA, pH 2	(158)
Sasagawa 2	As above but weighted towards smaller peptides	(158)
Meek 1	HPLC, Bio-Rad ODS, 0.1 M $NaClO_4$, pH 7.4	(155)
Meek 2	As for Meek 1 but also 0.1% H_3PO_4, pH 2.1	(155)
Meek 3	As for Meek 2 but averaged over 100 peptides	(157)
Meek 4	As for Meek 3 but 0.1 M NaH_2PO_4-0.2% H_3PO_4	(157)
Rekker	Octanol/water partioning	(158,175)
Bull & Breese	Surface tension of amino acids at isoelectric point	(129)
Jones	Solubility of amino acids in aqueous organic solv.	(178)
Manavalan	Statistical, surrounding hydrophobicity in 14 proteins	(177)
Pliska 1	t.l.c. of amino acids at pH 3.2	(176)
Pliska 2	t.l.c. of amino acids at pH 8.0	(176)
Wolfenden	Affinities of side chains for water	(179)
Kyte & Doolittle	Mixture of Wolfenden and statistical protein study	(272)

The hydrophobicities of each amino acid measured by each of the scales are given in table A-2.

Table A-2 The Hydrophobicities of the Amino Acids Measured by Different Scales.

	SASAGAWA	SASAGAWA 2	MEEK 1	MEEK 2	MEEK 3	MEEK 4	REKKER	BULL & BREESE[b]	JONES	MANAVALAN	PLISKA 1	PLISKA 2	WOLFENDEN	KYTE & DOOLITTLE
C CYS	0[a]	0[a]	0[a]	0[a]	0[a]	0[a]	0.93	+0.45	1.52	14.63	0.82	0.82	-1.24	2.5
H HIS	0.34	8.8	-3.5	0.8	-0.7	-2.2	-0.23	+0.12	0.87	12.16	-0.84	0.39	-10.27	-3.2
I ILE	1.38	27.4	13.9	11.8	8.5	7.0	1.99	+2.26	3.15	15.67	1.55	1.55	2.15	4.5
M MET	0.85	14.5	4.8	7.1	5.4	4.0	1.08	+1.47	1.67	14.39	1.42	1.42	-1.48	1.9
S SER	0.18	1.1	1.2	-3.7	-3.2	-2.9	-0.56	+0.39	0.07	11.23	-0.08	-0.08	-5.06	-0.8
V VAL	0.38	7.4	2.7	3.3	5.9	4.6	1.46	+1.36	1.87	15.71	1.18	1.18	1.99	4.2
A ALA	0.13	2.4	0.5	-0.1	1.1	1.0	0.53	+0.20	0.87	12.97	0.40	0.40	1.94	1.8
G GLY	0.22	4.0	0	-0.5	-0.2	0.2	0.00	0	0.10	12.43	0	0	2.39	-0.4
L LEU	1.34	26.4	8.8	10.0	11.0	9.6	1.99	+2.46	2.17	14.90	1.64	1.64	2.28	3.8
P PRO	0.48	7.9	6.1	8.0	4.4	3.1	1.01	+0.98	2.77	11.37	0.77	0.77	0[a]	-1.6
T THR	0.12	7.4	2.7	1.5	-1.7	-0.6	-0.26	+0.52	0.07	11.69	0.33	0.33	-4.88	-0.7
F PHE	1.71	31.4	13.2	13.9	13.4	12.8	2.24	+2.33	2.87	14.00	1.63	1.63	-0.76	2.8
R ARG	0.26	0	0.8	-4.5	-0.4	-2.0	0[a]	+0.12	0.85	11.72	-0.90	-0.90	-19.92	-4.5
Y TYR	1.23	21.0	6.1	8.2	7.4	6.7	1.70	+2.24	2.67	13.42	0.88	0.88	-6.11	-1.3
W TRP	2.34	35.8	14.9	18.1	17.1	15.1	2.31	+2.01	3.77	13.93	1.41	1.41	-5.88	-0.9
D ASP	0.10	-0.1	-8.2	-2.8	-1.6	-0.5	-0.02	+0.20	0.66	10.85	-0.07	-1.05	-10.95	-3.5
N ASN	-0.45	-11.3	0.8	-1.6	-4.2	-3.0	-1.05	-0.08	0.09	11.42	-0.16	-0.16	-9.68	-3.5
E GLU	0.27	2.7	-16.9	-7.5	0.7	1.1	-0.07	+0.30	0.67	11.89	0.36	-0.98	-10.20	-3.5
Q GLN	0.36	3.2	-4.8	-2.5	-2.9	-2.0	-1.09	-0.16	0	11.76	0.10	0.10	-9.38	-3.5
K LYS	0.05	-3.1	0.1	-3.2	-1.9	-3.0	0.52	+0.35	1.64	11.36	-1.14	-1.14	-9.52	-3.9

a) No value given therefore arbitrarily chosen at zero.

b) The Bull & Breese hydrophobicity scale shown here is that of reference (129) multiplied by negative one. This was necessary to make the sign of the scale positive for increasing hydrophobicity and hence make the scale compatible with the computer program in section A.3.

A.3 Computer Program for the Calculation of Non-polar Side Hydrophobicities of Peptides

The computer program detailed below calculates the total and the average hydrophobicity of the non-polar surface of the peptide when in the α-helical conformation.* The calculation is performed for a particular 180° of the helix surface then the face is shifted around the helix by an increment of 20° and the hydrophobicity recalculated. The last step is performed repeatedly until the face is back at its original position. The maximum total hydrophobicity from all of the different positions of the face is then called the "non-polar side hydrophobicity". The average hydrophobicity of the non-polar side is then calculated by dividing by the number of residues on the non-polar side.

* The α-helix is assumed to have 3.6 residues per turn and hence each residue is separated by 100°.

Input

"Hydrophobicity scale":	As defined in table A-2.
"Penetration of helix":	The area of face over which hydrophobicity is to be summed (180° for all the calculation made in this study).
"Peptide Sequence":	in one letter or three letter code.

Output

"Tothyd":	the sum of the hydrophobicities of all the amino acids in a sequence.
"Avtot" :	"Tothyd" divided by the number of amino acids in a sequence.
"Test":	the maximum hydrophobicity of the non-polar face as described above (also called the "Non-polar Side Hydrophobicity").
"Avnpol":	"Test" divided by the number of amino acids on the maximum non-polar face.
"Polar":	"Tothyd" - "Test"
"Avpol":	"Polar" divided by the number of amino acids not on the maximum non-polar face.

```
program peptides;

  type  amino_acids = (cys, his, ile, met, ser, val, ala, gly, leu, pro,
                       thr, phe, arg, tyr, trp, asp, asn, glu, gln, lys);

        char3       = packed array[1..3] of char;

  var   acid_names  : array[amino_acids] of char3;

                (*   Parameters   *)
        scale       : array[amino_acids] of real;
        penetration : integer;
        peptide     : array[1..60] of amino_acids;
        pepchar     : packed array[1..60] of char;

        no_peptides : integer;
        tothyd      : real;
        totres      : integer;
        biggest_nonpolar : real;
        first       : boolean;
        formfeed    : char;

        no_biggest  : integer;
        save_pol    : array[1..17] of record
                                        incr  : integer;
                                        numbnp: integer
                                      end;
        filename    : packed array[1..32] of char;
        filelen     : integer;

  procedure initialise;
  begin
    acid_names[cys] := 'CYS';    acid_names[his] := 'HIS';
    acid_names[ile] := 'ILE';    acid_names[met] := 'MET';
    acid_names[ser] := 'SER';    acid_names[val] := 'VAL';
    acid_names[ala] := 'ALA';    acid_names[gly] := 'GLY';
    acid_names[leu] := 'LEU';    acid_names[pro] := 'PRO';
    acid_names[thr] := 'THR';    acid_names[phe] := 'PHE';
    acid_names[arg] := 'ARG';    acid_names[tyr] := 'TYR';
    acid_names[trp] := 'TRP';    acid_names[asp] := 'ASP';
    acid_names[asn] := 'ASN';    acid_names[glu] := 'GLU';
    acid_names[gln] := 'GLN';    acid_names[lys] := 'LYS';

    first := true;
    formfeed := chr(140);
  end;

  procedure readparameters;

    var responce: char;
        f       : text;
        acid    : amino_acids;


    function valid_peptide: boolean;
      var cnt  : integer;
          ch   : char;
          valid: boolean;
    begin
      valid := true;
```

```
    cnt := 1;
    repeat
      case (pepchar[cnt]) of
        'c', 'C': peptide[cnt] := cys;
        'h', 'H': peptide[cnt] := his;
        'i', 'I': peptide[cnt] := ile;
        'm', 'M': peptide[cnt] := met;
        's', 'S': peptide[cnt] := ser;
        'v', 'V': peptide[cnt] := val;
        'a', 'A': peptide[cnt] := ala;
        'g', 'G': peptide[cnt] := gly;
        'l', 'L': peptide[cnt] := leu;
        'p', 'P': peptide[cnt] := pro;
        't', 'T': peptide[cnt] := thr;
        'f', 'F': peptide[cnt] := phe;
        'r', 'R': peptide[cnt] := arg;
        'y', 'Y': peptide[cnt] := tyr;
        'w', 'W': peptide[cnt] := trp;
        'd', 'D': peptide[cnt] := asp;
        'n', 'N': peptide[cnt] := asn;
        'e', 'E': peptide[cnt] := glu;
        'q', 'Q': peptide[cnt] := gln;
        'k', 'K': peptide[cnt] := lys;

        otherwise begin
            valid := false;
            writeln('Invalid Peptide Character - ''', pepchar[cnt],
                    ' in column ', cnt:3);
        end;
      end;
      cnt := cnt + 1;
    until (cnt > no_peptides) or not valid;

    valid_peptide := valid;
  end (* Valid Peptide *);

begin
  if first
  then responce := 'y'
  else
    repeat
      write('Do you want to change the Hydrophobicity scale? ');
      readln(responce);
    until (responce in ['n', 'y', 'N', 'Y']);

  if responce in ['y', 'Y'] then begin    (* Must get new values *)
    repeat
      write('Do you want to enter a new Hydrophobicity scale? ');
      readln(responce);
    until (responce in ['n', 'y', 'N', 'Y']);

    if responce in ['n', 'N'] then begin
      write('Name of current Hydrophobicity scale: ');
      readln(filename: filelen);

      reset(f, filename);
      for acid := cys to lys do    (* Read in the scale for each acid *)
        readln(f, scale[acid]);

    end else begin      (*  Read in values from terminal  *)
```

```
      for acid := cys to lys do begin
        write('Enter value for ', acid_names[acid], ': ');

        readln(scale[acid]);
      end;

      writeln;
      write('Name of new Hydrophobicity scale: ');
      readln(filename: filelen);
      rewrite(f, filename);
      for acid := cys to lys do
        writeln(f, scale[acid]:8:2, '      (* ', acid_names[acid], ' *)');
      writeln('Scale saved in file ''', filename: filelen, '''');
    end;
  end;

  write('Enter Depth of Penetration: ');
  readln(penetration);

  write('Enter Peptide Name: '); readln(pepchar);
  repeat
    write('Enter Peptide: ');
    readln(pepchar: no_peptides);
  until valid_peptide;
end (* Read parameters *);

procedure processpeptide;

  var   no_degrees: integer;
        cnt       : integer;


  procedure sum_nonpolar(lower, upper: integer; polar: boolean);
    var   val  : real;
          no   : integer;
          cnt  : integer;
          angle: integer;
  begin
    val := 0;
    no := 0;

    for cnt := 1 to no_peptides do begin
      angle := (100 * cnt) mod 360;

      if (lower < angle) and (angle < upper) then begin
        val := val + scale[peptide[cnt]];
        no := no + 1;
      end;
    end;

    if polar then begin
      val := tothyd - val;
      no := totres - no;
    end;

    if val >= biggest_nonpolar then begin
      if val > biggest_nonpolar then begin
        no_biggest := 1;
        biggest_nonpolar := val
      end else no_biggest := no_biggest + 1;
```

```
      with save_pol[no_biggest] do begin
        numbnp := no;
        incr := no_degrees;
      end;
    end;
  end (* Sum Non polar *);

begin
  tothyd := 0;
  for cnt := 1 to no_peptides do
    tothyd := tothyd + scale[peptide[cnt]];

  totres := no_peptides;


  biggest_nonpolar := -1000;
  no_degrees := 10;
  repeat
    sum_nonpolar(no_degrees, no_degrees+penetration, false);

    no_degrees := no_degrees + 20;
  until (no_degrees + penetration) >= 360;

  repeat
    sum_nonpolar(no_degrees+penetration-360, no_degrees, true);

    no_degrees := no_degrees + 20;
  until (no_degrees >= 360);
end (* Process Peptide *);

procedure total_and_print;
  var   cnt     : integer;
        acid    : amino_acids;
        npres   : integer;
        polar   : real;
begin
  npres := save_pol[1].numbnp;
  polar := tothyd - biggest_nonpolar;

  writeln('Peptide is :', pepchar);
  for cnt := 1 to no_peptides do begin
    write(acid_names[peptide[cnt]], ' ');

    if cnt mod 10 = 0
    then writeln;
  end;
  writeln;
  writeln;

  writeln('Hydrophobicity scale chosen is: ', filename: filelen);
  for acid := cys to lys do
    writeln(acid_names[acid], scale[acid]: 8:2);
  writeln;

  writeln('Depth of Penetration = ', penetration:3);
  writeln;

  writeln('Tothyd =', tothyd:8:2);
  writeln('Avtot  =', (tothyd / totres):8:2);
```

```
    writeln('Test   =', biggest_nonpolar:8:2);
    writeln('Avnpol =', (biggest_nonpolar / npres):8:2);
    writeln('Polar  =', polar:8:2);
    writeln('Avpol  =', (polar /(totres - npres)):8:2);
    writeln;

    writeln('Non polar Face');
    for cnt := 1 to no_biggest do
      with save_pol[cnt] do
        if incr + penetration < 360
        then writeln(incr:4, ' to', incr+penetration:5)
        else writeln(incr+penetration-360:4, ' to', incr:5);
    writeln;
  end (* Total and Print *);

  function finished: boolean;
    var ch: char;
  begin
    writeln;
    writeln;
    write('Do you want to continue? ');
    readln(ch);
    if (ch in ['y', 'Y']) then begin
      writeln; writeln(formfeed);
      finished := false;
      first := false;
    end else finished := true
  end (* Finished *);

begin (* Main Line of Program *)
  initialise;
  repeat
    readparameters;
    processpeptide;
    total_and_print;
  until finished;
end.
```

A.4 Plots of Various Hydrophobicity Parameters v's Retention of Peptide in an Acidic Reversed-Phase HPLC System for the Synthetic Peptide Series.

The plots shown for each of the parts A, B, C and D of figures A-4 to A-17 were all derived in the same manner. The vertical axis is the point of elution of each peptide in the acidic reversed-phase HPLC system on the particular column as detailed below.

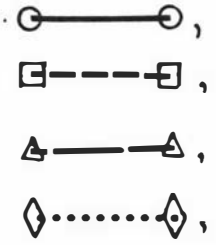

Radial-PAK CN (ambient temp.)

μBondapak alkylphenyl ($40^{o}C$)

μBondapak alkylphenyl (ambient temp.)

Radial-PAK C18 (ambient temp.)

These values were taken from table 5-1.

The horizontal axis represents respectively the total hydrophobicity of the peptide (A), the total non-polar side hydrophobicity of the peptide (B), the average hydrophobicity of the peptide (C) and the average non-polar side hydrophobicity of the peptide (D), calculated by the computer program in section A.3 using the hydrophobicity scale shown under the particular figure (section A.2). The plots which consider average hydrophobicity (C) and average non-polar side hydrophobicity (D) are not strictly relevant to the currently accepted methods of predicting peptide retentions on RP-HPLC systems (155-158). Nevertheless, these plots are included for completeness since the currently accepted model for affinity of peptides to another hydrophobic surface (phospholipid) considers the average non-polar side hydrophobicity of the peptides (33).

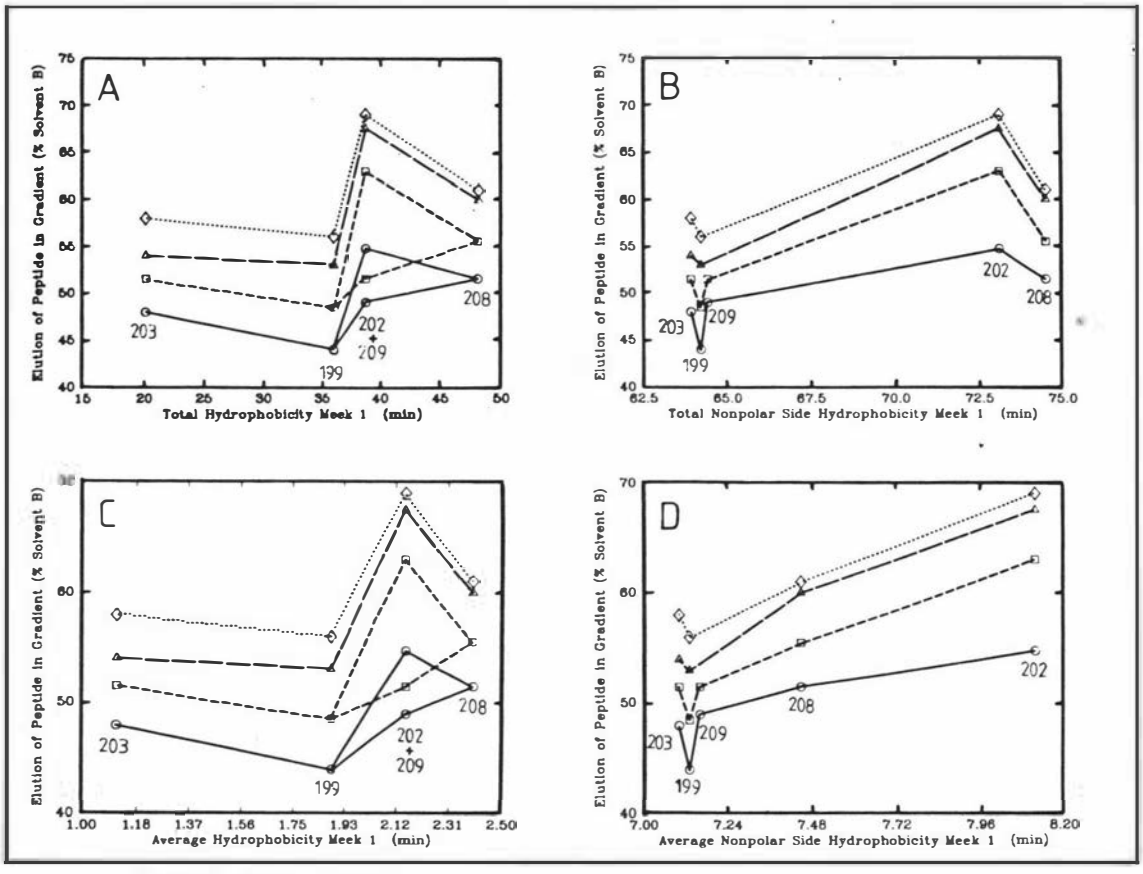

Figure A-4 Meek1

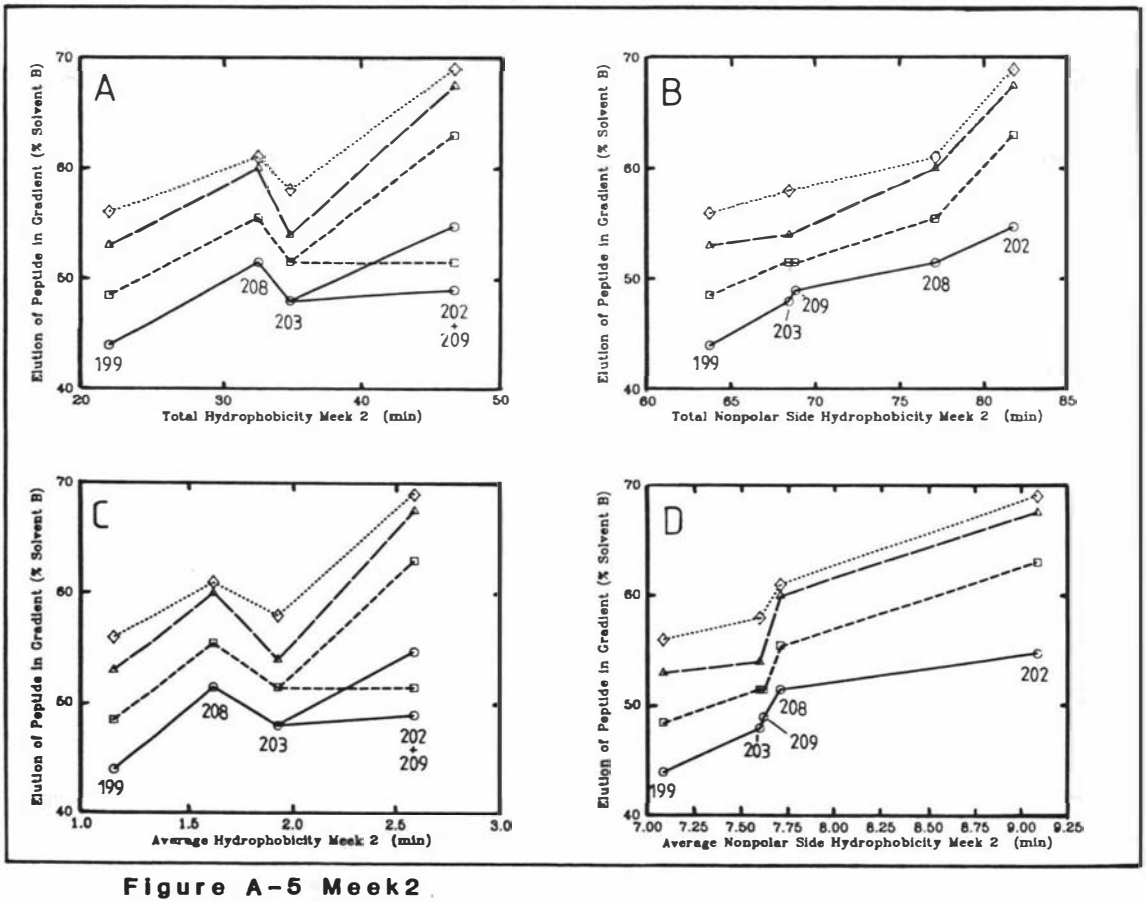

Figure A-5 Meek2

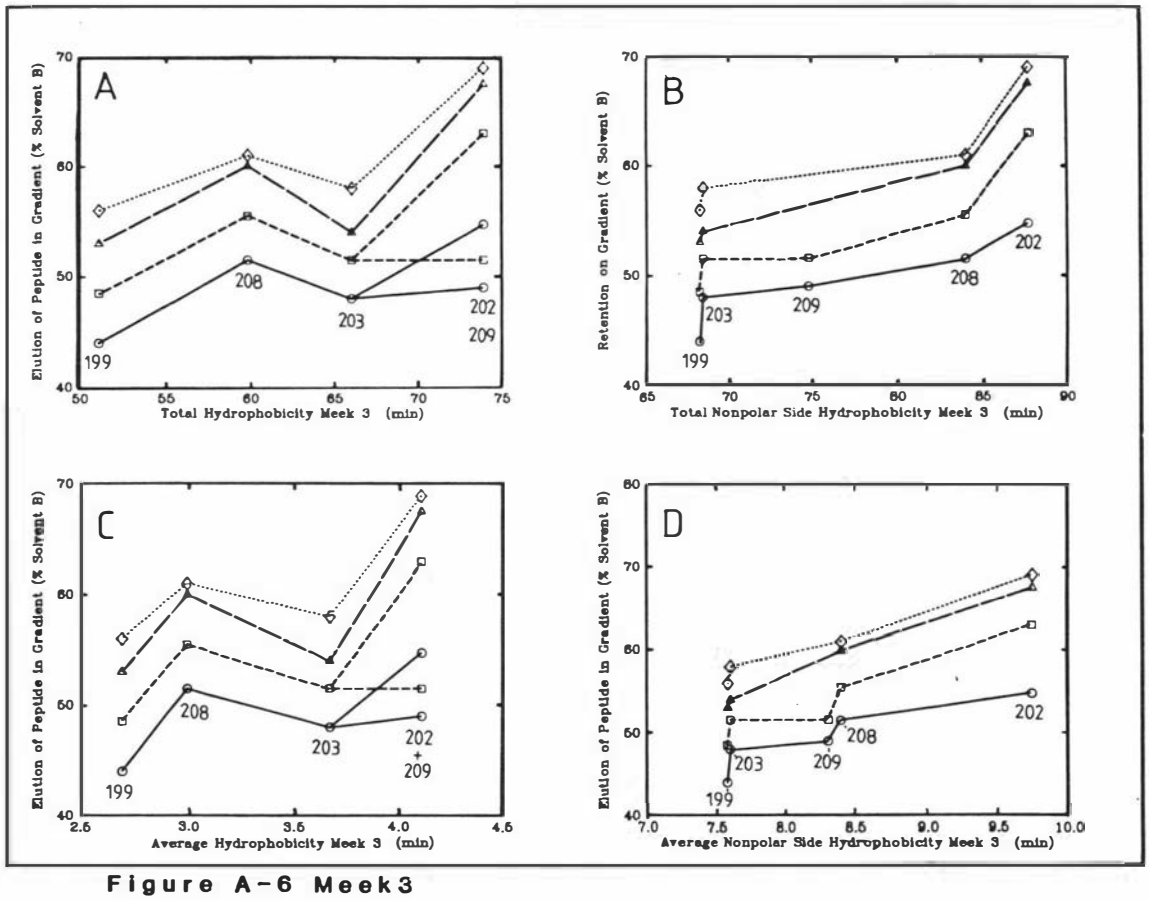

Figure A-6 Meek3

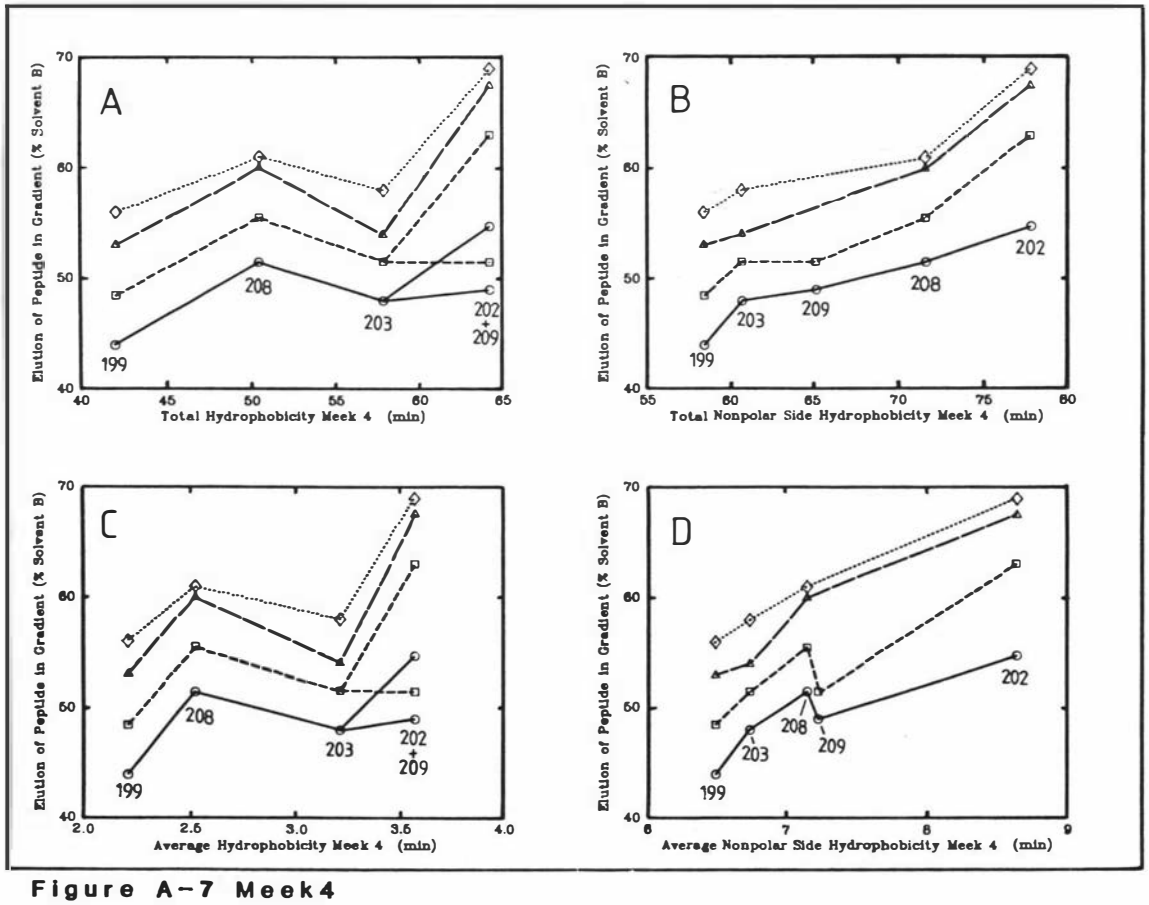

Figure A-7 Meek4

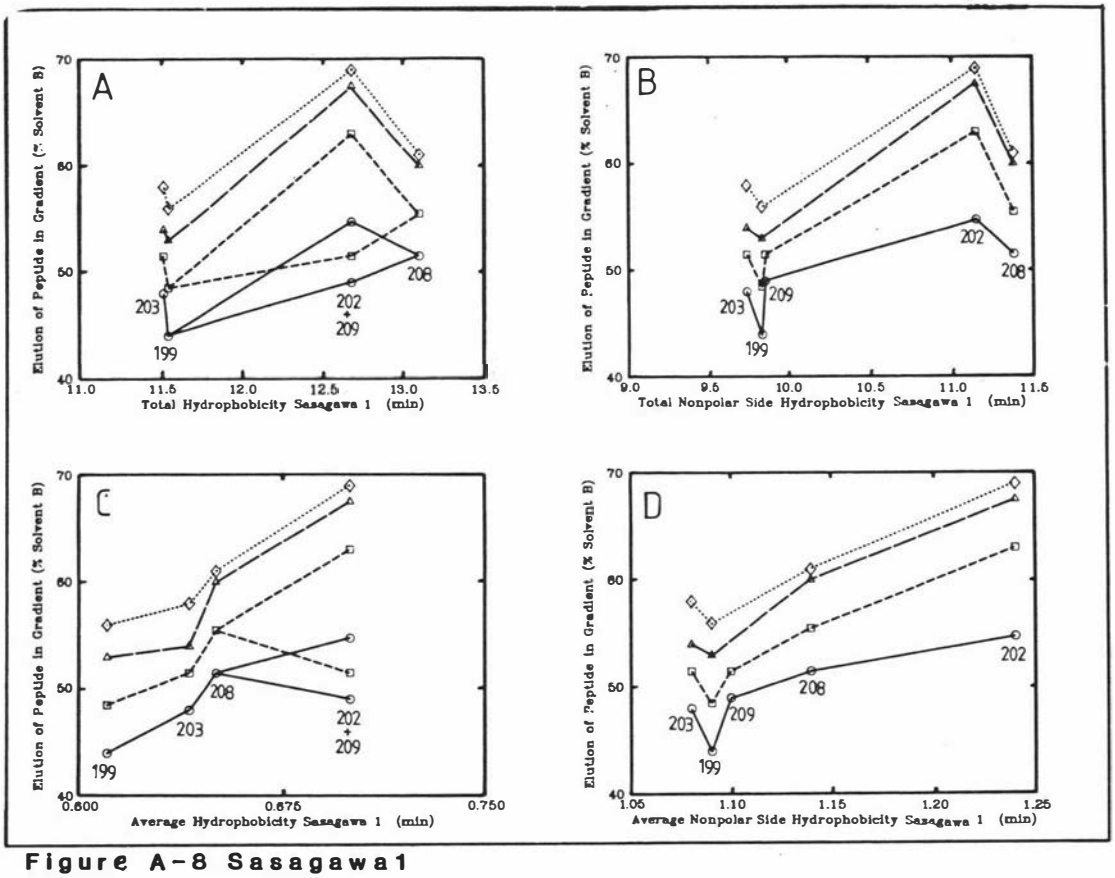

Figure A-8 Sasagawa1

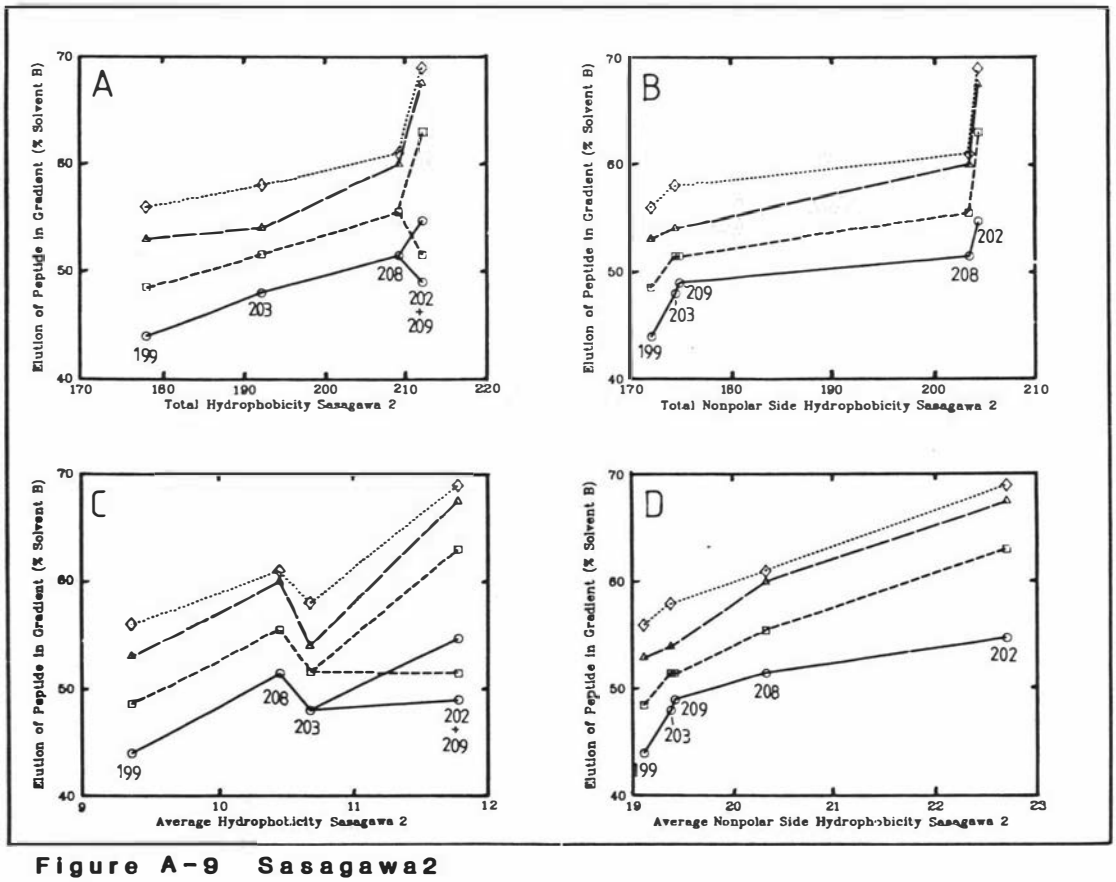

Figure A-9 Sasagawa2

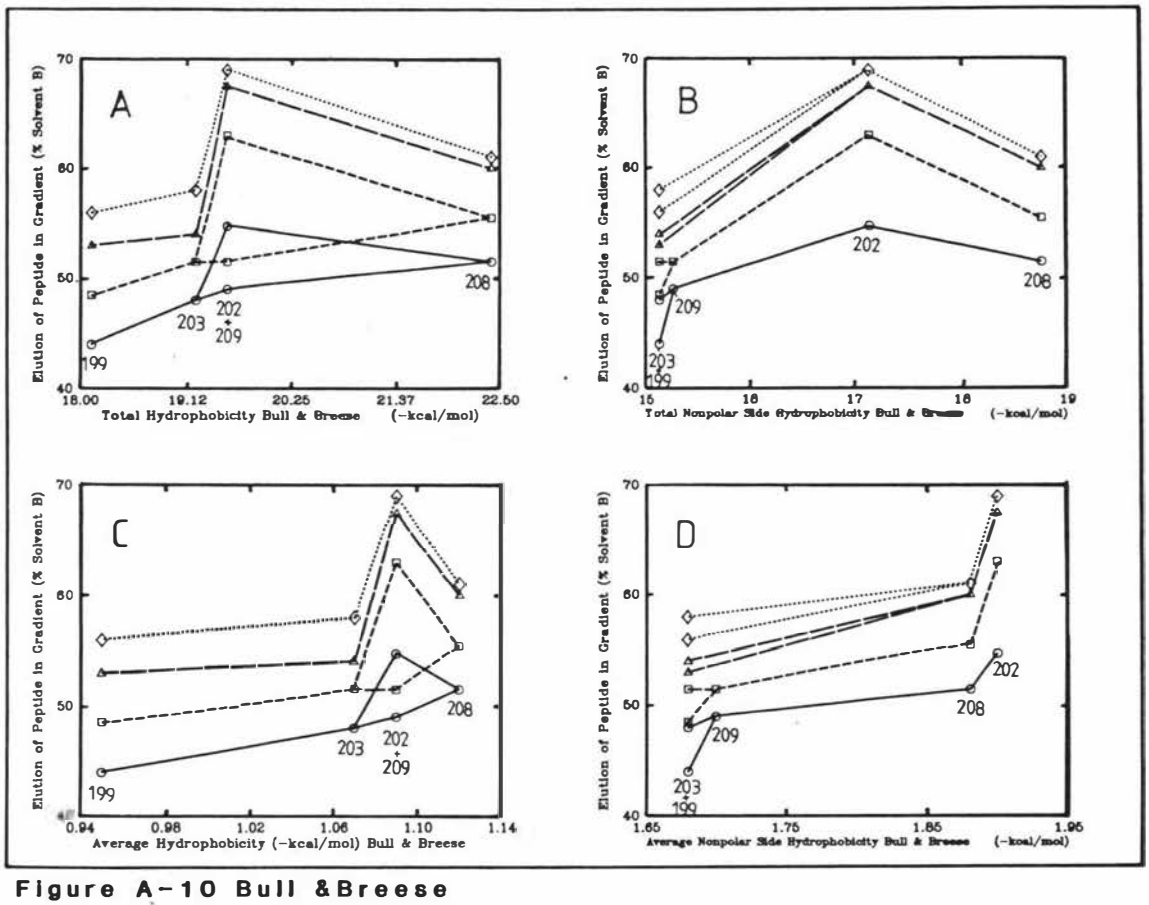

Figure A-10 Bull &Breese

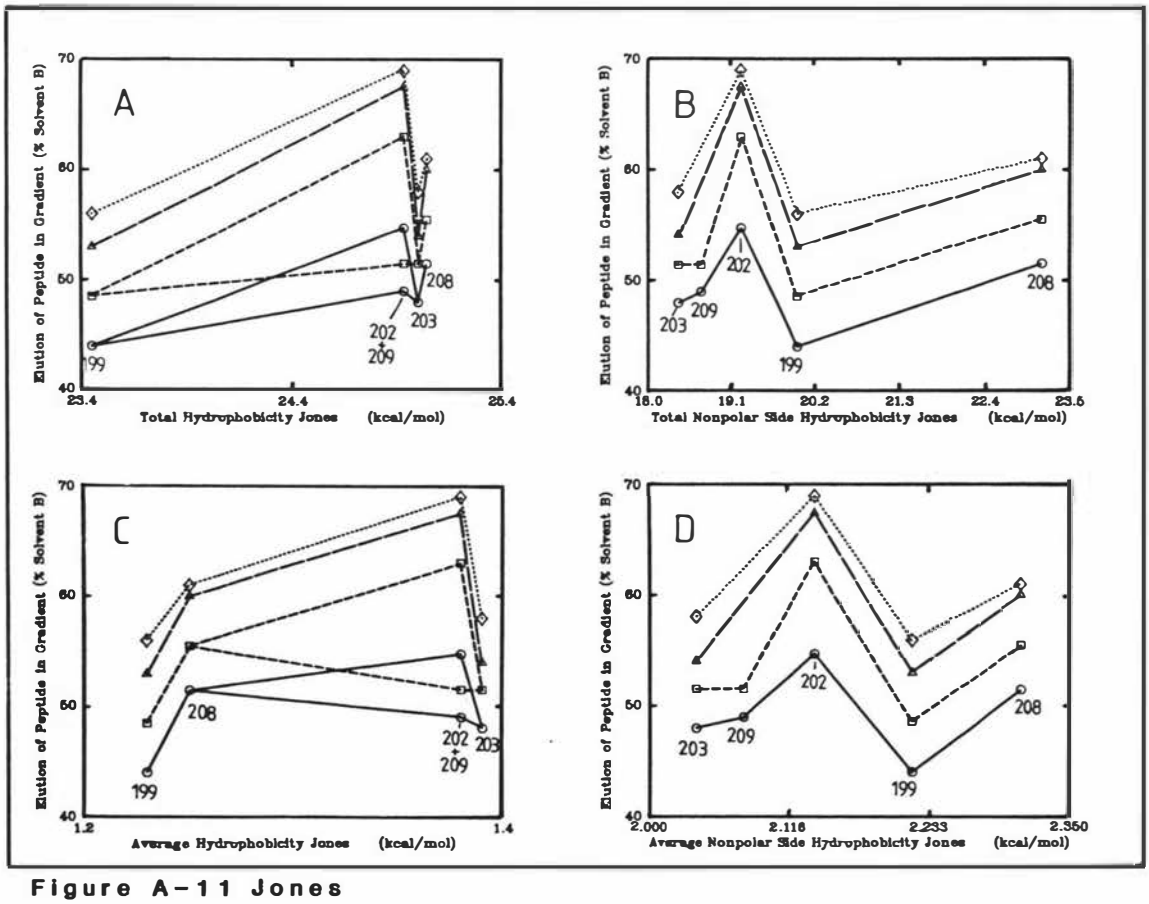

Figure A-11 Jones

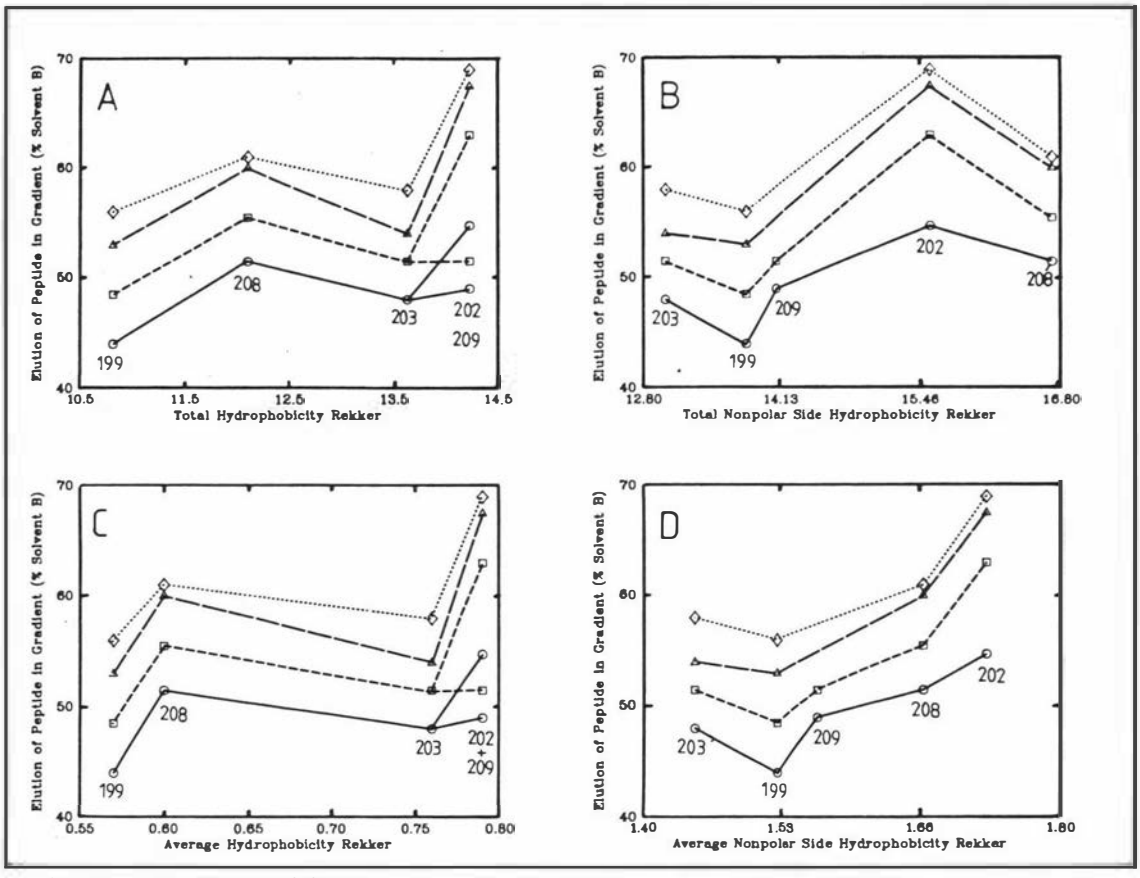

Figure A-12 Rekker

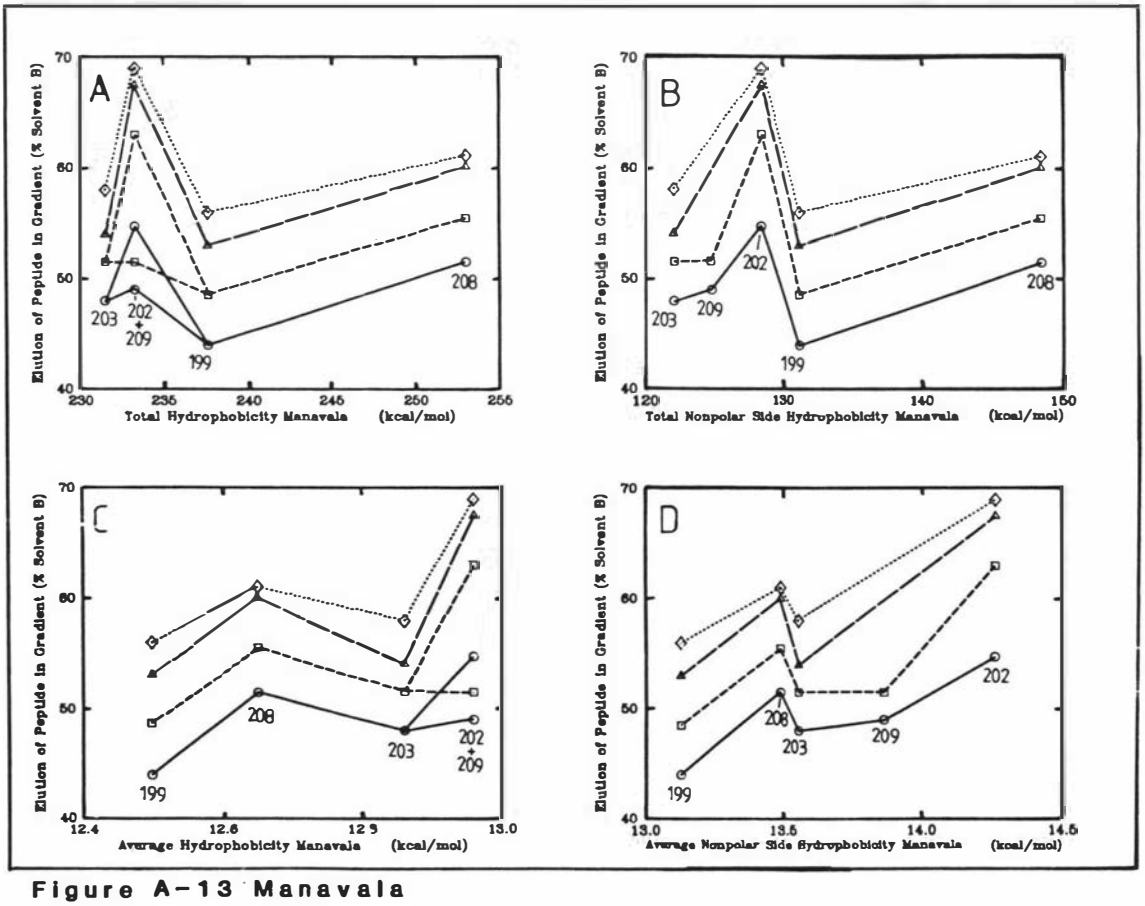

Figure A-13 Manavala

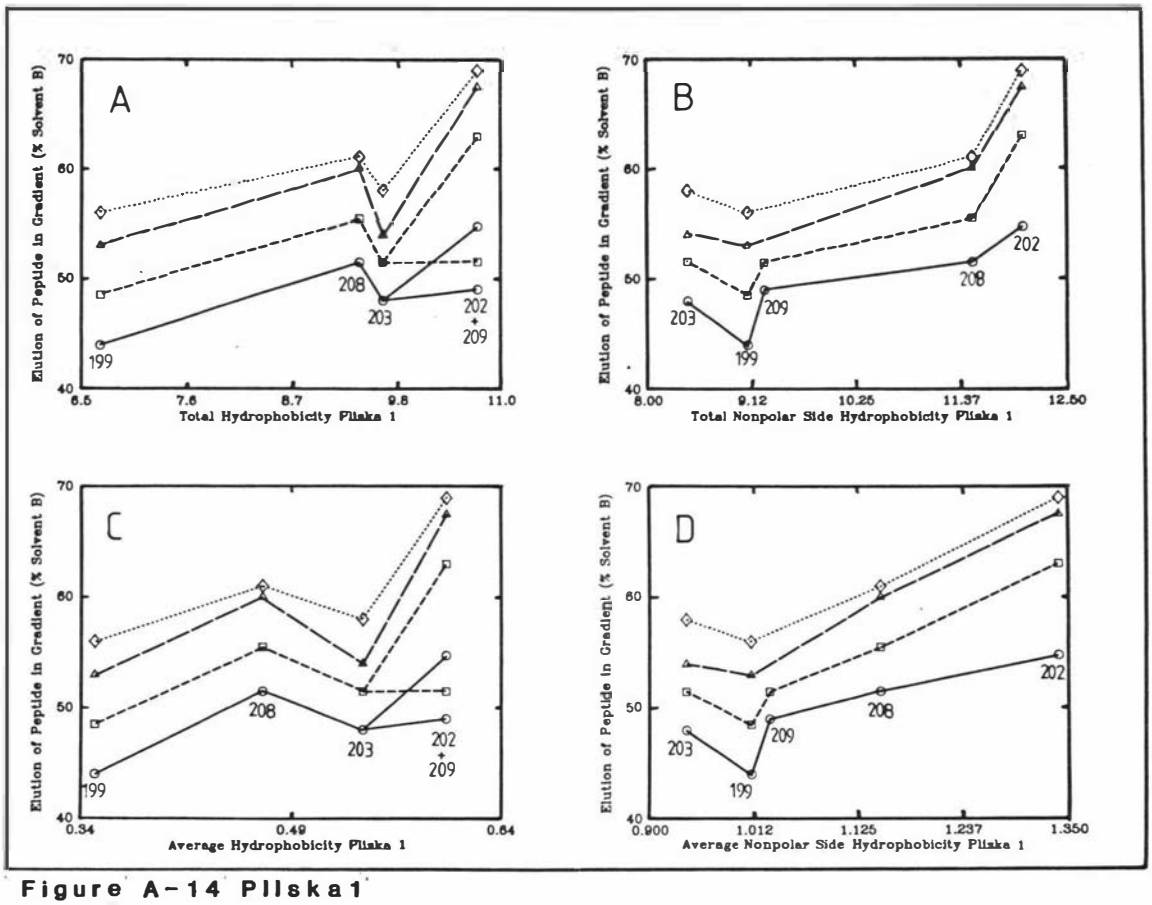

Figure A-14 Pliska1

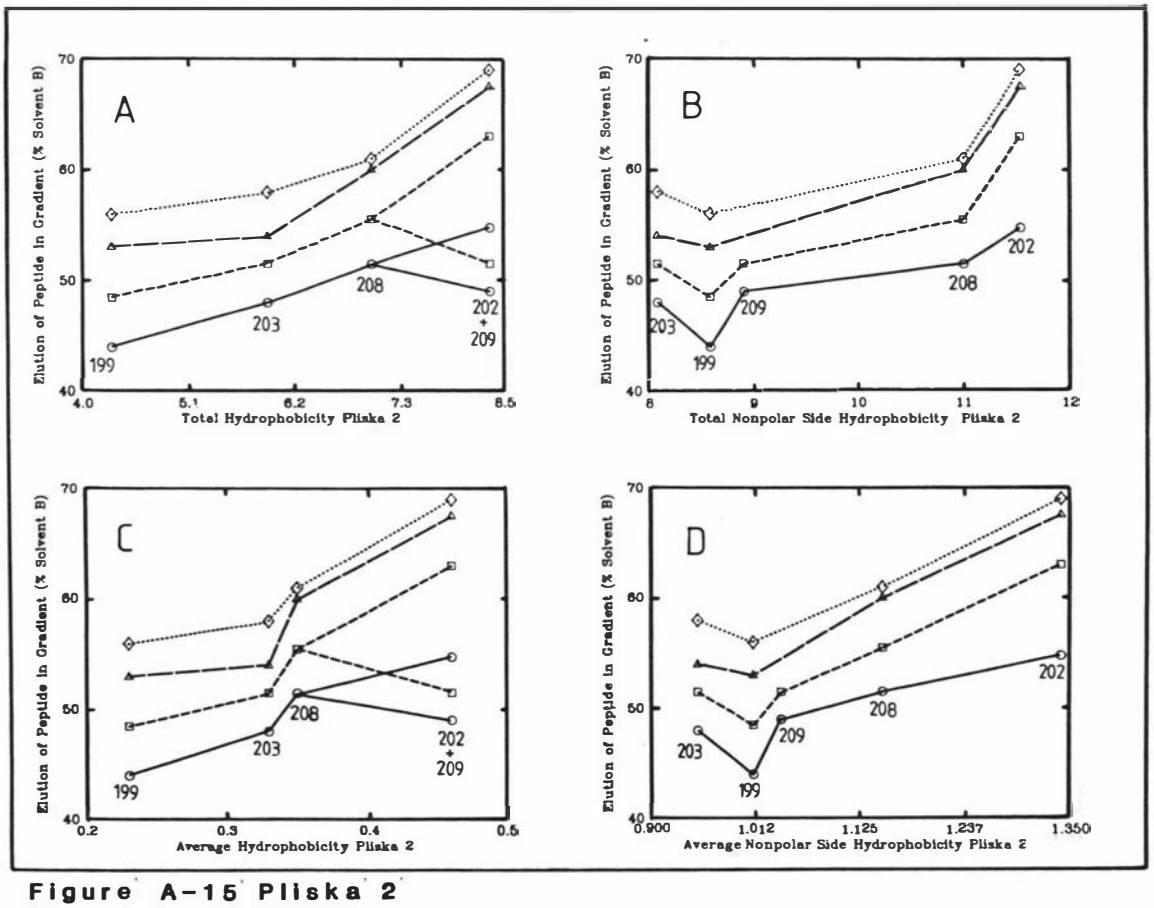

Figure A-15 Pliska 2

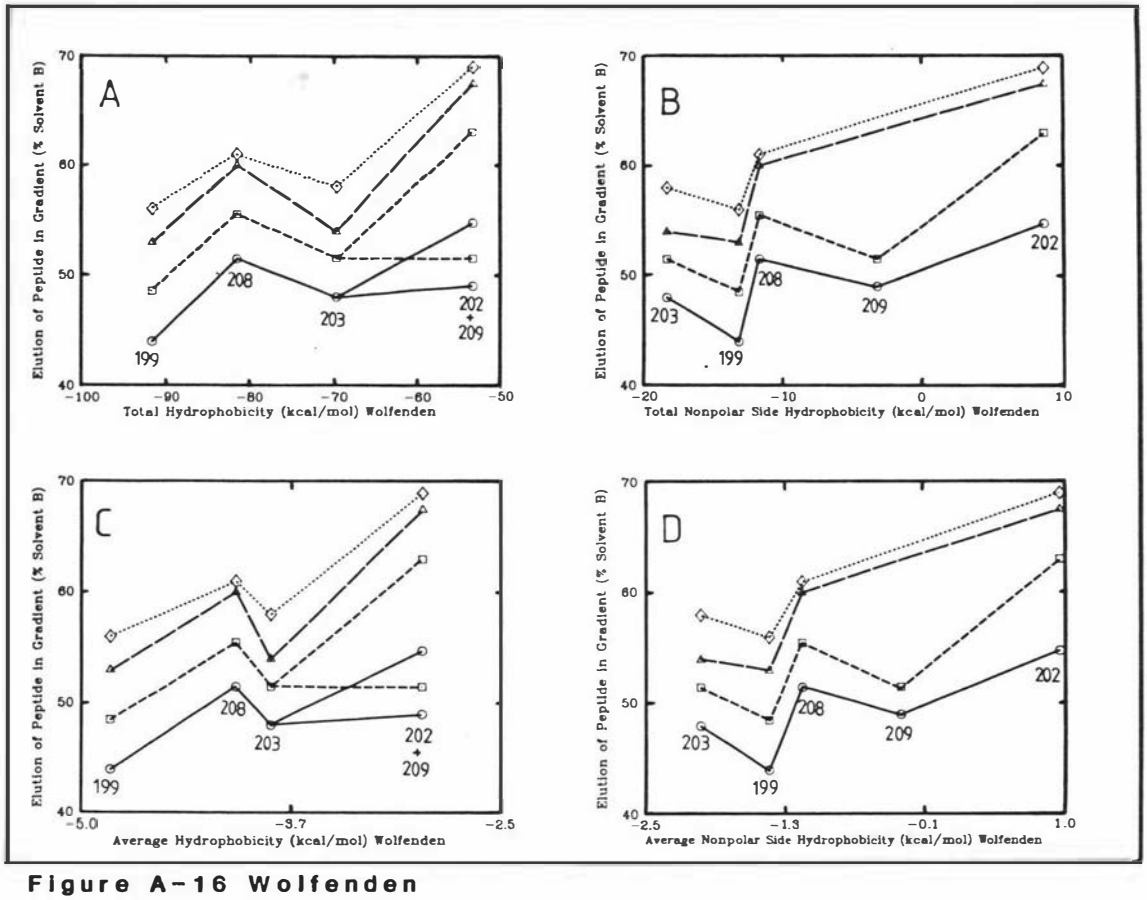

Figure A-16 Wolfenden

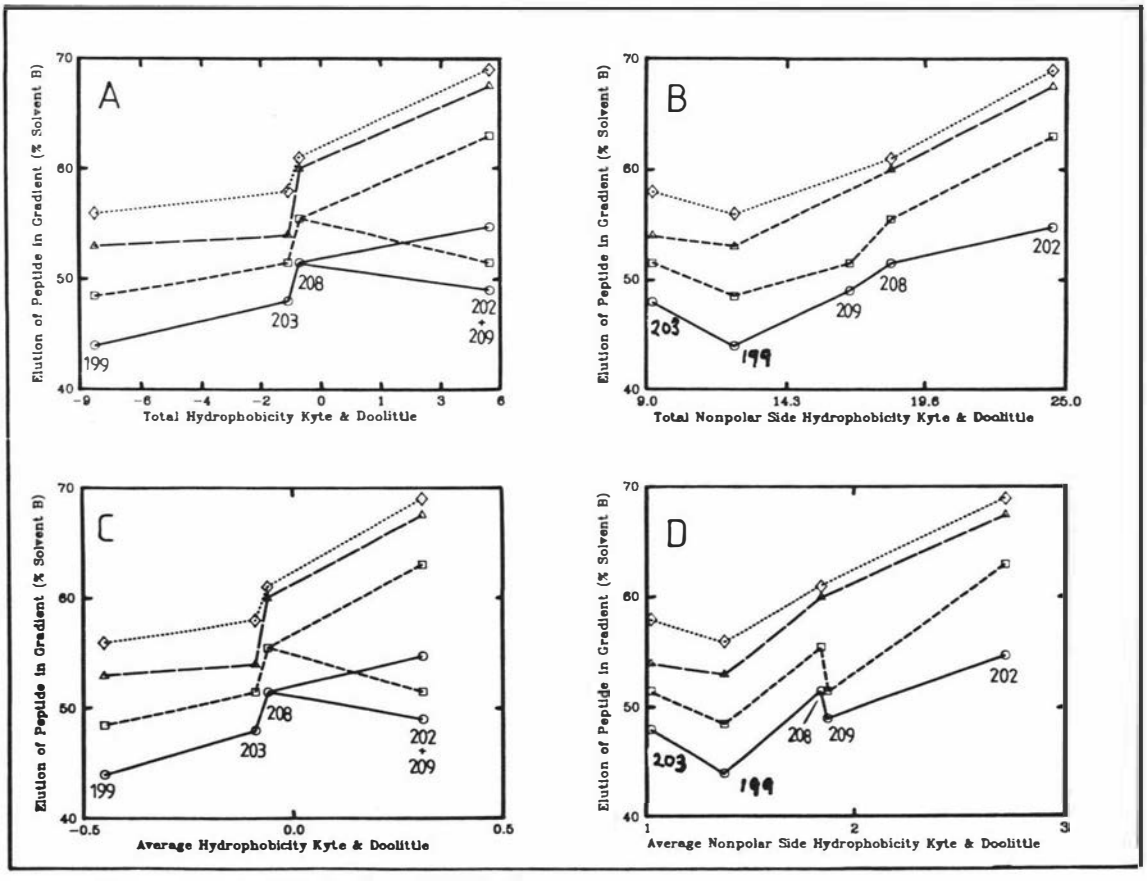

Figure A-17 Kyte & Doolittle

A.5 Purification of Acetonitrile for HPLC

The acetonitrile was purified by a 4 step process as detailed below. This is a modification of method B from reference (273).

STEP 1 — reflux over anhydrous $AlCl_3$ (15 g/l) for one hour - distill rapidly (no column) until temperature exceeds $82^{o}C$.

STEP 2 — reflux over alkaline $KMnO_4$ (10 g $KMNO_4$/10 g Li_2CO_3/1) for a quarter hour - distill rapidly (no column) until temperature exceeds $82^{o}C$.

STEP 3 — reflux over pot. bisulfate (15 g/l) for one hour - cool - decant and/or filter through glass wool.

STEP 4 — reflux over CaH_2(2 g/l) for one hour - distill rapidly (no column) - collect acetonitrile until temperature begins to exceed $82^{o}C$.

A.6 Abbreviations

RP	-	reversed-phase
HPLC	-	high performance liquid chromatography
DMPC	-	dimyristoyl phosphatidylcholine
DPPC	-	dipalmitoyl phosphatidylcholine
PC	-	phosphatidylcholine
AUFS	-	absorbance units full scale
GdnCl	-	guanidine hydrochloride

Table A-3 A List of Peptides Plotted on Figures 7-2 and 7-3.

No.	Peptide	Ref.	No.	Peptide	Ref.
1	Peptide I (Sparrow)	(33)	37	ApoA-II(52-77)	(33)
2	Peptide II (Sparrow)	(33)	38	ApoA-II(50-77)	(33)
3	Peptide III(Sparrow)	(33)	39	No. 38 with $Ala_{52}Ala_{53}$	(33)
4	LAP 16 (Sparrow)	(33)	40	No. 38 with $Ser_{54}Ser_{55}$	(33)
5	Peptide V (Sparrow)	(33)	41	ApoA-I(227-245)	(33)
6	Peptide VI (Sparrow)	(33)	42	ApoA-I(220-245)	(33)
7	LAP 20 (Sparrow)	(33)	43	ApoA-I(213-245)	(33)
8	LAP 24 (Sparrow)	(56)	44	ApoA-I(204-245)	(33)
9	Peptide I (Kaiser)	(33)	45	ApoA-I(197-245)	(33)
10	Peptide II (Kaiser)	(276)	46	ApoA-I(124-167)[i]	(85)
11	18Aa (Segrest)	(274)	47a	ApoA-I(147-168)[j]	(33)
12	18As (Segrest)	(274)	47b	ApoA-I(147-168)[k]	(33)
13	18Al (Segrest)	(274)	48	peptide 202	
14	18 Asr(partial) (Segrest)	(274)	49	peptide 203	This study
15	ApoC-I(1-38+39-57)[a]	(33)	50	peptide 209	
16	ApoC-I(1-38)[b]	(33)	51	peptide 199	
17	ApoC-I(39-57)[f]	(33)	52	ApoC-I(17-57)	(33)
18	ApoC-III(41-79)[c]	(33)	53	ApoC-I(24-57)	(33)
19	ApoC-III(1-40)	(33)	54	ApoC-I(32-57)	(33)
20	ApoC-III(61-79)	(33)	55	ApoC-I(39-57)[g]	(33)
21	ApoC-III(55-79)	(33)	56	ApoA-I(164-185)	(33)
22	ApoC-III(48-79)	(33)	57	ApoA-I(157-185)	(33)
23	ApoC-II(55-78)	(33)	58	ApoA-I(152-185)	(33)
24	ApoC-II(50-78)	(33)	59	ApoA-I(148-185)	(33)
25	ApoC-II(43-78)	(33)	60	ApoA-I(145-185)	(33)
26	ApoA-II(1-26)[b,d]	(33)	61	18Asr(total)(Segrest)	(205)
27	ApoA-II(27-77)[e]	(33)	62	ApoC-I(1-22)	(275)
28	ApoA-II(17-31)	(33)	63	LAP-20(Glu_9)	(193)
29	ApoA-II(12-31)	(33)	64	LAP-20(Glu_{16})	(193)
30	ApoA-II(7-31)	(33)	65	LAP-20(Glu_9,Glu_{16})	(193)
31	ApoA-II(22-31)	(33)	66	LAP-20(Ala_4)	(193)
32	ApoA-II(65-77)	(33)	67	LAP-20(Ala_5)	(193)
33	ApoA-II(56-77)	(33)	68	LAP-20(Ala_8)	(193)
34	ApoA-II(47-77)	(33)	69	LAP-20(Ala_{11})	(193)
35	ApoA-II(40-77)	(33)	70	LAP-20(Ala_{15})	(193)
36	ApoA-II(54-77)	(33)	71	ApoA-I(114-133)[l]	(33)

Footnotes to Table A-3

a) Calculated in 2 segments (1-38) and (39-57) followed by addition of the calculated hydrophobicities.

b) This peptide is a cyanogen bromide fragment and therefore the carboxy terminal methionine residue has been converted into a homoserine residue. Since the hydrophobicity of homoserine is not available in most scales the value used in the calculation of hydrophobicity of the peptide was that of threonine.

c) Both native and synthetic sequences.

d) The hydrophobicity of this sequence was calculated for ApoA-II (2-26) since the hydrophobicity for the N-terminal pyroglutamic acid was not known.

e) Calculated in 4 segments (27-31), (32-50), (51-73) and (74-77) followed by addition of the hydrophobicities calculated.

f) The native fragment. Compare with the synthetic peptide (No. 55) which apparently has a different lipid affinity.

g) This is the synthetic peptide. Compare with the native peptide (No. 17) which apparently has a different lipid affinity.

h) Every acidic and basic residue in this peptide has swopped positions compared to peptide No. 12. This is only partially true for peptide No. 14.

i) This peptide has Gln_{148}, Gln_{149} because it was based on the Brewer sequence (60).

j) At pH below 7.

k) At pH above 7.

l) Since this peptide only binds to PC below pH 5 it is designated as interacting strongly with PC but not forming stable complexes with PC.

REFERENCES

(1) Mathews, B.W., in Lipid-Protein Interactions Vol.1, edited by Jost, P.C. and Griffith, O.H., Wiley, New York, 1982. p.1-23.

(2) Brown, J.R., and Shockley, P., p.25-68 of reference (1).

(3) Wirtz, K.W.A., p.151-231 of reference (1).

(4) Calvert, G.D., and Abby, M., in Atherosclerosis VI edited by Schettler, G., Gotto, A.M., Meddelhoff, G., Habenicht, A.J.R., and Jurutka, K.R., Springer-Verlag, Berlin, 1983. p.428-431.

(5) Metzler, D.E., Biochemistry: The Chemical Reactions of Living Cells, Academic Press, New York, 1977. p.256.

(6) Chapman, D., in Membrane Reconstitution, Cell Surface Reviews - Vol.8, edited by Post, G., and Nicholson, G.L., Elsevier Biomedical Press, Amsterdam, 1982. p.34.

(7) Gurr, M.I., and James, A.T., Lipid Biochemistry: An Introduction, 3rd ed., Chapman and Hall, London, 198-. p.183.

(8) Boggs, J.M., Moscarello, M.A., and Papahadjopoulos, D., in Lipid-Protein Interactions Vol.2, edited by Jost, P.C., and Griffith, O.H., Wiley, New York, 1982. p.1-51.

(9) Robson, R.J., Radhakrishnan, R., Ross, A.H., Takagaki, Y., and Khorana, H.G., p.149-192 of reference (8).

(10) p.3-4 of reference (6).

(11) Trumpower, B.L., in Membrane Proteins In Energy Transduction, edited by Capaldi, R.A., Marcel Dekker, New York, 1979. p.89-200.
Senior, A.E., ibid p.233-278.
Olson, J.M., ibid p.279-340.

(12) Tanford, C., The Hydrophobic Effect: Formation of Micelles and Biological Membranes, 2nd ed. Wiley-Interscience, New York, 1979. p.208.

(13) Dailey, H.A., and Strittmatter, P., J. Biol. Chem. 256, 3951-3955 (1981).

(14) p.271 of reference (5).

(15) Roelofsen, B., in Membrane Proteins, Proceedings of the 11th FEBS Meeting Vol.45, edited by Nicholls, P., Moller, J.V., Jorgensen, P.L., and Moody, A.J., Pergamon, Oxford, 1978. p.183-190.

(16) Gremlich, H., Fringeli, U., and Schwyzer, R., Biochemistry 22, 4257-4264 (1983).

(17) p.345 of reference (5).

(18) Epand, R.M., Trends Biochem. Sci. 8, 205-206 (1983).

(19) Hammonds, R.G., Jr., Hammonds, A.S., Ling, N., and Puett, D., J. Biol. Chem. 257, 2990-2995 (1982).

(20) Craig, S.W., and Cuatrecasas, P., in Immunology of Receptors, edited by Cinader, B., Marcel Dekker, New York, 1977. p.63-76.

(21) De Grado, W.F., Kezdy, F.J., and Kaiser, E.T., J. Am. Chem. Soc. 103, 679-681 (1981).

(22) Prendergast, F.G., Lu, J., Wei, G.J., and Bloomfield, V.A., Biochemistry 21, 6963-6971 (1982).

(23) Volwerk, J.J., and De Haas, G.H., p.69-149 of reference (1).

(24) Shields, D., Biochem. Biophys. Res. Commun. 98, 242-249 (1981).

(25) Engelman, D.M. and Steitz, T.A., Cell 23, 411-422 (1981).

(26) Chapman, M.J., J. Lipid Res. 21, 789-853 (1980).

(27) Schultz, R.M., in Textbook of Biochemistry With Clinical Correlations, edited by Delvin, T.M., John Wiley & Sons, New York, 1982. p.113-119.

(28) Gotto, A.M., Jr., p.469-479 of reference (4).

(29) Patsch, J.R., Gotto, A.M., Jr., Olivecrona, T., and Eisenberg, S., Proc. Natl. Acad. Sci. USA 75, 4519-4523 (1978).

(30) Nye, E.R., Harding, D.R.K., Hancock, W.S., and Janus, E.D., N.Z. Med. J. 96, 85-88 (1983).

(31) Houslay, M.D., and Stanley, K.K., Dynamics of Biological Membranes, Wiley, New York, 1982. p.299.

(32) Morrisett, J.D., Jackson, R.L., and Gotto, A.M., Jr., Biochim. Biophys. Acta 472, 93-133 (1977).

(33) Sparrow, J.T., and Gotto, A.M., Jr., CRC Crit. Rev. Biochem. 13, 87-107 (1982).

(34) Scanu, A.M., Edelstein, C., and Shen, B.W., p.259-316 of reference (1).

(35) Owen, J.S., and McIntyre, N., Trends Biochem. Sci. 7, 95-98 (1982).

(36) Basu, S.K., Goldstein, J.L., and Brown, M.S., Science 219, 871-873 (1983).

(37) Brown, M.S., Basu, S.K., Falck, J.R., Ho, Y.K., and Goldstein, J.L., J. Supramolecular Structure 13, 67-81 (1980).

(38) Fowler, S.D., p.452-456 of reference (4).

(39) Hancock, W.S., Manuscript in preparation.

(40) Smoking and Health a Report of the Surgeon General, DHEW publication no. (PSH) 79-50066, U.S. Department of Health, Education and Welfare, 1979.

(41) Le Pape, A., Gutman, N., Guitton, J.D., Legrand, Y., and Muh, J.P., Biochem. Biophys. Res. Commun. 111 602-610 (1983).

(42) Stevens, V.J., Fantl, W.J., and Newman, C.B., J. Clin. Invest. 67 361-369 (1981).

(43) Goldstein, J.L., and Brown, M.S., Annu. Rev. Biochem. 46 897-930 (1977).

(44) Cardin, A.D., Witt, W.R., Barnhart, C.L., and Jackson, R.L., Biochemistry 21, 4503-4511 (1982).

(45) Rall, S.C., Jr., Weisgraber, K.H., and Mahley, R.W., J. Biol. Chem. 257, 4171-4178 (1982).

(46) Innerarity, T.L., Pitas, R.E., and Mahley, R.W., J. Biol. Chem. 254, 4186-4190 (1979).

(47) Mahley, R.W., Klin. Wochenschr 61, 225-232 (1983).

(48) Innerarity, T.L., Friedlander, E.J., Rall, S.C., Jr., Weisgraber, K.H. and Mahley, R.W., Circulation 66 (Supp.II), 11 (1982)

(49) Jackson, R.L., Morrisett, J.D., and Gotto, A.M., Jr., Phys. Rev. 56, 259-315 (1976).

(50) Havel, R.J., Chao, Y., Windler, E.E., Kotite, L., and Guo, L.S.S., Proc. Natl. Acad. Sci. USA 77, 4349-4353 (1980).

(51) Gordon, J.I., Sims, H.F., Lentz, S.R., Edelstein, C., Scanu, A.M., and Strauss, A.W., J. Biol. Chem. 258, 4037-4044 (1983).

(52) Silvius, J.R., p.239-281 of reference (8).

(53) Zannis, V.I., and Breslow, J.L., Mol. Cell. Biochem. 42, 3-20 (1982).

(54) Sparrow, J.T., and Gotto, A.M. Jr., Ann. N.Y. Acad. Sci. 348, 187-211 (1980).

(55) Pownall, H.J., Hu, A., Albers, J.J., Gotto, A.M., and Sparrow, J.T., Proc. Natl. Acad. Sci. USA 77, 3154-3158 (1980).

(56) Sparrow, J.T., Ferenz, C.R., Gotto, A.M., Jr., and Pownall, H.J., in Peptides: Proc. 7th Am. Peptide Symp., edited by Rich, D.H., and Gross, E., Pierce Chemical Company, Rockford, 1981. p.253-256.

(57) Baker, H.N., Gotto, A.M. Jr., and Jackson, R.L., J. Biol. Chem. 250, 2725-2738 (1975).

(58) Sparrow, J.T., Warman, A.H., and Gotto, A.M. Jr., in Peptides: Proc. 6th Amer. Pept. Symp., edited by Gross, E. and Meienhofer, J., Pierce Chemical Company, Rockford, 1979. p.523-526.

(59) Dr J.T. Sparrow, Baylor College of Medicine, Houston, personal communication.

(60) Brewer, H.B., Jr., Fairwell, T., La Rue, A., Ronan, R., Houser, A., and Bronzert, T.J., Biochem. Biophys. Res. Commun. 80, 623-630 (1978).

(61) Figure 6 of reference (2).

(62) Kent, S.B.H., Mitchell, A.R., Engelhard, M., and Merrifield, R.B., Proc. Natl. Acad. Sci. USA 76, 2180-2184 (1979).

(63) p.7 of reference (64).

(64) The Peptides: Analysis, Synthesis, Biology, edited by Gross, E., and Meinhoffer, J., Academic Press, London, Vol.1, 1979; Vol.2, 1980; Vol.3, 1981.

(65) Bodanszky, M., Klausner, Y.S., and Ondetti, M.A., Peptide Synthesis, 2nd ed., Wiley, New York, 1976.

(66) Harding, D.R.K., Battersby, J.E., Husbands, D.R., and Hancock, W.S., J. Am. Chem. Soc. 98, 2664-2665 (1976).

(67) Harding, D.R.K., Husbands, D.R., and Hancock, W.S., Abstracts New Zealand Institute of Chemistry Conference, Aug 1975, No.24, p.47.

(68) Hancock, W.S., Prescott, D.J., Vagelos, P.R., and Marshall, G.R., J. Org. Chem. 38, 774-781 (1973).

(69) Gutte, B., and Merrifield, R.B., J. Biol. Chem. 246, 1922-1941 (1971).

(70) Wang, S., and Merrifield, R.B., J. Am. Chem. Soc. 91, 6488-6491 (1969).

(71) Barany, G., and Merrifield, R.B., p.119 of reference (64), vol. 2.

(72) Merrifield, R.B., J. Am. Chem. Soc. 85, 2149-2154 (1963). Bayer, E., Eckstein, H., Hagele, K., Konig, W.A., Bruning, W., Hagenmaier, H., and Parr, W., J. Am. Chem. Soc. 92, 1735-1738 (1970).

(73) Erickson, B.W., and Merrifield, R.B., J. Am. Chem. Soc. 95, 3757-3763 (1973).

(74) Mitchell, A.R., Erickson, B.W., Ryabtsev, M.N., Hodges, R.S., and Merrifield, R.B., J. Am. Chem. Soc. 98, 7357-7362 (1976).

(75) Sparrow, J.T., J. Org. Chem. 41, 1350-1353 (1976).

(76) Gisin, B.F., Helv. Chim. Acta 56, 1476-1482 (1973).

(77) Stewart, J.M., and Young, J.D., Solid Phase Peptide Synthesis, Freeman, San Francisco, 1969. p.32.

(78) P.53 of reference (77).

(79) Cabral, F., and Schatz, G., in Methods In Enzymology Vol.LVI, edited by Fleischer, S., and Packer, L., Academic Press, London, 1979. p.613.

(80) Wilson, K.J., Honegger, A., Stotzel, R.P., and Hughes, G.J., Biochem. J. 199, 31-41 (1981).

(81) Pearson, J.D., Lin, N.T., and Regnier, F.E., Anal. Biochem. 124, 217-230 (1982).

(82) Hearn, M.T.W., and Hancock, W.S., Trends Biochem. Sci. 4, N58-N62 (1979).

(83) Dinner, A., and Lorenz, L., Anal. Chem. 51, 1872-1873 (1979).

(84) Blanc, J.P., Taylor, J.W., Miller, R.J., and Kaiser, E.T., J. Biol. Chem. 258, 8277-8284 (1983).

(85) Fukushima, D., Yokoyama, S., Kroon, D.J., Kezdy, F.J., and Kaiser, E.T., J. Biol. Chem. 255, 10651-10657 (1980).

(86) P.1-4 of reference (12).

(87) Haschemeyer, R.H., and Haschemeyer, A.E.V., Proteins: A Guide To Study By Physical Methods, Wiley-Interscience, New York, 1973. p.120-124.

(88) Tanford, C., Science 200, 1012-1018 (1978).

(89) Hartley, G.S., Aqueous Solutions Of Paraffin-Chain Salts, Hermann & Cie., Paris, 1936.

(90) Ben-Naim, A., Hydrophobic Interactions, Plenum Press, New York, 1980).

(91) Diamond, J.M., and Katz, Y., J. Membrane Biol. 17, 121-154 (1974).

(92) P.63 and 102 of reference (31).

(93) Hildebrand, J.H., Proc. Natl. Acad. Sci. USA 76, 194-194 (1979).

(94) P.1-6 of reference (90).

(95) Kauzmann, W., in A Symposium On The Mechanism of Enzyme Action, edited by McElroy, W.D., and Glass, B., John Hopkins University Press, Baltimore, 1954.

(96) P.14 of reference (90).

(97) P.37 of reference (90).

(98) P.52 of reference (90).

(99) McKenzie, H.A., John Curtin School of Medicine, Australian National University, Canberra, personal communication.

(100) P.19-24 of reference (12).

(101) Franks, F., and Ives, D.J.G., J. Chem. Soc. 1960, 741-754.

(102) Wertz, D.H., J. Am. Chem. Soc. 102, 5316-5322 (1980).

(103) Wilhelm, E., Battino, R., and Wilcock, R.J., Chem. Rev. 77, 219-262 (1977).

(104) Rogers, J.A., and Wong, A., Int. J. Pharmaceutics 6, 339-348 (1980).

(105) P.8 and 16 of reference (12).

(106) Gill, S.J., and Wadso, I., Proc. Natl. Acad. Sci. USA 73, 2955-2958 (1976).

(107) Smith, R., and Tanford, C., Proc. Natl. Acad. Sci. USA 70, 289-293 (1973).

(108) Snyder, L.R., Kirkland, J.J., Introduction To Modern Liquid Chromatography, 2nd ed., Wiley-Interscience, New York, 1979.

(109) High-Performance Liquid Chromatography: Advances and Perspectives Vol. 2, edited by Horvath, C., Academic Press, New York, 1980.

(110) Hearn, M.T.W., in Advances In Chromatography Vol. 20, edited by Giddings, J.C., Grushka, E., Cazes, J., and Brown, P.R., Marcel Dekker, New York, 1983. p.13.

(111) Sinanoglu, O., and Abdulnur, S., Photochem. Photobiol. 3, 333-342 (1964).

(112) P.39 of reference (90).

(113) Wells, M.J.M., and Clark, C.R., J. Chromatogr. 243, 263-277 (1982).

(114) Grushka, E., Colin, H., and Guiochon, G., J. Chromatogr. 248, 325-339 (1982).

(115) Colin, H., Diez-Masa, J.C., Guiochon, G., Czajkowska, T., and Miedziak, I., J. Chromatogr. 167, 41-65 (1978).

(116) Kikta, E.J., Jr., and Grushka, E., Anal. Chem. 48, 1098-1104 (1976).

(117) Knox, J.H., and Vasvari, G., J. Chromatogr. 83, 181-194 (1973).

(118) This thesis, Chapter 5.

(119) Assman, G., and Brewer, H.B., Jr., Proc. Natl. Acad. Sci. USA 71, 1534-1538 (1974).

(120) P.60-78 of reference (12).

(121) Andrews, A.L., Atkinson, D., Barratt, M.D., Finer, E.G., Hauser, H., Henry, R., Leslie, R.B., Owens, N.L., Phyllips, M.C., and Robertson, R.N., Eur. J. Biochem. 64, 549-563 (1976).

(122) Stoffel, W., Zierenberg, O., Tunggal, B., and Schreiber, E., Proc. Natl. Acad. Sci. USA 71, 3696-3700 (1974).

(123) Seeman, P., Roth, S., and Schneider, H., Biochim. Biophys. Acta 225, 171-184 (1971).

(124) Wright, E.M., and Bindslev, N., J. Membrane Biol. 29, 289-312 (1976).

(125) Jain, M.K., and Wray, L.V., Jr., Biochem. Pharmacol. 27, 1294-1296 (1978).

(126) Wise, M.B., thesis, Ph.D. University of Pennsylvania, 1981.

(127) Massey, J.B., Gotto, A.M., Jr., and Pownall, H.J., J. Biol. Chem. 254, 9359-9361 (1979).

(128) Massey, J.B., Gotto, A.M., Jr., and Pownall, H.J., Biochemistry 20, 1575-1584 (1981).

(129) Bull, H.B., and Breese, K., Arch. Biochem. Biophys. 161, 665-670 (1974).

(130) P.126 of reference (87).

(131) P.128 of reference (87).

(132) Barrow, G.M., Physical Chemistry, 3rd ed. McGraw-Hill Kogakusha, Tokyo, 1973. p.272.

(133) P.356 of reference (87).

(134) P.209 of reference (90).

(135) Privalov, P.L., Adv. Protein Chem. 33, 167-241 (1979).

(136) Perutz, M.F., Kendrew, J.C., and Watson, H.C., J. Mol. Biol. 13, 669-678 (1965).

(137) Lim, V.I., J. Mol. Biol. 88, 857-872 (1974).

(138) Kanehisa, M.I., and Tsong, T.Y., Biopolymers 19, 1617-1628 (1980).

(139) Cid, H., Bunster, M., Arriagada, E., and Campos, M., FEBS Lett. 150, 247-254 (1982).

(140) Kabsch, W., and Sander, C., FEBS Lett. 155, 179-182 (1983).

(141) Melander, W., Campbell, D.E., and Horvath, C., J. Chromatogr. 158, 215-225 (1978).

(142) Snyder, L.R., J. Chromatogr. 179, 167-172 (1979).

(143) Hall, D.G., in Aggregation Processes In Solution, edited by Wyn-Jones, E., and Gormally, J., Elsevier, Amsterdam, 1983. p.7-69.

(144) Chen, T., Knapp, R.D., Rohde, M.F., Brainard, J.R., Gotto, A.M., Jr., Sparrow, J.T., and Morrisett, J.D., Biochemistry 19, 5140-5146 (1980).

(145) Molnar, I., and Horvath, C., Clin. Chem. 22, 1497-1502 (1976).

(146) Horvath, C., Melander, W., and Molnar, I., J. Chromatogr. 125, 129-156 (1976).

(147) Colin, H., and Guiochon, G., J. Chromatogr. 158, 183-205 (1978).

(148) Karger, B.L., Gant, J.R., Hartkopf, A., and Weiner, P.H., J. Chromatogr. 128, 65-78 (1976).

(149) Horvath, C., and Melander, W., J. Chromatogr. Sci. 15, 393-404 (1977).

(150) Davis, M.A.F., Hauser, H., Leslie, R.B., and Phillips, M.C., Biochim Biophys. Acta 317, 214-218 (1973).

(151) Abraham, M.H., J. Am. Chem. Soc. 102, 5910-5912 (1980).

(152) Israelachvili, J., and Pashley, R., Nature 300, 341-342 (1982).

(153) Hancock, W.S., and Sparrow, J.T., HPLC Analysis Of Biological Compounds. A Laboratory Guide, Marcel Dekker, New York, 1984.

(154) Yonker, C.R., Zwier, T.A., and Burke, M.F., J. Chromatogr. 241, 257-268 (1982).

(155) Meek, J.L., Proc. Natl. Acad. Sci. 77, 1632-1636 (1980).

(156) Meek, J.L., Anal. Chem. 52, 1370-1371 (1980).

(157) Meek, J.L., and Rossetti, Z.L., J. Chromatogr. 211, 15-28 (1981).

(158) Sasagawa, T., Okuyama, T., and Teller, D.C., J. Chromatogr. 240, 329-340 (1982).

(159) Imoto, T., and Yamada, H., Mol. Cell. Biochem. 51, 111-121 (1983).

(160) Grego, B., and Hearn, M.T.W., Chromatographia 14, 589-592 (1981).

(161) Mahoney, W.C., Biochim. Biophys. Acta 704, 284-289 (1982).

(162) Wehr, C.T., Correla, L., and Abbott, S.R., J. Chromatogr. Sci. 20, 114-119 (1982).

(163) Heukeshoven, J., and Dernick, R., J. Chromatogr. 252, 241-254 (1982).

(164) Vigh, G., Varga-Puchony, Z., Hlavay, J., and Papp-Hites, E., J. Chromatogr. 236, 51-59 (1982).

(165) Wilson, K.J., Wieringen, E.V., Klauser, S., and Berchtold, M.W., J. Chromatogr. 237, 407-416 (1982).

(166) Nice, E.C., Capp, M., and O'Hare, M.J., J. Chromatogr. 185, 413-427 (1979).

(167) Hancock, W.S., Bishop, C.A., Prestidge, R.L., Harding, D.R.K. and Hearn, M.T.W., Science 200, 1168-1170 (1978).

(168) Kohr, W.J., Keck, R., and Harkins, R.N., Anal. Biochem. 122, 348-359 (1982).

(169) Schoenmakers, P.J., Billiet, H.A.H., Tijssen, R., and De Galan, L., J. Chromatogr. 149, 519-537 (1978).

(170) Billiet, H.A.H., Keehnen, P.D.M., and De Galan, L., J. Chromatogr. 185, 515-528 (1979).

(171) Snyder, L.R., Dolan, J.W., and Gant, J.R., J. Chromatogr. 165, 3-30 (1979).

(172) Dolan, J.W., Gant, J.R., and Snyder, L.R., J. Chromatogr. 165, 31-58 (1979).

(173) Schoenmakers, P.J., Billiet, H.A.H., and De Galan, L., J. Chromatogr. 185, 179-195 (1979).

(174) Krstulovic, A.M., Colin, H., and Guichon, G., Anal. Chem. 54, 438-2443 (1982).

(175) Molnar, I., and Horvath, C., J. Chromatogr. 142, 623-640 (1977).

(176) Pliska, V., Schmidt, M., and Fauchere, J., J. Chromatogr. 216, 79-92 (1981).

(177) Manavalan, P., and Ponnuswamy, P.K., Nature 275, 673-674 (1978).

(178) Jones, D.D., J. Theor. Biol. 50, 167-183 (1975).

(179) Wolfenden, R., Andersson, L., Cullis, P.M., and Southgate, C.C.B., Biochemistry 20, 849-855 (1981).

(180) Tanford, C., J. Am. Chem. Soc. 84, 4240-4247 (1962.

(181) Nozaki, Y., and Tanford, C., J. Biol. Chem. 245, 2211-2217 (1971).

(182) Zimmerman, J.M., Eliezer, N., and Simha, R., J. Theor. Biol. 21, 170-201 (1968).

(183) Snyder, L.R., Principles of Adsorption Chromatography, Marcel Dekker, New York, 1968. p.134.

(184) Bij, K.E., Horvath, C., Melander, W.R., and Nahum, A., J. Chromatogr. 203, 65-84 (1981).

(185) Hancock, W.S., Bishop, C.A., Meyer, L.J., Harding, D.R.K., and Hearn, M.T.W., J. Chromatogr. 161, 291-298 (1978).

(186) Unger, K., in Handbook On The Use Of HPLC For The Separation Of Amino Acids, Peptides And Proteins, edited by Hancock, W.S., CRC Press, Boca Raton, in press.

(187) Knox, J.H., Kaliszan, R., and Kennedy, G.J., Faraday Symp. Chem. Soc. 15, paper 7 (1981).

(188) Deming, S.N., in reference (186), in press.

(189) Tanaka, N., and Thornton, E.R., J. Am. Chem. Soc. 99, 7300-7307 (1977).

(190) Segrest, J.P., Jackson, R.L., Morrisett, J.D., and Gotto, A.M. Jr., FEBS Lett. 38, 247-253 (1974).

(191) Segrest, J.P., FEBS Lett. 69, 111-115 (1976).

(192) Segrest, J.P., and Feldman, R.J., Biopolymers 16, 2053-2065 (1977).

(193) Sparrow, J.T., and Gotto, A.M., Jr., Ann. N.Y. Acad. Sci. USA 348, 187-211 (1980).

(194) Sparrow, J.T., Pownall, H.J., Sigler, G.F., Smith, L.C., Soutar, A.K., and Gotto, A.M., Jr., in Peptides, edited by Sigler, G.F., and Meienhofer, J., Wiley, New York, 1977. p.149-152.

(195) Mao, S.J.T., Jackson, R.L., Gotto, A.M., Jr., and Sparrow, J.T., Biochemistry 20, 1676-1680 (1981).

(196) Kroon, D.J., Kupferberg, J.P., Kaiser, E., and Kezdy, F.J., J. Am. Chem. Soc. 100, 5975-5977 (1978).

(197) Rosseneu, M., Soeteway, F., Lievens, M., Vercaemst, R., and Peeters, H., Eur. J. Biochem. 79, 251-257 (1977).

(198) Jackson, R.L., Mao, S.J.T., and Gotto, A.M., Jr., Biochem. Biophys. Res. Commun. 61, 1317-1324 (1974).

(199) Hauser, H., FEBS Lett. 60, 71-75 (1975).

(200) Pattnaik, N.W., Kezdy, F.J., and Scanu, A.M., J. Biol. Chem. 215, 1984-1990 (1976).

(201) Scanu, A., Reader, W., and Edelstein, C., Biochim. Biophys. Acta 160, 32-45 (1968).

(202) Finer, E.G., Henry, R., Leslie, R.B., and Robertson, R.N., Biochim. Biophys. Acta 380, 320-337 (1975).

(203) Henderson, T.O., Kruski, A.W., Davis, L.G., Glonek, T., and Scanu, A.M., Biochemistry 14, 1915-1920 (1975).

(204) Zimm, B.H., and Rice, S.A., Mol. Phys. 3, 391-407 (1960).

(205) Segrest, J.P., Chung, B.H., Brouillette, C.G., Kanellis, P., and McGahan, R., J. Biol. Chem. 258, 2290-2295 (1983).

(206) P.63-65 of reference (31).

(207) Janiak, M.J., Small, D.M., and Shipley, G.G., Biochemistry 15, 4575-4580 (1976).

(208) Papahadjopoulos, D., Moscarello, M., Eylar, E.H., and Isac, T., Biochim. Biophys. Acta 401, 317-335 (1978).

(209) Chatelain, P., Berliner, C., Ruysschaert, J.-M., and Jaffe, J., J. Colloid Interface Sci. 51, 239-244 (1975).

(210) Montal, M., J. Membrane Biol. 7, 245-266 (1972).

(211) Hartmann, W., and Galla, H.J., Biochim. Biophys. Acta 509, 474-490 (1978).

(212) Hammes, G.G., and Schullery, S.E., Biochemistry 9, 2555-2563 (1970).

(213) De Kruijff, B., and Cullis, P.R., Biochim. Biophys. Acta 610, 235-240 (1980).

(214) P.71-75 of reference (31).

(215) Fookson, J.E., and Wallach, D.F.H., Arch. Biochem. Biophys. 189, 195-204 (1978).

(216) Nakagaki, M., and Okamura, E., Bull. Chem. Soc. Jpn. 55, 1352-1356 (1982).

(217) Nakagaki, M., and Okamura, E., Bull. Chem. Soc. Jpn. 56, 1607-1611 (1983).

(218) Riordan, J.F., McElvany, K.D., and Borders, C.L., Jr., Science 195, 884-886 (1977).

(219) Cotton, F.A., Hazen, E.E., Jr., Day, V.W., Larsen, S., Norman, J.G., Wong, S.T.K., and Johnson, K.H., J. Am. Chem. Soc. 95, 2367-2369 (1973).

(220) P.98-105 of reference (31).

(221) Paddy, M.R., Dahlquist, F.W., Davis, J.H., and Bloom, M., Biochemistry 20, 3152-3162 (1981).

(222) Jahnig, F., Vogel, H., and Best, L., Biochemistry 21, 6790-6798 (1982).

(223) Bierzynski, A., Kim, P.S., and Baldwin, R.L., Proc. Natl. Acad. Sci. USA 79, 2470-2474 (1982).

(224) Segrest, J.P., Chem. Phys. Lipids 18, 7-22, (1977).

(225) Nemethy, G., and Scheraga, H.A., J. Phys. Chem. 66, 1773-1789 (1962).

(226) Blundell, T., Barlow, D., Borkakoti, N., and Thornton, J., Nature (in press).

(227) Hermans, J., Jr., J. Phys. Chem. 70, 510-516 (1966).

(228) Poland, D.C., and Scheraga, H.A., Biopolymers 3, 275-282 (1965).

(229) Laskowski, M., Jr., and Scheraga, H.A., J. Am. Chem. Soc. 76, 6305-6319 (1954).

(230) Mantulin, W.W., Massey, J.B., Gotto, A.M., Jr., and Pownall, H.J., J. Biol. Chem. 256, 10815-10819 (1981).

(231) Pownall, H.J., Hickson, D., and Gotto, A.M., Jr., J. Biol. Chem. 256, 9849-9854 (1981).

(232) Gilman, T.G., Kauffman, J.W., and Pownall, H.J., Biochemistry 20, 656-661 (1981).

(233) Pownall, H.J., Hsu, F.J., Rosseneu, M., Peters, H., Gotto, A.M., and Jackson, R.L., Biochim. Biophys. Acta 488, 190-197 (1977).

(234) Heyn, M.P., Cherry, R.J., and Dencher, N.A., Biochemistry 20, 840-849 (1981).

(235) Bergelson, L.D., Lipid Biochemical Preparations, Elsevier/ North-Holland Biomedical Press, Amsterdam, 1980. p.124-132.

(236) Pownall, H.J., Pao, Q., Sparrow, J.T., Kusserow, S.K., and Massey, J.B., Biochemistry 20, 6630-6635 (1981).

(237) Swaney, J.B., J. Biol. Chem. 255, 8791-8797 (1980).

(238) Pownall, H.J., Morrisett, J.D., Sparrow, J.T., and Gotto, A.M., Biochem. Biophys. Res. Commun. 60, 779-786 (1974).

(239) P.11 of reference (12).

(240) Roth, R.I., Jackson, R.L., Pownall, H.J., and Gotto, A.M., Jr., Biochemistry 16, 5030-5036 (1977).

(241) Lebl, M., J. Chromatogr. 242, 342-345 (1982).

(242) Hammers, W.E., Meurs, G.J., and De Ligny, C.L., J. Chromatogr. 246, 169-168 (1982).

(243) Hammers, W.E., Meurs, G.J., and De Ligny, C.L., J. Chromatogr. 247, 1-13 (1982).

(244) Hafkenscheid, T.L., and Tomlinson, E., Int. J. Pharmaceutics 16, 225-239 (1983).

(245) Quay, S.C., and Condie, C.C., Biochemistry 22, 695-700 (1983).

(246) Chen, T.C., Sparrow, J.T., Gotto, A.M., Jr., and Morrisett, J.D., J. Am. Chem. Soc. 18, 1617-1622 (1979).

(247) Soutar, A.K., Sigler, G.F., Smith, L.C., Gotto, A.M., Jr., and Sparrow, J.T., Scand. J. Clin. Lab. Invest. 38 (Suppl. 150), 53-58 (1978).

(248) Chou, P.Y., and Fasman, G.D., Biochemistry 13, 222-245 (1974).

(249) Dijkstra, B.W., Kalk, K.H., Hol, W.G.J., and Drenth, J., J. Mol. Biol. 147, 97-123 (1981).

(250) McLachlan, A.D., Nature 267, 465-466 (1977).

(251) Kaiser, E.T., and Kezdy, F.J., Proc. Natl. Acad. Sci. USA 80, 1137-1143 (1983).

(252) Gavilanes, J.G., Lizarbe, M.A., Municio, A.M., and Onderra, M., FEBS Lett. 126, 253-256 (1981).

(253) Wu, C.C., Hachimori, A., and Yang, J.T., Biochemistry 21, 4556-4562 (1982).

(254) Cockle, S.A., Epand, R.M., Boggs, J.M., and Moscarello, M.A., Biochemistry 17, 624-629 (1978).

(255) Shirahama, K., and Yang, J.T., Int. J. Pept. Protein Res. 13, 341-345 (1979).

(256) Sugihara, T., Blout, E.R., and Wallace, B.A., Biochemistry 21, 3444-3452 (1982).

(257) Brack, A., and Spack, G., J. Am. Chem. Soc. 103, 6319-6323 (1981).

(258) Grupe, R., Zschatsch, U., Preuber, E., and Goring, H., Studia Biophysica 66, 31-46 (1977).

(259) Phillips, M.C., Hauser, H., Leslie, R.B., and Oldani, D., Biochim. Biophys. Acta 406, 402-414 (1975).

(260) Walton, A.G., Polypeptides And Protein Structure, Elsevier, New York, 1981. p.42.

(261) Wu, C.S., Lee, N.M., Loh, H.H., Yang, J.T., and Li, C.H., Proc. Natl. Acad. Sci. USA 76, 3656-3659 (1979).

(262) Kaiser, E.T., and Kezdy, F.J., Science 223, 249-255 (1984).

(263) Bhakoo, M., Birkbeck, T.H., and Freer, J.H., Biochemistry 21, 6879-6883 (1982).

(264) Fitton, J.E., Dell, A., and Shaw, W.V., FEBS Lett. 115, 209-212 (1980).

(265) Epand, R.M., Epand, R.F., Orlowski, R.C., Schlueter, R.J., Boni, L.T., and Hui, S.W., Biochemistry 22, 5074-5084 (1983).

(266) Van Scharrenburg, G.J.M., Puijk, W.C., Egmond, M.R., De Haas, G.H., and Slotboom, A.J., Biochemistry 20, 1584-1591 (1981).

(267) Epand, R.M., and Sturtevant, J.M., Biochemistry 20, 4603-4606 (1981).

(268) Epand, R.M., and Epand, R., Biochim. Biophys. Acta 602, 600-609 (1980).

(269) Pownall, H.J., Knapp, R.D., Gotto, A.M., Jr., and Massey, J.B., FEBS Lett. 159, 17-23 (1983).

(270) Van Scharrenburg, G.J.M., Puijk, W.C., De Haas, G.H., and Slotboom, A.J., Eur. J. Biochem. 133, 83-89 (1983).

(271) Blanc, J.P., Taylor, J.W., Miller, R.J., and Kaiser, E.T., J. Biol. Chem. 258, 8277-8284 (1983).

(272) Kyte, J., and Doolittle, R.F., J. Mol. Biol. 157, 105-132 (1982).

(273) Walter, M., and Ramaley, L., Anal. Chem. 45, 165-166 (1973).

(274) Kanellis, P., Romans, A.Y., Johnson, B.J., Kercret, H., Chiovetti, R., Allen, T.M., and Segrest, J.P., J. Biol. Chem. 255, 11464-11472 (1980).

(275) Dr W.S. Hancock, Massey University, personal communication.

(276) Fukushima, D., Yokoyama, S., Kezdy, F.J., and Kaiser, E.T., Proc. Natl. Acad. Sci. USA 78, 2732-2736 (1981).